https://ntrs.nasa.gov/search.jsp?R=19790021032 2020-03-21T22:21:40+00:00Z

CASD-ASP78-016

NASA CR-
160288

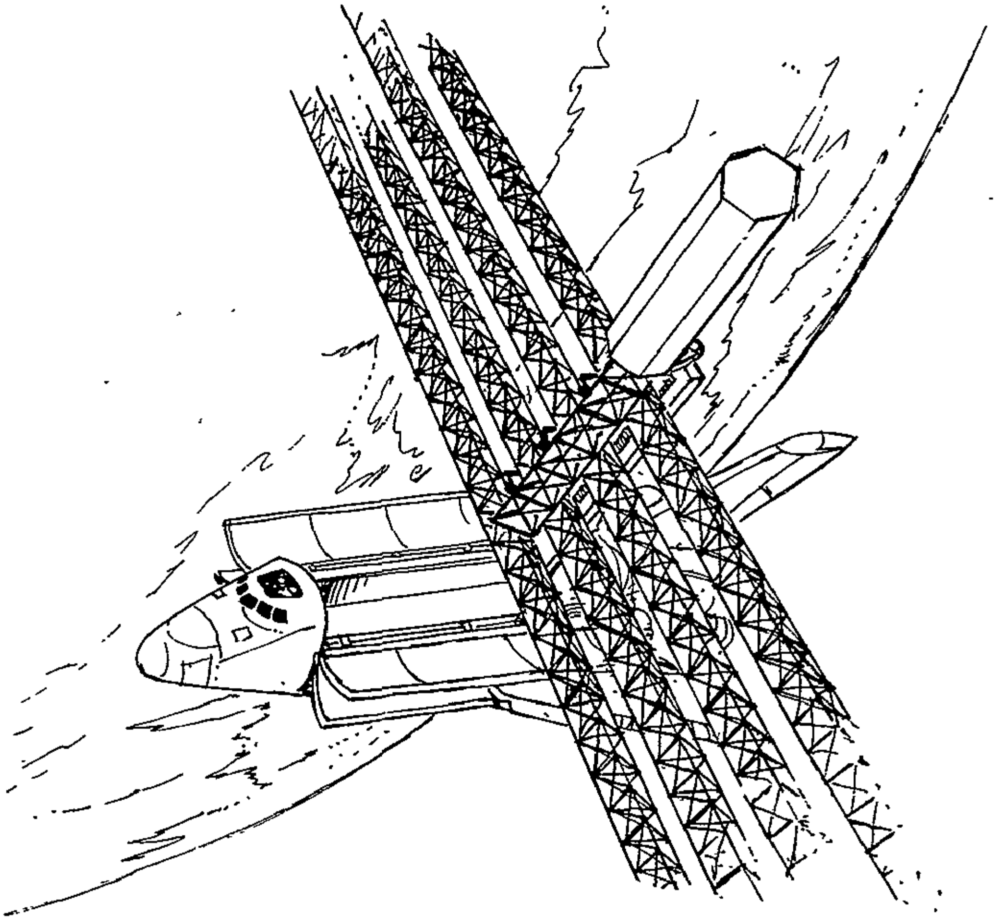

SPACE CONSTRUCTION AUTOMATED FABRICATION EXPERIMENT DEFINITION STUDY (SCAFEDS) PART III

FINAL REPORT

VOLUME II ✦ STUDY RESULTS

CONTRACT NO. NAS9-15310
DRL NO. T-1346
DRD NO. MA-664T
LINE ITEM NO. 3

GENERAL DYNAMICS
Convair Division

Kearny Mesa Plant, P.O. Box 80847
San Diego, California 92138
Advanced Space Programs

(NASA-CR-160288) SPACE CONSTRUCTION AUTOMATED FABRICATION EXPERIMENT DEFINITION STUDY (SCAFEDS), PART 3. VOLUME 2: STUDY RESULTS Final Report (General Dynamics/Convair) 309 p HC A14/MF A01 CSCL 22B

N79-29203

Unclas
G3/12 31642

SPACE CONSTRUCTION AUTOMATED FABRICATION EXPERIMENT DEFINITION STUDY (SCAFEDS) PART III

FINAL REPORT

VOLUME I ✦ EXECUTIVE SUMMARY
VOLUME II ✦ STUDY RESULTS
VOLUME III ✦ REQUIREMENTS

CASD-ASP78-016

SPACE CONSTRUCTION AUTOMATED FABRICATION EXPERIMENT DEFINITION STUDY (SCAFEDS) PART III

FINAL REPORT

VOLUME II - STUDY RESULTS

CONTRACT NO. NAS9-15310
DRL NO. T-1346
DRD NO. MA-664T
LINE ITEM NO. 3

29 June 1979

Submitted to
National Aeronautics and Space Administration
LYNDON B. JOHNSON SPACE CENTER
Houston, Texas 77058

Prepared by
GENERAL DYNAMICS CONVAIR DIVISION
P.O. Box 80847
San Diego, California 92138

FOREWORD

This final report was prepared by General Dynamics Convair Division for NASA-JSC in accordance with Contract NAS9-15310, DRL No. T-1346, DRD No. MA-664T, Line Item No. 3. It consists of three volumes: (I) a brief Executive Summary; (II) a comprehensive set of Study Results; and (III) a compilation of Requirements.

The principal study results were developed from August 1978 through April 1979, followed by final documentation. Reviews were presented at JSC on 13 December 1978 and 24 April 1979, and at NASA Headquarters on 17 May 1979.

Due to the broad scope of this study, many individuals were involved in providing technical assistance. General Dynamics Convair personnel who significantly contributed to the study include:

Study Manager	Lee Browning
Mechanical Design	John Bodle, Steve Hardy, Hans Stocker
Avionics & Controls	Jack Fisher, Ed Kleidon, Bill Snyder, Doug Burgess
Requirements	Jim Peterson
Development Plans	John Maloney
Structural Design	Gary Tremblay, Lee Browning
Structural Analysis	Keith Kedward
Structural Dynamics	Des Pengelley, Shih-How Chang
Thermodynamics	Dick Pleasant
Mass Properties	Dennis Stachowitz
Mfg. Technology	Steve Hardy
Economic Analysis	Bob Bradley
Test Integration	George Copeland

The study was conducted in Convair's Advanced Space Programs department, directed by J. B. (Jack) Hurt. The NASA-JSC COR is Lyle Jenkins of the Spacecraft Design Division, under Allen J. Louviere, Chief.

For further information contact:

Lyle M. Jenkins, Code EW4
NASA-JSC
Houston, Texas 77058
(713) 483-3405

D. Lee Browning, MZ 21-9504
General Dynamics Convair Division
P. O. Box 80847
San Diego, California 92138
(714) 277-8900, Ext. 2815

PRECEDING PAGE BLANK NOT FILMED

TABLE OF CONTENTS

PRECEDING PAGE BLANK NOT FILMED

TABLE OF CONTENTS (Continued)

TABLE OF CONTENTS (Continued)

TABLE OF CONTENTS (Continued)

LIST OF FIGURES

LIST OF FIGURES (Continued)

LIST OF FIGURES (Continued)

LIST OF FIGURES (Continued)

LIST OF TABLES

1

INTRODUCTION

1.1 SCOPE

This is the second of three volumes comprising the SCAFED Study Part III Final Report. It contains the detailed results of all Part III study tasks. Other volumes provide an Executive Summary (Volume I) and an updated comprehensive Requirements Document (Volume III). A corresponding 3-volume set was prepared at the conclusion of the Part I/II study effort in May 1978. Together they fully document all SCAFEDS effort to date.

This section provides an overview and a top level summary of prior and current study effort.

1.2 STUDY OVERVIEW

1.2.1 PART I/II SUMMARY. In Part I/II a wide range of tasks was focused on a baseline system concept, shown in Figure 1-1, in which fabrication/assembly systems and prepackaged raw materials were delivered by Shuttle to LEO. Upon system deployment from the stowed position, a beam builder, moving to successive positions along a Shuttle-attached assembly jig, automatically fabricated four long triangular beams and then nine shorter, but otherwise identical, cross-beams. Beams were retained in position and translated as required, to accommodate automated joining, by jig-mounted mechanisms. Upon platform assembly completion, subsystems were installed, with difficult-to-automate tasks done by EVA, followed by structural and thermal response tests and development of RMS/platform release/recapture techniques.

Part I/II outputs of particular significance to the Part III effort are also shown in Figure 1-1, and principal Part I/II conclusions applicable to Part III activity are summarized in Table 1-1.

1.2.2 PART III. Part III of the SCAFED Study started in July 1978, with midterm and final reviews in December 1978 and April 1979, respectively, and will be concluded in July 1979. Part III major task groups build on inputs from Part I/II and relate to each other per the flow illustrated in Figure 1-2. The approximate percentage of study budget allocated to each task group is indicated. Subjects presented in the midterm review are highlighted with solid borders; and those presented in the final review with dashed borders. Each of the major Part III task groups is divided into subtasks as shown in Figure 1-3. Specific objectives of these six task groups are:

I BEAM BUILDER FUNCTIONS. Perform selected analysis and design trades of development or cost-critical details of the Part II beam builder conceptual design.

II BEAM BUILDER DEVELOPMENT ARTICLE. Define a ground test beam builder as an article for use in the development of the capability to automatically fabricate space structures from composite materials.

III ALTERNATIVE ASSEMBLY JIG CONCEPTS. Develop assembly jig and fixture concepts capable of constructing the six illustrated structural configurations, using the beam builder as the basic construction tool and the Orbiter as a construction base. The truss produced by the beam builder, as updated in Tasks I and II, above, will be the basic element used in building the various structural configurations.

IV DEVELOPMENT EXPERIMENTS. Define individual "suitcase" experiments requiring flight tests by the Shuttle.

V BEAM BUILDER DEVELOPMENT PLAN. Update Part I/II programmatics.

VI REPORTING. Establish a permanent record of study progress and outputs and present significant findings to NASA/industry representatives.

Table 1-1. Part I/II summarized conclusions.

- **Fabrication Equipment**
  - Automated fabrication: feasible
  - Electromechanical devices: state-of-the-art, some development needed
  - Control functions: current μP memory/speed adequate
  - Control/monitor concepts & software; orbiter compatible
  - Power: 2kW required, 7kW available
- **Structure**
  - Open section cap: easy to form, large M.S.
  - Hybrid laminate: low energy, high E, low CTE
  - Dynamic/thermal response: low
  - Loads: low
- **Flight Mission Integration**
  - Single flight, 7-days
  - EVA: non-repetitive tasks
  - Orbiter compatibility: weight/CG, supports, orientation, VRCS, power, no radiator interface
- **Programmatics**
  - Mid-1982 flight achievable
  - Total payload cost: $41.9M

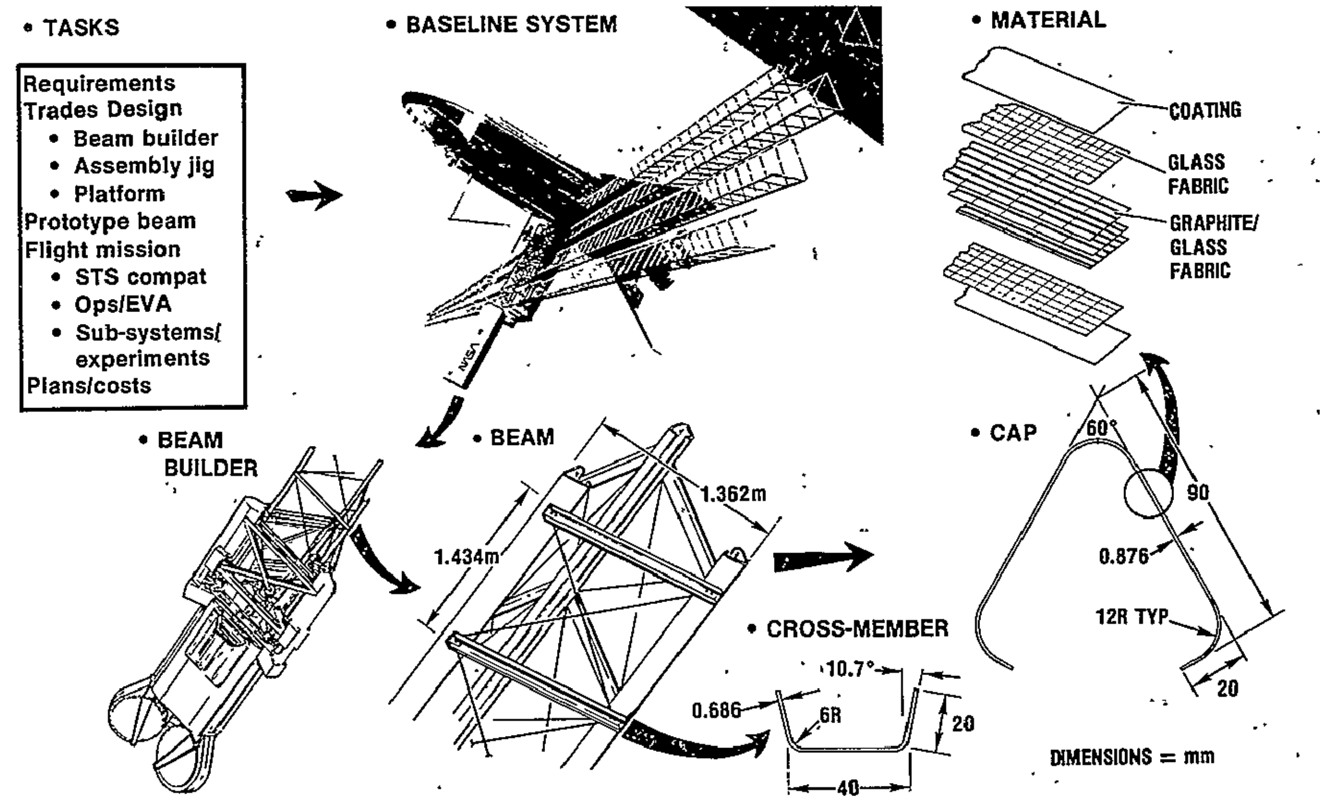

Figure 1-1. Part I/II summary.

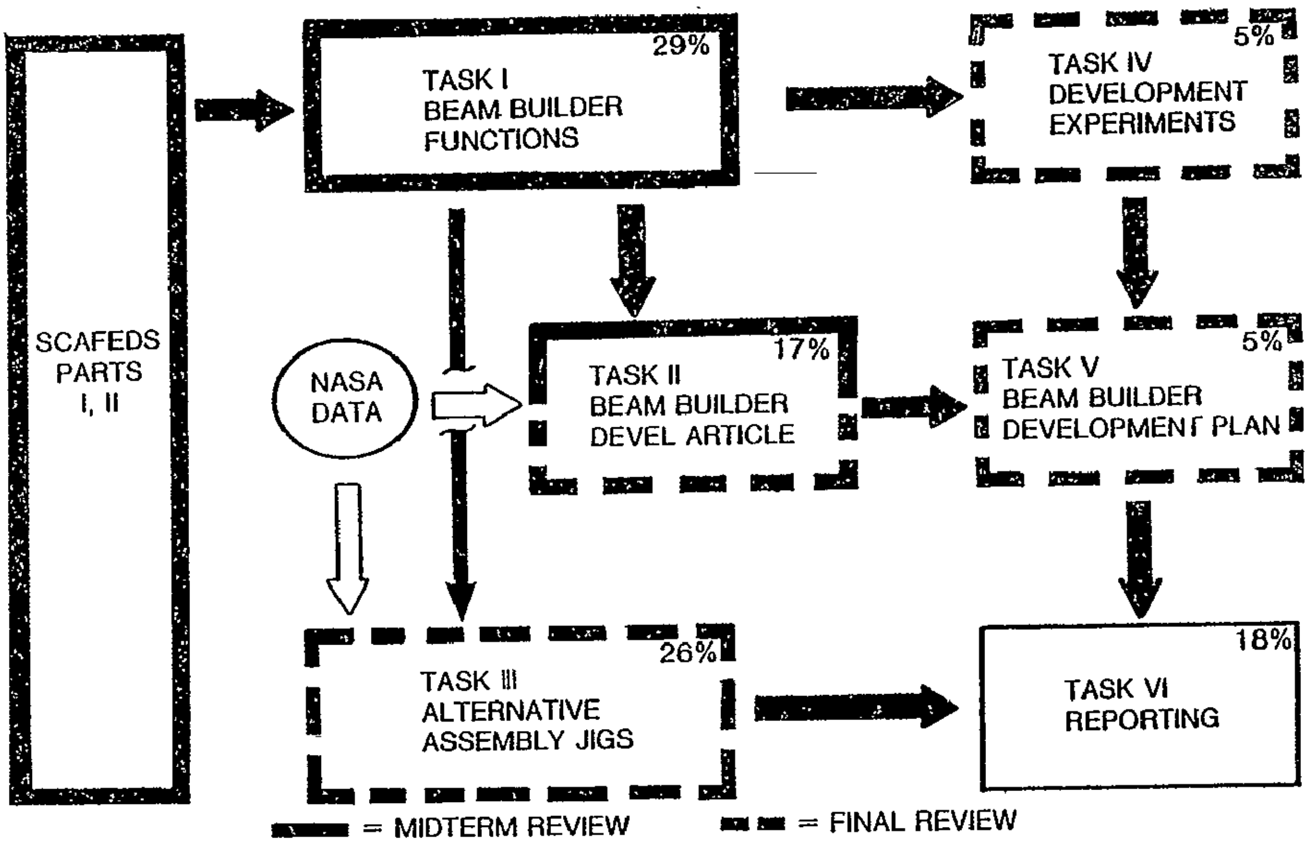

Figure 1-2. Part III task relationships.

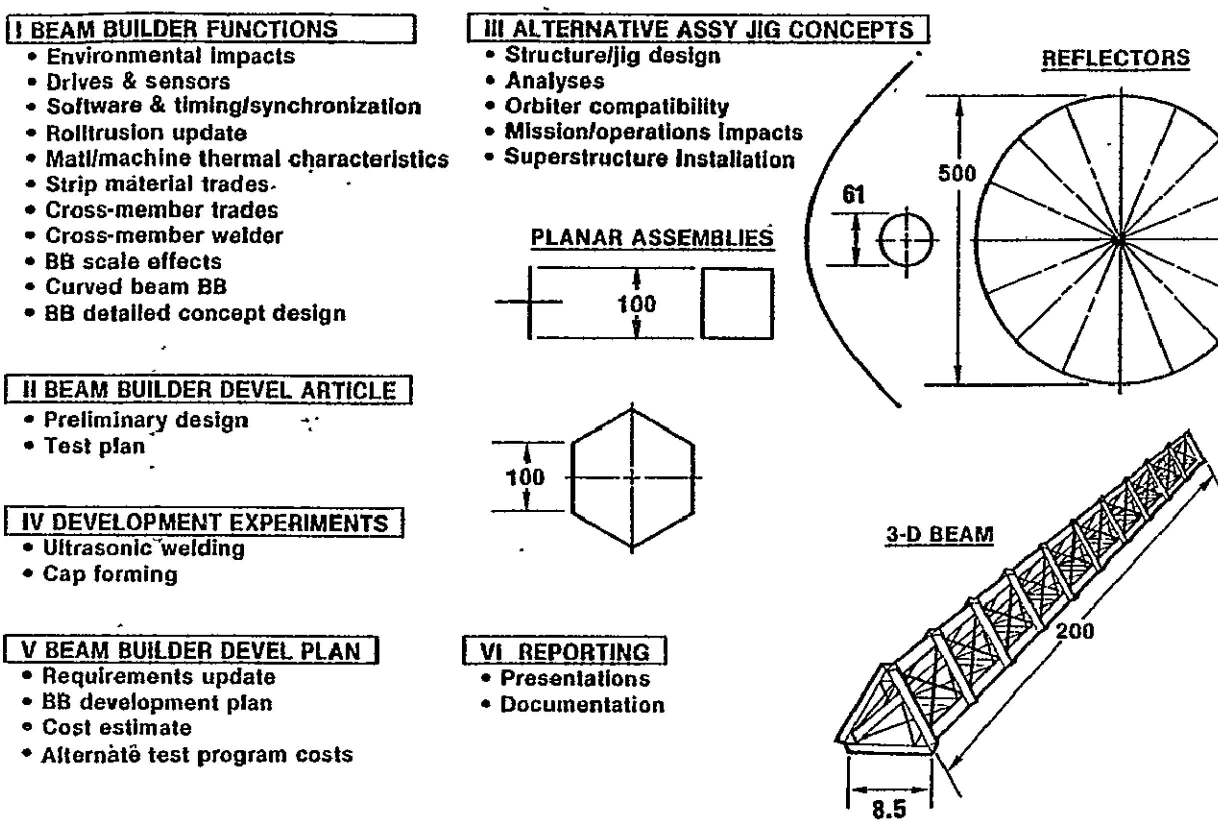

Figure 1-3. Part III detail tasks.

2

BEAM STRUCTURE/MATERIALS

The Part I/II structural design effort developed a baseline experimental "ladder" platform using a triangular beam concept selected as a result of an integrated beam and beam builder trade study. The ladder platform and the overall beam size/arrangement were retained as program baselines for Part III. However, new materials evaluations and machine/material compatibility considerations have since led to: (1) selection and optimization of a single-ply strip material in lieu of the previous multi-ply laminate; (2) prediction of the thermal characteristics of this material; and (3) trades and selection of both an improved cross-member section and improved weld joint configuration for joining cross-members and cords to the beam caps. The results of these activities and the resulting updated beam characteristics are presented in this section.

2.1 NEW STRIP MATERIAL

During the Part I/II effort, a material design evolved which combined the benefits of two fibers (glass and graphite), thermoplastic resin, and a white pigmented resin coating into a strip material suitable for the SCAFE fabrication process and service environments. Predicted properties of this "sandwiched-graphite" multi-ply laminate, using then-available materials (first unidirectional graphite tape, then 0° graphite/90° glass fabric) were reported previously. Coupon tests of the cross-member laminate (using two interior plies vs. three in the cap) were reported under Contract NAS8-32471 and generally substantiated strength and modulus predictions as shown in Figure 2-1.

At the start of laminate evolution, however, the benefits to be achieved by combining the desirable features of the constituent materials into a single-ply woven strip were already recognized. As "weavable" high-modulus graphite yarn became available, private development of single-ply strip material began, adopting the SCAFE cap and cross-member laminates as fiber percent/orientation baselines.

The first trial, a cross-member simulation, showed good strength translation but insufficient thickness and modulus due to underestimation of the required graphite content. The next trial, based on the 5-ply cap laminate, resulted in close-to-nominal thickness and provided a significant strength increase (due to a change in graphite fiber) and a combination of modulus decrease and CTE increase probably caused by the up/down crimp of graphite yarn in the fabric.

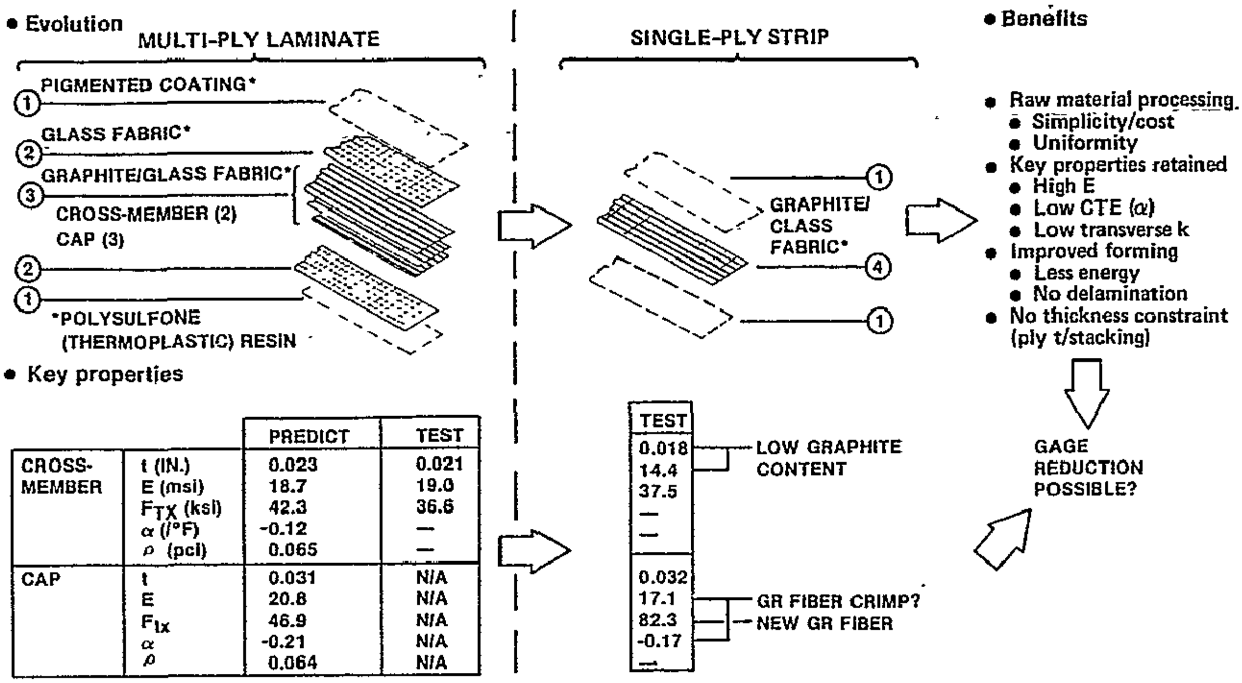

		Multi-ply laminate PREDICT	Multi-ply laminate TEST	Single-ply strip TEST
CROSS-MEMBER	t (IN.)	0.023	0.021	0.018
	E (msi)	18.7	19.0	14.4
	F_{TX} (ksi)	42.3	36.6	37.5
	α (/°F)	-0.12	—	—
	ρ (pci)	0.065	—	—
CAP	t	0.031	N/A	0.032
	E	20.8	N/A	17.1
	F_{tx}	46.9	N/A	82.3
	α	-0.21	N/A	-0.17
	ρ	0.064	N/A	—

Figure 2-1. Strip material evolution and benefits.

For the most part, the anticipated processing/property/forming benefits of single-ply construction were realized and this approach was adopted for the SCAFE application. However, a further valuable asset of the single-ply material lies in the flexibility in gage selection since the ply thickness and stacking symmetry constraints of the laminate approach are eliminated. This feature, plus the very large margin of safety in the cap section, reported previously, made it a prime target for gage reduction.

The principal objective in further strip material optimization was weight reduction via cap gage decrease. With sufficient gage reduction, cap/cross-member material commonality also becomes desirable.

Two primary concerns govern the extent of cap gage reduction as indicated in Figure 2-2. The current cap exhibits a very large safety margin with respect to conservatively high loads (N_{CR} = 133.26 N/cm vs. 16.64 N/cm limit load) but capability drops with t^3 and, in thin materials, a "comfortable" margin - say 2.0 is desirable. Furthermore, previous analyses have shown relatively low dynamic response, which is, of course, desirable. To maintain this condition, the beam fundamental frequency should be maintained, which implies minimum reduction of the frequency parameter $\sqrt{EI/m}$.

OBJECTIVES
- Reduced weight
- Cap/cross-member commonality

CONCERNS
- Cap local buckling (N_{CR})
- Beam dynamics ($f_n = f\sqrt{EI/m}$)

INITIAL TRADE
- Use single-ply material properties
- Include cross-member trade effects
- Use Part I/II cap load: $N_{max} = 16.6$ N/cm

CAP			BEAM EFFECTS				
t (cm)	E GN/m^2	N_{CR} (N/cm)	Cross-Member	Mass (kg/m)	I (cm^4)	$\sqrt{EI/m}$ $\left(\frac{N-m^2}{kg}\right)^{1/2}$	Δ %
0.0787	143.42	113.27	Original	1.1072	12077.3	13676.98	BASE
0.0813	117.90	112.96	Original	1.1429	12662.3	12492.53	-8.7
0.0635	117.90	53.94	Original	0.9643	9904.2	12023.22	-12.1
0.0635	117.90	53.94	Heavy alt	1.0536	9904.2	11509.22	-15.8
0.0635	117.90	53.94	Light alt	0.9822	9904.2	11911.48	-12.9

NEW MATERIAL DEFINED
- Increased stiffness
- New weave
- Revised fiber percentages

t	E	N_{CR}	Cross-Member	Wt	I	$\sqrt{EI/m}$	Δ %
0.0610	131.69	52.71	NEW	0.8750	9490.1	13095.93	-4.2

Figure 2-2. Strip thickness optimization.

An initial trade study assumed that the properties of the single-ply 0.0813-cm cap material would translate unchanged to lower gages (which is probably conservative for E since crimp effects would lessen). The table compares the original laminate, its single-ply analog at full thickness, and three cross-member alternatives in combination with 0.0635-cm caps. The 0.0635-cm cap maintains a buckling margin above 2.0, but exhibits a fairly significant frequency reduction, largely due to the sacrifice in modulus in the single ply material.

Consequently, a new material, designed for increased stiffness plus improvement in various "second-order" characteristics is now in development. Comparing it with the initial trade candidates shows a further gage reduction, significant weight decrease, a small but acceptable frequency penalty, and essentially unchanged local stability. It also permits cap/cross-member material commonality and has been used in the new cross-member design developed in a companion trade discussed in the following section.

2.2 MATERIAL THERMAL CHARACTERISTICS

The strip material used in the cap forming process is a consolidated strip of impregnated glass and graphite fibers with a top and bottom coating layer. The value of overall effective thermal conductivity (or thermal resistance) in the thickness direction is required to determine the temperature difference between the strip top and bottom surfaces as the material passes the heaters. The overall laminate thermal resistance is equal to the sum of the four layer resistances. Impregnated graphite composite transverse thermal conductivity is shown in Figure 2-3 as a function of the graphite fiber thermal conductivity. At the thermal conductivity of PAN50 graphite fibers (k = 100 W/m-K, 58 Btu/hr-ft-F), the transverse composite conductivity is 0.904 W/m-K (0.523 Btu/hr-ft-F). The calculated effective thermal conductivity of the total laminate is 0.484 W/m-K (0.280 Btu/hr-ft-F). Thermal conducitivity of the strip material is independent of the weave and has a low sensitivity to the graphite fiber conductivity. Calculations indicate that the strip thickness-direction ΔT in the heating section will be between 3 and 6 C (5 and 10 F).

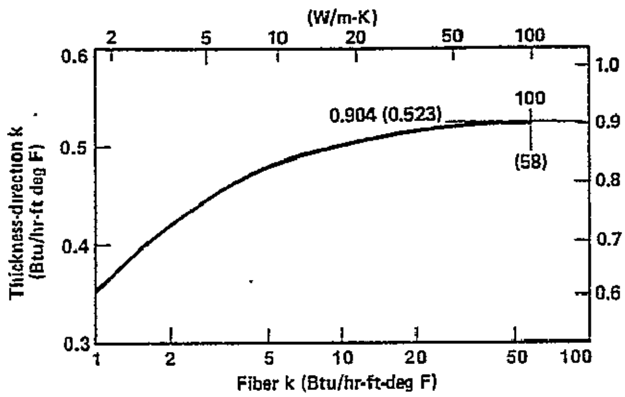

Figure 2-3. Transverse conductivity of impregnated graphite.

2.2.1 THICKNESS-DIRECTION THERMAL CONDUCTIVITY.

Definition of the strip material assumed for this thermal analysis is given in Figure 2-4. The overall effective thermal conductivity (or thermal resistance) in the thickness direction is required to determine the temperature difference between strip top and bottom surfaces as the material passes under the heaters. Overall laminate thermal resistance is calculated from top to bottom: 0.005 cm (0.002 in) top coating layer, 0.051 cm (0.021 in) layer of graphite fibers impregnated with resin, 0.010 cm (0.004 in) layer of glass fibers impregnated with resin, and 0.005 cm (0.002 in) bottom coating layer. The effective thermal conductivity of each layer is calculated or estimated, and the overall resistance is the sum of the four layer resistance.

The 3000 or 6000 graphite filaments making up each yarn are assumed to be uniformly separated by the polysulfone resin. Transverse thermal conductivity of a composite material consisting of circular cross-section fibers in a homogeneous matrix is given by the following equation from Reference 2.

$$k_{22} = k_m \left[\left(1 - \frac{r}{b}\right) + \frac{2a}{b} \int_0^r \frac{dy}{2a + h(1 - k_m/k_f)} \right] \qquad (2-1)$$

where k_{22} = transverse thermal conductivity of composite
k_m = matrix thermal conductivity
k_f = fiber thermal conductivity (fiber geometry is shown in Figure 2-4).

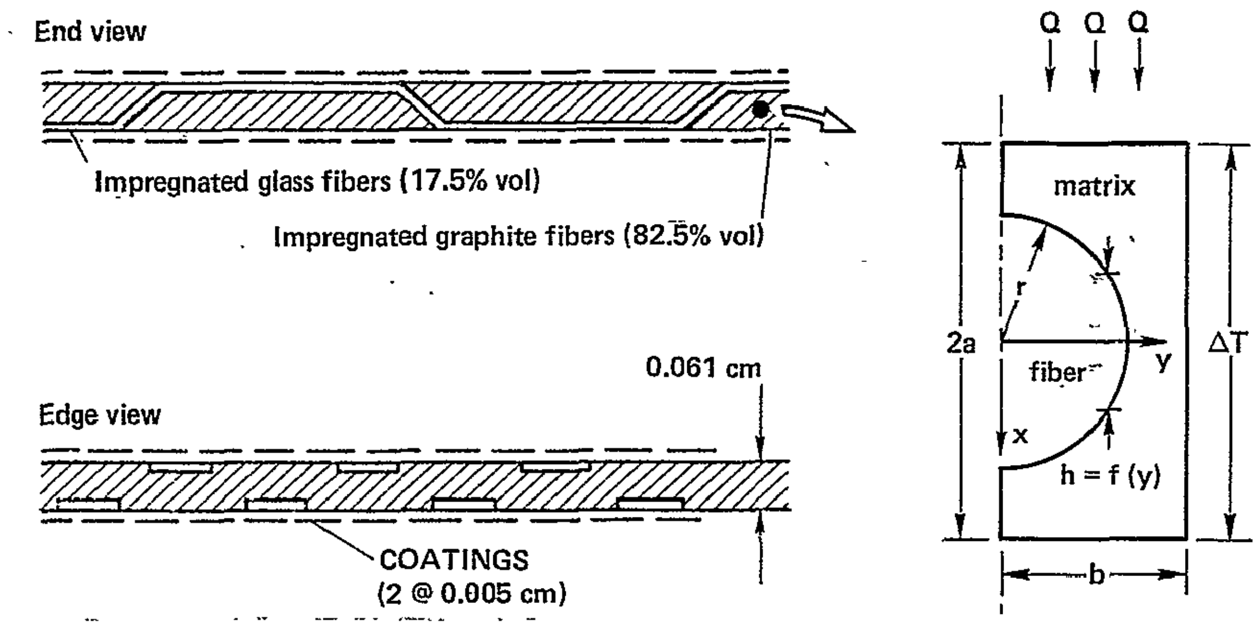

Figure 2-4. Consolidated strip material cross-section.

For a uniform square packing of fibers (assumed in this case), a = b and integration of the above equation yields:

$$k_{22} = k_m \left[\left(1 - 2\sqrt{\frac{v_f}{\pi}}\right) + \frac{1}{B}\left[\pi\left(1 - \frac{1}{C}\right) + \frac{2}{C}\tan^{-1}\left(\frac{B}{C}\sqrt{\frac{v_f}{\pi}}\right)\right]\right] \qquad (2\text{-}2)$$

where $B = 2\left(\frac{k_m}{k_f} - 1\right)$

$$C = \sqrt{1 - \frac{B^2 v_f}{\pi}}$$

In the impregnated graphite fiber region, the graphite volume fraction is 57% and the resin volume fraction is 43%. Composite transverse thermal conductivity, calculated for Equation 2-2, is shown in Figure 2-3 as a function of graphite fiber thermal conductivity. The composite k is seen to be relatively insensitive to fiber k, especially in the region of fiber k = 70 to 170 W/m-K (40 to 100 Btu/hr-ft-F). At the thermal conducitivity of PAN50 graphite fibers (k = 100 W/m-K, 58 Btu/hr-ft-F), the transverse composite k = 0.904 W/m-K (0.523 Btu/hr-ft-F).

Transverse thermal conductivity in the impregnated glass fiber region was calculated to be 0.206 W/m-K (0.119 Btu/hr-ft-F) using the same equation. The polysulfone coating layer thermal conductivity was estimated to be 0.26 W/m-K (0.15 Btu/hr-ft-F), the known value without pigment addition. Overall thermal resistance through the strip (per square foot) is given by the sum of the layer resistances.

$$R = \frac{(0.020/12)}{0.523} + \frac{(0.004/12)}{0.119} + \frac{(0.004/12)}{0.15} = 0.00832 \frac{\text{hr-F}}{\text{Btu}}$$

Effective thermal conductivity of the total laminate is given by

$$k = \frac{(0.028/12)}{0.00832} = 0.280 \text{ Btu/hr-ft-F}$$
$$= 0.484 \text{ W/m-K}$$

2.2.2 THICKNESS-DIRECTION ΔT IN HEATING SECTION. Heating of the strip from one side with essentially zero heat leaving the opposite side corresponds to the classical case of a slab heated on one side and perfectly insulated on the other side. From Reference 3, the general equation describing the temperature change from the unheated condition at any point in the slab at any time is:

$$\Delta T_x = \frac{Q\ell}{k}\left\{\frac{\alpha t}{\ell^2} + \frac{3x^2 - \ell^2}{6\ell^2} - \frac{2}{\pi^2}\sum_{n=1}^{\infty}\frac{(-1)^n}{n^2} e^{\frac{-\alpha n^2\pi^2 t}{\ell^2}} \cos\left(\frac{n\pi x}{\ell}\right)\right\} \quad (2\text{-}3)$$

where Q = absorbed heat rate per unit area
ℓ = slab thickness
k = material thermal conductivity
α = material thermal diffusivity = $\frac{k}{\rho C_p}$
ρ = material density
C_p = material specific heat
x = distance into slab from insulated side
t = time

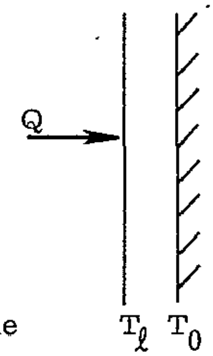

Substituting ℓ and zero for x gives the time-dependent change at the slab faces:

$$\text{At } x = \ell \quad \Delta T_\ell = \frac{Q\ell}{k}\left\{\frac{\alpha t}{\ell^2} + \frac{1}{3} - \frac{2}{\pi^2}\sum_{n=1}^{\infty}\frac{(-1)^n}{n^2} e^{\frac{-\alpha n^2\pi^2 t}{\ell^2}} \cos n\pi\right\} \quad (2\text{-}4)$$

$$\text{At } x = 0 \quad \Delta T_0 = \frac{Q\ell}{k}\left\{\frac{\alpha t}{\ell^2} - \frac{1}{6} - \frac{2}{\pi^2}\sum_{n=1}^{\infty}\frac{(-1)^n}{n^2} e^{\frac{-\alpha n^2\pi^2 t}{\ell^2}}\right\} \quad (2\text{-}5)$$

The transient temperature difference across the slab is the difference between Equation 2-4 and Equation 2-5.

$$\Delta T = \Delta T_{\ell} - T_0 = \frac{Q\ell}{k}\left\{\frac{1}{2} + \frac{2}{\pi^2}\left[\sum_{n=1}^{\infty}\frac{(-1)^n}{n^2}e^{\frac{-\alpha n^2\pi^2 t}{\ell^2}} - \sum_{n=1}^{\infty}\frac{(-1)^n}{n^2}e^{\frac{-\alpha n^2\pi^2 t}{\ell^2}}\cos n\pi\right]\right\} \tag{2-6}$$

Terms within the { } brackets equal zero at time zero and equal 1/2 as the heating reaches the slab (or strip in this case) backside. Solving Equation 2-6 for t = several values between 0 and 1 second (using strip properties described earlier) shows that by 0.5 second, 98.6% of the full ΔT is developed. In other words, for all but the first half-second of heating, the strip thickness-direction ΔT is given by:

$$T = \frac{1}{2}\frac{Q\ell}{k} \tag{2-7}$$

During the first half-second, ΔT is less than that given by Equation 2-7.

Note that, if a small amount of heat were to leave the strip backside by radiation and/or conduction, the 1/2-factor would increase slightly. In this case, the 1/2-factor would be approximated by:

$$\text{1/2-factor} = 1/2 + \left(1/2\,\frac{\text{Qout}}{\text{Qin}}\right)$$

For example, if heat loss from the backside were 5% of the total heat absorbed, the factor would be 0.5025 instead of 0.500. We will, therefore, consider the factor to be 1/2 for all cases.

If all the heat generated by one cap center heater (127 watts) were absorbed by the strip (no losses to the reflector, out the ends of the reflector, or around the edges of the reflector) and no heat were conducted laterally in the strip away from the heat zone, Q, the absorbed heat rate per unit area, would be given by:

$$Q = \frac{127 \text{ watts} \times 3.413 \text{ (Btu/hr)/watt}}{(1.0 \times 27.6/144)\text{ ft}^2} = 2261 \text{ Btu/hr-ft}^2 = 7133 \text{ W/m}^2$$

Thickness-direction ΔT is given by Equation 2-7.

$$\Delta T = 1/2\,\frac{2261 \text{ Btu/hr-ft}^2 \times (0.028/12)\text{ ft}}{0.280 \text{ Btu/hr-ft-F}} = 9.4 \text{ F} = 5.2 \text{ C}$$

For the more realistic case where the strip heating system sustains some losses and the on-off power control results in just enough heat addition to the strip to bring it to the desired forming temperature in 80 seconds, the net heat absorbed from one cap center heater is 75.6 watts, and the thickness-direction ΔT is given by:

$$\Delta T = 9.4 \text{ F} \times \frac{75.6}{127} = 5.6 \text{ F} = 3.1 \text{ C}$$

We can, therefore, conclude that the strip thickness-direction ΔT in the heating section will be between 3 and 6 C (5 and 10 F).

2.3 CROSS-MEMBER TRADES

The cross-member trade study was conducted to both improve the reliability of mechanized handling by the clip feed subsystem and to increase the structural capability of the cross-section for differential drive. A lipped-channel section was selected since it met both objectives. Structural analysis of the original simple channel and several lipped-channel cross-members, with a variety of section depths, widths, corner radii, and/or material thicknesses was conducted and is summarized in Figure 2-5. For each lipped-channel section considered, the section properties, weights, and maximum end-moment capabilities were determined.

The progression of improvements to the cross-member builds on configuration (1), the initial (baseline) design. The first improvement to the cross-member was the addition of lips to the baseline cross-member design (configuration (2)), which greatly increased the differential drive capability and improved the clip feed capability. But this change also increased the section's depth and mass, and it affected the size of the cross-member storage clip and the clearances encountered during the cross-member handling movements. Next, in configuration (3) , the section's depth was reduced approximately to that of the baseline design, while the lips and corner radii of (2) were retained. This change lowered the mass of the section, yet retained most of the substantial increase in structural performance capability over the initial design. However, the problem of the increased section width affecting the cross-member storage canister size and handling movement clearances remained. It was found that the initial section width and depth dimensions had to be retained in order to maintain the design envelope of the cross-member storage canister and its handling motions. This constraint made it necessary to develop tighter corner radii and shorter lips in order to simultaneously retain both the initial weld pattern width and the side flares. Structural analysis of this latest section showed that it had the best combination of weight, structural performance, and mechanical handling capability, and it was selected as the new baseline.

Objectives

- Improve clip feed capability
- Improve differential drive capability

Initial trade candidates (dimensions in mm)

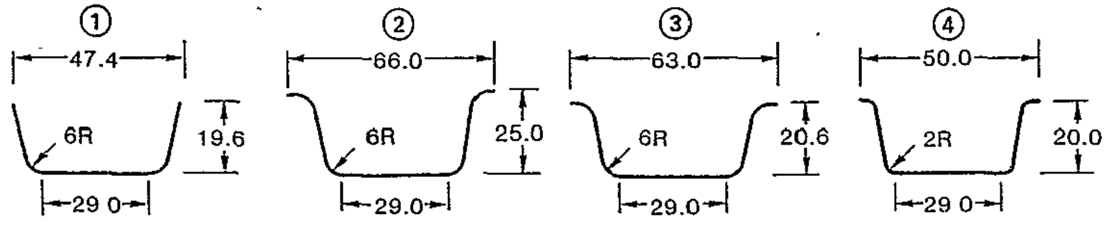

(BASELINE DESIGN)

FEATURE	EVALUATION			
Configuration	①	②	③	④
Material*	A	B	B	B
Mass (Kg/m)	0.075	0.102	0.091	0.081
Beam column M.S.	1.75	2.12	1.82	1.35
M_{max} (N-m)	1.9	54.6	45.3	28.0
Mechanism compat.	Poor	Good	Good	Best
Selected Design				✓

*Material: A: Original laminate, t = 0.584mm, E = 128.7 GN/m^2
B: Single ply, t = 0.635mm, E = 117.9 GN/m^2

Final configuration definition

- Strip material trade
- Final mechanism design
- Weld joint trade

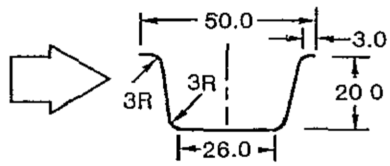

Matl "t"	0.610
Mass	0.079
M.S	1.29
M_{max}	30.0

Figure 2-5. Cross-member trade/selection.

The selected design was used in the concurrent strip material and weld pattern trade studies, each of which suggested further minor modifications to the geometry which would improve the structural performance and fabricability of the overall beam. These changes were adopted when it was found that the same strip material could be used for both the cap and cross-member and that a somewhat smaller flat weld area could be used at the cap-to-cross-member joint. The final design is similar to ④ with two minor exceptions: the flat web area of the lipped channel is shortened from 29 to 26 mm while the corner radii are increased from 2 to 3 mm.

Improved reliability of both the clip feed and clip/handler interface mechanisms resulted due to the addition of lips to the channels. The weight of the cross-member has increased slightly (approximately 5%), but this weight gain is more than offset by a weight reduction in the cap section through the use of thinner strip material. Although the margin of safety decreased slightly for the final selected geometry, it remains adequate. As in the prior analyses (SCAFEDS Part I/II Final Report), stresses were calculated using the final internal ultimate member loads resulting from the final beam limit reaction loads at the assembly jig interface, and were based on elastic buckling of flat orthotropic plates with specific edge conditions.

The governing equation is:

$$F_{cr} = \frac{2\pi}{tb^2}\left[\sqrt{D_{11}D_{22}} + D_{12} + 2D_{66}\right]$$

and the flexural plate rigidity matrix, D, for the selected material is:

$$D\ (N\text{-}m) = \begin{vmatrix} 2.4928 & 0.0313 & 0. \\ 0.0313 & 0.1567 & 0. \\ 0. & 0. & 0.0911 \end{vmatrix}$$

The channel web flat, which is widest and also sees the highest edge load, is the critical element of the cross-member section.

A more important concern, resolved by the cross-member trade study, was the improvement to the differential drive capability of the cross-member. For the final selected cross-member geometry, the differential-drive induced end moment capability was increased from 1.9 N-m for the original simple-channel design to 30.0 N-m for the final design.

2.4 WELD JOINT TRADES

The weld joint pattern trade was initiated to evaluate and increase, if required, the in-plane end moment resistance necessary for differential drive, and to assess the increase in welding power required for larger weld patterns. The baseline weld pattern consists of U_1/L_1 in Figure 2-6. Alternative concepts for the upper (U) cap/cross-member weld(s) and the lower (L) cap/cross-member/cord weld were developed and evaluated in terms of spot quantity, size, spacing, cord capture geometry, pattern width, and moment capability. The illustrated series of spots and bars of varying sizes was evaluated. A critical requirement of the lower weld was to provide complete cord capture in the weld and to eliminate any prying action between the cap and cross-member.

As before, a limit shear stress of $F_s = 10.34\ MN/m^2$ was adopted for design use.

The maximum allowable in-plane moment capacity of the weld joint and the shearing stress in the joint due to a differential drive (2.54 mm) was computed based on all of the geometry options shown in Figure 2-6. The selected weld pattern geometry U_1/L_2, also shown, is quite similar to the initial pattern with a slight area reduction.

The allowable spotweld shear loads, assuming full effectivity, are:

U_1: 334 N

L_2: 2606 N

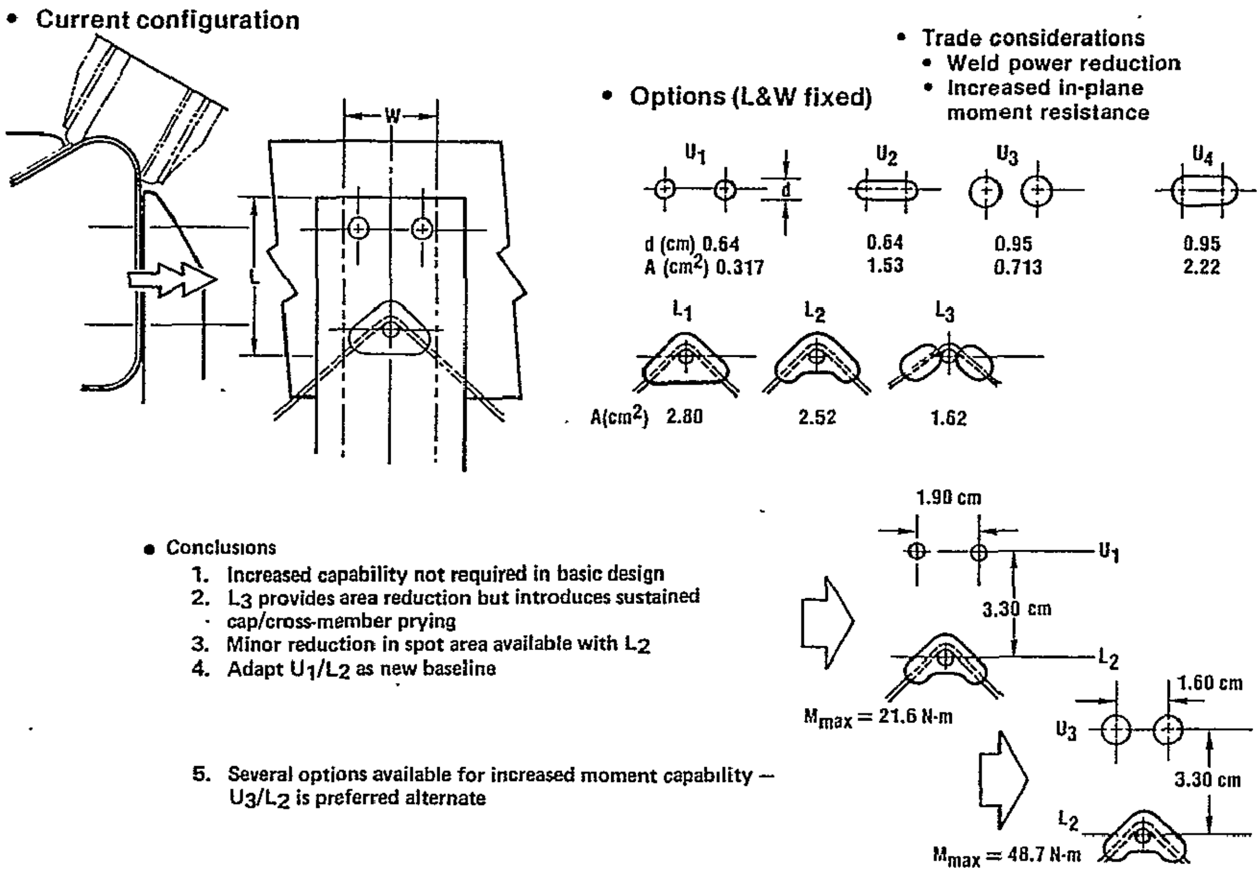

Figure 2-6. Weld joint trade.

The maximum in-plane moment capacity of the weld joint pattern is calculated with the axis of rotation acting about the centroid of the joint and the maximum shear stress being equal to the design allowable at the centroid of an individual spot weld.

The joint geometry and loads associated with a differential drive of 2.54 mm are:

M = 12.2 N-m VX = 277 N

XBAR = 0.665 cm YBAR = 0.00 cm

	Location (cm)			Force (N)				
Weld	X	Y	Area (cm^2)	Allow	VX	VY	V_M	MS
L_2	0.0	0.0	2.520	2606	138	147	371	2.00
U_1	3.30	0.953	0.316	327	69	73	185	1.50

The allowable pure moment capacity (no net in-plane shear) for the joint is:

$M_{allow} = 21.6$ Nm

The allowable differential drive (ΔL) for this weld pattern is:

$$\Delta L = (MS + 1)\ (\Delta L \text{ applied})$$
$$= 2.50\ (2.54) = 6.35 \text{ mm}$$

The weld pattern can be modified to match the capability of the cross-member (30.0 Nm), but it is concluded that the increased joint capability is not required in the basic weld design for a straight beam which remains inside the anticipated differential drive limits of the cap drive mechanism. To increase the degree of curvature beyond that available with this moment limit, several options are available, including the increased-area upper spots, U_3, also shown in Figure 2-6.

2.5 BEAM CHARACTERISTICS

As a result of the selection of a new strip material and a new cross-member section, several beam and beam element characteristics have changed. Although the overall beam dimensions remain unchanged, new values have been computed for both the mass and all mechanical properties except torsional stiffness. Figure 2-7 summarizes the updated characteristics. The torsional stiffness, KG, is unchanged since the previous bay geometry and cord design have been retained.

The detailed structural properties of both the cap and cross-member have also changed, and are summarized in Table 2-8. Two material thicknesses are shown, in fractional form, for both the cap and cross-member. The larger value is the total strip material thickness, whereas the smaller value represents the "effective" thickness for structural analysis, excluding the surface coatings

PHYSICAL

L = 1.434m
H = 1.180m
S = 1.362m
MASS = 0.870 kg/m
(0.584 LB_m/FT)

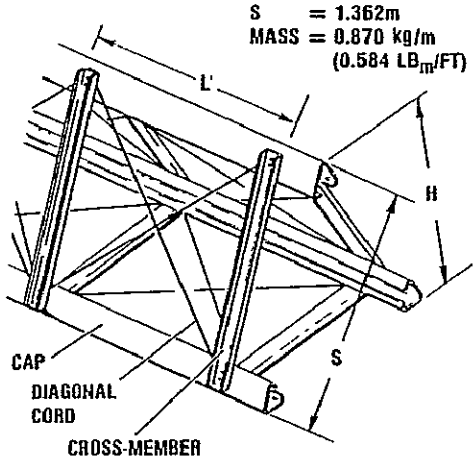

MECHANICAL

AE	-4.586 E7 N	1.031 E7 LB_f
I	1.078 E4 cm^4	2.591 E2 IN^4
EI	1.420 E7 $N \cdot m^2$	4.949 E9 $LB_f \cdot IN^2$
KG	1.111 E4 $N \cdot m^2$	3.871 E6 $LB_f\ IN^2$

Figure 2-7. Updated beam characteristics.

• CAP

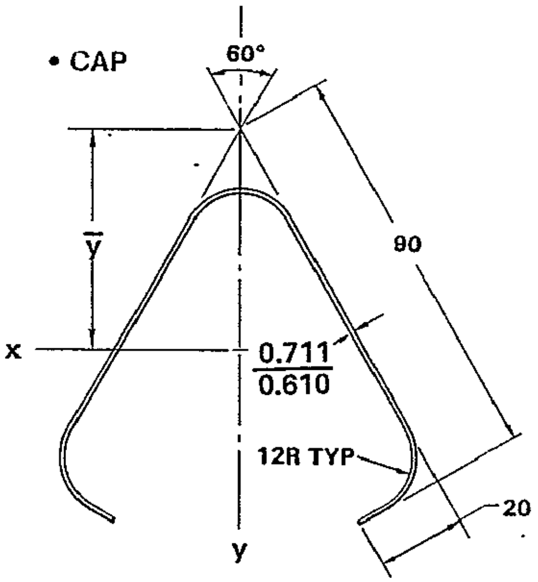

A	1.16 cm^2	0.180 in^2
$\overline{y}$	48.67 mm	1.916 in
I_x	6.43 cm^4	0.155 in^4
I_y	8.97 cm^4	0.215 in^4
ρx	23.52 mm	0.926 in
ρy	27.79 mm	1.094 in

• CROSS-MEMBER

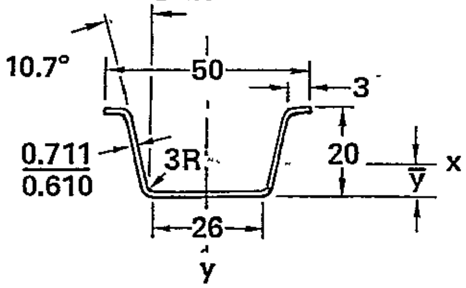

A	0.48 cm^2	0.075 in^2
$\overline{y}$	7.85 mm	0.309 in
I_x	0.26 cm^4	0.006 in^4
I_y	1.25 cm^4	0.030 in^4
ρx	7.32 mm	0.288 in
ρy	16.10 mm	0.634 in

Figure 2-8. Beam element characteristics.

3

BEAM BUILDER DESIGN

Preliminary design and analysis and design trades were conducted on structural, mechanical, and controls details of the SCAFEDS Part II beam builder conceptual design. These analyses and trades defined a beam builder development configuration and identified critical design criteria for compatibility with Space Shuttle payload operational, environmental, and safety requirements. The beam builder development article is described in Section 6. The details of the baseline concept update are presented in this section. The effects of curved beam manufacture and beam builder scale-up are also described.

3.1 BEAM BUILDER CHARACTERISTICS

Updated characteristics of the baseline beam builder are summarized in Figure 3-1. Beam builder physical characteristics include the new length changes described in Subsection 3.3.7 and the updated mass properties given in Table 3-1. The strip material change (Subsection 2.1) is incorporated in the productivity data. The energy and rate data have not changed from those of the baseline previously reported.

Table 3-1. Beam builder mass properties update.

Item	Mass			
	kg		lb_m	
Principal Subsystems		2,474		5,451
Basic structure	829		1,826	
Cap forming machine	565		1,245	
Cross-member positioner & handler	38		83	
Cross-member clip & feed mechanism	359		791	
Cord tensioner mechanism	165		364	
Cord plyer mechanism	154		339	
Beam welding mechanism	26		58	
Beam cutoff mechanism	68		150	
Avionics & controls	270		595	
Stored material		801		1,764
Cap material	588		1,295	
Cross-member material	201		442	
Cord material	12		27	
Flight article subsystems		129		284
Cooling system	7		16	
Thermal shroud	9		20	
Latch/deployment mechanisms	113		248	
Total	3,404		7,499	

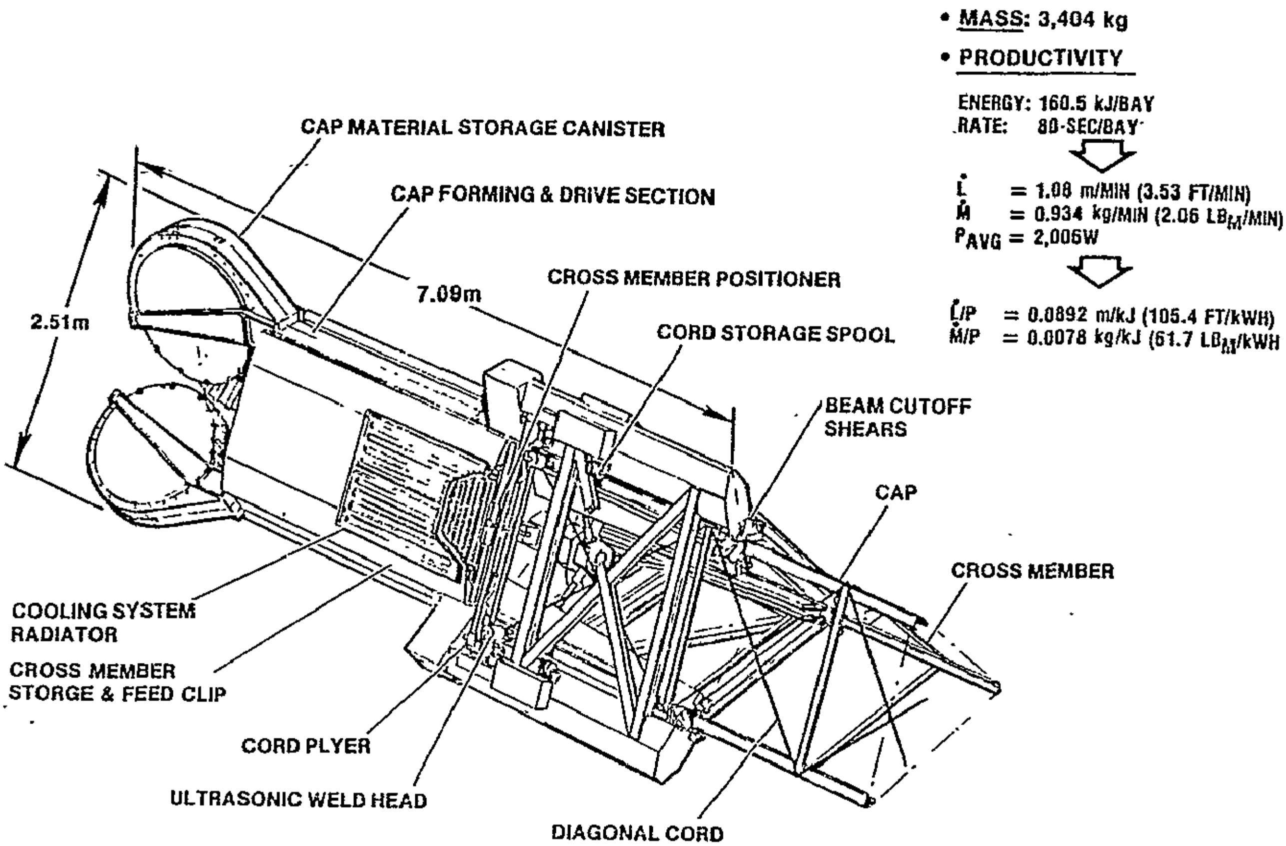

Figure 3-1. Beam builder characteristics update.

The mass properties data reflect the updated materials and subsystem design information. All items include a contingency of 10 to 15%.

3.2 DRIVES AND SENSORS

The baseline beam builder conceptual design identified the need for numerous electromechanical drives and controls sensors. The Part III study included tasks to define and select electromechanical drives and sensors for the beam builder functions. This definition also required identification of special materials, lubricants, and environmental protection techniques. Finally, the subsystem and system design concepts were refined and analyzed to minimize the overall number of drives and sensors and to use common elements for cost-effectiveness where practical. The results of these tasks are presented in this section.

3.2.1 BEAM BUILDER FUNCTIONS ANALYSIS. In developing the preliminary design of the beam builder subsystems, each of the subsystem functions was analyzed for sensor and drive requirements. These analyses included Failure Mode and Effects Analyses (FMEA), Failure Detection Analyses (FDA), and drive duty cycle analyses. The FMEA established the effects produced by a component failure and the criticality of the failure. The FDA defined the sensors required to physically detect the failure or failure symptoms. The criticality, repairability, and detectability factors were then evaluated and used to determine sensor requirements and redundancy requirements using the ground rules of Subsection 3.3.1 as guidelines. An example of the FMEA/FDA is shown in Table 3-2.

As a result of these analyses, the required number of primary and backup sensors, drives, and heaters has been defined for each subsystem module as summarized in Table 3-3.

3.2.2. SENSOR TRADES. The most commonly used sensors and the most critical sensors were analyzed and trades performed on various candidates of each type to select the sensor technologies best suited for beam builder applications. These trades are discussed in the following subsections.

3.2.2.1 Discrete Position Sensor Trades. Discrete position sensors are devices used to generate an electric signal (or interrupt a signal) when activated (or deactivated) by placing a triggering device in a preset position with respect to the sensor. Discrete position sensing can be accomplished by either of two types of devices: (1) electromechanical or (2) solid state. A comparison of both types is shown in Table 3-4.

Electromechanical position sensors most commonly used are limit switches (microswitches or snap-action switches) and magnetically activated reed switches. These devices are used extensively in commercial and GSE and launch facilities process control applications. With the exception of reed switches, electromechanical position sensors are rarely used in spacecraft applications because of major disadvantages as indicated in Table 3-4. For beam builder requirements, solid state position sensing devices are clearly the choice because of their unique advantages.

Solid state position sensors have three operating modes to select from: (1) interrupted mode, (2) proximity mode, and (3) mechanical switch mode. The optional types of devices available for operation in each of these modes are compared in Table 3-5.

The three types of interrupted sensors evaluated are opto-electronic, Hall effect, and sonic. The opto-electronic sensing device provides an accurate, high speed method for measuring equipment position control. Low power, immunity to RFI noise, and ease of transmitting data over long lengths makes this system ideal for position sensing in space. The main disadvantage is the reliability of the light emitting diode (LED). The half life period is now 25,000 hours but, as LEDs are improved, the reliability will increase. This method of position sensing is a future candidate for the beam builder design.

Table 3-2. Beam builder sensor and redundance evaluation.

COMPONENT	FAILURE MODE	FAILURE EFFECTS	CRITICALITY	REPAIRABILITY	DETECTABILITY	RECOMMENDED DEGREE OF REDUNDANCY
CAP FORMING SUBSYSTEM						
HEATER	1. Ni-Chrome wire failure - wire melts or fatigues, or power supply lines fail.	1. Material fails to heat. Heater draws zero power.	1. Mission failure. Inability to produce beams.	1. Medium-High difficulty to replace wires or elements.	1. Temp. sensor detects low temp. condition, or low heater current may be measured.	Use dual nichrome wire elements.
	2. Heater breaks loose from support & moves away from bend zone.	2. Material fails to heat across full bend zone, material not formable, or is damaged by forming rollers.	2. Same as 1.	2. Same as 1.	2. Temp. sensor detects low temp. condition.	Monitor heater currents for condition assessment capability.
	3. High contact resistance in connection reduces heat rate.	3. Material fails to reach forming temperature.	3. Same as 1.	3. High difficulty to trouble shoot and repair poor connection.	3. Temp. sensor detects low temp. condition. Heater current increase may be measured.	
TEMP. SENSOR	Sensor fails with electrical open or low output.	Heater controller turns heater on. Heater is not shut off at proper temperature of material. Material overheats, resin outgases, material damaged.	Mission failure. Inability to produce beams.	Medium difficulty to replace sensor wires.	Downstream sensors can detect overheat (except if last sensor fails).	Use dual temperature sensors. Operate on sensor with highest output.
CAP DISPLACEMENT SENSOR						
OPTION #1 Encoded Magnetic tape strips on cap material with tape reading sensor.	OPTION #1 1. Tape reader head becomes contaminated & fails to read tape.	OPTION #1 Inability to control cap displacement. Cap and beam damage will occur.	OPTION #1 Mission failure. Inability to produce beams.	Medium to high difficulty to repair beam & faulty tape. Low difficulty to replace tape reader.	1. Loss of signal is detectable by processor.	Use automatic equipment to verify condition, position and accuracy of tape as material is rolled up.
	2. Damaged tape generates intermittent signals.				2. Intermittent signals are detectable by processor.	
	3. Tape mislocated. Tape reader not in contact.				3. Loss of signal is detectable by processor.	Use redundant tape strips and tape readers. Processor to switch to control with redundant strip and reader when fault is detected in primary tape or reader.
	4. Tape improperly encoded.				4. Not sure.	

Table 3-3. Sensors, drives, and heaters summary.

Subsystem	Module	Sensor	Prime	B/U	Drive/Heater	Prime	B/U
Forming	Heater/Temp.	IR Sensors	12	12	Heater Coil	12	12
		Current Sensors	12	12			
		Voltage Sensors	12	12			
	Cap Drive	Travel	1	1	Motor	1	1
		Current	1	1			
	Platen Drive	Position	4	4	Motor	1	1
		Current	1	1			
Cutoff	Cap Cutter	Position	2	2	Motor	1	1
		Current	1	1			
Cross-Member	Cross-Member Clip Feed	Position	1	1	Motor	1	1
		Current	1	1			
	Cross-Member Handler/Pos.	Position	2	2	Motor	1	1
		Encoder	2	2	Clutch	3	0
		Current	1	1			
Cord	Cord Plyers/ Tensioners	Force	2	2	Motor	2	2
		Encoder	2	2	Brake	2	0
		Current	2	2			
Joining	Weld Anvil	Position	1	1	Motor	1	1
		Current	1	1			
	Weld Head	Position	3	3	Motor	3	3
		Force	3	3			
		Power	3	3			
		Current	2	2			

B/U = Backup

The Hall effect sensor (vane) configuration described in Figure 3-2 consists of a Hall sensing generator and a permanent magnet mounted in one package. The sensor is operated by passing a ferrous vane through the gap between the magnet and the Hall sensor. The ferrous vane diverts the magnetic flux from the Hall sensor causing the digital output from the sensor to change status. Additional signal conditioning, logic, and output circuitry are required as shown in Figure 3-3 to produce a digital output.

Table 3-4. Position sensor technology trade.

TECHNOLOGY	ADVANTAGES	DISADVANTAGES
Electromechanical	• Cost-effective • Easily mounted	• Creates RFI • Limited switch life • Low operating speed • Contact material migration • Mechanical deterioration • Possible cold weld of contacts in vacuum • Contact bounce, arcing • Vibration sensitive contacts
Solid State Sensors √	• No internal wear-out phenomena • High switch reliability • No contact arcing, RFI • High switching speeds	• Higher cost • Can become misaligned • Limited at high ambient temperatures

√ Sensing technology performance best suited for beam builder.

The "0" and "1" digital states can be programmed by varying the shunt width and space width of the vane, so the same sensor is capable of being used in different applications. The shunting indication characteristics are shown as the ferrous vane is moved through the air gap. For maximum applied gauss, the output is normally high ("1" state). For minimum applied gauss the output is normally low ("0" state). Thus, an electronic equivalent of the snap-action electromechanical switch is achieved.

Sonic type interrupted sensing devices are not feasible for use in space because of the absence of air through which to transmit audio beams. The four types of proximity sensors evaluated were Hall effect, eddy current, capacitance, and variable reluctance. Hall effect proximity sensors are actuated by an external magnetic field that emanates from a traveling permanent magnet. Although several types of motion of the magnet may be used, e.g., slide-by, head-on pendulum, or rotary, the slide-by motion was selected for use in the beam builder design. Figure 3-4 shows the slide-by form of Hall sensor actuation. The induction gauss change at a gap of 0.254 mm is illustrated as the magnet is moved by the Hall sensor. The advantage of the slide-by actuation over the head-on type is increased slope of the induction curve vs. travel distance. Therefore, less actuation travel is required to produce the same gauss change, producing a sharper trip point.

Table 3-5. Comparison of solid state sensors.

ACTUATING MODE	TECHNOLOGY	OPERATION	ADVANTAGES	DISADVANTAGES
Interrupted	*Opto-electronic	Emits a narrow beam of IR light	• High speed-10mHz • Accurate • Good resolution	• Complex • Easily contaminated
	✓Hall-effect (vane)	Ferrous vane shunts magnetic flux	• Medium speed-100KHz • Not rate sensitive • Integral design	• Low resolution
	Sonic	Audio beam interrupted	• Large sensing gap • Detects all material	• Triggered by noise • Higher cost
Proximity	✓Hall-effect	Magnet brought in proximity of Hall generator	• Medium speed-100kHz • Not rate sensitivity • Simplicity	• Low resolution • Magnet required
	Eddy current	Eddy current sensing detects metal	• Operates at high frequency • Not easily contaminated	• Poor resolution • Higher cost
	Capacitance	Material in close proximity exhibits dielectric change	• Detects low dielectric material	• False triggering • Temperature sensitive
	Variable Reluctance	Magnetic materials brought hear magnet	• High speed • Good resolution	• Complex • Higher cost for accuracy
Mechanical Switch	✓Hall effect	Mechanical actuated hall generator	• High reliability • Digital output • Solid state	• Mechanical switch plunger

✓ Sensing technology best suited for the beam builder design
* Promising future candidate

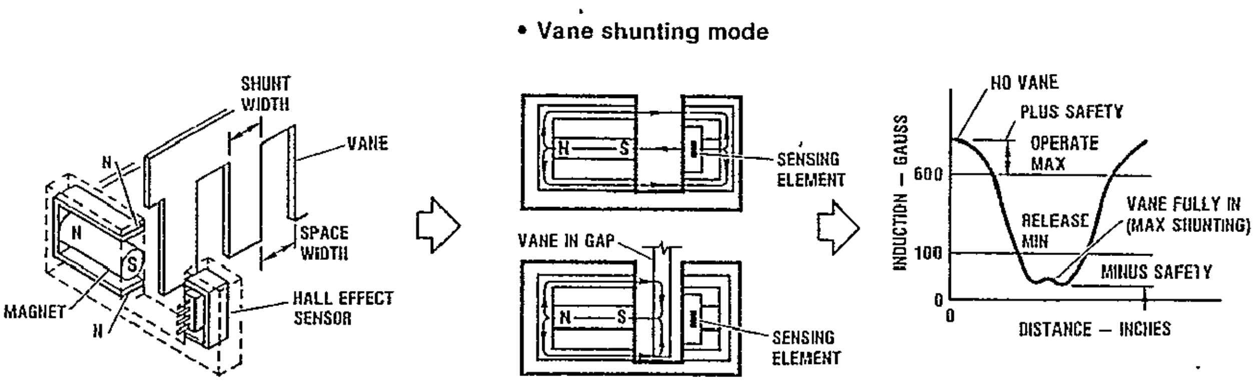

Figure 3-2. Vane type Hall effect sensor.

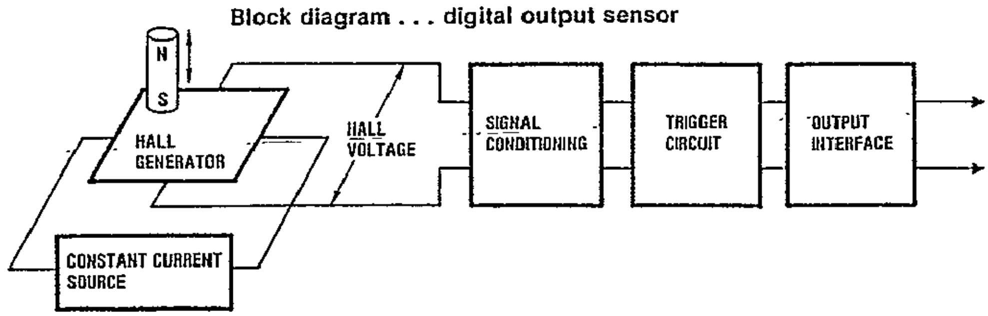

Figure 3-3. Digital output circuit diagram.

The Hall effect sensor was selected as the best proximity type position sensor over the other candidate sensors because it will provide the best performance with the highest degree of reliability.

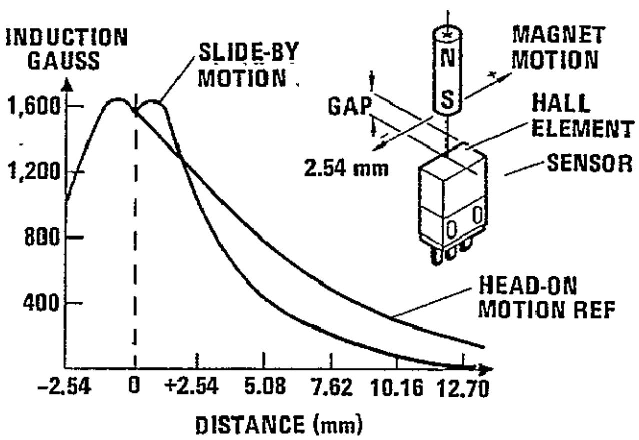

Figure 3-4. Slide-by proximity Hall effect sensor.

The mechanically operated Hall effect switch is a combination of a mechanical operating switch and solid state reliability. The switch consists of a Hall effect element with an integrated circuit actuated by a magnet in the operating plunger as shown in Figure 3-5. The integrated circuit produces a digital output as previously described. Unlike the electromechanical switch, the Hall effect switch has no electrical contact and is, therefore, immune to contact bounce and contact contamination problems. This device will be used where it is difficult or impractical to use either interrupted or proximity devices.

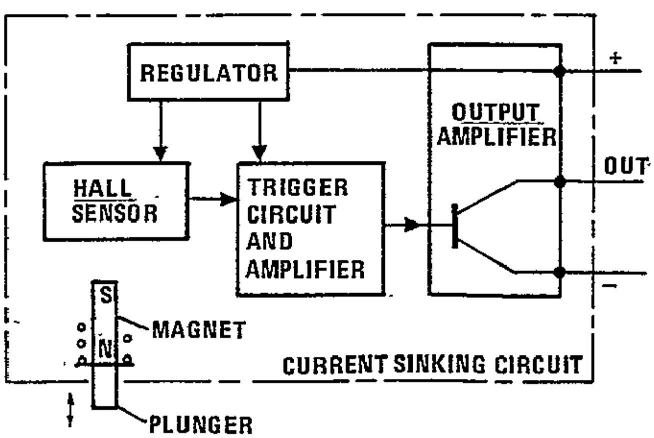

Figure 3-5. Mechanical Hall effect sensor.

3.2.2.2 Rotary Shaft Encoder Trade. Rotary shaft encoders are electromechanical devices which provide a digital code output representing the absolute position of the rotary shaft. Incremental encoder output is a series of pulses which must be counted by external logic to determine absolute position relative to a starting point.

Rotary shaft encoders were determined to be the preferred technique for measuring cord plyer position, cross-member positioner position, and cross-member carriage position. The advantages of rotary shaft encoders over discrete position sensors in these cases are: (1) better accuracy and (2) minimum number of sensors by measuring multiple positions with one sensor. In the case of the cord plyers, there are six discrete positions for each of the six cord plyers which must be monitored. Using four bi-directional shaft encoders (two active, two redundant) in the cord subsystem eliminated a potential requirement for 24 discrete position sensors.

Rotary shaft encoders are of two basic types, contacting and noncontacting. Contact encoders are those which use a mechanical contact, brush or pin, between the coded disk and the output circuitry. The coded disk contains a series of metallic concentric rings with 8 tracks having a coded output of 256 counts per revolution.

Contact encoders are limited by the minimum practical segment and sensor size. Making disks smaller causes the life of the resulting encoder to be severely limited by contact wear and bridging of the disk segments. In addition, contact encoders are limited to relatively low input shaft speeds.

The noncontact type encoder eliminates contaminated and scratched commutator segments, providing high accuracy of resolution. There are three basic types of noncontact encoders: magnetic, capacitive, and optical. Magnetic encoders are limited in speed capability and have accuracies equivalent to contact encoders. Capacitive encoders are not generally available because problems in design, manufacture, and operation have limited their use. This leaves optical encoders as the selected sensor for beam builder applications.

Optical encoders have disks with opaque and transparent segments. The substrate, usually glass, provides excellent dimensional stability. The readout is effected by an array of carefully aligned light emitting diodes (LED), phototransistors aligned in front and behind the rotating disk as shown in Figure 3-6. As the disk rotates, the opaque areas pass between the light source and the sensors modulating the output light beam in accordance with the coded disk. Optical encoders focus the light on the coded disk.

The optical encoder selected for the cord and cross-member subsystem mechanism uses a gallium arsenide light emitting diode (LED), a phototransistor sensor, and an optical quality glass commutator disk with a chromium deposition pattern. The design facilitates use of an encoder that can operate in a high shock and vibration environment, yielding high MTBF rate and the utmost in reliability.

Since the rotary shaft reverses during the beam fabrication cycle, a bidirectional encoder will be necessary. The encoder operates with a standard +5 Vdc power supply and provides fully buffered TTL compatibility. Encoder output pulses will either be decoded or counted in a 2^{16} count and stored for the BCU. The final design approach will be determined after several system concepts have been analyzed. The BCU will sample the output (encoder or counter) every 25 milliseconds to control the movement and direction of the cord plyer mechanism. Characteristics for the optical encoder are compiled in Table 3-6.

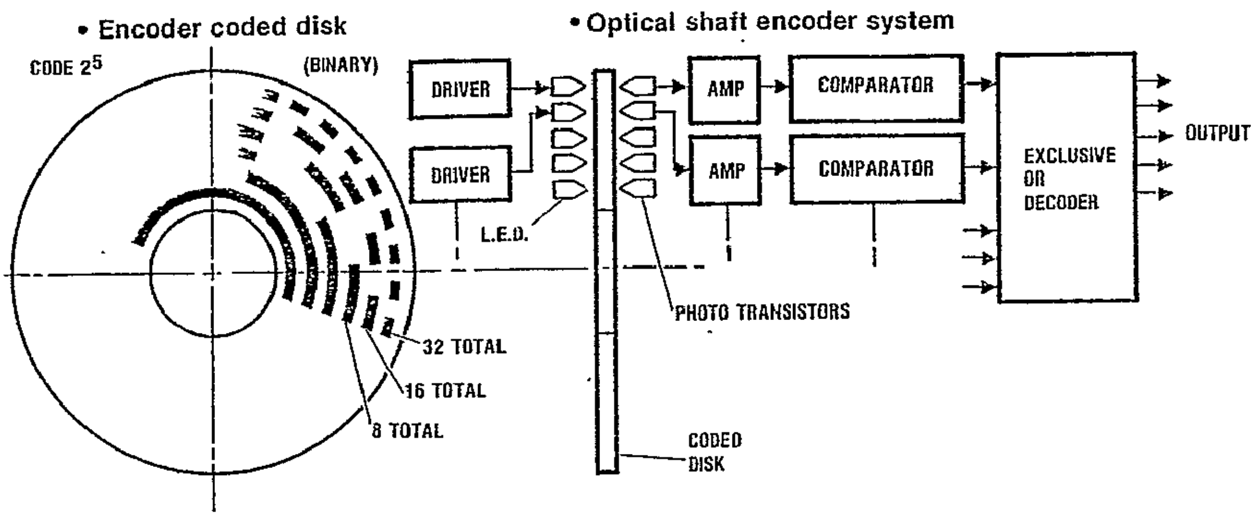

Figure 3-6. Optical rotary shaft encoder.

3.2.2.3 Cap Displacement Sensor Trades. In SCAFEDS Part II, differential cap drive was the recommended approach for beam straightness (or curvature) accuracy and control. The differential cap drive concept uses three individual cap drive and displacement control systems, one for each cap. Details of the drive control system and technique are described in Subsection 3.3.2.4.

The ability to accurately drive each cap in accordance with a prescribed displacement vs. time function, accurately determine the length of each bay produced, and to correct for random errors in bay length all depend upon the accuracy and reliability of the cap displacement sensor. Investigations of two candidate sensors, optical shaft encoders and coded magnetic tapes and reader heads, have shown the need for development of an acceptable sensor configuration for high accuracy and high reliability.

The first sensor candidate is an optical rotary shaft encoder with a friction wheel mounted on the shaft to make contact with the moving cap material. By choosing the correct wheel diameter, the proper resolution per inch can be achieved. Two encoders would be mounted on each cap section to simulate system redundancy. The digital output would be sent to the computer for counting and maintaining the precision movement required between all three cap sections. This system has these potential sources of error:

a. Out of roundness of friction wheel
b. Flat spots on friction wheel
c. Slippage between wheel and material
d. Transmission error between wheel and encoder disk.

Table 3-6. Optical encoder characteristics.

PERFORMANCE CHARACTERISTICS	
Maximum rate of operation	200 cycles/revolution
Minimum rate of operation	0 cycles/revolution
Input voltage	+5 Vdc
Input current	750 mA @ 5 Vdc
Output current	12 mA maximum
Operating speed	500 rpm, maximum
Slewing rate	1000 rpm, maximum
Power dissipation	4.0 watts, maximum @ 5 Vdc
PHYSICAL CHARACTERISTICS	
Starting torque	2.0 oz-in, maximum @ 25 C
Operating temperature	-40 to +125 C
Actuation	Shaft bidirectional rotation
Shaft loading	10 lb, maximum
Vibration	10 g's @ 5 to 500 Hz
Reliability	100,000 hr, minimum
Mounting concept	TBD shaft - frame
Enclosure size	10.16 x 6.35 cm (4 x 2.5 inches)
Light source	GaAs
MISCELLANEOUS CHARACTERISTICS	
Code format	Binary
Interfacing output	TTL
Circuit protection	External
Output circuitry	Counter

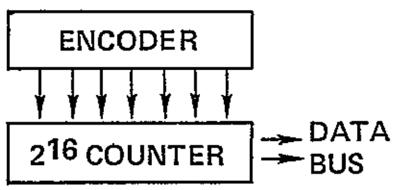

As previously reported, beam straightness requirements could result in manufacturing error limits on the order of 0.1 mm/m (overall average for a 200-m beam).

Test and evaluation of a prototype rotary shaft encoder sensor setup would be required to determine the true range of error in the measurement. The potential for slippage, however, will always exist. This problem precludes this approach for use where a high degree of accuracy in beam geometry is critical.

The second sensor candidate is coded magnetic tape with a reader head shown in Figure 3-7. Mounting a coded magnetic tape on the unheated flats of the cap section will allow a magnetic read head to count the recorded bits. The low output signal must then be amplified and sent to the BCU to control precision travel of the three caps.

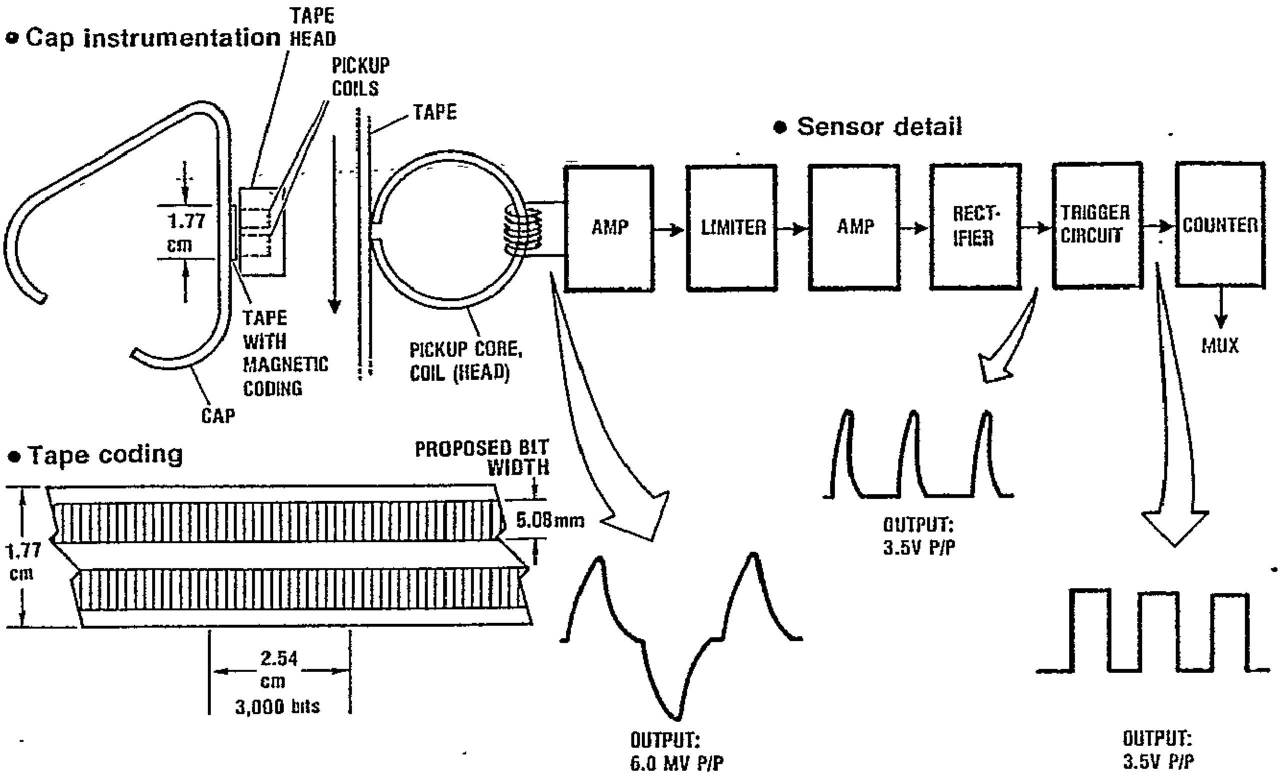

Figure 3-7. Cap displacement sensor concept.

Reading recorded data on magnetic tape at 3.81 cm/sec presents design problems that can be partially eliminated by proper redesign. The slow speed lowers the tape head output voltage to the 0.1 to 0.2 millivolt level. (Normal computer heads outputs are 6.0 to 10.0 millivolts.) The lower signal output level lowers the system S/N ratio and increases the bit error rate for data transmission.

The maximum bit density that can effectively be put on a tape is between 1600 and 3200 bits/2.54 cm (inch). Increasing the bit density causes the output amplitude to decrease and the rise time to approach a sine wave. This slower rise time would create output pulse jitter and loss of the precision timing required between all three cap sections. Rectifying both the positive and negative tape head output pulse doubles the counting rate. This allows greater output timing precision.

The low voltage output necessitates the use of a high gain, low noise preamplifier to achieve the faster rise time. Amplification, limiting, and further amplification are necessary. Rectifying the pulse doubles the bit density and improves the travel error for each cap section. The trigger circuit decreases the pulse output rise time to an acceptable microsecond time to maintain the timing precision required.

The computer tape bit has a nominal width of 0.58 mm but, with a tape speed of 317.5 cm/sec, can produce an output voltage from 6.0 to 10.0 millivolts. The slower tape speed of the beam builder (3.81 cm/second) drastically lowers the output voltage.

To overcome this problem the bit width will be increased to 5.08 mm. This produces a tape output voltage gain of 8.76. On a 1.27-cm wide tape, two tracks will be placed (one redundant) for total system redundancy. Another tape will be placed on the opposite flat side for further redundancy should one tape break during system operations.

The beam builder tape head will incorporate only a read head to simplify the design. The read head must be a high input impedance device for maximum signal pickup. The write head will be a separate design, used to program the data bits on the tape after it has been mounted on the cap material. The magnetic tape read head will be a special design, the width being controlled by stacking together 0.76 mm thick metal laminations for the 5.08 mm core width. The increase the induced flux on the tape, NRZ recording will be utilized in the write head. Maximum bit density will be 3000 to 4000 bits/2.54 cm; exceeding this limit causes the output voltage to approach a sine wave and possible output jitter.

3.2.2.4 Temperature Sensor Trades. Sensing the cap material temperature to ensure proper temperature for composite material forming can be accomplished by the use of either contacting or noncontacting temperature sensors.

Contacting sensors such as thermocouples, thermistors, or other thermostatic devices in contact with the composite material cause scratching and scuffing of the material which removes the external coating and displaces material fibers. Because of these problems, the contacting sensor is not suited for the beam builder application.

Noncontacting sensors are basically all infrared detectors. Infrared detectors are devices which generate an electrical output in response to energy absorbed from a source of infrared radiation. In the beam builder strip material heating process, the material is passed over radiant heaters along the bend zones. The temperature sensors are placed on the opposite side of the material from the heaters. As discussed in Subsection 2.1.3, the predicted temperature differential across the material is between 2.8 and 5.6 C. The infrared radiation emitted from the material surface has an intensity, frequency, and wavelength that vary as a function of the temperature, area, and emmissivity of the source material.

There are two basic groups of infrared detectors: (1) thermal detectors and (2) photon detectors. Thermal detectors absorb energy from the source. This causes the detector's chip temperature to rise causing the electrical output voltage to change. The basic characteristic of thermal detectors is that they absorb energy over a wide spectral band and are uniformly sensitive to all wavelengths.

Photon detectors are semiconductors that utilize energy contained in photons arriving from the source to raise electrons within the material of the detector from nonconducting to conducting states. The basic characteristics of the photon detector are that they have fast response time, require cryogenic cooling for longer wavelengths, and have high but non-uniform sensitivity.

Several types of sensors selected from each group as candidate temperature sensors for the beam builder are compared in Table 3-7.

The pyroelectric detector consists of ferroelectric crystal on which electrodes have been deposited. The high impedance of the crystal requires an ultra-high input impedance amplifier. The device is fragile, which restricts using the device in the present design.

Thermistor bolometers are heat-sensitive resistors that change resistance when radiation strikes the cobalt-nickel flakes. The assembly is rugged and resistant to vibration, shock, and other extreme environmental conditions.

The bolometer is operated in a bridge circuit with two units oppositely biased. One device is exposed to radiation and the compensating device is shielded. When the exposed device receives radiation, its resistance changes and the output voltage is changed proportional to the incident radiation.

Table 3-7. Noncontacting temperature sensor comparison.

ACTUATING MODE	TECHNOLOGY	ADVANTAGES	DISADVANTAGES
Thermal	Pyroelectric	• Good S/N ratio • No bias current	• Fragile • High impedance amplifier required • Hard to use
	Thermistor bolometer	• Small • Rugged • No bias	• Requires bridge circuit • Low output • Low detectivity
	✓ Thermopile	• Rugged • High output • No bias • D.C. stability • Flat response	• Slow response, but adequate
Photon	Photoconductive	• Fast response	• Low temperature cooling • Bias current
	Photovoltaic	• High sensitivity • Rugged with metal jackets	• Requires liquid nitrogen • Sharp cutoff near 6 micrometers

✓ Sensing technology perfomance best suited for beam builder design

Low detectivity and the need for bridge circuitry make this approach unfeasible for the beam builder design. To improve detectivity, optical gain is required. The optics, however, are not desirable for shock and vibration environments.

Thermopile sensors consist of many junctions (in series) of dissimilar metals deposited onto a substrate. One junction is in good thermal contact with the heat sink by conductor, the other junction is isolated by a thin insulating film.

The two dissimilar metals, like bismuth and antimony, will produce a voltage output that is proportional to the junction temperature. Thin-film techniques have miniaturized thermopile devices, but their response time remains relatively slow.

This detector was selected for the beam builder because it offers excellent electrical and environmental characteristics for temperature sensing including:

a. Compact size
b. Rugged construction
c. Accepts broad spectral response
d. No low temperature cooling required
e. No bias required

The use of photon detectors was found to be unacceptable. Photo-conductive sensors require external bias and low temperature cooling to achieve sensitivity to longer wavelengths. Therefore, this detector is not suited for space systems application. Photovoltaic detectors consist of a junction of P-type and N-type semiconductor material. The sensitivity of this device operates within a range of 6 to 7 micrometers which is below the IR spectral output of the cap material. This device also requires low temperature cooling making it unsuitable for this system application.

3.2.2.5 Current Sensor Trades. Current sensing can be classified into seven different approaches. Although seven methods are listed, four are eliminated from the beam builder because of size, weight, and circuitry. The seven are listed below:

Type		Comment
(1)	Shunt (resistor)	Excellent
(2)	Current transformer	Cannot measure dc; excessive weight
(3)	Clamp-on transformer	Not suited; cannot measure dc
(4)	Ferromagnetic saturation	Not suited; cannot measure dc
(5)	Clamp-on tong	Low accuracy; sensitive to wire position
(6)	Hall effect generator	Excellent
(7)	Meter	Good

A comparison of the three remaining candidates is shown in Table 3-8. Shunt resistor current sensing is an old technology that has been successfully used in many space programs. The simplicity of the transducer, using a single resistor, to sample low dc current levels yields high system reliability. Since the output signal level is normally low, an amplifier is required to amplify the signal to a level acceptable for the A/D converter. A disadvantage is that power will be lost in the resistor proportional to the sensor current. The resistor must be derated sufficiently to prevent burnout during a temporary overload. This method of sensing is an excellent approach for the beam builder.

Table 3-8. Current sensor comparisons.

TYPE	OPERATION	ADVANTAGE	DISADVANTAGE
✓ Resistor	Voltage sensed across precision resistor	• Small size • Accurate • Cheap	• Power loss • Burn out
✓ Hall effect generator with flux concentrator	• Coil wound around core • Hall generator mounted in air gap	• Accurate • No power loss • Medium speed • Can't burn out	• External excitation • Needs magnetic core • Larger than resistor
Meter	• Measures voltage across resistor	• Direct meter reading	• Meter must be in the Shuttle • Large size • Hard to mount

✓ Sensing technology performance best suited for beam builder design

Hall effect sensing is the newest method of measuring current. The Hall effect sensor consists of a magnetic core, a Hall generator, and a coil winding, as shown in Figure 3-8. The configuration shown is the most sensitive system, designed to measure lower level currents (0.5-10 A). The core is wound with a coil and the core concentrates the magnetic flux density to the Hall generator positioned in the core gap. To prevent core saturation, the gap flux density must never exceed one-half the core saturation levels. The Hall output voltage is proportional to the current, a low output requires an amplifier to raise the voltage level compatible with an A/D converter.

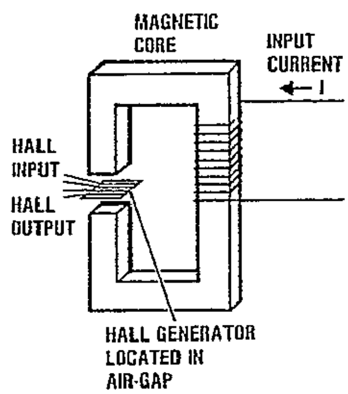

Figure 3-8. Hall effect generator diagram.

Meters are widely used in ground-based and spacecraft equipment that is accessible to operating personnel. This approach is unacceptable for automatic feedback control applications.

3.2.2.6 <u>Force Sensor Trades.</u> Force sensors are required in two of the beam builder subsystems. In the cord subsystem, force transducers will measure cord tension in each of the six cord tensioner mechanisms. In the joining subsystem, the force applied to each weld head must be measured to ensure proper pressure on the weld joints during the welding operations.

Force sensors can be classified into three major types. These types are compared in Table 3-9.

Table 3-9. Force transducer comparisons.

TYPE	OPERATION	COMPONENTS	ADVANTAGES	DISADVANTAGES
PIEZOELECTRIC	HARD IMPACT ON CRYSTAL	• CRYSTAL	• NO STANDBY POWER • LOW COST	• NEEDS IMPACT • PULSE OUTPUT
PIEZO RESISTANCE	PRESSURE OR TWIST	• INTEGRATED CIRCUIT	• NO MECHANICAL LINKAGE	• COMPLEX • EXPENSIVE FOR GOOD ACCURACY
LOAD CELL ✓	STRAIN GAGE BRIDGE CIRCUIT	• WIRE • IC	• ACCURATE • REPEATABILITY	• EXCITATION • SLOW RESPONSE

✓ SENSING TECHNOLOGY PERFORMANCE BEST SUITED FOR BEAM BUILDER DESIGN

a. Piezoelectric. This type requires an impact input to develop a pulse voltage output. Not suited for small pressure changes.

b. Piezo-resistance. This type is extremely sensitive, the limitations are complexity and cost. Not suited because of complexity.

c. Load Cells. This type has excellent accuracy, is easy to use, and is in a small package. Best suited for cord tension measurement and welder force measurement.

3.2.3 MOTOR TRADES. The direct current (dc) motor is an ideal motor for applications where high efficiency is required. The dc motor has a higher ratio of torque output to motor weight than ac motors. The outstanding characteristic of a dc motor is its adaptability to control of its torque and speed. For this reason, dc motors are used in applications requiring a wide range of motor speeds or precise control of motor output.

Figure 3-9 shows three alternative types of dc motor construction evaluated for the beam builder application. These types include: (1) shunt wound induction; (2) permanent magnet (PM); and (3) brushless.

The main advantages of permanent magnet motors over shunt wound induction motors include: (1) linear speed-torque characteristics; (2) higher stall or starting torque; and (3) magnetic output.

Recent advances in magnet technology (smarium cobalt) and semiconductor technology have led to increased emphasis in the development of brushless dc motors. The brushless motor exhibits several advantages over the conventional permanent magnet motors.

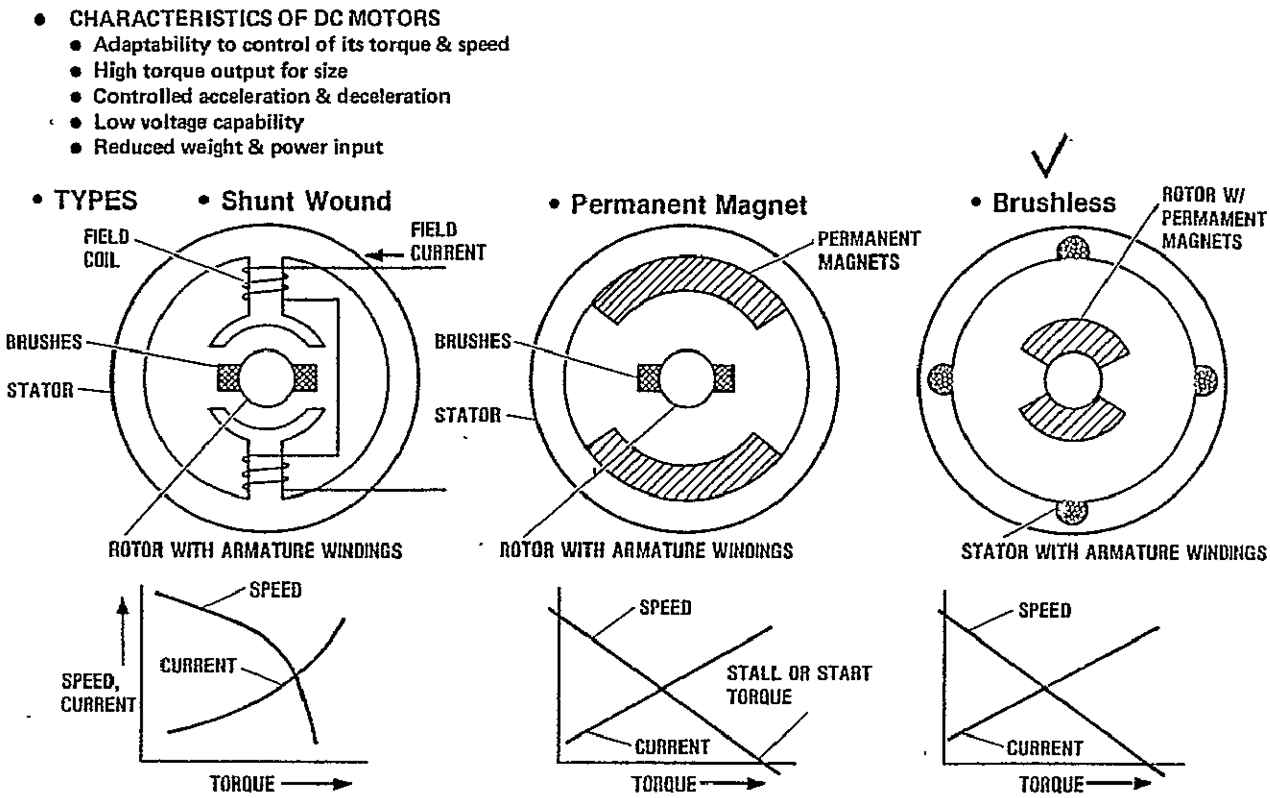

Figure 3-9. Alternative drive motors evaluated.

A brushless motor may be operated at higher speeds at full torque resulting in greater power output for its size. High speed operation is difficult in conventional brush type motors since high energy that must be switched by brushes is destructive and results in shorter life. The brushless motor is capable of more rapid response and generally has higher efficiency. Omitting the brushes results in elimination of EMI, brush particles, explosion hazards caused by arcing, and less or no required maintenance. The "inside-out" design, i.e., permanent magnet rotor and armature windings placed in slots in the frame, allows for better heat dissipation to prevent temperature rise and prolong bearing life, thereby resulting in greater life expectancy. The life of the brushless motor is limited only by wear of the main shaft bearings and the reliability of the electronic controller.

The increased performance characteristics, reliability, greater versatility, and proven usage in aerospace applications have led to selection of the brushless motor as the baseline motor.

3.2.4 BRUSHLESS DC MOTOR OPERATION. A brushless motor system consists of four basic subassemblies: (1) wound stator, including phased windings; (2) permanent magnet rotor; (3) rotor position sensors; and (4) a solid state switching assembly.

The wound stator consists of windings embedded in slots in the housing. The number of slots is dependent upon many factors such as motor size and desired operating characteristics. The rotor consists of field magnets. Significant output power may be achieved through the use of rare-earth magnetic material, which has ten times the magnetic strength of Alnico. Rotor position sensors generate a set of signals describing actual rotor position. The two types of sensors commonly used for rotor position sensors are LEDs and Hall elements. These signals are used to properly energize the commutation circuitry. The solid state switching assembly consists of the circuitry needed to connect and disconnect each motor coil to and from the dc power supply at the appropriate time and with the correct polarity.

A brushless dc motor duplicates the performance characteristics of a PM motor only if it is properly commutated. Proper commutation involves excitation of the stator windings in a sequence that keeps the magnetic field produced by the stator approximately 90 electrical degrees ahead of the rotor field.

Figure 3-10 shows a typical example of electronic commutation of a three-phase Delta motor. Three position sensors are placed 60 degrees apart and are energized by a wheel having a magnet which is 180° wide. The sensor outputs are processed by exclusive-or gates. The control input line allows for rotation to be reversed. A logic "1" on the control input will invert the sense of the sensor output, which in turn will reverse the polarity of each motor terminal thus, making it produce torque in the opposite direction. The motor speed or torque can be controlled by controlling the input to the power switches or by pulse-width modulating the input to the exclusive-or gates. Pulse-width modulated control input waveforms are shown in Figure 3-11.

Since motor inductance causes high voltage spikes to appear across the power transistors as they are switched off, protective zener diodes or transient suppressors will be used in the power driver stages. Higher efficiency or lower ripple torque may be achieved by increasing the number of phases at the cost of increased motor and circuit complexity.

3.2.5 DRIVE MOTOR COMMONALITY EVALUATION. The use of a single drive motor to meet all driving requirements in the beam builder has a significant cost advantage in procurement, test, and logistics. In order to evaluate the feasibility of using a common drive motor, an initial baseline motor was selected which appeared to have adequate power to accomplish all of the drive functions within acceptable time limits. The size and characteristics of the baseline motor are shown in Figure 3-11.

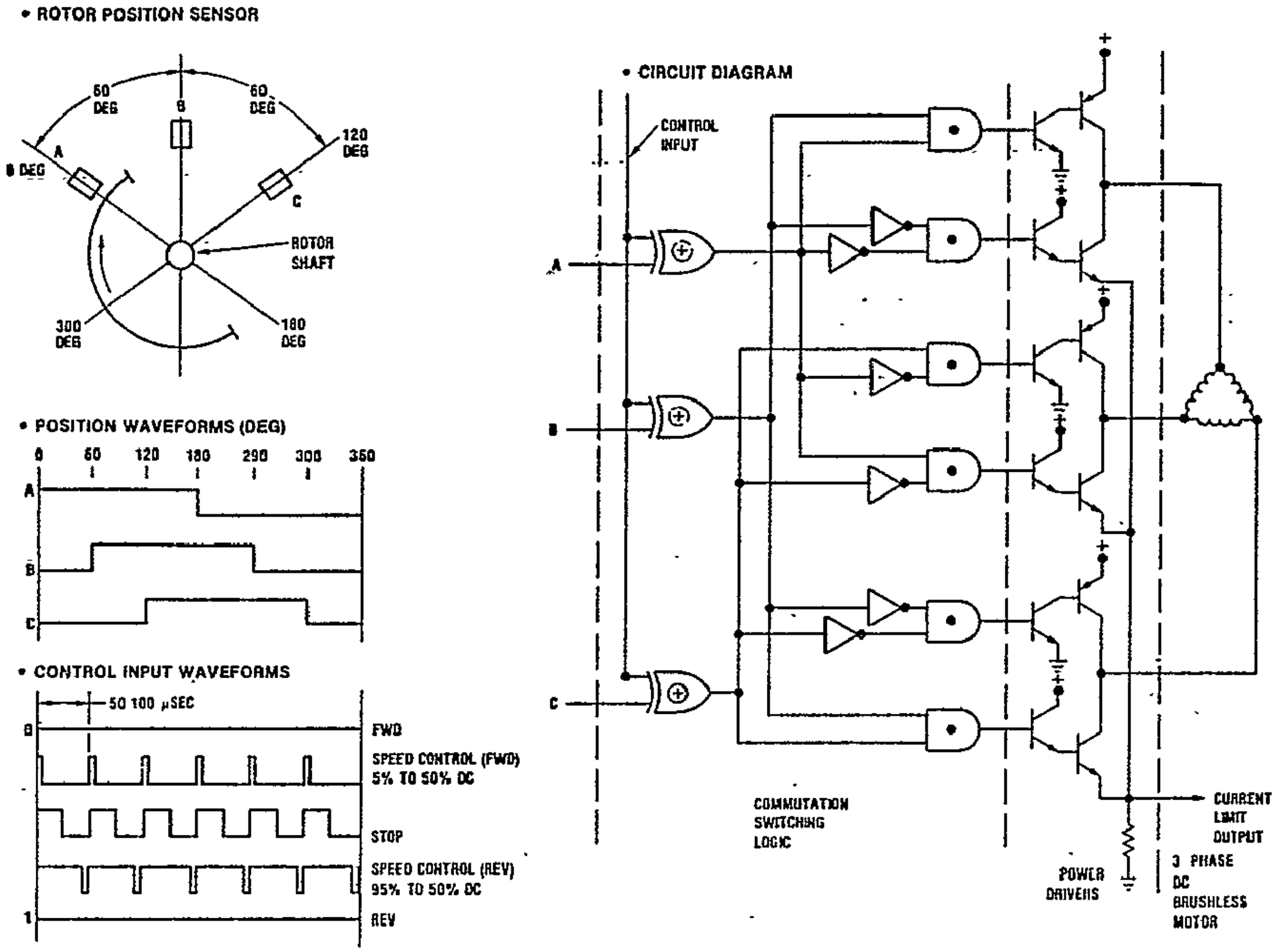

Figure 3-10. Electronic commutation and motor speed control.

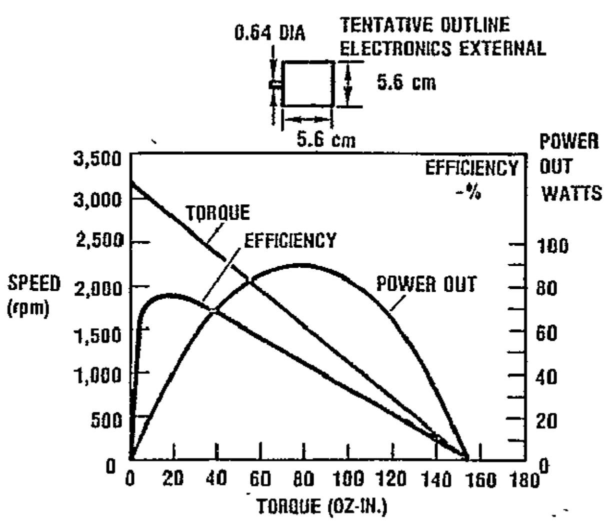

Figure 3-11. Baseline motor characteristics.

Evaluation of a universal drive motor required calculation of load duty cycles for each drive application. Operating time allocations were determined by developing an operational sequence timeline. As a result of this analysis, the speed ratios for each drive and peak torque loads on the motor were determined and are summarized in Table 3-10.

The one drive application which is probably marginal is the weld head positioner. To reduce torque, a greater speed ratio is required. This causes the duration of weld head engagement to be reduced to an undesirable time (10 to 12 seconds). Until such time that welder force requirements and drive mechanism configuration are firmly established, a final recommendation cannot be made.

The detail design of all of the drivers will require a more detailed analysis before the optimum common drive motor selection is made, however, it appears feasible to use one motor configuration to meet all beam builder drive requirements.

3.2.6 UNIVERSAL DRIVE UNIT. A decision to provide a backup to each drive motor was made to ensure high reliability and fail-safe operation. The goal was to develop a design concept of a dual motor driver which would fit all of the drive applications. With the exception of the cooling platen drive, this goal was achieved.

The universal drive unit concept, shown in Figure 3-12, may be operated with either or both motors but will normally be operated with one motor only. Each motor inputs to one side of a differential. Since the output of the differential is the average of the two inputs, the differential provides a 2:1 speed reduction when only one motor is operating.

The bidirectional torque feedback preventing clutches (no-backs) prevent a loss of output which will occur if the operating motor torque input to the differential causes the passive motor to rotate. The no-backs also prevent the motors from being back driven by torque loads applied to the output shaft. A range of speed reductions within the same housing configuration permits the units to be in applications as shown in Table 3-11.

Table 3-10. Summary of motor speed/torque analysis.

Subsystem Drives	Speed Ratio	Peak Motor Torque (Oz-in.)
Forming		
• Cooling platen	10	37 normal 59 back-up
• Cap	124	18
Crossmember		
• Clip feed	347	18
• Handler	353	18
• Positioner rotate	1,236	40
• Positioner translate	8.4	30
Cord		
• Aft cord plyer	15	40
• Forward cord plyer	15	40
Joining		
• Weld anvil	7.1	40
• Weld head positioner	108.4	80
Cutoff		
• Cap cutter	4.2	5

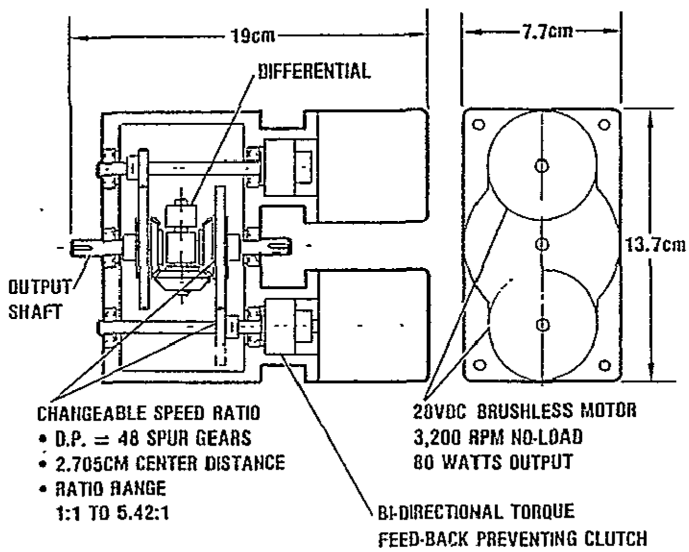

Figure 3-12. Universal drive unit concept.

Table 3-11. Universal drive unit summary.

APPLICABLE SUBSYSTEM DRIVES	NO. REQD	UDU* SPEED REDUCTION
FORMING		
• CAP DRIVE	3	3.31:1
CROSS MEMBER		
• CLIP FEED DRIVE	1	10.84:1
• HANDLER/POSITIONER DRIVE	1	7.06:1
CORD		
• AFT CORD PLYER	1	18.32:1
• FWD CORD PLYER	1	18.32:1
JOINING		
• WELD ANVIL DRIVE	1	7.08:1
• WELD HEAD POSITIONER DRIVE	3	10.84:1
CUTOFF		
• CUTTER DRIVE	3	4.16:1
TOTAL	14	

*ONLY ONE MOTOR IS OPERATED AT A TIME

As a result of the preliminary design effort, the total number of drives required to energize subsystem mechanisms has been reduced from a total number of 62 motors and solenoids to 34 motors, as summarized in Table 3-12. This updated count includes redundant motors. No solenoids will be used in the updated system. Principal benefits of drive reduction are:

a. Fewer actuators results in cost savings

b. The lower drive motor count reduces the total system power consumption.

c. Elimination of solenoids reduces EMI.

d. System reliability is improved.

Table 3-12. Drive motor/solenoid summary.

SUBSYSTEM DRIVES	INITIAL COUNT	UPDATED COUNT
Forming		
• Cap drive	6	6
• Cooling platens	18	6
Cross-Member		
• Clip feed	12	2
• Handler	6	2
• Positioner	2	
Cord		
• Aft	2	2
• Forward	2	2
Joining		
• Weld anvil	2	2
• Weld head	6	6
Cutoff		
• Cap cutter	6	6
Totals	62	34

Note: Counts include redundant motors

3.3 PRELIMINARY SUBSYSTEMS DESIGN

The preliminary design of the beam builder development article or Ground Test Beam Builder (GTBB), as it will be referred to, is the same as the Flight Test Beam Builder (FTBB) with few exceptions. This allows the major portion of the GTBB design to be used for the FTBB in constructing a flight qualifiable beam builder.

The preliminary design drawings and data presented in this section not only represent the GTBB configuration, within the guidelines presented in the ground rules section, but also represent the updated configuration of the Part II final configuration of the SCAFE beam builder.

3.3.1 GROUND RULES. The following ground rules were established for the preliminary design:

1. The integrated beam builder system shall include modular subsystems for forming, joining, cross-member, cord, cutoff, controls and structure.

2. The system shall automatically fabricate the beam configuration established herein.

3. For the GTBB, storage capacity shall be sufficient to prove the functional capability of the cap material storage and feed concept and the cross-member clip feed mechanism. Modular storage clips and canisters shall be used to allow storage capacity to be varied conveniently.

4. All materials and components for the GTBB shall be selected for compatibility with space environment or for their suitability for spacecraft applications. Substitutions for space compatible materials and components may be made where future retrofit is feasible and use of the preferred material or component impacts budget or schedule.

5. The degree of redundancy in subsystems design required to achieve the optimum safety and reliability for the flight article may be reduced for the GTBB where implementation of the redundant system element would significantly affect program budget or schedule.

6. Redundant system elements shall be provided as follows:

   a. Wherever the failure of a system element affects orbiter or flight crew safety.

   b. Wherever the failure of a system element will result in damage to the beam or beam builder equipment.

   c. Wherever the manual repair of a failed system element in space is either not feasible or would require too much time.

7. Condition monitoring and fault detection (CMFD) provisions shall be incorporated. The control subsystem shall diagnose a failure and initiate corrective action before damage occurs and shall either stop the beam builder in a safe mode or automatically switch over to a redundant element.

3.3.2 FORMING SUBSYSTEM. The forming subsystem consists of the three cap forming machines used to process the preconsolidated graphite-glass-polysulfone strip material into the formed cap members and deploy the cap members to the assembly processes and beyond. The cap forming machine design concept from Part II has been updated to reflect the latest roll forming process features, the cooling platen actuation mechanism design update, and the drive unit design update. The controls and sensors configurations have been defined in more detail, and thermal analysis of the heaters was accomplished to further define heater design requirements.

3.3.2.1 Cap Forming Machine Description. The cap forming machine assembly shown in Figure 3-13 is functionally unchanged from the initial concept. It contains all elements necessary to continuously process flat strip glass/graphite/thermoplastic material into the baseline cap configuration. Approximately a 918 m length of material is coiled in a roll which is retained in the storage canister. The roll turns freely on bearing-mounted rollers and unwinds uniformly as material is used. The canister is halved with one half hinged to permit the material roll to be inserted. When the canister is closed and latched, an access panel in the hinged half is opened to allow the material to be manually routed over the heating section guide rollers into the forming section.

The heating section is partially built into the storage canister with resistance strip heaters and parabolic reflectors mounted on the access panel. The heating section extends from the access panel up to the point where the material starts to form.

The material passes from the heating section through the forming section. The rolltrusion forming section is also equipped with strip heaters, which heat the material in preparation for start-up of the machine. The material then passes from the forming section into the cooling section where it is contacted and cooled by aluminum platens during the 40-second pause period. Cooling fluid is supplied to the inside cooling platens and expelled as waste heat either by the Orbiter cooling system or by an independent cooling system in the beam builder.

The drive section provides the necessary pull force on the cap to draw the material from the storage roll through the heat/form/cool sections. As a result of changes to the roll forming section, the length of the machine grew 30.5 cm. An additional 15.2 cm was added to accommodate changes to the drive section.

The cap member subsystem control equipment diagram is shown in Figure 3-14. The numbers in parentheses ( ) indicate the quantity of each type of sensor/actuator used in the subsystem.

A common multiplex bus is shared by each subsystem. A central multiplex unit will be interfaced to the BCU, and four remote multiplex units (RMU) will interface to each of the four subsystems. Each RMU will have a receive and transmit channel. Control signals from the BCU will be sent to the subsystem via the receive channel and signal monitoring will be provided via the transmit channel. Analog signals will be processed via a data acquisition module and digital data signals will be available via a digital interface.

The control equipment diagram is the same for each of the three cap forming machines. Each of these machines contains identical equipment to control the processes of heating, forming, cooling, and cap drive. The design and analysis tasks performed on each of these processes are described in the following sections.

3.3.2.2 <u>Heating Section.</u>

3.3.2.2.1 <u>Heater Thermal Analysis.</u>

a. <u>Summary</u>. A study was performed to define and analyze a small-diameter heating element which will provide the beam builder with the required radiant heating levels in both vacuum operation and ground test conditions. A heater element of nickel-chrome wire double-spiral wrapped around a helically grooved ceramic core was analyzed and sized to meet heating requirements determined from earlier analyses. A 21-gage wire size was found to provide enough excess heat at 28 Vdc to make up vacuum operation losses totalling

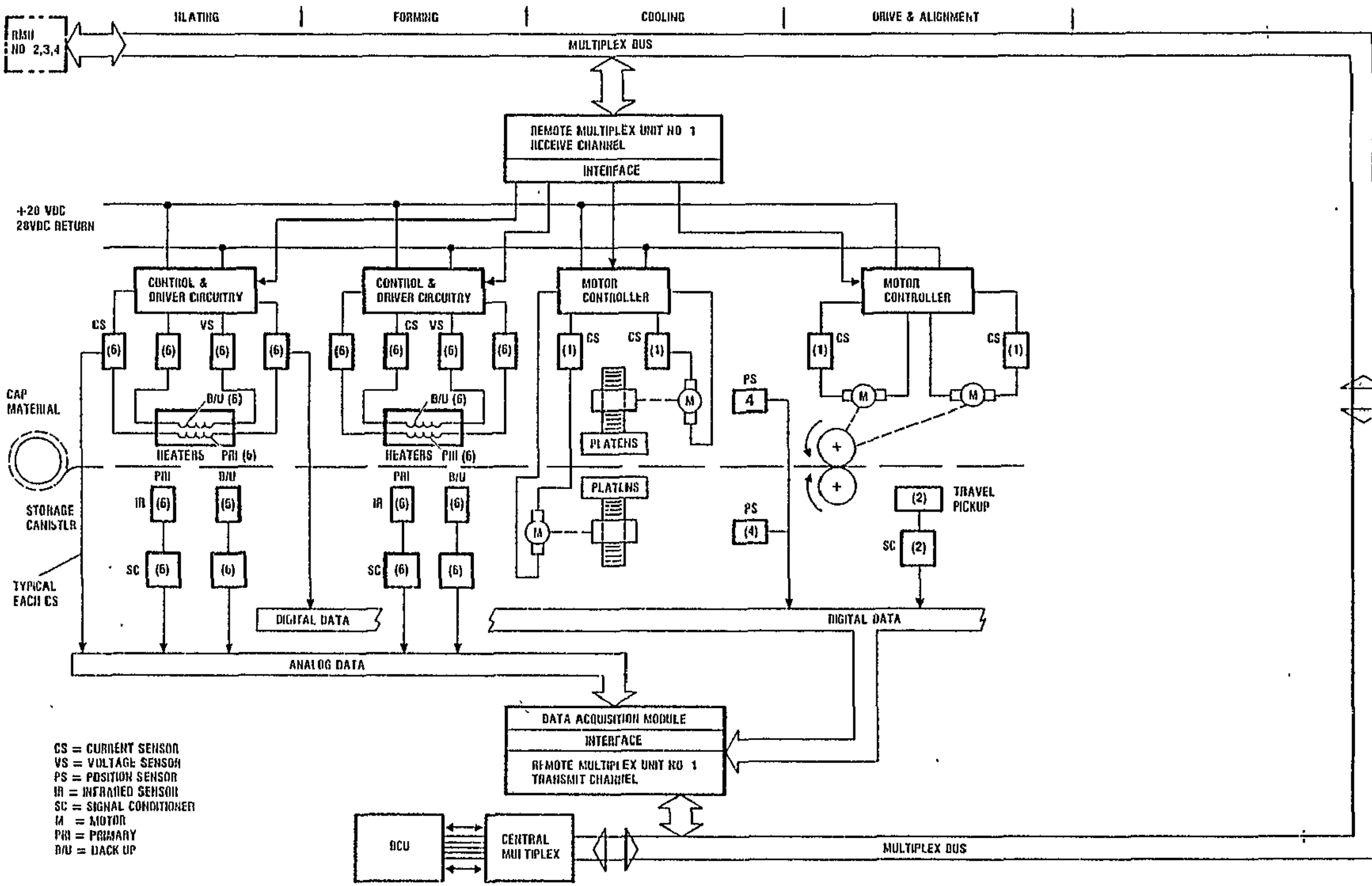

Figure 3-14. Forming subsystem control equipment diagram.

48% of the required heating (a 6% loss is currently estimated). Reduction in thickness of the thermoplastic material to less than 0.076 cm (0.030 in.), will reduce the heater power requirement in proportion to the thickness, and even more performance margin will have been designed into the system.

A parametric analysis was performed to determine heater surface average temperature as a function of heater diameter, emittance, and power level. Predicted heater element temperatures were around 538 C (1000 F). A detailed computer analysis was performed on a small symmetrical section of heater element to determine temperature differences between hot wire, core surface, and passive redundant wire. For a worst case assumption of no contact between wire and core, the wire temperature was only 624 C (1156 F) compared to the Ni-Cr wire melting temperature of 1400 C (2552 F).

A feasibility analysis was conducted to determine if use of the redundant wire would be sufficient to make up convective heat losses during ground testing. The redundant wire was found to provide an extra 254 watts to make up a maximum predicted 101 watts of convective heat loss. Thus, the double wire design has sufficient margin for air operation.

Thermal design of the reflector could follow either of two opposite approaches; cooling to reduce its temperature or insulating to conserve energy. For a given amount of backside insulation, reflector temperature will depend on the actual reflectance achieved by the coated surface. Testing is required to determine effective reflectance and maximum use temperature. The final selected design approach (whether to cool or insulate the reflector) will depend on test results.

b. Heater Requirements. Heaters used in the heating section of the cap forming machine are required to heat the strip material bend areas to the forming temperature 491 K (425 F) in 80 seconds. Thermal analysis of Reference 1 showed the required heater power to be 172 watts for the center bend, assuming a 6% heat loss to the reflector. Heater power required for each of the two outer bends is 125 watts. The center heater is therefore the more severe case and will be used as the design case. Heater power capability greater than 172 watts must be designed into the system to accommodate any heat losses beyond the very preliminary estimate of a 6% reflector loss. Note that the analysis of Reference 1 was based on a material thickness of 0.076 cm (0.030 in.), and thinner material is now being considered. If the final selected material is less than 0.076 cm (0.030 in.) thick the heater power requirement will be decreased proportionally, and the heater system will have a greater performance margin.

The heater element must be small diameter to approximate the point focus of the parabolic reflector, to be responsive to controller power setting changes, and to prevent excessive temperatures on the element backside caused by heat reflection back from the center of the parabolic reflector. Redundancy in the heater element design is desirable.

c. Heater Configuration, Sizing and Materials. A heater element of nickel-chrome wire double-spiral wrapped around a helically grooved ceramic core was analyzed and sized to meet the above requirements. Total active heater length in the heating section is approximately 140 cm (55.1 in.). Heater wire wrapped as shown in Figure 3-15 has 551 wraps and a running length of 462 cm (182 in.). Since the heating section will be composed of two separately controlled elements, the analysis from this point on will deal with only one of these heaters (power = 86 watts, length = 70 cm, etc.).

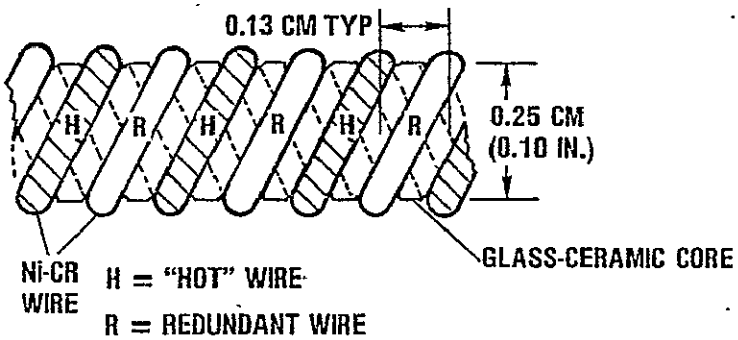

Figure 3-15. Heater configuration.

The most stable nickel-chrome alloy used for resistance heating is that of 80%-20% composition. The melting point of this material is 1400 C (2552 F), which makes it suitable for high temperature applications such as this one. It is available in wire sizes from 40 gage (0.0079 cm dia) to 14 gage (0.163 cm dia).

Table 3-13 summarizes the electrical resistance, required effective voltage, and heating power available at 28 Vdc for heaters using four different Ni-Cr wire gages. Resistivity of 80-20 Ni-Cr is 110×10^{-6} ohm-cm. Heater resistance is computed by

$$R = \frac{\text{Resistivity} \times \text{Running Length}}{\text{Wire Cross-Section Area}}$$

Required effective voltage is given by

$$E = \sqrt{\text{Power} \times \text{Resistance}}$$

The three power level columns of Table 3-13 represent heater power required to accommodate heat losses of 6%, 10%, and 20%. Since the Shuttle provides a nominal 28 Vdc, the 23-gage wire, which requires voltages greater than 28, will not work. As wire size increases, less effective voltage is needed to generate a given amount of heat. For the full 28 volts, the 21-gage wire can provide enough excess heat to make up losses totalling 48%. The recommended wire size is, therefore, 21-gage.

Corning Glass Works manufactures a machinable glass-ceramic, identified as MACOR, which is suitable for the heater core material. Machining (with standard metalworking tools) tolerances of ±0.0013 cm are routinely achieved with this material. It does not outgas in a vacuum environment. Thermal conductivity is 0.004 cal/sec-cm-°C (1.0 Btu/hr-ft-°F). MACOR is available in rod form, which would be used in this application.

Table 3-13. Heater performance as a function of wire size.

Gage	Wire Dia., cm	Wire Area, cm^2	Resis. for each of two Heaters, Ω	Required Effective Voltage* 6% Loss P = 86W	10% Loss P = 89.2W	20% Loss P = 97.4W	Power for Full 28 Volts
23	0.0574	2.59E-3	9.81	29.1	29.6	30.9	80W – Not Sufficient
22	0.0643	3.25E-3	7.82	25.9	26.4	27.6	100W (23% Loss)
21**	0.0724	4.12E-3	6.17	23.0	23.5	24.5	127W (57% Loss†)
20	0.0813	5.19E-3	4.90	20.5	20.9	21.9	160W (98% Loss)

* Method of reducing effective voltage will be determined by heater control approach. On-off pulsing is one possibility.

** Selected wire size.

† Enough power to heat strip plus make up an additional 57% heat loss.

d. Analysis of Uniform Temperature Heater Element. Thermal analysis was conducted on a one-foot long section of heater element assumed to have a uniform surface temperature. Heater element temperature was calculated from the following equation

$$Q_{h-s} = F_{h-s} A_h F_\epsilon \sigma (T_h^4 - T_s^4)$$

where

Q_{h-s} = heat rate absorbed by the strip = 119.9 Btu/hr-ft = 35.14 watts/ft

F_{h-s} = geometric view factor from heater to strip = 0.94 (assumes all energy striking the reflector is reflected onto the strip except 6% which is absorbed by the reflector)

A_h = heater element surface area = $\pi D/12$, ft^2

F_ϵ = emittance factor = $\dfrac{1}{\dfrac{1}{\epsilon_h} + \dfrac{A_h}{A_s}\left[\dfrac{1}{\epsilon_s} - 1\right]}$

A_s = thermoplastic material heated strip area = $(1.0/12) \times 1.0 = 0.083\ ft^2$

ϵ_h = heater element emittance, dimensionless

ϵ_s = thermoplastic material emittance = 0.88

σ = Stefan-Boltzmann constant = 0.1714×10^{-8} Btu/hr-ft^2-°R^4

T_h = heater element temperatures, °R

T_s = heater material temperature = 425 F = 885 R

Heater diameters of 0.25, 0.32, and 0.38 cm (0.10, 0.125 and 0.15 inch) were analyzed. Heater emittance was varied from 0.2 to 1.0. Two power levels corresponding to a 6% loss (86 watts per heater) and a 20% loss (97.4 watts per heater) were analyzed. Uniform heater element temperatures are shown in Figure 3-16 as a function of heater emittance, diameter, and power level.

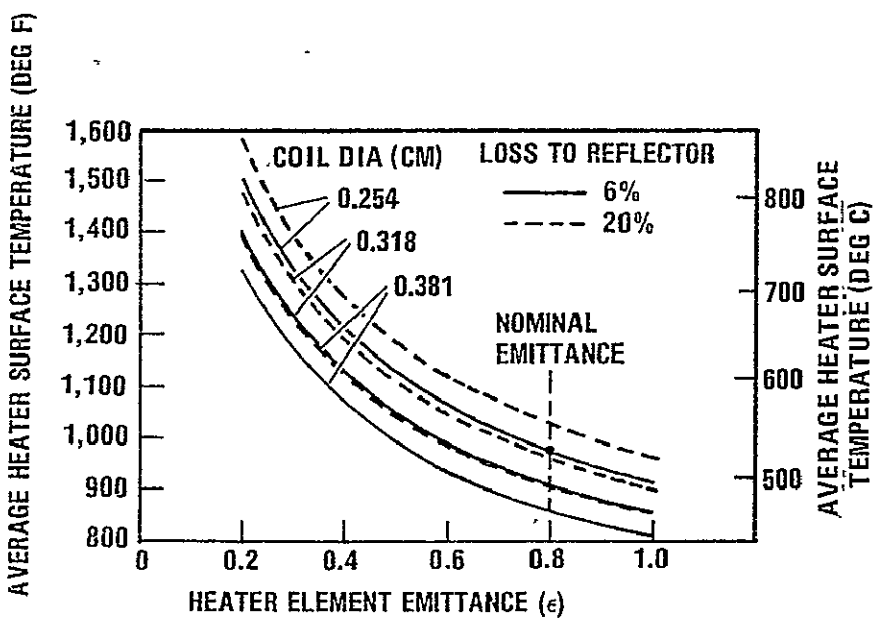

Figure 3-16. Heater surface temperature variation as a function of emittance, coil diameter, and reflector loss.

An effective emittance of 0.8 is estimated for the wire/core heating element surface. Bright Ni-Cr wire has an emittance of 0.73 at 593 C (1100 F) and oxidized Ni-Cr wire has an emittance of 0.96 at 593 C (1100 F) (Reference 4). An oxidized wire surface is clearly the choice here, but it is not known how stable the oxidized surface would be after repeated heating cycles in vacuum. Emittance of MACOR glass-ceramic was not available. Glass has an emittance greater than 0.9.

From the curves of Figure 3-16, a 0.25 cm (0.10 in.) diameter heating element with an emittance of 0.8 will have average surface temperatures of 527 C (980 F) and 554 C (1030 F) for the two power levels shown.

e. Detailed Analysis of Heater Section. A small symmetrical section of heater was modeled in detail (Figures 3-15 and 3-17) for analysis using the Convair Thermal Analyzer computer program. The analysis was conducted to determine temperature differences between the hot wire, core surface, and passive redundant wire. As the Ni-Cr wire heats up, it will lengthen and tend to loosen away from the core. The looser the wire, the greater the temperature difference between hot wire and core. Two cases of wire/core contact were considered. In the first, the wire was assumed to contact the core groove over 10% of the wire circumference (a contact conductance coefficient of 56.7 W/m^2-K was assumed). In the second case, an even more severe condition was simulated where the wire has expanded away from the core resulting in no contact. In this case, heat is transferred from the wire to the core only by radiation. Predicted temperatures are shown below.

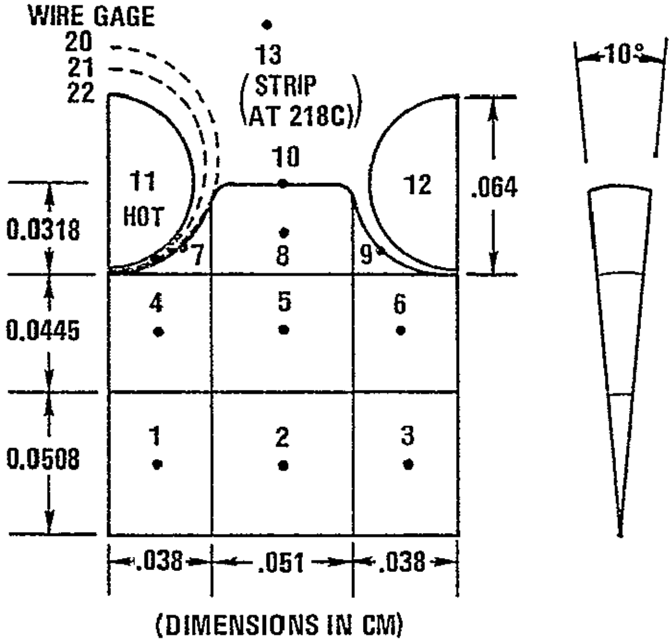

Figure 3-17. Detailed thermal model for temperature gradients.

	Case 1, Contact Over 10% of Wire Circumference	Case 2, No Contact
Hot Wire	564 C (1048 F)	624 C (1156 F)
Core Surface	498 C (929 F)	469 C (876 F)
Redundant Wire	473 C (884 F)	408 C (766 F)

Note that even for the worst case assumption of no contact between wire and core, the wire temperature is not excessive and remains within 100 C of the perfect case of uniform heater temperature (527 C).

f. Heater Operation in Air Environment. Precise thermal analysis of heater operation in an air environment is not possible at this time without detailed definition of the total beam builder machine. However, a feasibility analysis was conducted to determine if use of the redundant heater wire is sufficient to make up worst case convective heat losses. A very conservative assumption was made that 21 C (70 F) air surrounds the heater element and both sides of the 2.54 cm wide heated section of strip material. Strip temperature was taken to be 173 C (343 F), which is the one-baylength heating section average after 80 seconds of heating. A still air convection heat transfer coefficient of 5.7 W/m^2-°K (1.0 Btu/hr-ft^2-°F) was assumed. The following heat losses were calculated for the cap center heater over the full baylength heating section:

Heater Convective Loss

$$Q = 1.0 \text{ Btu/hr-ft}^2\text{-°F} \times 0.132 \text{ ft}^2 \times (1070 - 70)\text{F}$$

$$= 132 \text{ Btu/hr} = 39 \text{ watts}$$

Heater Strip Convective Loss

$$Q = 2 \times 1.0 \text{ Btu/hr-ft}^2\text{-°F} \times 0.382 \text{ ft}^2 \times (343 - 70)\text{F}$$

$$= 208 \text{ Btu/hr} = 62 \text{ watts}$$

The total convective heat loss is, therefore, 101 watts. Since one of the 21-gage wire wraps can provide 2 × 127 watts (Table 3-13) = 254 watts at 28 Vdc, using the redundant wire could provide an extra 254 watts to make up 101 watts of convective heat loss. Thus, the heater has sufficient margin for test operations in an air environment.

g. Reflector Cooling. Two opposite reflector thermal design approaches are under consideration: (1) to cool the reflector with a coolant loop or conductive path to a heat sink or, (2) to insulate it to conserve energy. Conventional tungsten filament infrared heaters require cooling if the heater is on more than three minutes to prevent reflector damage. Thermal design of the reflector of this study will depend entirely on the actual reflectance achieved by the surface and the damage threshold temperature of the reflective coating layer. A perfect reflector would not absorb any of the heat generated in the heating element, and so would come to the temperature of the backside surroundings. The reflective surface will not be perfect and will therefore absorb some small percent of the generated heat. The lower the reflectance, the greater is the heat absorbed and the higher is the reflector surface temperature for a given amount of backside insulation. Testing is required to determine the effective reflectance of the coated surface and its maximum use temperature. The final selected design approach (i.e., whether to cool or to insulate the reflector) will depend on testing results.

3.3.2.2.2 Strip Material Heating Analysis.

a. Summary. Strip temperatures at two planned sensor locations (at the midpoint and end of the heating section) were calculated as a function of cycle time. Parametric transient temperature curves were generated as a function of heat absorbed by the strip (given as a percent of the total heat generated in the heating element).

A strip temperature overshoot condition was simulated in which power to the heating element is turned off and the heat stored in the element is radiated to the strip. Strip heated zone thermal capacity is approximately three times that of the heater element, so the strip temperature increases 1K for each 3K drop in element temperature. The heating element was found to drop from 922K (1200F) to 700K (800F) in 17 seconds, while the strip temperature increases from 492K (425F) to 569K (565F) in the same time. Strip temperature overshoot is a potential problem unless the heater power profile accounts for continued heating from heat stored in the element.

b. Strip Temperature at Sensor Locations. Planned locations for strip temperature sensors in the heating section are at the downstream ends of the two heaters. This locates the sensors at the midpoint of the heating section and at the end of the heating section, just before the start of the forming section.

Detailed multi-node strip analysis performed under the initial SCAFEDS contract resulted in the strip temperature vs. time curves shown in Figure 3-18. The strip material has changed, but the longitudinal temperature distributions shown in Figure 3-18 are still very close to those of the current material. No thickness ΔT was considered for the earlier analysis, so strip temperatures are actually strip thickness-average temperatures. Since the analysis of Subsection 2.2 showed the thickness ΔT's to be only 2.8 C to 5.6 C, they will also be neglected in this discussion. Note that the distance along the abscissa of Figure 3-18 is the

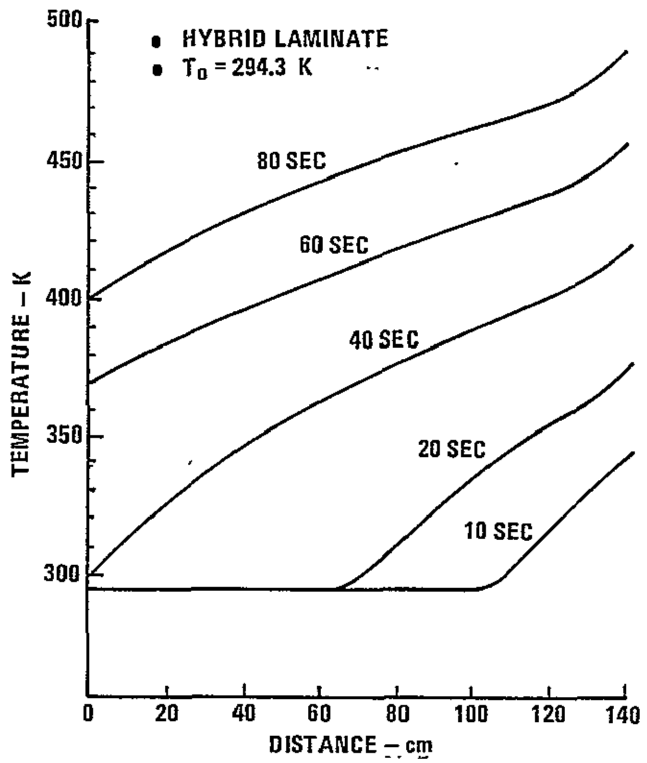

Figure 3-18. Longitudinal temperature distribution in strip heated zone.

distance along one baylength of material which is moving during the first 40 seconds and pausing during the second 40 seconds.

Strip temperatures at two stationary locations on the heaters (the sensor locations) are shown as the solid lines in Figure 3-19. These data are taken directly from Figure 3-18. The slight bend to the curves as the temperature rises during the pause period is caused by the material increase in specific heat with temperature. At a higher temperature, a given amount of heat addition results in a lower temperature rise rate.

Since the heaters are designed with sufficient performance margin to make up unknown heating section losses, full power with no losses during the pause period would result in achievement of the desired temperature in less than 40 seconds. This is shown by the long dashed curves (— — — —) of Figure 3-19. Just enough heat addition to the strip to bring its temperature to the total heat rate available (75.6 watts required vs. 127 watts available). Two other intermediate curves corresponding to 87% and 71% of the total power available are also shown in Figure 3-19.

Figure 3-19 shows that the strip production rate could probably be increased, if desired, using the current heater design. The achievable shortening of the 80-second cycle depends on system heat losses. The time reduction achieved during the pause period would also be achieved during the moving period.

c. Sensor Temperature Sampling Rate and Strip Temperature Overshoot. Currently planned temperature sampling rate is one sample per second at each sensor. The curves of Figure 3-19 show a maximum temperature rise rate of 1.1 C to 2.2 C per second. Since the strip will be changing temperature several hundred degrees C as it heats up, a maximum temperature change of 2.2 C between samples is not excessive. One temperature sample per second at each sensor, therefore, appears adequate.

Strip temperature overshoot is defined as a continued strip temperature rise above a desired level after the heater is switched off. Strip temperature overshoot could occur as a result of radiation to the strip of heat stored in the heating element and in the reflector. It is assumed that other surfaces facing the strip within the heating section would be at temperatures lower than the strip.

Heating element temperature will be in the 538 C to 649 C range during heating. Figure 3-20 shows a strip warm-up with heater element cooldown. Strip heated zone thermal capacity is approximately three times that of the heater element, so the strip temperature increases one degree for each three degree drop in element temperature. Heat given up by the nichrome wires and ceramic core as the element cools from 649 C (1200 F) to 429 C (800°F) in 17 seconds is enough to raise the strip heated zone from 218 C (425 F) to 286 C (565 F). Note that

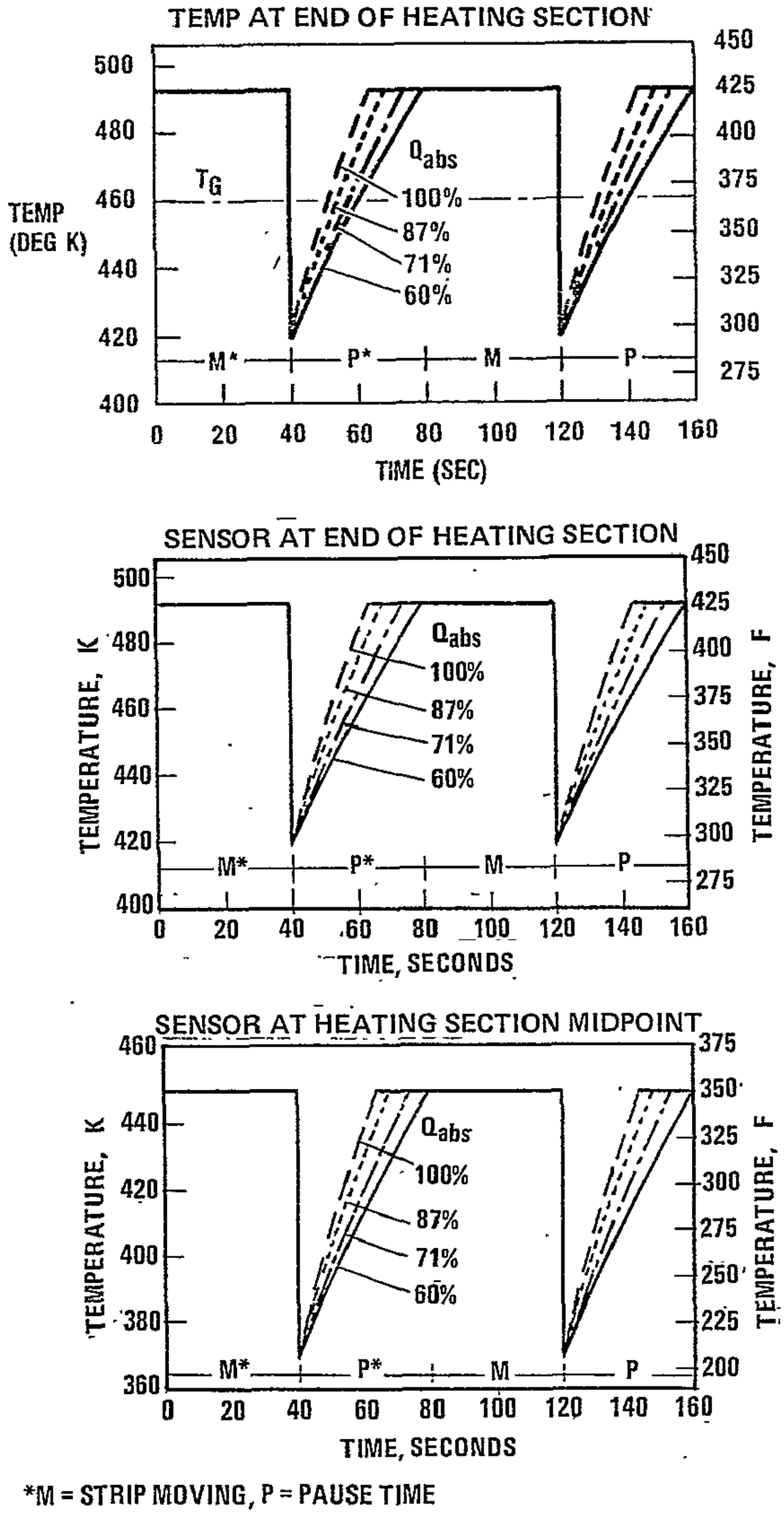

Figure 3-19. Strip temperature at sensor locations, cap center heater.

this analysis does not account for heat radiated from the reflector. Strip temperature overshoot is a potential problem unless the heater power profile accounts for continued heating from heat stored in the element.

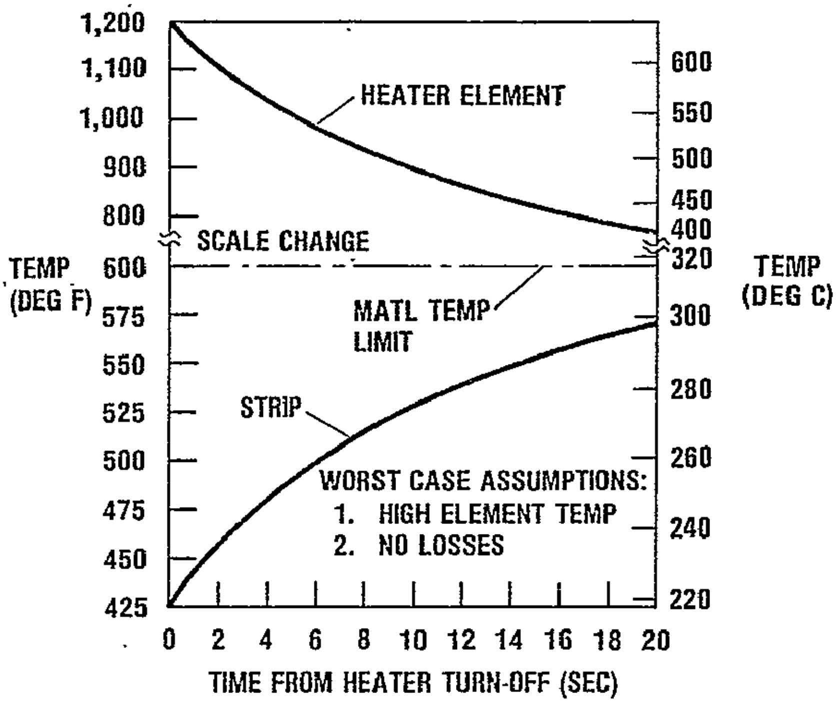

Figure 3-20. Heating element and strip temperatures after heater power turn-off.

Two options may be considered for control of the heater power profile. The first option shown in Figure 3-21 is to turn heater power off at a lower temperature and allow the material temperature to rise to the desired level using the overshoot phenomenon. This technique would complicate the control system since the controller would require both a transient and steady-state control mode. The steady-state mode would be required to maintain material temperature during standby operations.

A more practical solution would be to use pulse-width modulation of heater power as the temperature of the material approaches the control point as shown in Figure 3-21.

3.3.2.2.3 Temperature Sensor Configuration. As a result of the temperature sensor trades discussed in Subsection 3.2.2.4, a thermopile type of sensor was selected. An example of a suitable thermopile configuration is shown in Figure 3-22.

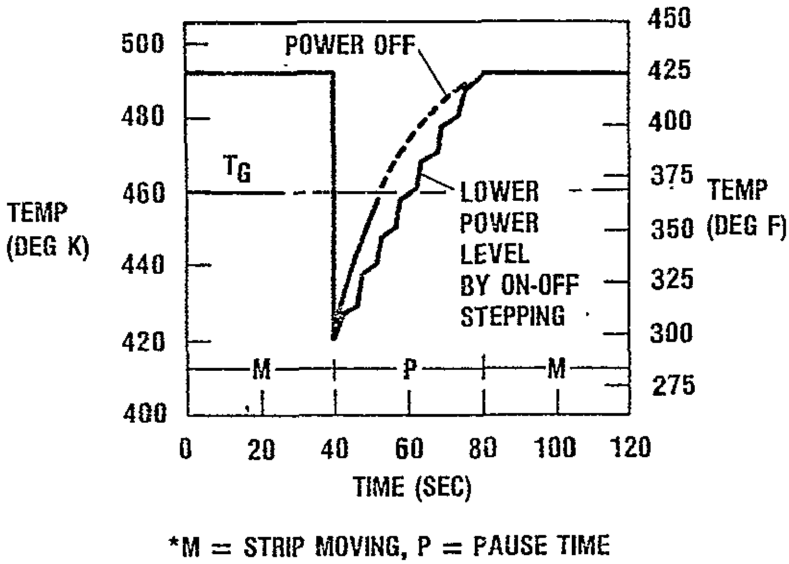

Figure 3-21. Solutions to temperature overshoot.

The thermopile aperture size determines the field of view (FOV) between the plane of the detector and the plane of the cap material. For a FOV of 1.77 cm and a viewing angle of 14.04°, the sensor can be placed 2.54 cm from the cap material. To limit the sensor's TO-5 can temperature, special heat sinking precautions must be followed. Mounting the sensor totally surrounded by space with radiating/receiving area = 3 — (emittance = 0.9) the final can temperature would rise to 77 C.

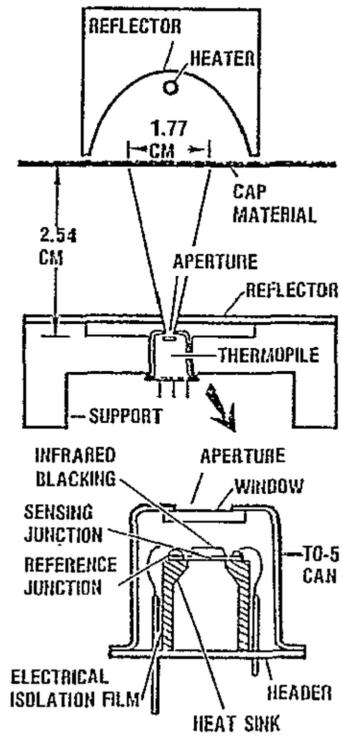

Figure 3-22. Thermopile installation concept.

To lower the can temperature further, the thermopile sensor will be mounted in an aluminum support that will conduct heat directly to the structure. A reflector will be placed in front of the thermopile sensor to limit the exposure of the sensor to IR radiation and reflect heat back to the cap material. This will also improve the heater efficiency.

The sensor can and aluminum heat sink will absorb heat from the cap material. Knowing the area exposed, emittance and conductive coupling, the final can temperature can be determined.

3.3.2.2.4 Heater/Temperature Control. The heaters and IR sensor described in previous sections are interconnected to the BCU via the multiplex bus and interface circuitry. The block diagram for heater/temperature control is shown in Figure 3-23.

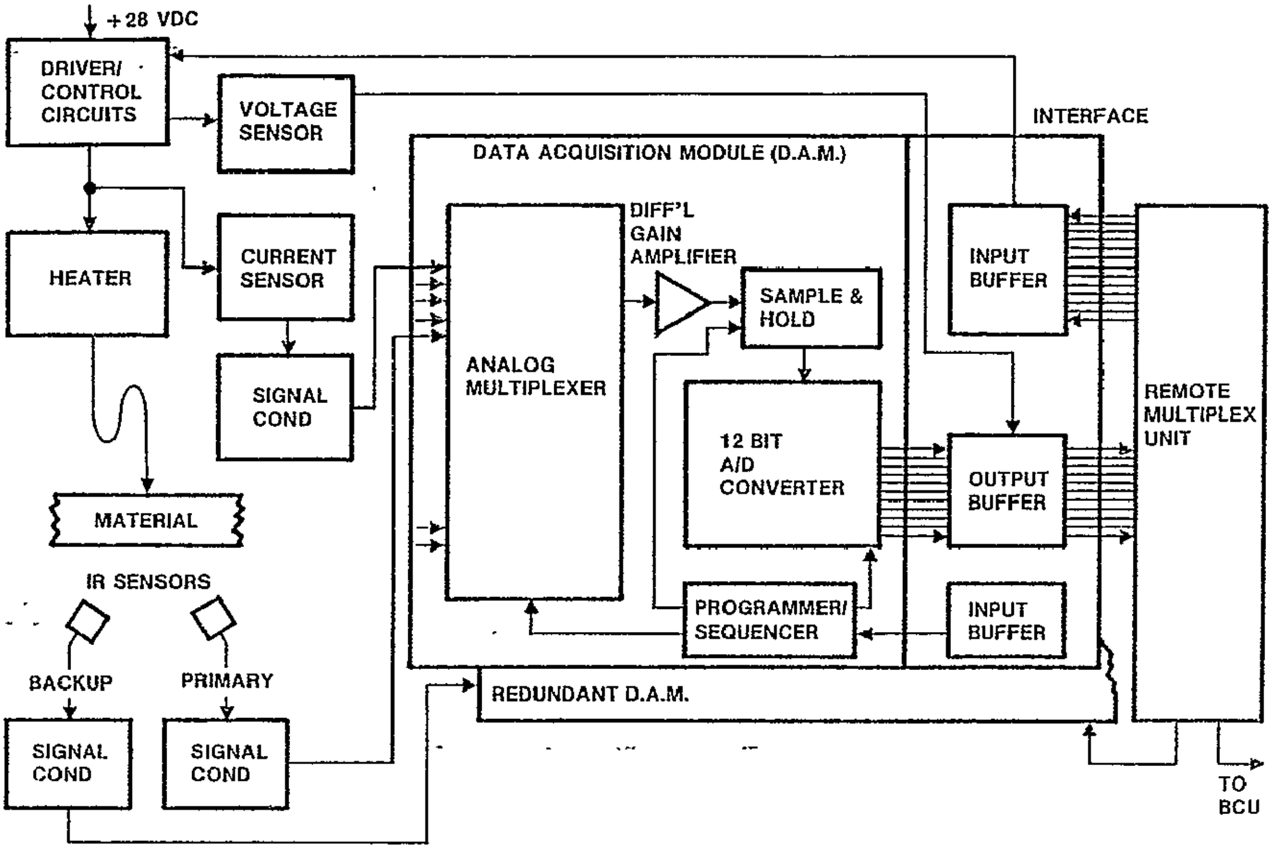

Figure 3-23. Heater/temperature control block diagram.

Depending upon mode of operation, the BCU will transmit control signals to the appropriate heater driver circuitry via the RMU and input buffer. Twelve bits will be needed to control the primary heater elements per cap subsystem. Twelve additional bits will be required for the redundant heater elements. Data acquisition modules will be used to process analog signals (thermopile IR sensors and current sensors) and convert them into digital form for subsequent transmission by the digital multiplexer to the BCU.

The input to the system (physical parameter) is converted to electrical form by the sensor and then fed to the signal conditioner. The signal conditioner converts the signal to a higher level voltage signal which can be used to drive the next analog circuit. This may be accomplished by using an operational amplifier or instrumentation amplifier. The signal conditioner will also include a low pass filter which will eliminate high frequency noise components from the signal.

The signal then goes to an analog multiplexer which multiplexes a number of different signal inputs. Each channel is sequentially connected to the output of the multiplexer for a specified period of time. The circuits beyond the analog multiplexer are time-shared between the input signals. The output of the analog multiplexer goes to a circuit which samples the multiplexer output at a specified time and then holds the voltage level at its output until the analog-to-digital conversion takes place. The timing and control of the analog multiplexer, sample-and-hold circuit, and A/D converter is accomplished by a programmer sequencer circuit. The programmer, in turn, is controlled by digital inputs from the BCU via a digital multiplexer.

3.3.2.3 Forming Section.

3.3.2.3.1 Heater Operation. The heaters will be operated in one of three distinct modes:

a. Preheat
b. Normal
c. Ground test (air)

The preheat sequence allows material to be heated to the forming temperature before start of the normal run cycle. Initially, the forming section heaters will be energized for 300 sec and then turned off. The heating section heaters will then be energized for 130 sec. This heating sequence is performed to obtain a temperature distribution approximating that at the end of a 40-sec. pause cycle during normal operation. The preheat sequence must be initialized after lengthy periods of heater shutdown before the beam builder machine operations are started.

During normal operation in space the forming heaters will be turned off. Heating section heaters will be energized and will provide sufficient material heating for the proper forming operation to occur. The heaters will be controlled such that the material leaving the heating section will be at a nominal temperature of 491K. Normal operation consists of a 40-second material run time and a 40-second pause time for fabrication.

Ground test operation in air will require the forming heaters to be turned on in addition to the heating section heaters. Air convection losses will necessitate energizing both of the dual elements in each heater.

3.3.2.3.2 Forming Section Update. The forming section configuration has been updated to reflect the latest changes established by Convair's experimental roll forming machine. The new forming roller geometries are as shown in Figure 3-13. The overall length of the forming section grew 30.5 cm as a result of these changes.

3.3.2.4 Cooling Section.

3.3.2.4.1 Cooling Platen Drive Mechanism Update. The initial concept for the cooling platen drive mechanism consisted of individual linear motors or solenoids driving each platen. There were two actuators for each outside platen and two actuators to operate the inside platens for a total of six actuators. Overall, the beam builder would require eighteen actuators for cooling platen operation. The new preliminary design, shown in Figures 3-13 and 3-24, uses a linkage mechanism which allows all platens within each of the three cap forming machines to be operated by a single actuator. Two sets of the linkage are provided along with a second actuator for redundant drive capability. The two linkage mechanisms are cross-coupled together. This, together with load springs in both ends of each actuator rod, permits one actuator to drive the platens with the other actuator not operating.

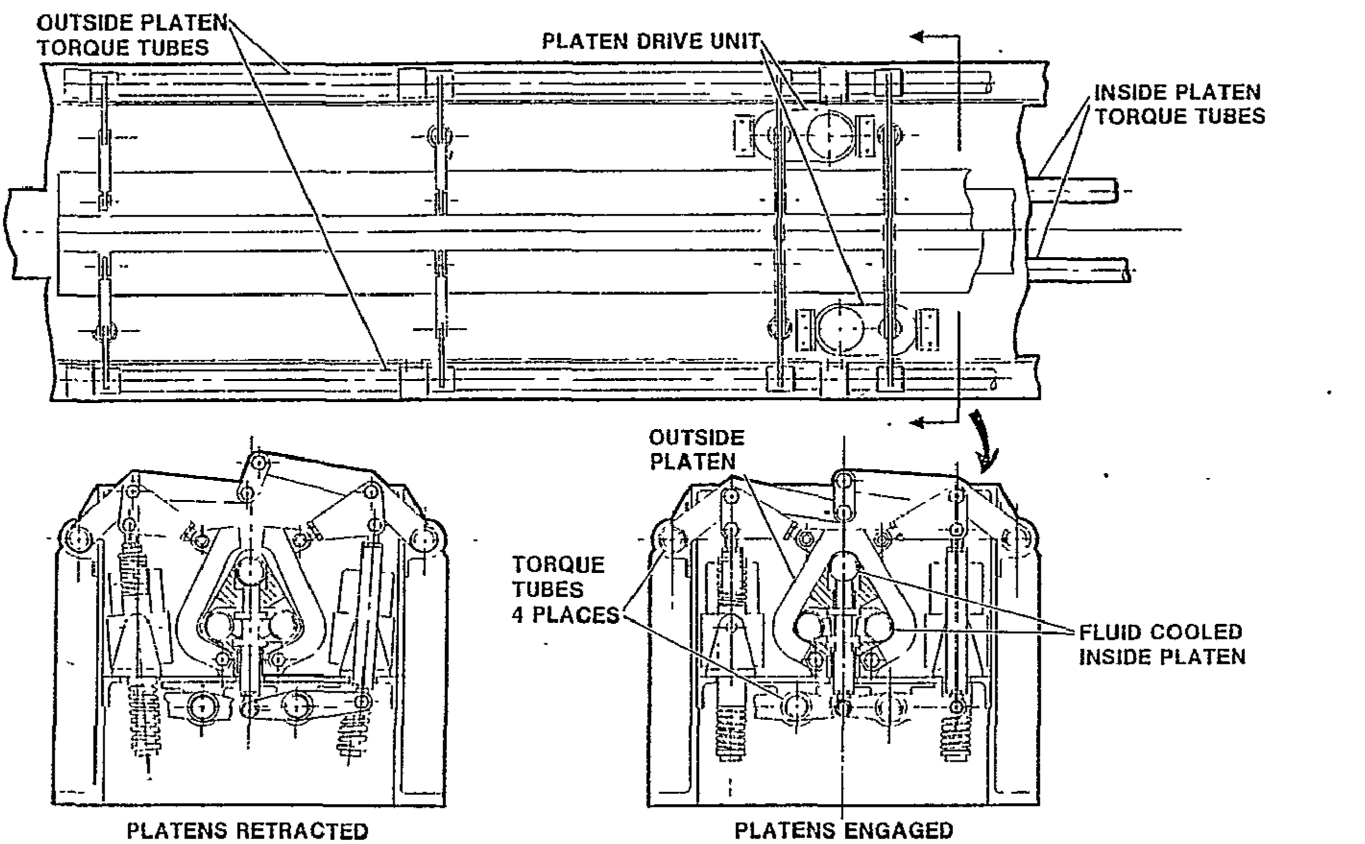

Figure 3-24. Cooling platen drive mechanism.

3.3.2.4.2 Cooling Platen Drive Unit Design. The cooling plate drive unit consists of a motor-driven screwjack, spring-loaded at both ends against a push rod which passes through the center of the lead screw as shown in Figure 3-25. The peculiarities of the mechanism and the space limitations in this area of the cap forming machine did not permit use of the universal drive unit in this application. However, the baseline DC brushless motor used throughout the beam builder is also used here.

The operating modes are illustrated to show how platen drive units behave in normal operation and with one unit not operating in the worst cases. Motor load cycles were calculated for the normal and worst case closing cycles in order to verify that the

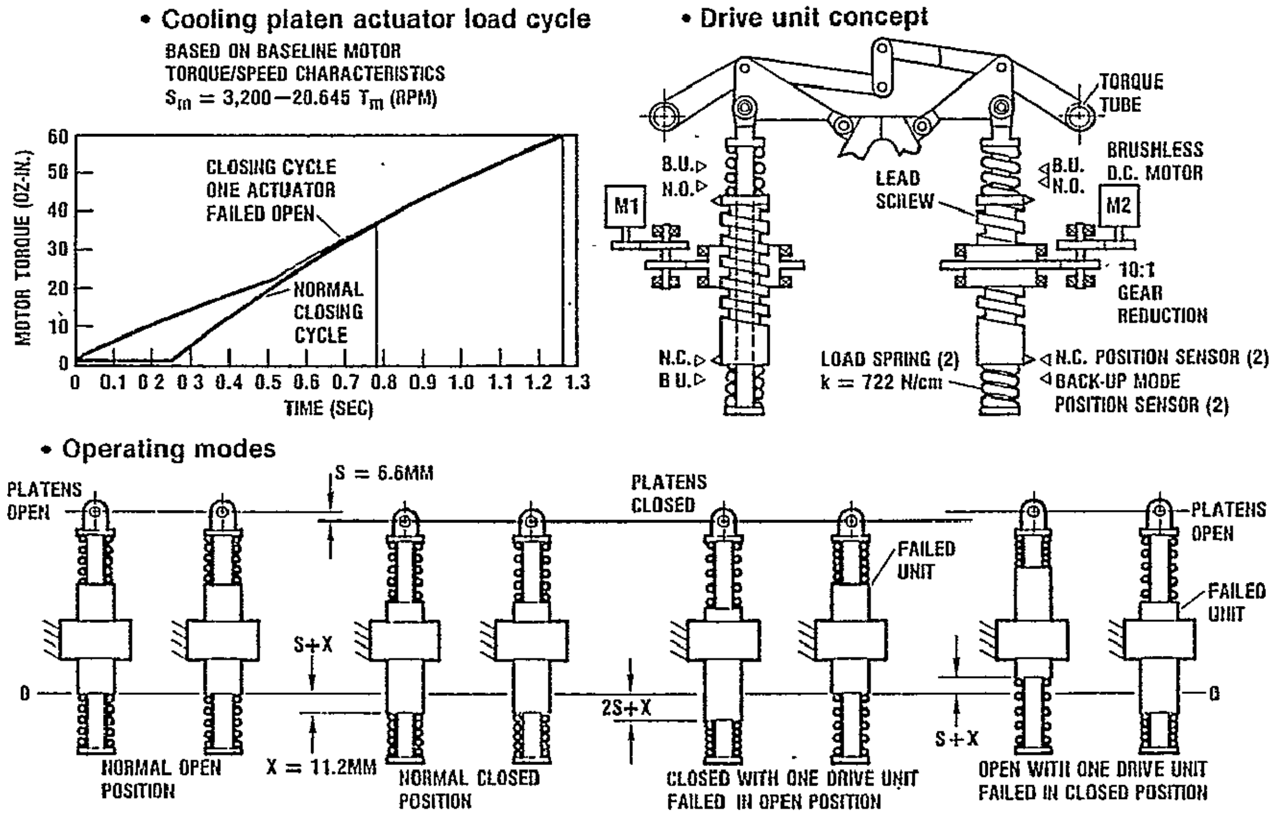

Figure 3-25. Cooling platen drive unit operating characteristics.

baseline motor would operate the platens within an acceptable time and an acceptable torque range. The opening cycle is the opposite of the closing cycle shown.

Both actuators are normally driven. The drive stroke is controlled by vane-interrupted Hall effect position sensors. One pair of sensors on each actuator detects normal open and normal closed position. A second pair of sensors is positioned to allow additional stroke if one actuator fails. Upon reaching the selected position, the motor is commanded to stop. If the normal position sensors should fail, the backup position sensors will take over their function automatically. In this case, the motor continues to drive until the backup sensor is activated.

The mechanism will operate the cooling platens within the following parameters:

1.	Actuation time (close/open)	1.5 sec max.
2.	Actuator load applied to platen (normal mode)	379 N/m or 534N
3.	Actuator load applied to platen (failed mode)	190 N/m or 267N

3.3.2.4.3 Cooling Platen Drive Control.

a. General. Under normal operation, both platen motors will be operated simultaneously. If a failure of one motor or duplicate mechanism occurs, the motor associated with the failure will be deactivated and cooling platen operation will continue via single motor operation with a longer actuator stroke to compensate for the failure condition.

b. Normal Operation. When the cap forming operation is occurring, the cooling platens are in the open position. After a 40-second run has been completed and the cap drive has stopped, the BCU will signal the cooling platen electronics to start the platen drive motors by sending a command word to the drive electronics.

Upon receiving start and direction signals (forward/reverse), the motors will drive the lead screws causing the lever mechanisms to close the cooling platens and move the cooling tubes inside the cap into contact with the heated cap radii. The BCU will also enable a set of four position sensors. When the appropriate sensors are activated by the mechanism (indicating that the cooling platens are in the closed position), the motors will be commanded to stop. The BCU will monitor sensor data to determine that a cooling platen cycle is occurring and has completed before starting the next operation. Sampling rate is established at 10 samples/sec. In addition to sampling status data, the BCU will use software timers to monitor timing of each mechanism operation for diagnostic and control purposes.

c. Backup Operation. If a motor bearing freezes or a mechanism locks up, motor current will rise because of greater torque required. Since the BCU is continually monitoring current data, the BCU will command a motor to stop if the motor or mechanism malfunctions. When this occurs, the BCU will also enable the backup position sensors and disable the normal position sensors.

The remaining motor will complete the platen cycle by increasing the stroke of the failure condition. The increased stroke positioning will be monitored by the backup position sensors. Cooling platen operation will continue in the backup mode until the failure condition has been corrected.

The force of the platens on the cap material is established by pretensioning of the springs on the lead screw actuators. Since overshoot will result in a larger, but still acceptable, platen force on the cap material, accurate positioning control is not required. Simple on-off control with electronic commutation will be used. Figure 3-26 shows the platen controller block diagram.

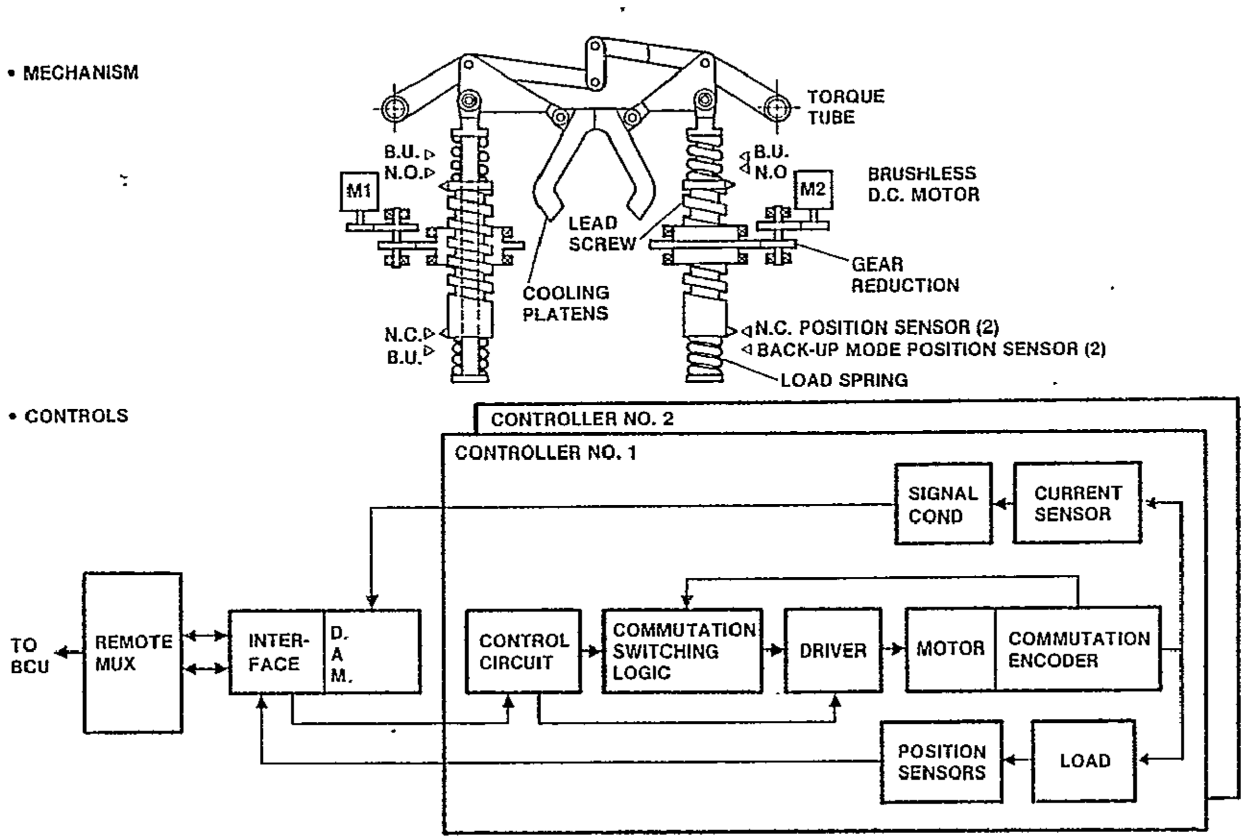

Figure 3-26. Cooling platen drive unit control block diagram.

d. Sensors. Vane-operated Hall effect sensors will be used as platen position sensors. Refer to Subsection 3.2.2.1 for a description of these sensors.

The ferrous vanes will be mounted on each lead screw and their physical movement will be dependent on the ball nut position. The Hall sensor will be physically mounted on brackets positioned to trip "on" (stopping the motors) at the required platen-to-cap material pressure (controlled by the spring preload). In the opposite position, the sensor will trip "on" when the cooling platens are fully open.

A second Hall sensor is mounted in the backup mode position. A failure will cause a switch to the backup sensor which will accommodate the lengthened lead screw stroke. This longer stroke applies sufficient, but reduced, platen pressure to accomplish cap cooling during the cooling cycle.

Hall effect current sensors will be used to monitor motor current. These sensors are described in Subsection 3.2.2.4. By sensing both the platen motor current and the platen position, the BCU can determine the operational condition of the platen drive unit and initiate the backup mode for failure conditions.

3.3.2.5 Drive Section.

3.3.2.5.1 Cap Drive Unit Update. The cap drive unit is the prime mover in the beam fabrication process, since it provides the pull force required to unroll the flat strip material from the storage roll and pass it through the heating, forming, and cooling sections. The cap drive unit also feeds the cap into the assembly section, thus causing the finished beam to be deployed from the beam builder.

The initial cap drive unit concept used only one set of rollers. Although one set of rollers provides adequate force, the failure of one roller could overload the functioning pair of rollers causing slippage. Failure to drive the cap in the prescribed displacement vs. time tolerance is detected through the cap displacement sensor and the beam builder process is automatically shut down. A second set of rollers was thus added to improve reliability as shown in Figure 3-13.

The universal drive unit has also been incorporated into the design as part of the effort to achieve drive commonality. The UDU drives a worm which, in turn, drives two worm gears that are cross-coupled through the roller drive gear trains. The anti-backlash worm gear, when properly set, will effectively remove all residual backlash in the roller drive train. This is essential to achieve the high degree of positioning accuracy required in the cap drive process.

3.3.2.5.2 Cap Drive Unit Load and Speed Requirements. During the run phase, the cap drive unit must be controlled such that the displacement of all three caps follows a prescribed displacement vs. time function within allowable limits to prevent placing high stress on the weld joints of the completed beam sections. This function will be similar to the one shown in Figure 3-27 and will result in the velocity profile shown. The caps will initially accelerate to a constant velocity in the first 3 seconds of travel and decelerate to zero velocity during the last 3 seconds.

During the run period, the cap drive unit may be subjected to cycle loading which will vary as a function of beam length and bending loads applied to the beam by the orbiter VRCS activity. The worst case cyclic load, shown in Figure 3-28, is conservatively based on a 200 m cantilevered beam experiencing load input as determined during Part II of the study.

The axial cap tension loads act to assist the cap drive. The drive transmission retards these assist loads through a high gear reduction which includes a worm drive. To provide accurate displacement control under these cyclic loading conditions, a velocity control loop will also be required to maintain stability.

3.3.2.5.3 Cap Drive Control.

a. Design Requirements. Differential displacement between cap sections, while running, shall be no greater than 5.08 mm. Each cap shall be stopped within

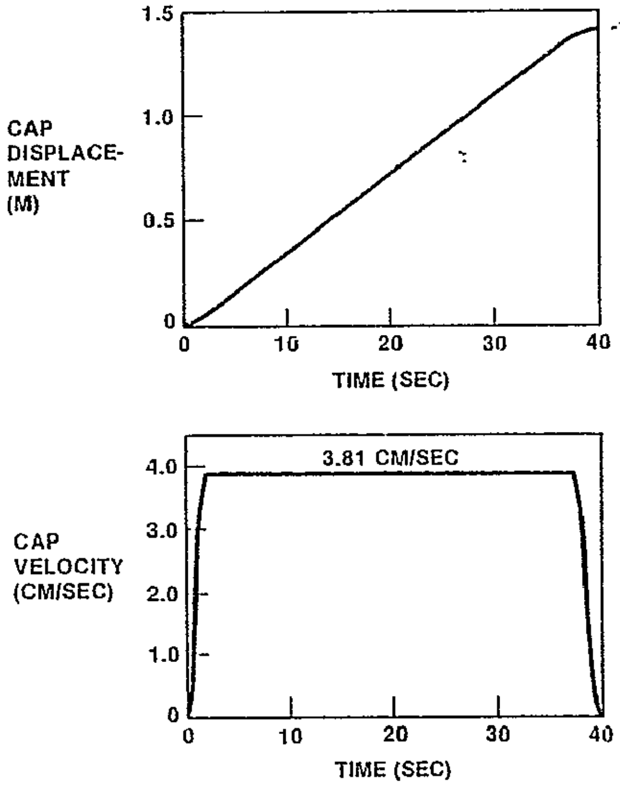

Figure 3-27. Cap drive displacement and velocity characteristics.

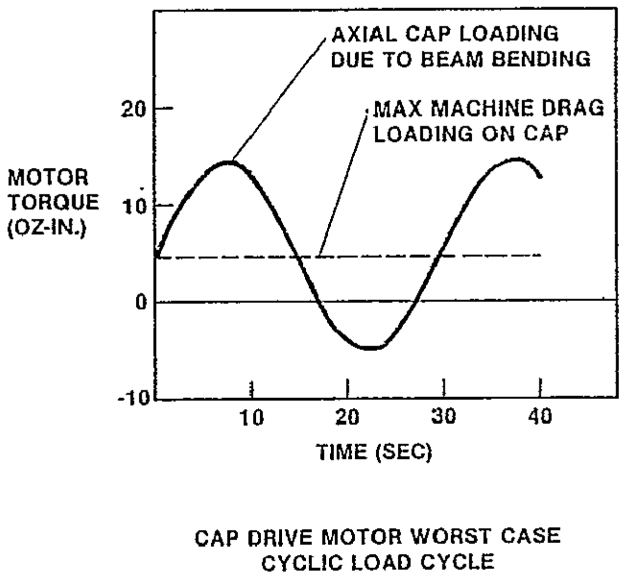

Figure 3-28. Cap drive motor worst case cyclic load cycle.

±0.1 mm/m of the required stopping location 50% duty cycle (40 sec on and 40 sec off). Duty cycles are described in Figure 3-27 and 3-28.

b. Description of Operation. The cap drive controller block diagram is shown in Figure 3-29. Precise position control will be required to achieve the design requirements. The BCU, which contains a cap displacement profile, will monitor cap displacement and determine the error with respect to the reference displacement profile. The error value will establish an adjusted reference signal, which is transmitted in digital form to the motor controller via the digital multiplexer. The digital data will be converted to an analog signal, which will be used to generate a reference signal, which is transmitted in digital form to the motor controller via the digital multiplexer. The digital data will be converted to an analog signal, which will be used to generate a reference frequency. This reference frequency will be compared to the pulse frequency generated by the travel sensor. This comparison will generate a pulse-width modulated signal, which is input to the commutation switching logic for motor speed control. This control signal will essentially lock the cap speed in phase with the reference frequency. Deceleration of the motor occurs by lowering the reference frequency. Motor current will be monitored by the BCU via the multiplexer and data acquisition module.

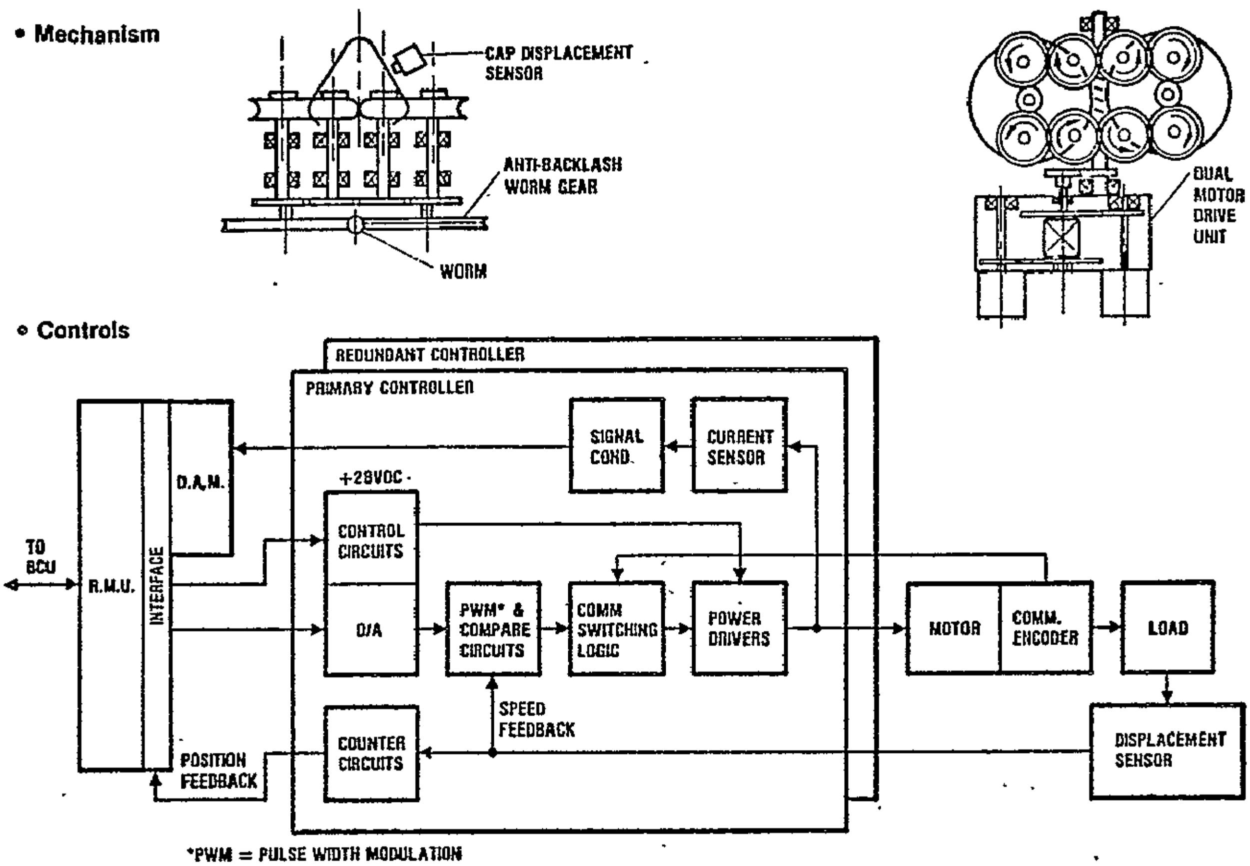

Figure 3-29. Cap drive controller block diagram.

As described in Subsection 3.2.2.4, Hall effect current sensors will be used to monitor motor current. The cap displacement sensors will be magnetic reader heads reading directly from encoded magnetic tape attached to the caps.

3.3.3 CROSS-MEMBER SUBSYSTEM. The design concept for the cross-member subsystem created in Part II had two major disadvantages. The first was that it used too many motors and actuators. The second was that the method of grasping each cross-member did not ensure a positive grip. As a result, trades were made during the preliminary design to reduce the number of drives and improve the reliability of the cross-member mechanisms. This included not only the cross-member configuration trades described in Subsection 2.2.1, but a number of mechanisms trades, which are described in the following subsection.

The updated cross-member subsystem has the same operation sequence as the original concept. This sequence is shown in Figure 3-30. The cross-member handler/positioner mechanism picks up one cross-member at a time from the storage clip. It then translates and rotates it to the installation position on the beam.

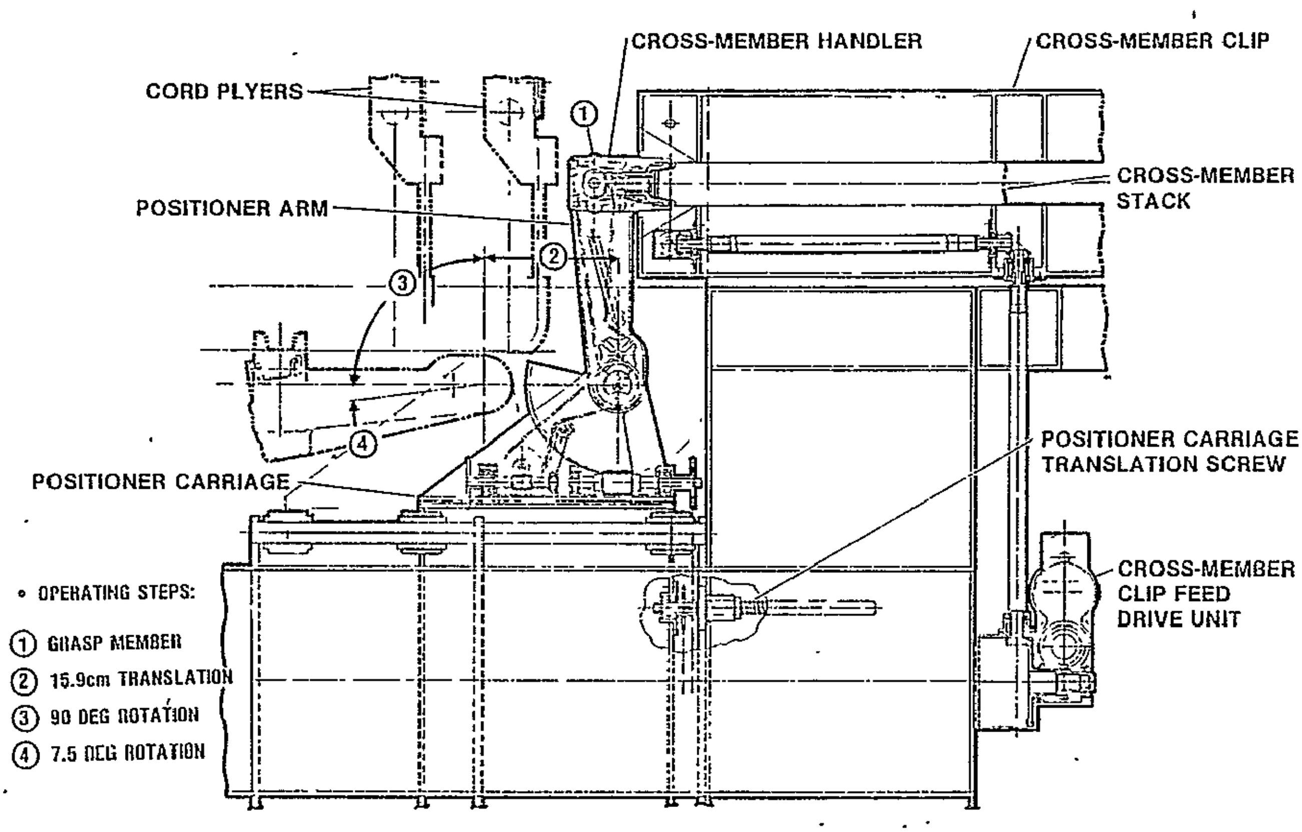

Figure 3-30. Cross-member subsystem functional sequence.

After welding of the cross-member and cord to the beam is complete, the handler fingers are opened and the positioner arm rotated to move the handler/positioner inboard of the plane of the beam side. This allows the last cross-member installed to clear the handler/positioner and the cord plyers to pass over the handler/positioner while the beam is advancing one bay length.

At some time after the cord plyers have completed their stroke, each positioner arm is rotated and translated into the position for receiving the next cross-member from the clip.

3.3.3.1 Cross-Member Mechanisms Trades.

3.3.3.1.1 Clip Feed Trades. Several options for feeding the stack of cross-members to the handler mechanism and ejecting only one cross-member at a time were considered, as shown in Figure 3-31.

The chain drive was selected to ensure high reliability of indexing under various loading conditions and because it offered the widest range of operating temperature over that of the flexible timing belt. Leadscrew feed mechanisms were rejected because of high weight and the potential wear they would induce on the cross-member bearing surfaces.

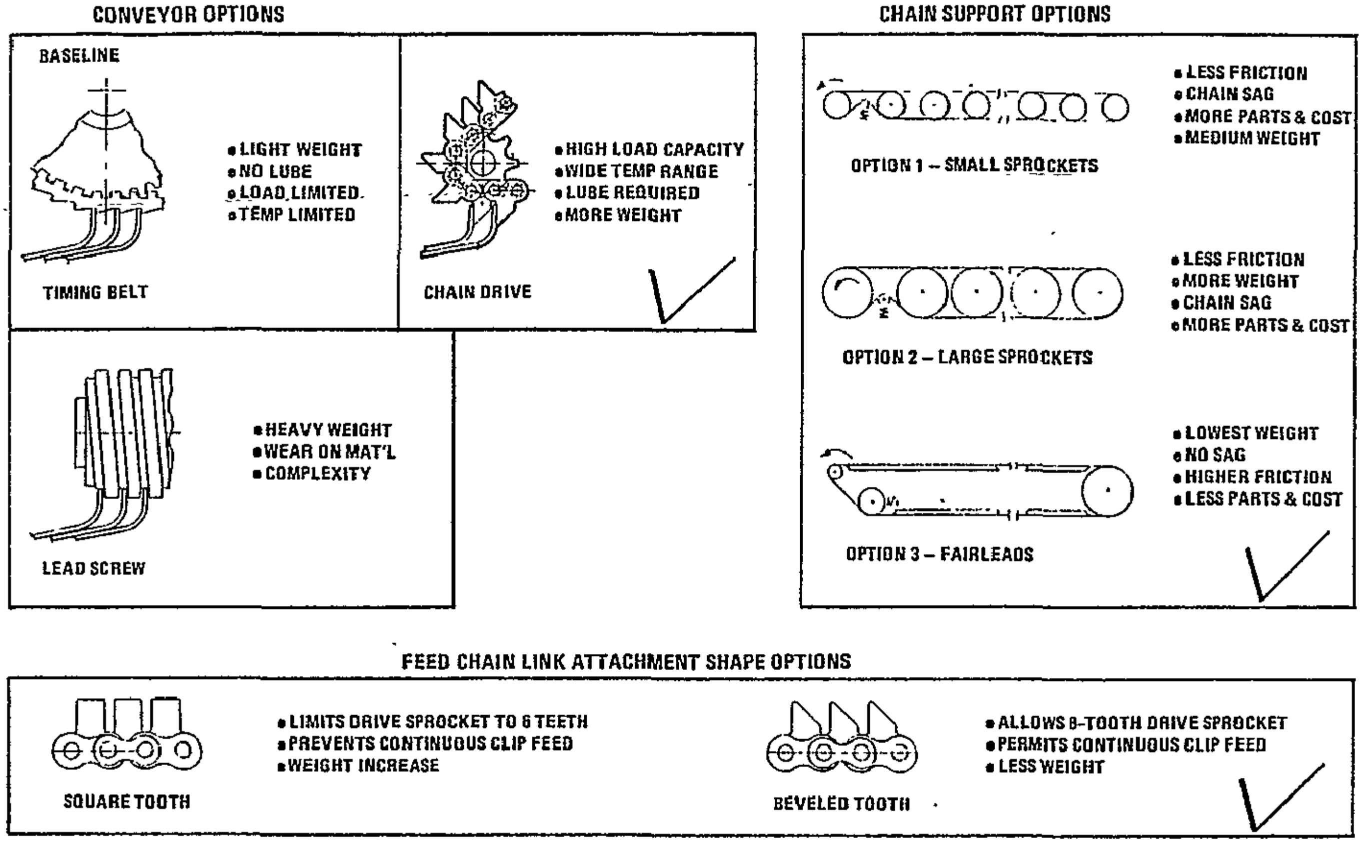

Figure 3-31. Clip feed options.

Although the fairlead chain supports create higher friction on the stack of cross-members, they do prevent the chains from sagging and eliminate the need for numerous sprockets along the path of the chain. The beveled tooth chain option used in conjunction with a small diameter feed sprocket was found to have the best feed and retention characteristics. Use of the square-tooth chain caused the size of the feed sprocket to become prohibitively small.

To eliminate use of separate motors for each feed clip and allow use of a common drive for all three clips, several feed drive options were evaluated, as shown in Figure 3-32.

The Option 4 mechanism was selected because of its lighter weight and minimum number of indexing mechanisms: A more detailed analysis of torque loads and deflection will be required to establish the overall indexing error at the chain feed sprockets due to wind-up or backlash in the drive train.

The initial cross-member handler concept used linear electromechanical actuators in each handler to open and close the grasping fingers. With one redundant actuator in each handler, six actuators were required for the three handlers. By using cam-operated fingers for each handler, the cams can all be operated through a drive mechanism by a common drive and the need for six actuators is eliminated.

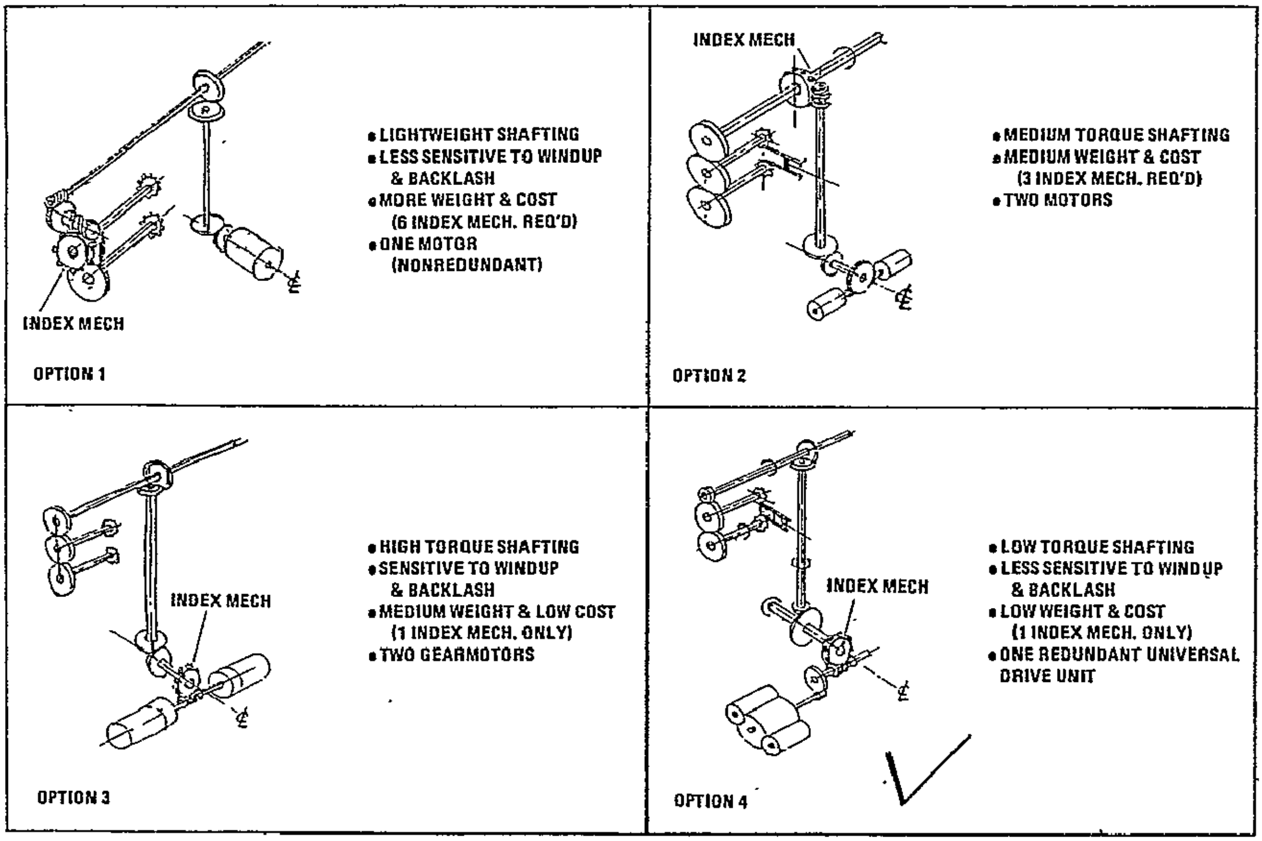

Figure 3-32. Feed drive trade options.

To ensure positive retention of each cross-member by the handler fingers, the configuration of the cross-member was changed to add lip flanges to each side of the channel. The final configuration was established through the trade discussion in Subsection 2.2.1. Although two options for grasping the cross-member with the cam-operated fingers are possible, as shown in Figure 3-33, Option 2 must be used if the flat of the cross-member is to be placed against the side of the caps for welding.

Finally, another group of options was evaluated for selection of the cross-member positioner mechanism. The originally selected baseline, which was a track-driven swing arm, shown as Option 1 in Figure 3-34, did not lend itself to common drive input for both the handler and positioner. After consideration of several alternatives, the Option 4 approach was selected because it allowed the use of a common drive input for each of the three handler/positioner functions: (1) grasping/release, (2) rotation, and (3) translation.

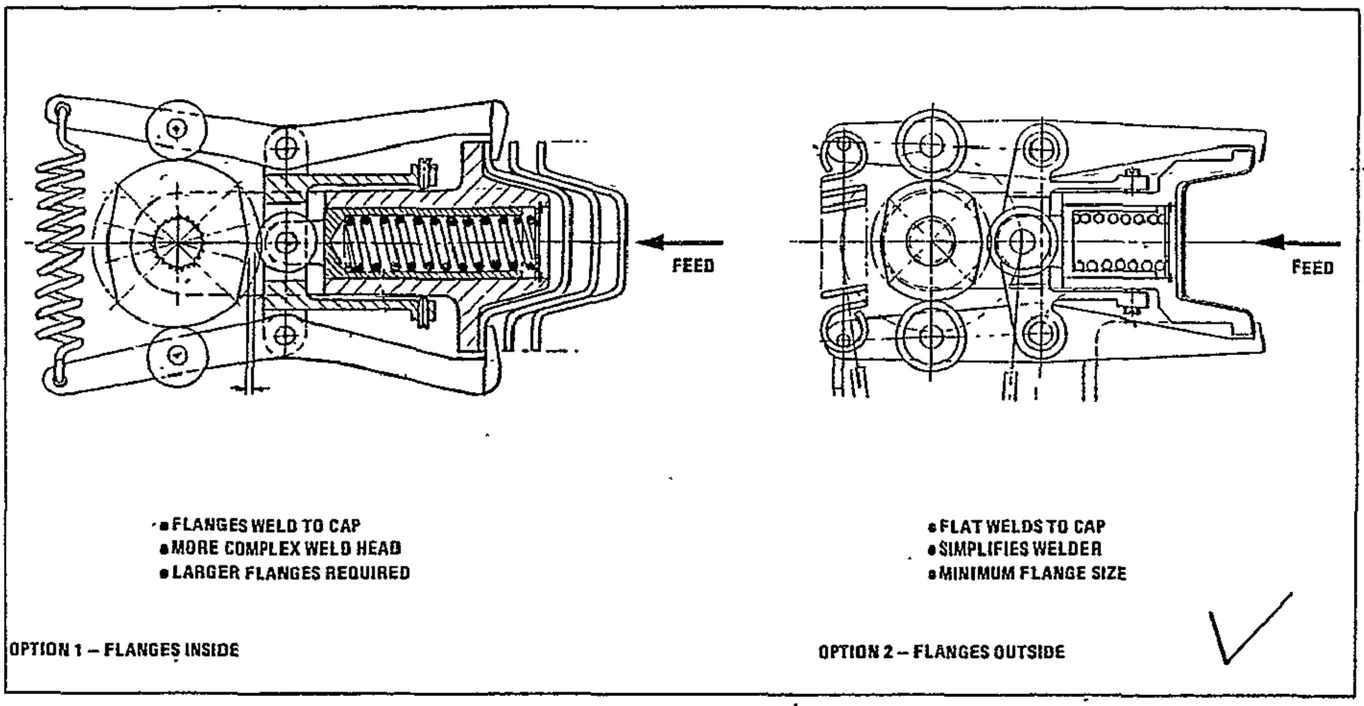

Figure 3-33. Cross-member grasping options.

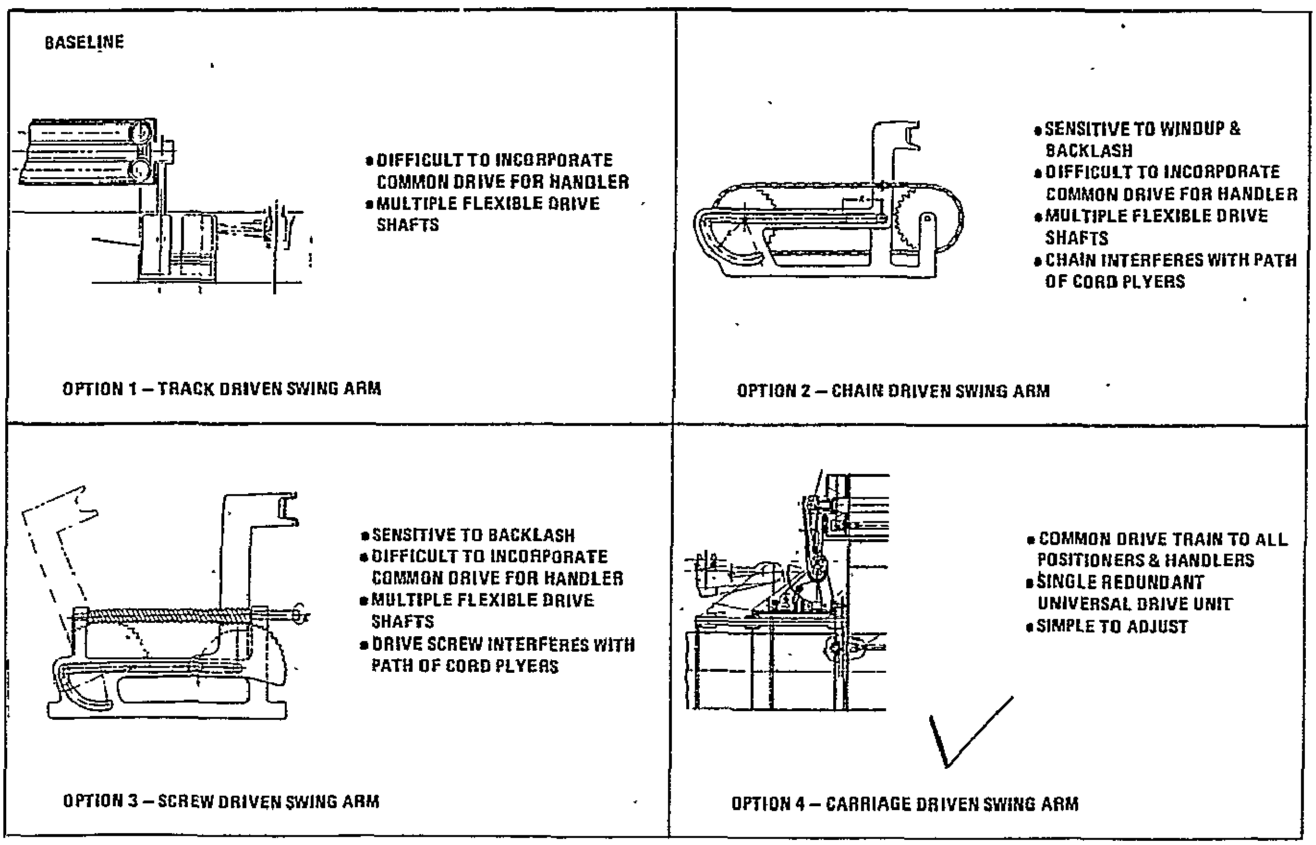

Figure 3-34. Cross-member positioner trade options.

3.3.3.2 Cross-member Storage and Feed Mechanism and Controls

3.3.3.2.1 Storage and Feed Clip Design. Each of the three cross-member storage clips is a self-contained, removable unit with its own transport drive and splined input shaft, and mounts on pads on the beam builder structure. The clip structure consists of two mated aluminum housing halves that are bolted together at the flanges. Each clip holds 650 cross-members.

The cross-member stack is supported and advanced by four chain loops whose toothed chain links mesh with the lipped flanges of the cross-members as seen in Figure 3-35, View B-B. The four chain loops are located approximately midway between the clip centerline and the edges of the clip. Each chain drive loop consists of a small drive sprocket at the forward end, a return sprocket at the aft end, and a spring-preloaded chain-tensioning sprocket near the drive sprocket. Chain supporting fairleads along the full straight length of the chain loop complete the chain drive system.

The drive sprockets have eight teeth and rotate 1/8 turn per feed cycle. This moves the chain and cross-members one pitch and rotates the chain link teeth forward of the first cross-member, just far enough to clear its path for pickup. The four chain drive sprockets are interconnected with shafting, spur gear, and bevel gear drives. The storage clip input bevel gear has a splined bore to facilitate coupling to the mating splined drive shaft on the beam builder structure.

The storage clip can either be loaded by feeding cross-members through the aft end opening or by opening the storage clip first and laying the stack of cross-members on the transport chain.

3.3.3.2.2 Feed Mechanism Design. The three cross-member storage clip assemblies are driven from a single, redundant-motor universal drive unit which is mounted on the aft face of the center pedestal structure as shown in Figure 3-35, View D-D. The drive train includes a spur gear reduction, a roller gear drive, and bevel gearing with splined output shafts. The indexing cam of the roller gear drive, shown in Figure 3-35, View E-E, makes one revolution per feed cycle and, with its dwell/acceleration/deceleration characteristics, assures precise, shock-free cross-member feed.

3.3.3.2.3 Storage and Feed Clip Performance Requirements. The storage and feed mechanisms and controls are designed to meet the following requirements:

Cross-member Increment Distance	3.75 ± 0.25 mm
Increment Stroke Time	1.0 sec, max
Worst Case Load:	
Full clips at 1 g,	
Max motor torque*	0.282 Nm

*Assumes 10% efficient mechanism due to fairlead friction

3.3.3.2.4 Cross-member Feed Controls. Figure 3-36 illustrates the cross-member clip feed control equipment. The cross-members in each storage canister are indexed simultaneously via operation of one common drive unit which operates for approximately one second, every 80 seconds.

The control equipment for this mechanism consists of dual (primary plus backup) brushless dc motors, current sensors, position sensors, and motor controllers. This control equipment will share the data acquisition module and the remote multiplex unit with the control equipment associated with the other fabrication processes (the cross-member handler/positioner, the cord plyers, the weld anvil, and the weld head).

The clip feed controls block diagram is shown in Figure 3-37. When the cross-member handler/positioner is ready to receive three cross-members, the BCU will issue a command to the motor controllers, starting the motor. The motor will rotate the indexing mechanism one revolution. One rotation of the indexing wheel will cause the cross-member to be driven forward 0.1475 inch via drive shafts and gear mechanisms. A sensor will monitor position of the indexing wheel and will provide a signal to the BCU after each revolution.

Since the index wheel will dwell at the same position for 1/4 revolution, the stopping accuracy of the motor is not critical. Since the stopping accuracy will be accomplished entirely by the mechanical system, simple on-off control with electronic commutation will be used.

3.3.3.3 Cross-member Handler/Positioner Mechanisms and Controls

3.3.3.3.1 Handler/Positioner Mechanism Design. The preliminary design of the handler/positioner is shown in Figure 3-38. Each of three cross-member positioner arms carries a cross-member handling mechanism and pivots on a common carriage that translates fore and aft on ball bushings on three parallel shafts mounted on the center pedestal of the beam builder structure.

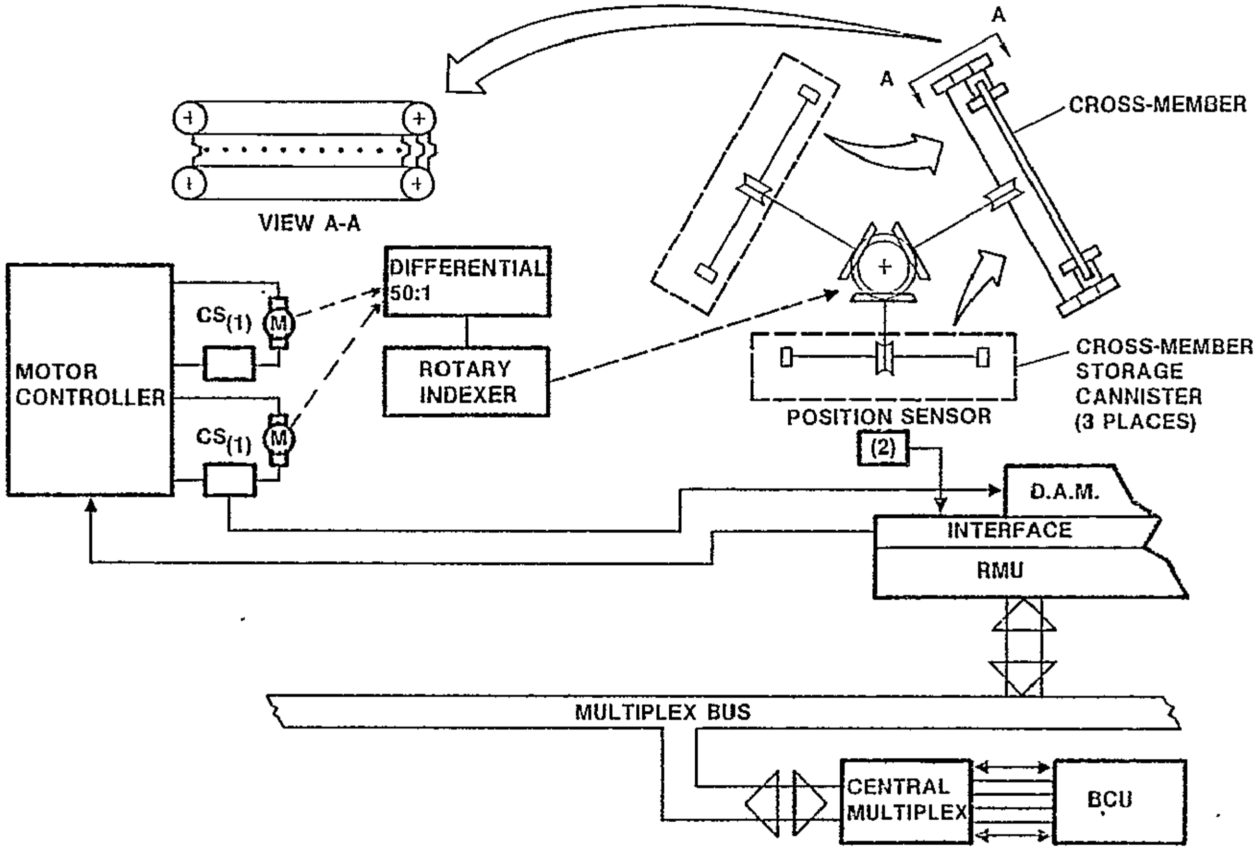

Figure 3-36. Cross-member clip feed control equipment diagram.

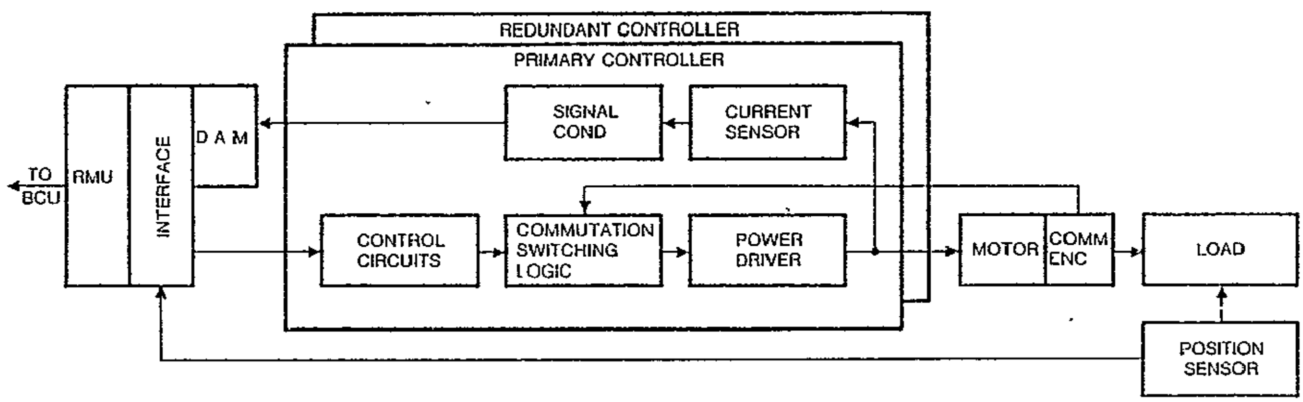

Figure 3-37. Cross-member clip feed controls block diagram.

A single redundant universal drive unit, mounted on the carriage, provides input to the three cross-member handling and positioning mechanisms. The scheduled operating sequence, shown in Figure 3-39, is accomplished by selective engagement of electromagnetic particle clutches. The input shafts of the clutches are driven and interconnected by a spur gear train and a coupling. Chain loops are used to interconnect the output shafts of the clutches with the three cross-member gripping worm gear drives, the three cross-member rotating worm gear drives, and the single carriage translating ballnut lead screw drive.

Each handler drive train contains a Geneva Wheel Indexing mechanism, a cam-operated gripping mechanism, and interconnecting chain loops with chain-tensioning devices.

The Geneva Wheel Input shaft is coaxial with the pivot axis of the positioner arm. Due to this arrangement and the large dwell of the Geneva Wheel, the position of the fingers of the gripping mechanism remains unchanged during the scheduled rotation of the positioner arm.

The cross-member gripping mechanism uses a single cam to schedule rotation and translation of the fingers. The fingers rotate on a pivoted and spring-loaded yoke. This assures equal gripping forces on both cross-member lips when squeezed by the fingers against the positioner structure. In the "open" position, the finger tips are centered between the lips of the stack's two most advanced cross-members to ensure clear entry.

3.3.3.3.2 Handler/Positioner Controls. Figure 3-40 illustrates the cross-member handler/positioner control equipment. The operation of the handler/positioner starts at the beginning of the fabrication sequence. The three handler arms will be located at the clearance position "E" prior to start of the sequence. See Figure 3-39 for translation/rotation positioning sequence.

The BCU transmits command data to start the drive motor and to energize the magnetic clutches. The handler/positioner will move from clearance position "E" to pickup position "A" in a sequence of rotation and translation movements activated by the magnetic clutches. The clutch activation sequence for movement to the pickup position is tabulated below.

Movement	Clutch Activated	Time	Distance
E to D	Rotation	1 sec	7 1/2°
D to B	Rotation	7 sec	90°
C to B	Translation	5 sec	132.1 mm
B to A	Translation	1 sec	26.4 mm

The C to B movement starts 2 sec after the D to B rotation begins.

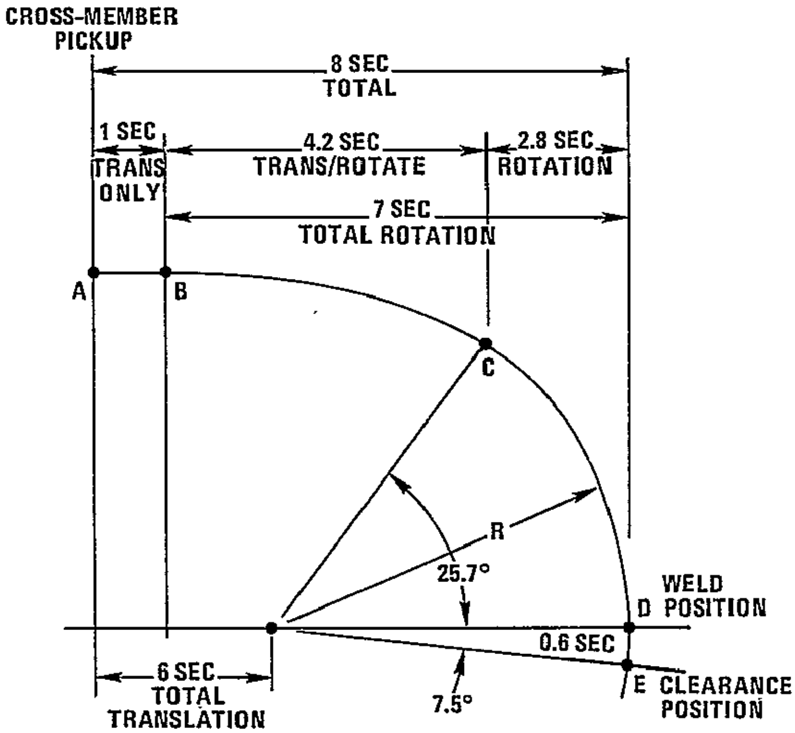

Figure 3-39. Cross-member translation/rotation schedule.

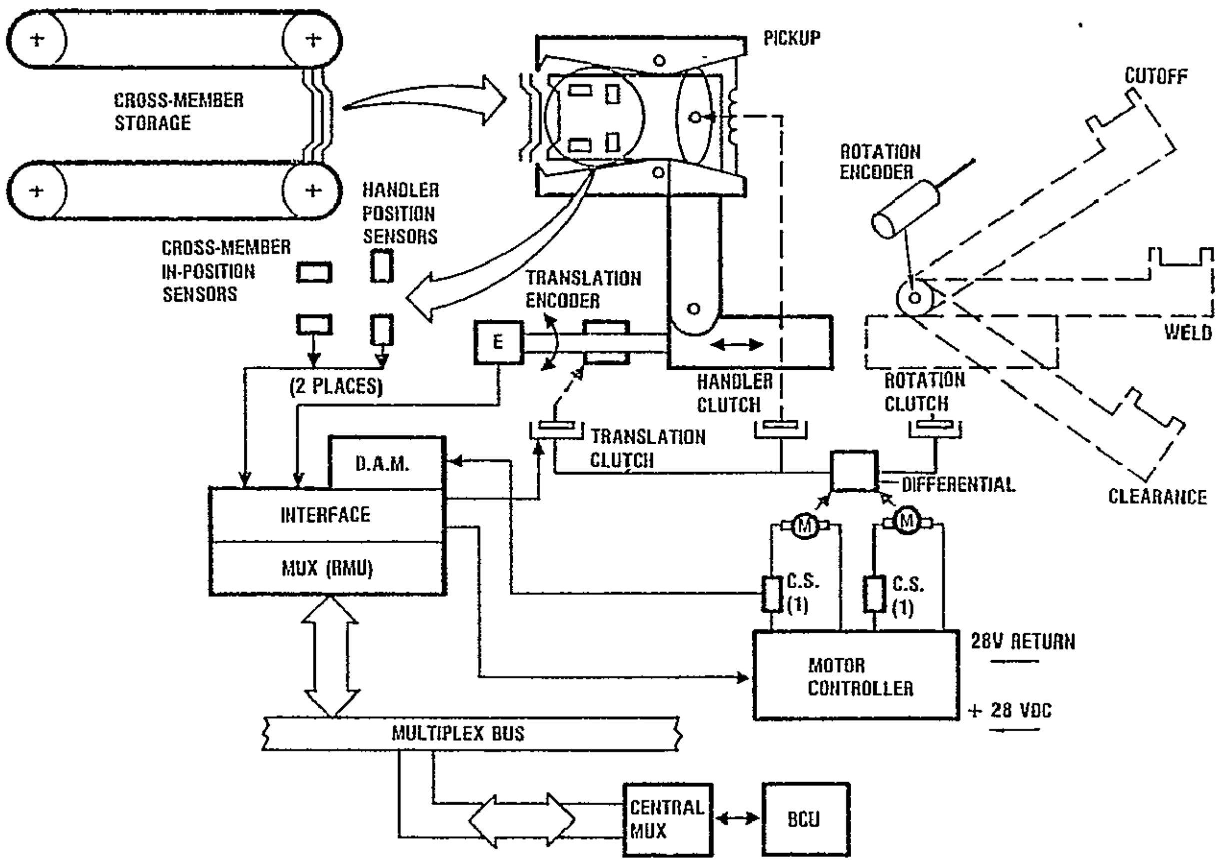

Figure 3-40. Cross-member handler/positioner control equipment diagram.

C-2

Shaft encoders will be used to monitor rotation and translation movements. Rotation of encoders will increment counters in the electronics. Figure 3-41 shows the handler/positioner controller block diagram. BCU monitors the counters every 25 ms and compares the data to predetermined position data stored in memory. The BCU will energize the clutches in accordance with these data. Software timers will be used for error detection. Since accurate stopping is required, the motor will be controlled by pulse-width modulation techniques.

After the handler arms have reached pickup position "A", the BCU will increment the cross-member clip feed as described previously.

Sensors in the handlers will assure that cross-members are properly seated. The BCU will then command the handler fingers to close, grasping the cross-member. Additional sensors will verify proper closing of the handler fingers.

The BCU will then energize the magnetic clutches to move the handler/positioner to the weld position "D" in the following sequence:

Movement	Clutch Activated	Time	Distance
A to B	Translation	1 sec	26.4 mm
B to C	Translation	5 sec	132.1 mm
B to D	Rotation	7 sec	90°

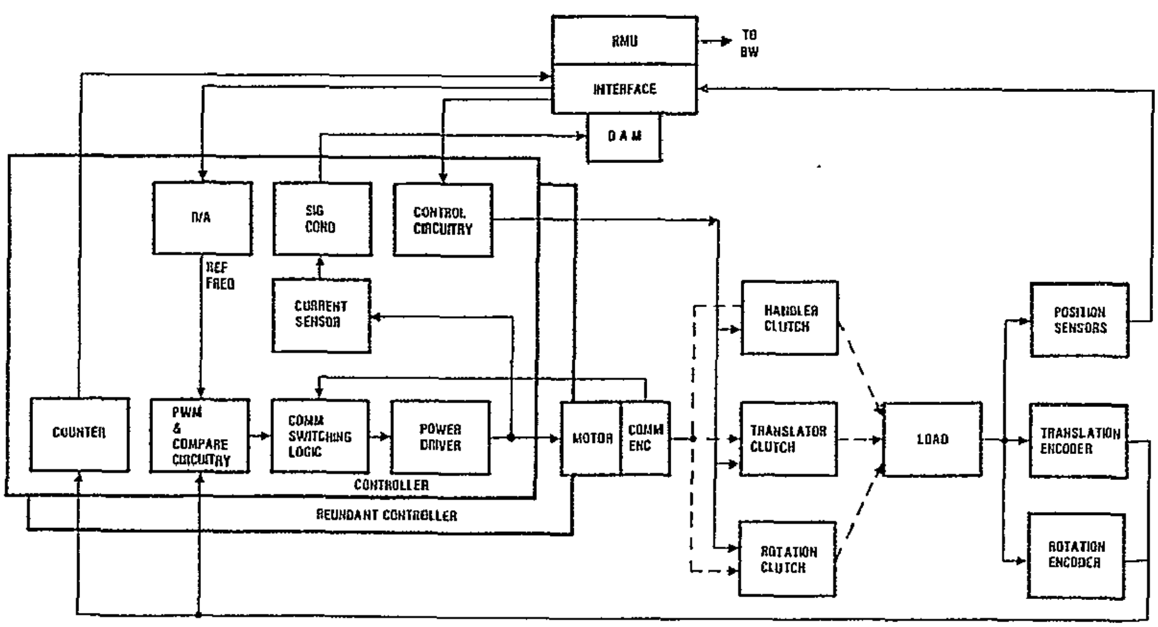

Figure 3-41. Cross-member handler/positioner controller block diagram.

The handler/positioner will pause momentarily at position "C" during the cutoff cycle only to allow for repositioning of the cord plyers. This operation is discussed in Subsection 3.3.4.2.

The handler/positioner will remain in the weld position until the welding operation is completed. The BCU will then command the handler fingers to open, releasing the cross-member. The handler/positioner will then be commanded by the BCU to rotate to clearance position "E" by energizing the appropriate clutch. The handler/positioner will be left in the clearance position until after the next drive sequence.

Hall effect current sensors and position sensors, described previously, will be implemented to monitor motor and handler operation. Shaft encoders will be used to provide positioner movement data and, in conjunction with the motor controller, for highly accurate position control.

3.3.4 CORD SUBSYSTEM. The cord plyer mechanism design, shown in Figure 3-42, has been updated to incorporate the selected drives, sensors, and reliability improvements. The functional characteristics are the same as the Part II conceptual design.

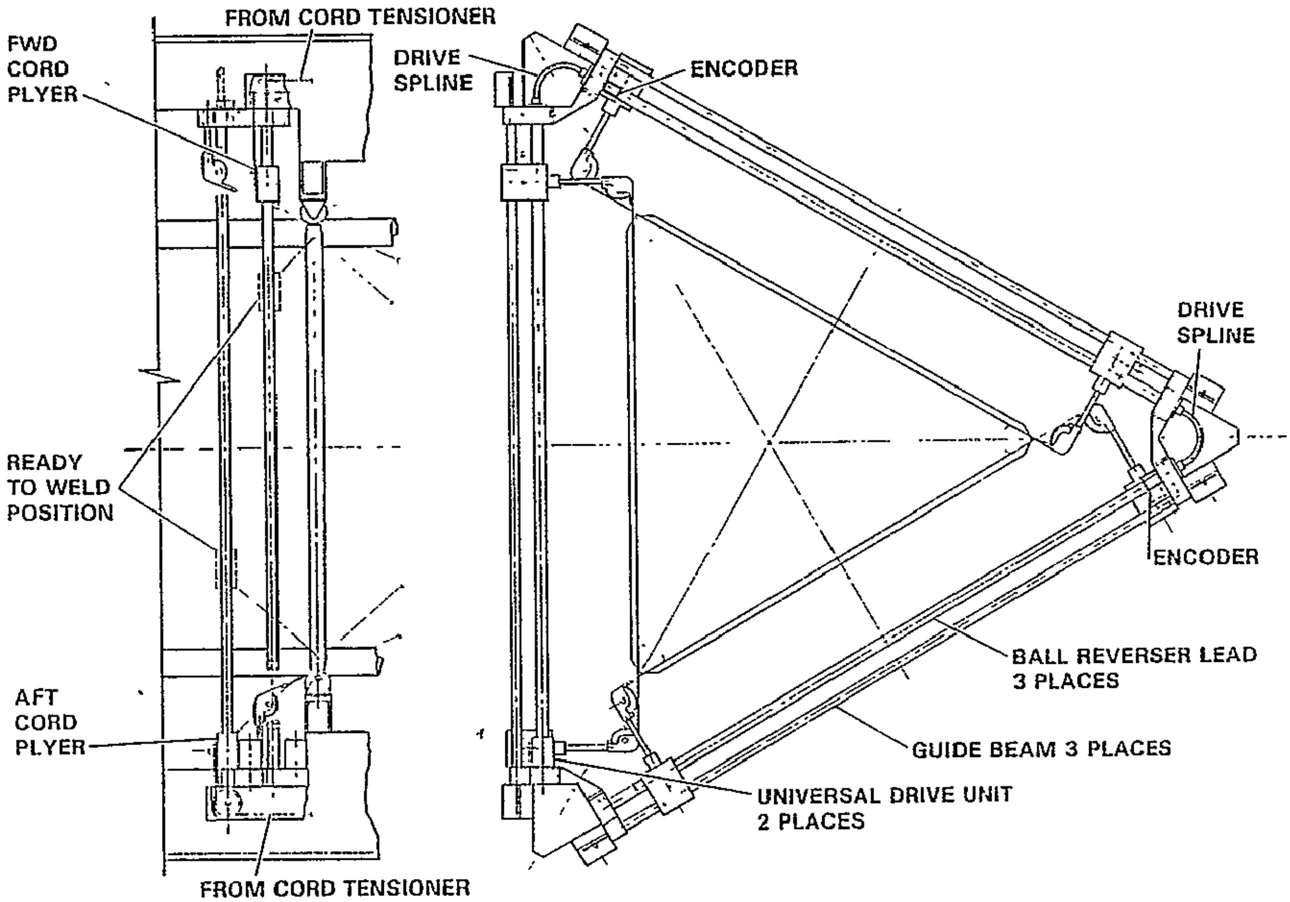

Figure 3-42. Cord plyer mechanism.

3.3.4.1 Cord Plyer/Tensioner Mechanisms. The cord plyer mechanism consists of six reciprocating cord plyer subassemblies. Each plyer is driven along a guide beam by a motor-driven ball reverser lead screw. Cord is supplied to each plyer from a cord tensioner mechanism. The inboard pulleys on the cord plyers are mounted on swivels to allow the cord to be properly aligned as the cord plyer changes position.

Forward and aft cord plyers permit the two cords on each side of the beam to be applied without interference between the moving plyers. The aft cord plyers have a longer stroke than the forward cord plyers because they are set back 13.5 cm from the forward cord plyers. This requires more lateral motion to achieve the required angle between the cord and the caps. Cord plyer strokes are 154.43 cm forward and 178.10 cm aft.

The forward cord plyer must always complete its stroke to the outboard position ahead of the aft cord plyer to avoid a collision with the cord of the aft plyer at the apex of the beam. Similarly, the aft cord plyer must always move from the outboard position first.

The forward and aft cord plyers each have dual motor universal drive units. One of the three lead screws is motor driven while the other two are driven at either end by flexible drive shafts. Should one of the flexible shafts fail, the other two would drive all three lead screws. The cord plyers are all driven at an average velocity of 10.7 cm/sec.

Two of the three cord plyers in each set are equipped with encoders for position control sensing of the six positions of each cord plyer. One encoder is the primary with the second encoder as backup.

A preliminary design layout of the cord plyer drive mechanism, shown in Figure 3-43, proves the feasibility of installing the universal drive unit to drive the forward and aft cord plyers. The cord plyer assembly has also been defined in more detail. The center of the pulley swivel has been moved to the center of the cord plyer in order to minimize the total stroke of the plyer. A third flexible drive shaft was added to each cord plyer set. This allows the three cord plyers to function if one flexible drive shaft breaks.

The cord tensioner mechanism concept is essentially unchanged except for an update of the installation drawing as shown in Figure 3-44. The mechanism operates in two modes. The first mode is the supply mode, where cord passes freely from the storage spool to the cord plyers. The second mode is the tensioning mode, whereby the free turning capstan is stopped and held by an electrically operated clutch brake. This causes the traveling pulley to extend under the force applied by the constant-force spring. A tension force equal to one-half the spring force is thus applied to the cord. Total spring force is measured by a force transducer attached to a guide pulley.

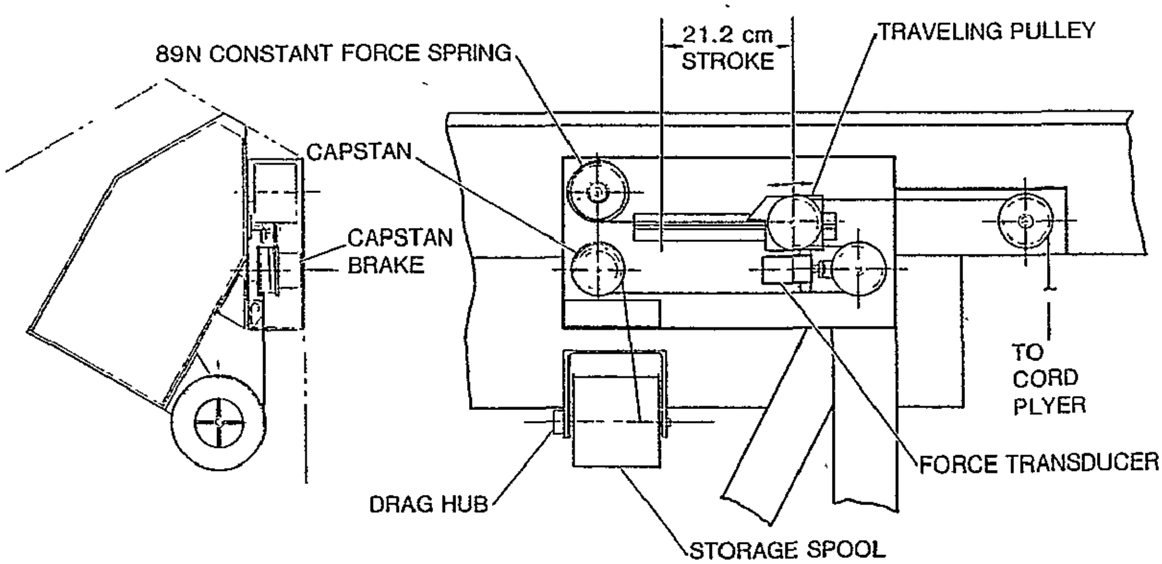

Figure 3-44. Cord tensioner installation update.

A cord tension force of 44.5 ±8.9 N is applied to each cord during assembly. This preloads the cords sufficiently to preclude any slackening or over-tensioning due to thermal and deflection effects. The ±8.9 N variation limits the amount of twist and deflection in the beam to less than 1.2° twist and 0.5 cm tip deflection of a 200 m beam.

The stroke of the traveling pulley ensures that a constant force is maintained on the cord throughout the assembly sequence. As the cord plyers move from the outboard position to the ready-to-weld position, the traveling pulley automatically compensates for the change in cord length.

3.3.4.2 Cord Plyer/Tensioner Controls. The cord plyer control equipment is diagrammed in Figure 3-45. Eight stopping positions are required for proper operation of the forward cord plyers during the normal and cutoff cycles. An additional eight stopping positions will be required for the aft plyers. These precalculated position data will be stored in the BCU memory and compared to encoder position data which are monitored at a rate of 40 times/sec (25 ms). The stopping accuracy required is ±1.27 cm.

Figure 3-46 shows the cord plyer/tensioner control block diagram. Identical sets of controls are required for the forward and aft cord plyers. Operation of the forward and aft cord plyers is similar, except for stroke and timing differences. For the sake of brevity, only operation of the forward cord plyer is described below.

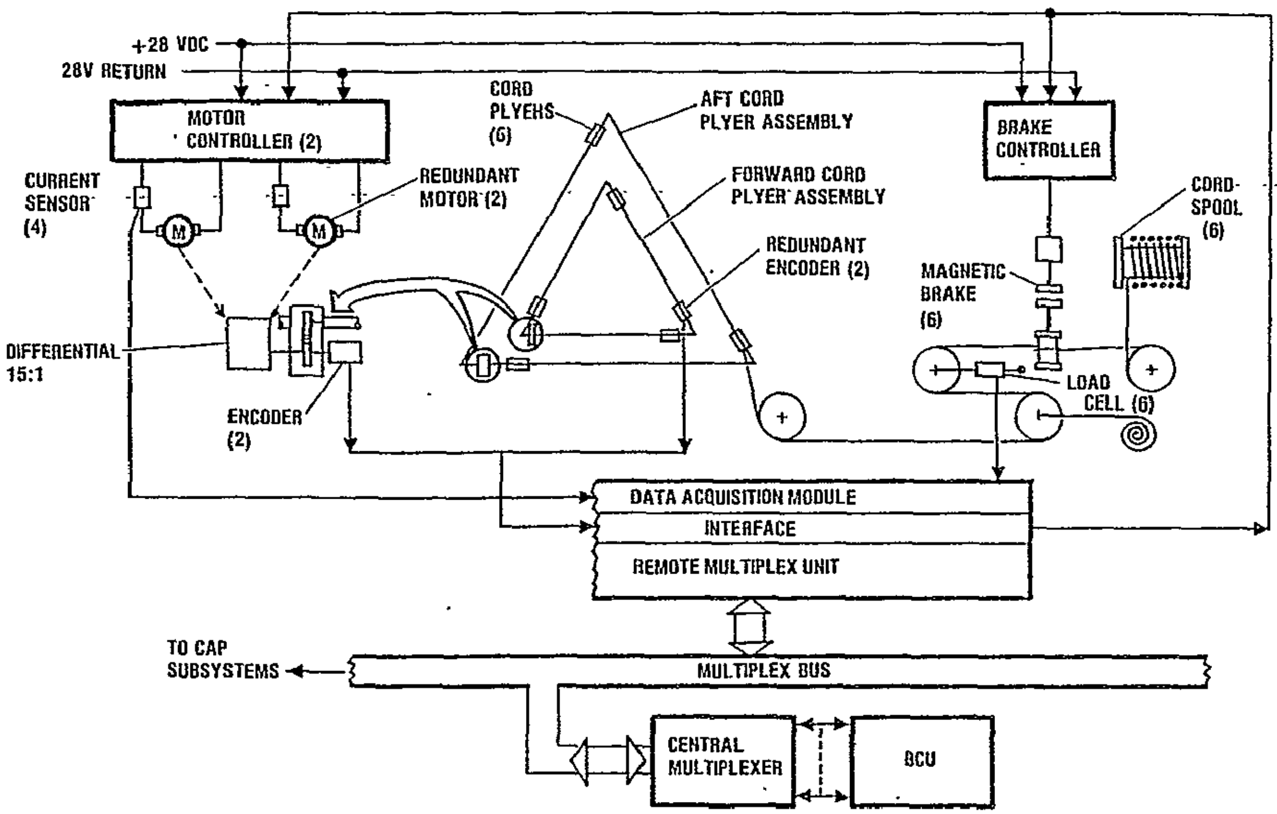

Figure 3-45. Cord plyer/tensioner control equipment diagram.

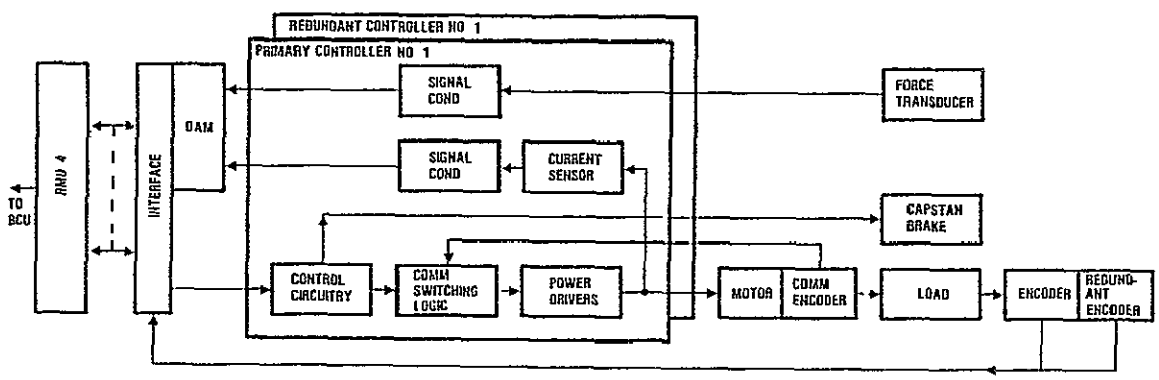

Figure 3-46. Cord plyer/tensioner controls block diagram.

Three cord plyers operate simultaneously because of mechanical interconnection of the three ball reversers with flexible couplings. If any one of the flexible couplings should fail, the three cord plyers will continue to operate. The cord plyers will operate in one of two distinct cycles, normal cycle or cutoff cycle. Timing diagrams for these two cycles for the forward cord plyers are shown in Figure 3-47 and Figure 3-48.

During normal cycle operation, the cord plyers will be initially positioned at the ready-to-weld "start" position. This position will provide a reference for encoder tracking. When the cord plyer operation is scheduled and ready for activation, the BCU will transmit a motor and capstan brake control command word to the cord plyer controller via the multiplexer. The command word will consist of 8 bits and will contain the following commands:

Motor Start/ Stop	Motor Fwd/ Rev	Redun Motor Start/ Stop	Redun Motor	Brakes On/Off	SP.	SP.	SP.

The motor controller electronics, upon receipt of motor "start" and direction (fwd/ rev) signals, will activate the drive causing the cord plyers to travel on the ball reversers to the "pierce" positions on the opposite ends. This operation will start at the beginning of a normal drive sequence and will occur simultaneously with cap movement.

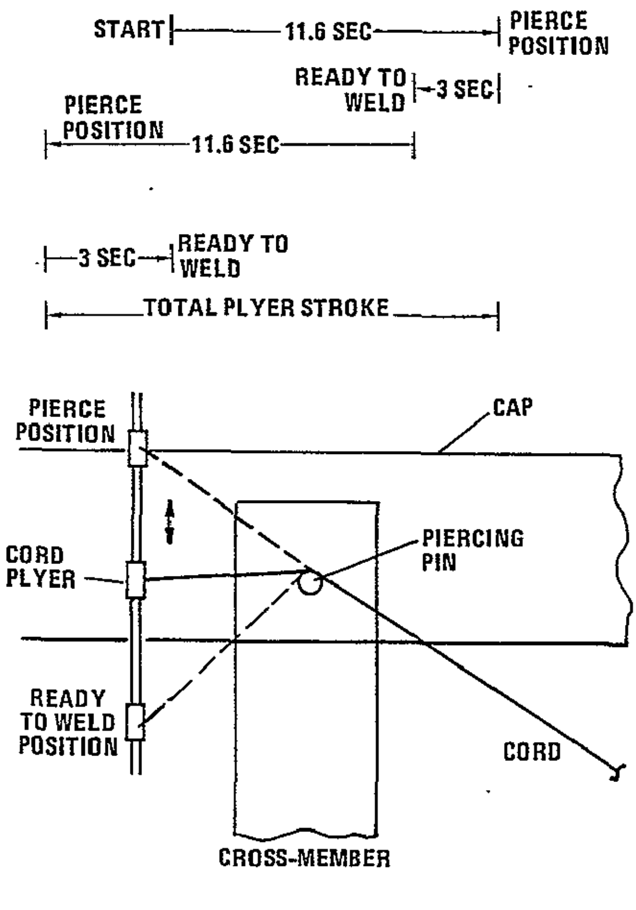

Figure 3-47. Normal cycle.

Using a 200 count/revolution incremental encoder will require a total of 19,456 counts for one complete cycle of the forward cord plyers. A 16-bit register will be used to count encoder pulses and will be reset to zero at the reference "start" position. The BCU will monitor the encoder data register located in the interface circuitry every 25 ms.

At a cord plyer speed of 10.7 cm/sec (4.2 in/sec), the travel distance between samples is 2.675 mm. Since the stopping tolerance of the cord plyer is ±1.27 cm, the sampling rate should be more than adequate.

The BCU will compare encoder data with the precalculated position data. Upon reaching the "pierce" position, the BCU will command the motor to stop. Dynamic braking techniques will be used because of low friction loads on the cord plyer. After the motor has stopped, encoder data will be examined for stopping error analysis.

Current sensors are implemented to monitor motor operation. Analog current readings will be presented to the data acquisition module which converts the analog data to an 8-bit digital word. The BCU will sample these data every 25 ms to analyze fluctuating current or overload conditions. If the BCU detects faulty motor operation, a new command word will be transmitted, shutting off the faulty motor and energizing the redundant motor. The BCU will notify the Orbiter crew of the failure.

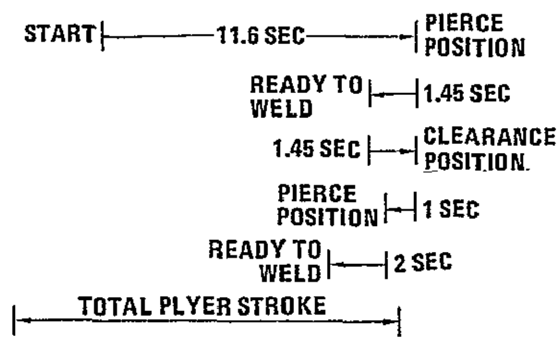

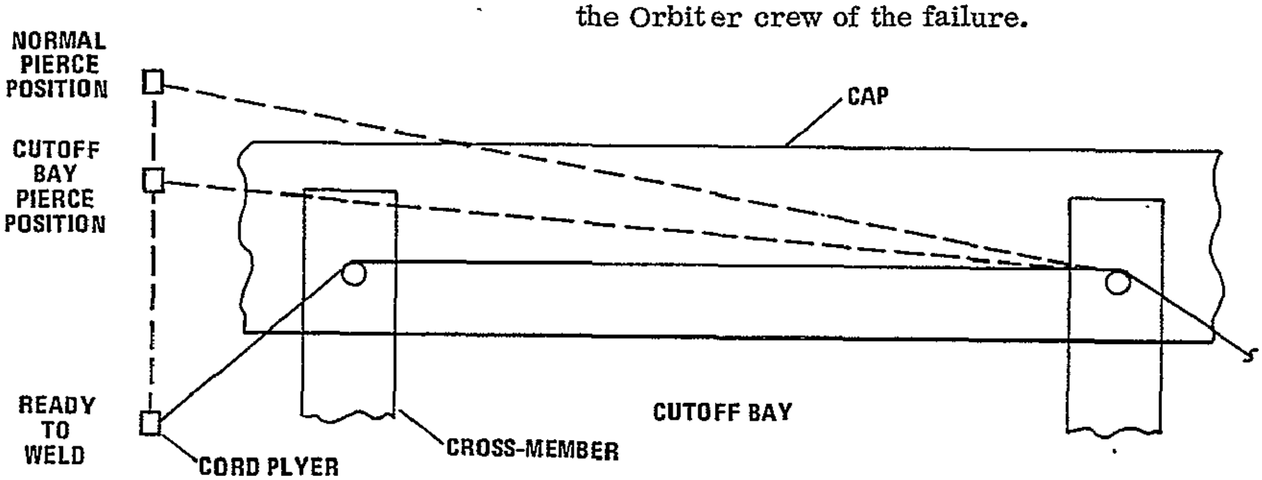

Figure 3-48. Cutoff cycle.

If encoder data are not being incremented while either motor is in the operation cycle, a redundant encoder, which has been monitoring the operation simultaneously, will provide data to the BCU for redundant tracking. If neither encoder is incrementing, the BCU will command the motor to stop.

After the cord plyers have stopped in the "pierce" position and after a predetermined time delay (23 sec after start of the cap drives), the BCU will issue the control command to energize the capstan brakes. These brakes provide tension to each cord as the cap sections progress through the beam builder. The brakes stay energized until the weld operation has been completed.

Force transducers measure cord tension. Force transducer output analog signals are converted to digital data by the data acquisition module. An 8-bit data word will provide adequate resolution of the force transducer readings. While the brakes are energized, the BCU will monitor the digital data, verifying that force applied to the cord by the tensioning mechanism is within allowable limits (44.5 ±8.9 N). If the cord tension is outside its limits, the BCU stops the beam building process until the error has been analyzed and corrective action has been taken.

After the cap drives stop, no further operation of the cord plyer mechanisms occurs until after the pin has pierced a hole in the caps and cross-members. When the piercing operation has been completed and determined to be satisfactory by the welder load cell, the BCU issues a command word energizing the cord plyer motor. The cord plyers will move to the ready-to-weld position as determined by prestored data in the BCU. When in position, the BCU commands the cord plyer motor to stop.

With the plyers in the ready-to-weld position, the BCU initiates the weld operation. After the weld operation is complete, the BCU issues a command releasing the capstan brakes. This completes 1/2 cycle operation of the cord plyer mechanism. The second 1/2 cycle operation occurs after the normal fabrication sequence has been completed and the cap drive has been initiated to form the next bay length. The second cycle operates in the same manner as previously discussed, but to the opposite cap member.

The cord plyer returns to its reference "start" position every two bay lengths. This process continues until the required number of bay lengths have been produced.

The cutoff cycle consists of the last-bay drive and fabrication sequences and the cutoff bay drive and fabrication sequences. The cutoff cycle is initiated prior to beam termination. The BCU keeps a count of completed normal bay lengths and initiates a cutoff cycle one bay prior to the required beam length.

The last-bay drive sequence is the same as a normal bay drive sequence. During fabrication of the last bay, the BCU commands the cord plyers to positions in line with the piercing pin after the piercing operation has been completed, as shown in Figure 3-48.

When the welding operation is completed, the BCU commands the cord plyers to reverse, returning them to their previous pierce positions. After the last-bay fabrication sequence is completed, the cutoff bay drive sequence is started. The cap drives are energized and the capstan brakes are also energized simultaneously to provide proper cord tension for the shortened cutoff bay.

After the cap drive completes its shortened drive cycle, the cutoff bay fabrication sequence begins. Because the cutoff bay is shorter, the cord will not be positioned correctly under the cross-member before the piercing operation. In order to allow time for this operation, the cross-member positioner stops before the cross-member comes in contact with the cap.

The BCU commands the cord plyers to move a short distance, bringing the cords into the proper cutoff bay pierce position under the cross-members. The cross-member is then positioned against the cap for the piercing operation. After piercing, the cord plyers are commanded to move to the ready-to-weld position. After completion of the welding operation, the system is ready for the next normal bay sequence. Completion of the next normal bay advances the cutoff bay into position for cutting operations.

3.3.5 JOINING SUBSYSTEM. The joining subsystem consists of six ultrasonic welders, three welder positioning mechanisms, one anvil drive mechanism, and associated controllers. The welders used in the preliminary design are 20 kHz units with multi-spot weld horns designed to produce the weld joint configuration selected in the Subsection 2.2.2 trades.

3.3.5.1 Cross-member Welder. Cord capture and attachment of the cross-members to the cap is accomplished by an array of six ultrasonic welders. Each pair of welders is powered by one power supply with an output signal of 20 kHz. This high frequency signal is fed to a piezoelectric transducer attached to each weld tip (Figure 3-49). The transducer converts the oscillations of electrical energy into mechanical vibrations of the same frequency. The weld tip is forced against the cap and cross-member. Heat is developed by the vibrational energy causing internal friction (hysteresis) in the composite material. When sufficient heat is generated to liquify the polysulfone, the ultrasonic energy is turned off. The material will flow under the constant pressure of the weld tip and as it cools and resolidifies, the bond is complete.

3.3.5.1.1 Ultrasonic Welder and Controls. The welder is controlled by a power supply (Figure 3-50) which draws on the Space Shuttle's 28-Vdc system. The power supply performs four major functions for the welder.

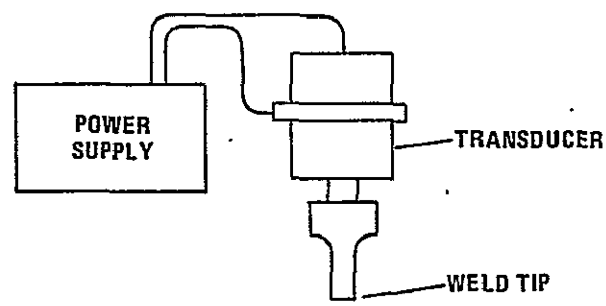

Figure 3-49. Ultrasonic welder.

a. The oscillator is an ac inverter, changing the 28-Vdc to a 20 kHz ac signal. The oscillator does not alter the voltage in any way and only stays on for a few microseconds to produce the initial high frequency oscillations in the total system.

b. The amplifier section of the power supply also runs directly from the 28-Vdc power of the Space Shuttle. The power output is a signal of 300 watts, 1500 volts at the initial frequency of 20 kHz provided by the oscillator. This high frequency, high voltage signal, when fed into the transducer, causes the piezoelectric crystals in the transducer to expand and contract. The conversion of electrical energy (300 watts) into mechanical oscillations is very nearly 100% efficient.

c. The efficiency analyzer "reads" the energy going into the material by comparing the input energy (wattage from the amplifier to the transducer) to that reflected (sonic waves) from the horn tip back to a sensor on the top of the horn. The efficiency analyzer is adjusted to the optimum energy (watt-seconds or joules) required to weld the graphite/polysulfone as determined by experiment. For example, the desired weld cycle might be 100 watts for one second

(100 joules) at 30 psi. If efficiency of input energy drops to 80 watts, the efficiency section of the amplifier will detect this loss through the efficiency sensor and will lengthen the weld cycle to 1.25 seconds, thus maintaining the desired 100 joule input.

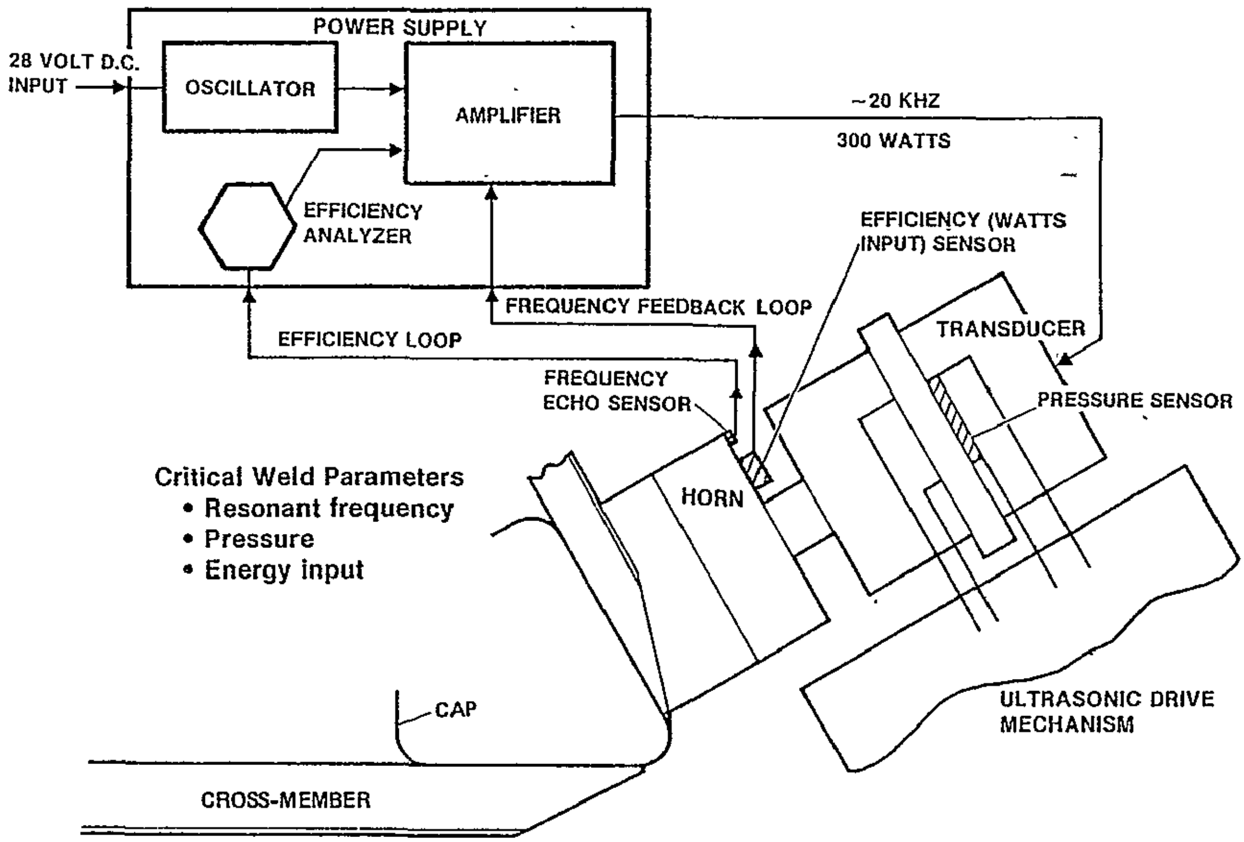

Figure 3-50. Ultrasonic welding control concept.

d. A frequency feedback loop is also used to ensure exact system frequency, regardless of environmental cycles and workload cycles. As the welder is used, temperature fluctuations can cause the resonant frequency of the system (transducer and weld tip) to change. The speed of sound in the horn and the distance this sound must travel are both functions of temperature and, therefore, affect resonant frequency. The oscillator only approximates the resonant frequency and sets up the initial vibrations in the horn. The horn then tries to oscillate at its own temperature-dependent resonant frequency exactly. A sensor at the top of the horn picks up this resonant frequency and, through the frequency feedback loop, the amplifier is fed this exact resonant frequency. This method ensures that the amplifier is continually producing the required frequency and the system is then independent of temperature fluctuations caused by environmental changes and workload cycles.

Three configurations of converting electrical energy to vibratory mechanical energy at ultrasonic frequencies are used to varying degrees in industrial applications. These are shown in Figure 3-51. Presently, the most common configuration for assembly line operations consists of a transducer, booster (with hold ring), and horn in a stack approximately 38 cm high. The three components are securely attached together to form a rigid path for transferring the ultrasonic mechanical energy produced by the transducer.

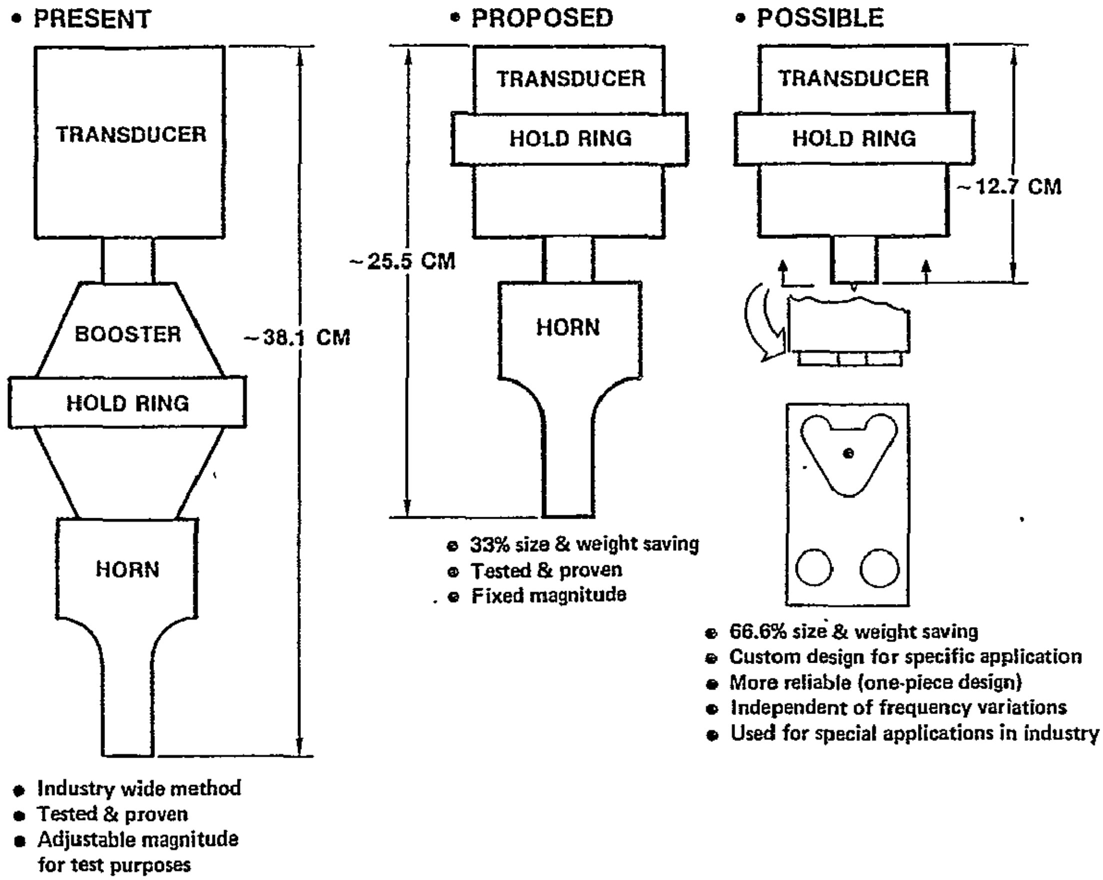

Figure 3-51. Ultrasonic welder design concepts.

The transducer is composed of piezoelectric crystals which are cut to produce the maximum expansion in the plane perpendicular to the plane of the weld surface. Due to a mass differential above and below the nodal plane, most of the mechanical energy travels toward the weld surface.

The booster may also have this characteristic of mass differential above and below its nodal plane. If, for example, the booster has equal mass above and below the plane, the magnitude of actual weld tip travel during ultrasonic vibration is exactly that of the lower tip of the transducer. However, if the booster has two thirds of its mass above the nodal plane, then magnitude of oscillation is doubled at the weld surface. This attachment is advantageous for experimental purposes to determine the optimum weld tip travel for a certain material and weld tip configuration. When this magnitude is determined, the booster can be removed and the horn can be designed to produce the required tip travel.

In the proposed configuration, removal of the booster from the weld stack reduces the length of the welder by 33% (12.7 cm for 20 kHz welding) and mass by approximately 40% since the mass of the booster is greater than any of the other components when the weld pattern is small.

For highly repetitive and critical weld requirements, it is possible to design the transducer itself to produce the optimum weld tip travel, thus eliminating the need for the stepped horn. The transducer tip is configured to provide the weld surface and the welder stack is again shortened by 33% becoming only 12.7 cm long. The diameter of the transducer can also be altered for specialized applications (e.g., the beam builder) and mass would also be reduced to approximately 25% of the original three-component welder design.

3.3.5.1.2 Quality Control. Reliability of ultrasonic spot welding can be assured by identifying all factors which can affect weld quality and controlling them in one of two ways. First, and most reliable, is to design the welding apparatus to completely eliminate the variability of critical factors. Second is to provide real-time in-process control of the variables so the system inspects and corrects during the cycle.

The design of the ultrasonic welder and the power supply has eliminated most of the critical parameters as variables. The remaining factors (frequency, amplitude, pressure, weld time, hold time, and efficiency) can be sufficiently controlled to ensure consistent weld quality.

Frequency of oscillation is initially provided electronically by the oscillator portion of the power supply. This frequency (approximately 20 kHz) is amplified to the required voltage and fed to the transducer. The transducer itself is somewhat independent of frequency (20 kHz ± 5 kHz is acceptable). The efficiency of energy transfer through the horn is very sensitive to even slightly out-of-phase frequency changes. This critical weld parameter is totally controlled by the implementation of a frequency feedback loop which uses the horn as the frequency-determining element and the frequency, therefore, is guaranteed to be exactly resonant in the horn.

The amplitude of oscillation is fixed by design. The weld tip is attached directly to the transducer, which is a special design for this application providing the precise 1.905×10^{-3} cm (0.00075") travel proven to be the most effective in laboratory tests.

The pressure applied by the weld tip on the cross-member and cap during the weld cycles is controlled by the positioning mechanisms discussed below. A sensor on or near the transducer hold ring indicates proper weld pressure.

The length of time the ultrasonic energy is on during horn tip pressure is the most critical of the variables since it determines the amount of energy which enters the spot weld. This weld time is controlled by the efficiency analyzer portion of the power supply. Welder efficiency is controlled by monitoring the input energy and reflected energy from the weld tip. The difference is the energy entering the parts to be welded. This quantity is continuously monitored and corrected to ensure constant energy input to the weld interface.

Hold time in the weld schedule is the time the pressure of the weld tip remains on the parts after ultrasonic vibration has ceased. It is required to ensure that the parts are pressed together while the molten resin cools and solidifies, and is typically fixed at approximately 0.5 second. Proper hold time is ensured by a timer in the ultrasonic welder drive circuitry which is activated when ultrasonic energy is turned off. A preprogrammed delay before raising the weld tip ensures that the resin has had time to cool and form a satisfactory bond.

Quality of the ultrasonic weld is further verifiable by direct ultrasonic inspection techniques. Experimentation with ultrasonic inspection of various composite materials has proven the feasibility of detecting very small voids in the material. Upon completion of the basic weld operation, a brief direct reading of ultrasonic energy transmissibility would be made, using the weld horn itself, to confirm weld quality during the beam builder pause cycle.

3.3.5.2 Welder and Anvil Positioning Mechanisms. The preliminary design drawing of the welder and anvil positioning mechanisms is shown in Figure 3-52. Each welder positioning mechanism is supported by an external support beam. It consists of two removable ultrasonic weld head assemblies, which are supported and translated by spring-preloaded, geared-parallelogram linkages and driven by one universal drive unit. A beam cap support roller completes the assembly.

The three weld head positions are: (1) the fully retracted position, which allows adequate clearance for the cross-members during transfer into the installation position; (2) the pierce position, where the piercing pin on each weld horn has penetrated the cross-member and cap; and (3) the weld position where the weld horn is engaged and properly loaded to enable the welds to be accomplished.

The anvil drive mechanism is supported by the center pedestal structure. It consists of one redundant universal drive unit, which is splined to a cam shaft that drives, by means of cam follower linkages, the three spring-preloaded anvil drive tubes. The anvil shaft slides in a bearing supported by the internal support beam.

After completion of the welds, the anvils are retracted to allow the weld zones to move on freely and to minimize friction drag on the caps while the beam is advancing one bay length.

3.3.5.3 Welder and Anvil Controls. Welder and anvil operating parameters are:

a. Anvil

Anvil engaged position travel distance	10.0 mm
Anvil closure time	1.0 sec
Anvil retraction time	1.0 sec

b. Weld Heads

Weld head engaged position travel distance	13.97 cm
Weld head pierce time	2.0 sec
Weld head activation time	3.0 sec
Weld head retraction time	3.0 sec
Weld head pressure	178 N

The joining subsystem control equipment is diagrammed in Figure 3-53. The sequence of operation is as follows.

The BCU commands the anvils to be inserted into the cap material at the start of the beam assembly process. The anvils will support the caps until completion of the welding process. The motor controller energizes the anvil drive motor. A position sensor will monitor cam position and will provide input data to the BCU for motor shutoff control. Figure 3-54 shows the weld subsystem controls block diagram. Current sensors are used to monitor motor operation.

After the cross-members have been positioned on the caps, the BCU issues a command to the weld head controllers to start the drive motors and move the heads through the piercing operation.

The piercing pins on each weld horn will be driven against the cross-members until the correct contact pressure is achieved. Pressure sensors located in the weld heads will measure this contact pressure and provide analog signals to the data acquisition module for monitoring by the BCU. When correct pressure is achieved, the BCU deactivates the weld head drive motors and signals the welder electronics to start the piercing operation.

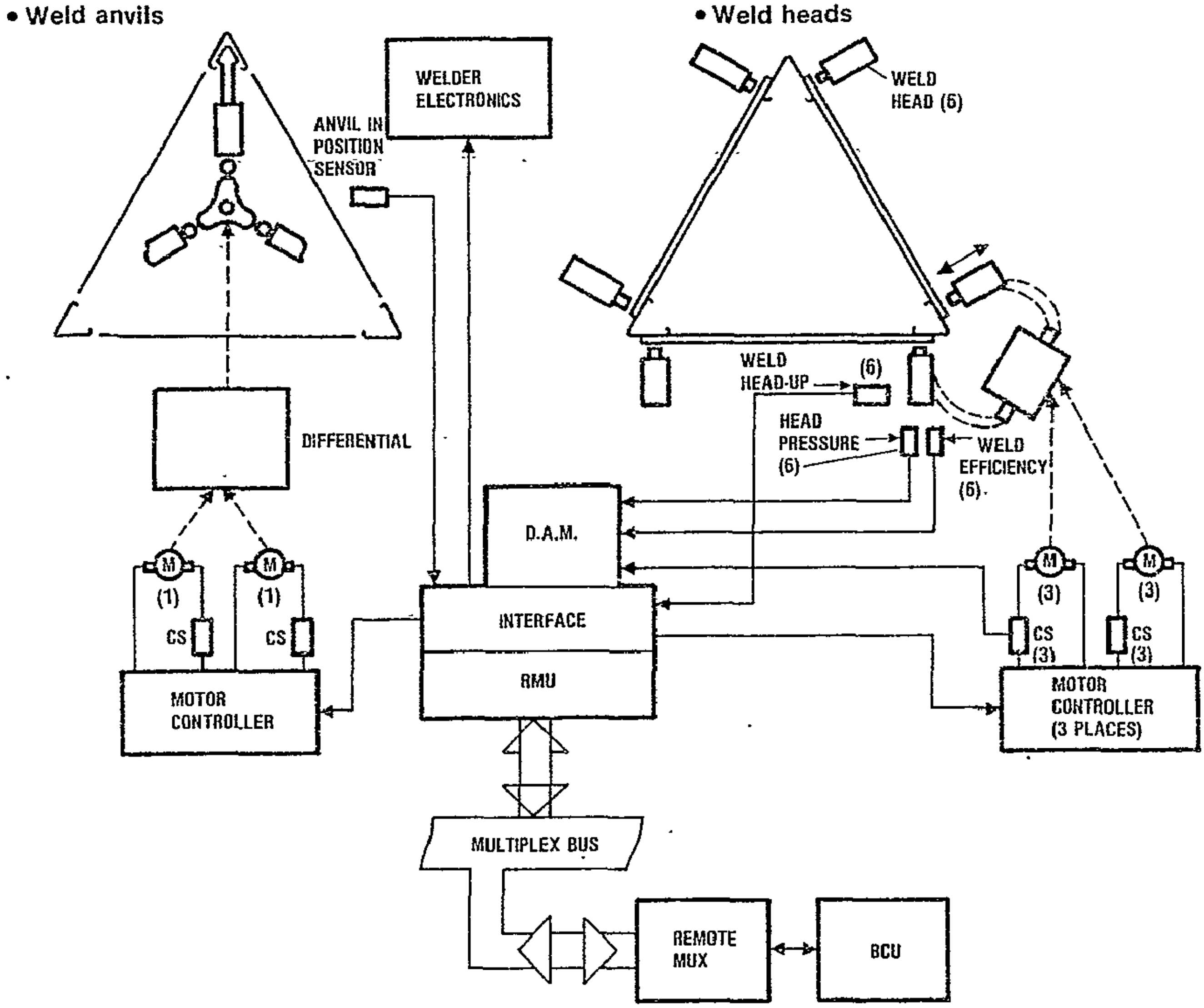

Figure 3-53. Joining subsystem control equipment diagram.

As energy is applied to the weld horn, the weld tip vibrates and transmits this mechanical energy into the material. As this heating occurs, the piercing pins pierce the cross-members and associated caps. Efficiency sensors and frequency sensors will provide feedback data to the welder electronics for process control. The BCU additionally monitors these data for diagnostic purposes. When the piercing operation is complete, contact pressure of the weld horn on the cross-member has been reduced. After sensing this reduced pressure, the BCU will signal the electronics to stop the energy flow and the cord plyers to move to the ready-to-weld position.

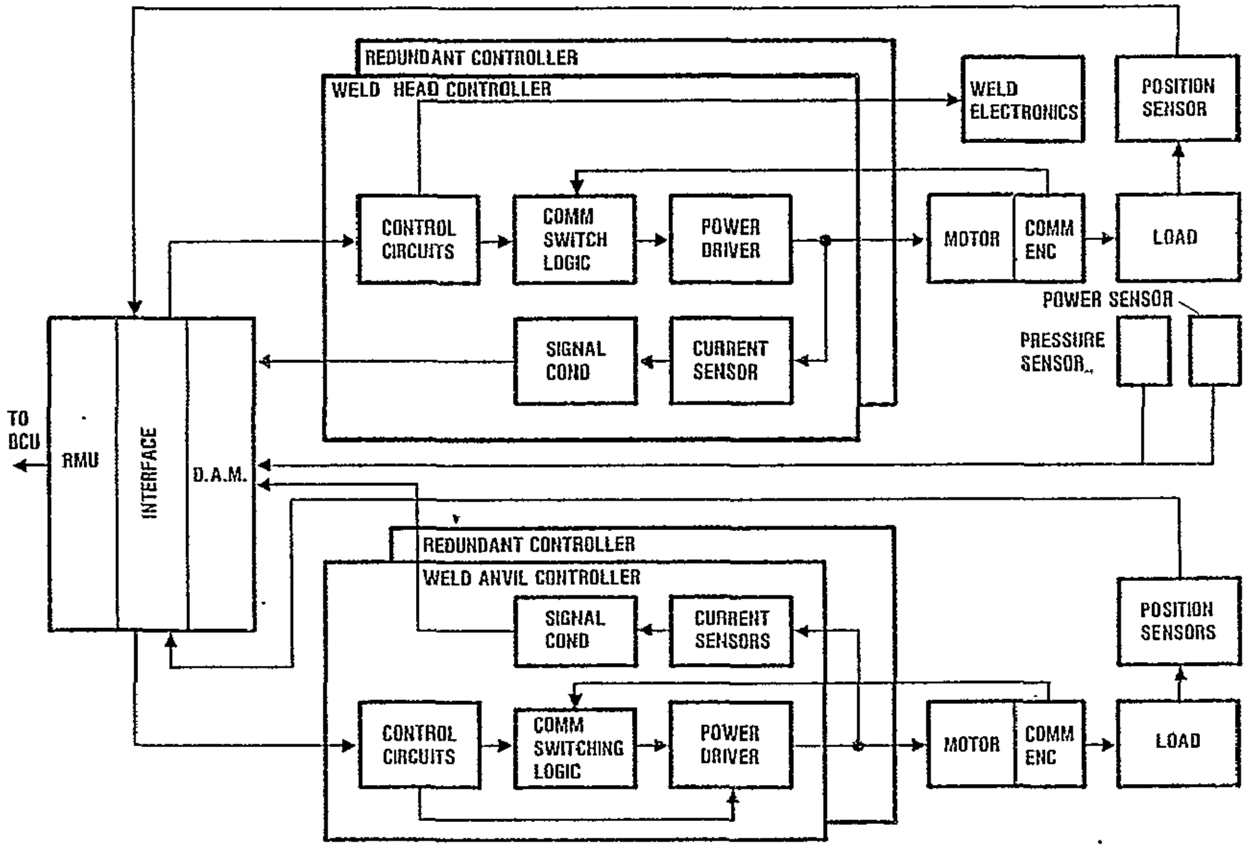

Figure 3-54. Joining subsystem controls block diagram.

With the cord plyers in the ready-to-weld position, the BCU signals the motor controllers, activating the motors until proper contact pressure is once again achieved. The drive motors are then deactivated by the BCU and welder electronics are commanded to start the welding process (discussed in Subsection 3.3.5.1).

After the welding has been completed, the BCU commands the motor controllers to retract the weld heads and anvils, allowing clearance for the next cap drive cycle. Position sensors provide signals indicating the heads and anvils have reached their retracted positions and the BCU deactivates the drive motors. Hall effect current and position sensor will be used to monitor motor current, and anvil and weld head positioning. Load cells will be mounted in each weld head assembly to monitor contact pressure.

3.3.6 CUTOFF SYSTEM. The cutoff subsystem consists of three beam cutoff mechanisms and associated controllers. The beam cutoff mechanism shown in Figure 3-55 shears each cap and cord member to separate a completed beam from the beam builder. The cutoff device is normally retracted to allow the cross-members to travel past the outer clamps.

In preparation for beam cutoff, a short cutoff bay (60 cm) is manufactured by the beam builder as described in Subsection 3.3.4.2. The short bay is advanced to the point where the cutoff shears are in the center of the short bay for cutoff.

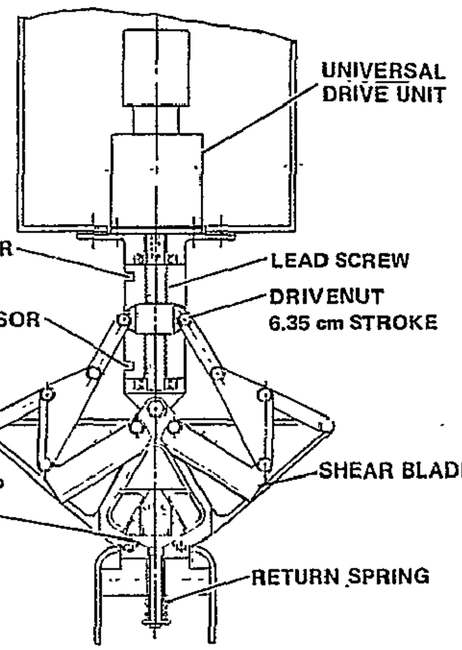

Figure 3-55. Beam cutoff mechanism.

The cap cutter drive has been revised to incorporate the universal drive unit. The drive unit rotates a single lead screw in a drive nut. As the drive nut is extended, the clamps engage the internal backup mechanism and force the backups into position. The shear blades are spring-loaded to allow the clamps to fully engage before the shear blades penetrate the cap. The shear blades are then driven through the caps as the actuators continue to extend. This also shears the cords as they lie along the sides of the cap.

The controller for the cap cutter drive is similar to the controller for the cooling platen drive, shown in Figure 3-27. Hall effect position sensors will monitor for open and closed cutter positions. Hall effect current sensors will be used to monitor motor current for excess motor load conditions and motor functioning conditions.

3.3.7 <u>STRUCTURE.</u> The beam builder structure preliminary design is the same as the initial conceptual design except for a few dimension changes and the addition of ground-handling provisions.

The initial structure design developed in Part II was composed of welded aluminum elements arranged as shown in Figure 3-56. This structure consists of three major segments: a forming section support, a central "spider", and an assembly section support. The forming section support is a trussed hexagonal system for supporting the cap forming mechanics and the cross-member storage clips. The central spider is a three-legged box structure for providing a transition load path from the internal forming section support to the external portion of the assembly section supports. Other subsystems modules are attached to the spider and cylindrical control hub. The assembly section support consists of three external beams and three internal beams for providing support for the cord plyers, welders, and cutoff subsystem modules.

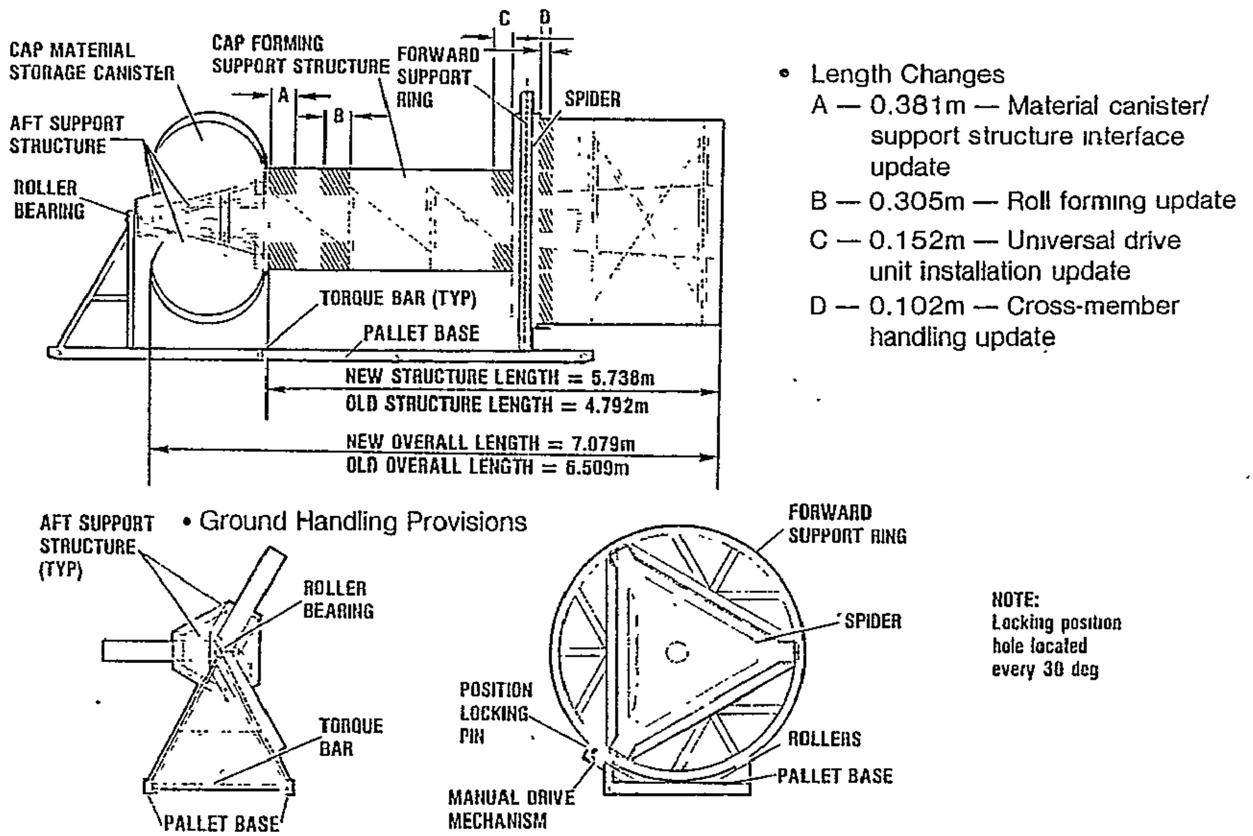

Figure 3-56. Beam builder structure update.

Length changes to the initial design total 0.946 meter. The major changes are:

a. Increase of 0.381 m in the forming section support to provide rigidity at the material canister/support structure interface.

b. Increase of 0.305 m in the forming section support for the updated roll forming process.

c. Increase of 0.152 m in the forming section support for installation of the universal drive unit in the forming subsystem.

d. Increase of 0.102 m in the assembly section to provide clearance for the cross-member handling mechanism.

The ground test beam builder structure unit is the same as the flight version. Both units will have detachable ground-handling provisions. These ground-handling provisions consist of:

a. Aft support structure and roller bearing to allow structure rotation.

b. Forward support ring for structure support and manual drive/positioning capability.

c. Pallet base for handling and transportation.

3.3.8 AVIONICS AND CONTROL SUBSYSTEM. The beam builder avionics and control subsystem concept created in Parts I and II has been revised and updated to provide more efficient data and control interfaces. The new subsystem interface arrangement is shown in Figure 3-57.

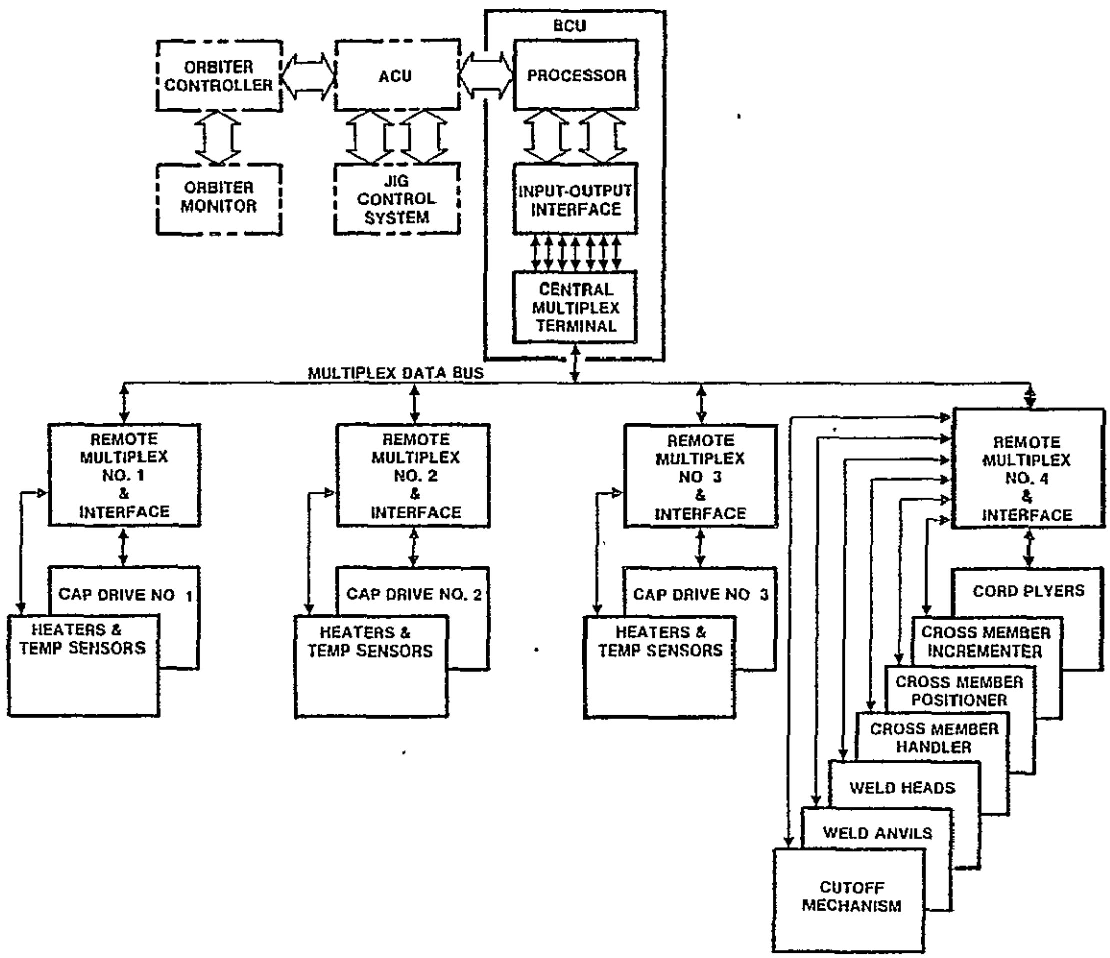

Figure 3-57. Beam builder avionics and control subsystem update.

The avionics and control subsystem contains one central controller, called Beam Controller Unit (BCU), which interfaces with the forming and assembly subsystem local controls via a multiplex system. The multiplex system provides the appropriate control circuitry necessary for transmission of sensor data and control data to and from the BCU. Data is transmitted in serial format over a 2-wire half duplex bus.

Controls for each individual subsystem have been described in previous sections. Remote multiplexers 1, 2, and 3, shown in Figure 3-57, are part of the forming subsystem with one multiplexer assigned to each cap forming machine. Remote multiplexer number 4 interfaces with the other fabrication subsystems associated with beam assembly operations.

SCAFE beam building operation is controlled by the Orbiter crew using Orbiter control and monitoring equipment located in the aft cabin, as reported in Parts I and II. The chain of communication will be from Orbiter controller to ACU to BCU, and return.

The overall control philosophy of centralized real-time process control, compared to localized sequential control, has these advantages and disadvantages:

Advantages	Disadvantages
Less hardware	Greater software effort
Less power	More I/O handling
Greater reliability	More complex local control at subsystem level
More flexibility	More test equipment

Overall inter-machine timing and synchronization and the real-time software executive for the beam builder have been defined and are described in the following sections.

3.3.8.1 Timing and Synchronization

3.3.8.1.1 Normal Bay. The excitation timeline for the feed and fabrication of a normal bay length is shown in Figure 3-58. The feed and fabrication sequence will be initiated by the Orbiter crew after the preheat sequence has been completed. The total time necessary for the feed and fabrication sequence is 80 seconds. The timing diagram indicates the start/stop times of the drives and actuators associated with each mechanism. The number within each time bar represents the actuation time for each drive or actuator. This timeline will be the basis for scheduling control to be provided by software application programs.

Before initialization, the cord plyers are positioned at the ready-to-weld positions. Upon initialization, three cap drives are energized and start pulling the strip material through the forming sections. One bay length is formed in 40 seconds.

The forward cord plyers are energized simultaneously with the cap drives. Three seconds later, the aft cord plyer is energized. This delay allows the forward cord plyer to reach the outermost pierce position before the adjacent aft cord plyer, thus eliminating interference. Cord plyers travel for 11.6 seconds.

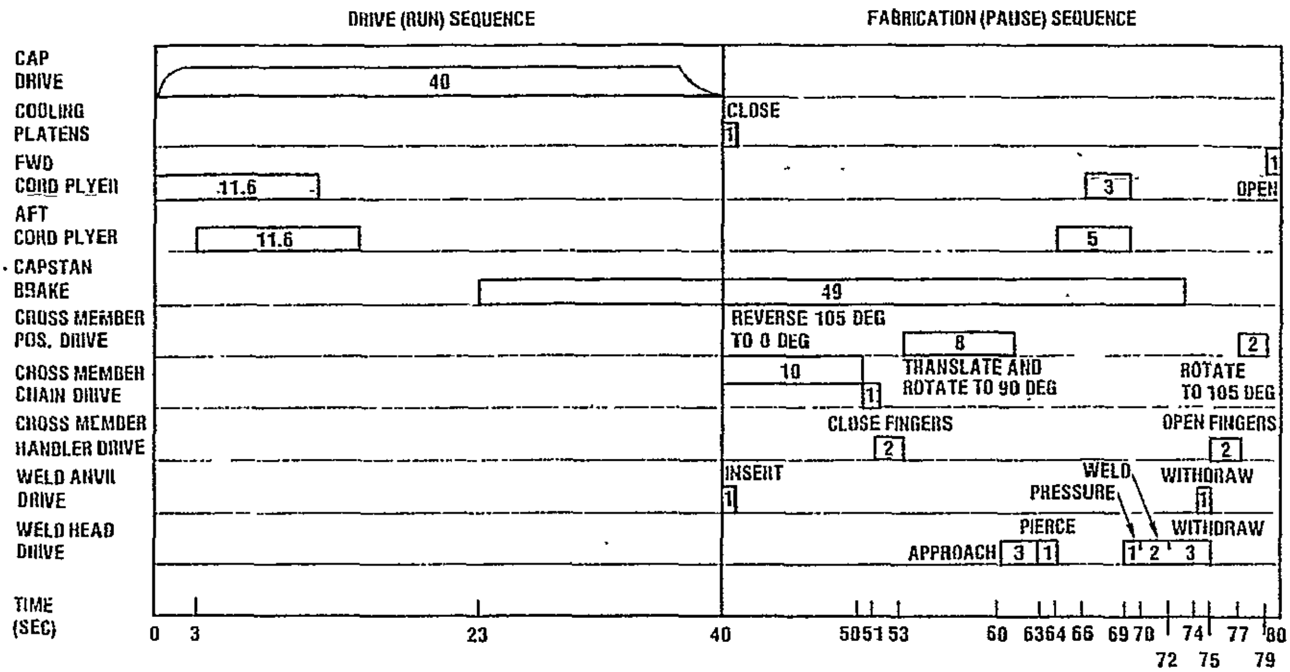

Figure 3-58. Normal bay timing and synchronization.

Approximately 8 seconds after the aft cord plyers are deactivated, the cord plyer capstan brakes are energized, providing tension to the cords. The brakes remain energized (49 seconds) until the welding operation is completed.

After the cap drives have stopped, the fabrication sequence begins with simultaneous operation of the cooling platens, the cross-member positioners, and the weld anvil drive.

The cooling platen drives are energized for approximately 1 second, closing the cooling platens around the formed cap. The cooling platens perform the final forming operation and cool the cap material. Although material cooling does not require platen closure for the entire fabrication sequence, the platens are kept closed until the end of the fabrication sequence.

The cross-member positioners rotate and translate the handler arms from the 105-deg position to the cross-member pickup position. This operation takes approximately 10 seconds.

The weld anvil drives are energized for 1 second, causing the anvil to be inserted against the caps. The primary purpose of the weld anvil is to provide support during the welding process. By inserting the anvil at the beginning of the fabrication sequence, cap support is provided for the duration of the entire sequence.

After the cross-member handler has reached the pickup position, the cross-member chain drive is energized (1 second), incrementing the cross-member storage clip. Three cross-members are then in position for closure of the handler fingers.

The handler drive is energized (2 seconds) causing the handler fingers to close around the cross-member lips. After the cross-members are clamped, the positioner is energized for approximately 8 seconds, translating and rotating the handler arms to the 90-deg position. The cross-members are now placed in proper position across the cap members.

One second prior to completion of positioner rotation, the weld head drives are energized. After approximately three seconds, the weld head piercing pins are in contact with the cross-member. When the proper amount of pressure has been established, the welder power supply is activated causing the pins to pierce the cross-members and caps.

With the pin in position in the pierced hole, the cord plyers are energized causing the cord to wrap around the piercing pin. The aft cord plyers are energized first to allow clearance for the forward plyers. After a 2-second delay, the forward plyers are energized. All plyers are deenergized when they reach the ready-to-weld position.

Since contact pressure of the weld heads had been reduced by the piercing operation, the weld head drives must be energized briefly to allow weld head pressure to be reestablished. The welder power supplies are activated resulting in the cross-members to be welded to the caps.

After the welding process has been completed, the weld heads and weld anvils are withdrawn to their fully retracted position. The cross-member handlers are then energized causing the finger grips to release the welded cross-member. After release, the cross-member handlers are rotated to the 105-deg position to allow clearance for the next drive and fabrication sequence.

The cooling platens are then opened, releasing the cap material. This operation completes the fabrication sequence. A drive and fabrication sequence is then repeated for each additional bay length required to complete the beam. Prior to beam cutoff, a special last-bay fabrication and cutoff bay drive/fabrication sequence is required. This sequence is described below.

3.3.8.1.2 Cutoff Bay. A deviation from the normal bay drive and fabrication sequence is required to terminate and cut off a beam builder. Termination of a beam will require a special last-bay fabrication sequence, a cutoff bay drive sequence, and a cutoff bay fabrication sequence. The excitation timeline for these sequences is shown in Figure 3-59.

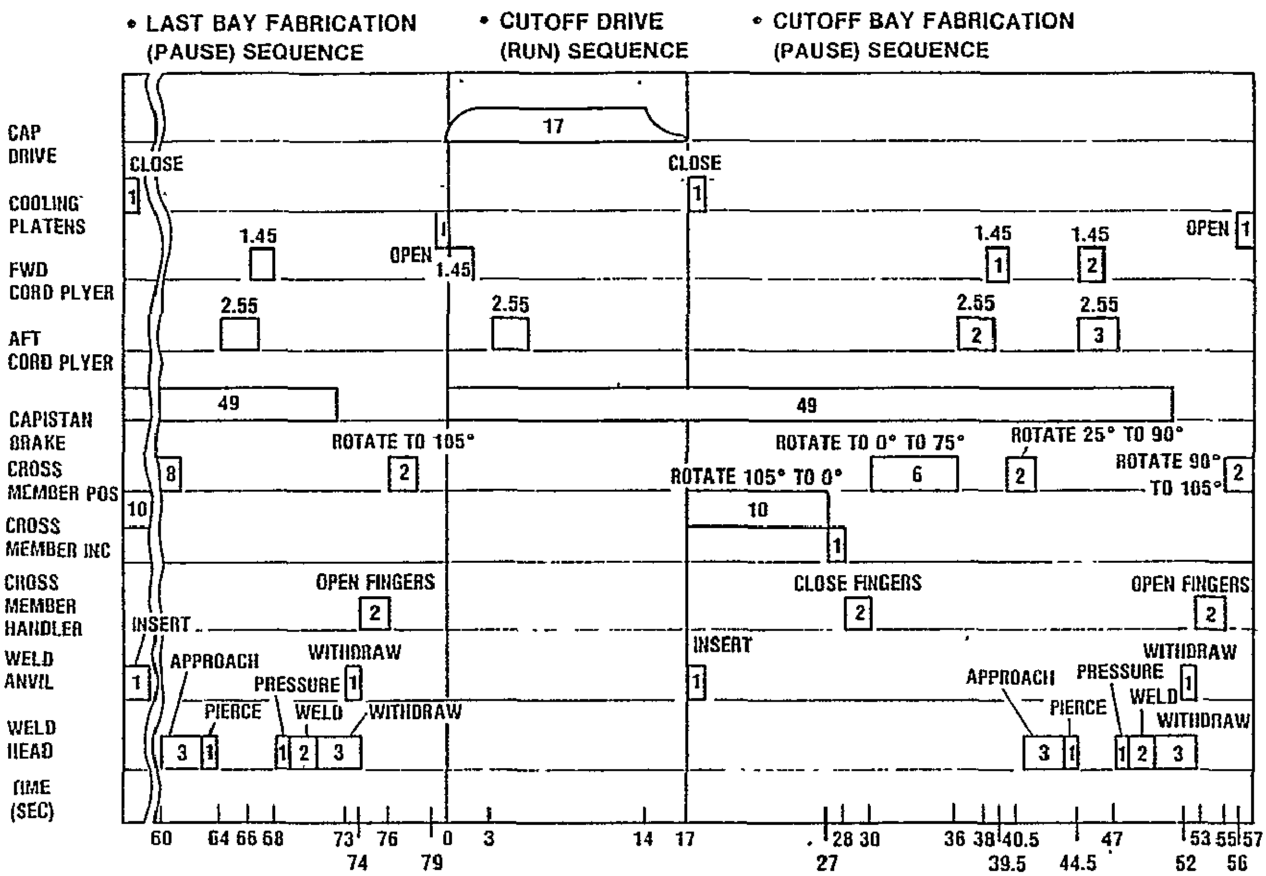

Figure 3-59. Cutoff bay timing and synchronization.

The only difference in the last-bay fabrication sequence from the normal bay fabrication sequence is the operation and positioning of the cord plyers. During last-bay fabrication, the cord plyers are moved to a position in line with the pierce pin instead of the normal ready-to-weld position, where the cord is wrapped around the pin. This positioning requires activation of the aft cord plyer drive for 2.55 seconds and, after a 2-second delay, activation of the forward cord plyer drive for 1.45 seconds. After the welding process has been completed and after the capstan brake has been deenergized, the cord plyers are reversed and moved back to the previous outermost pierce position to provide clearance for the cutoff bay fabrication process. This movement requires activation of the forward cord plyer for 1.45 seconds and, after a 3-second delay, the aft cord plyer is activated for 2.55 seconds. When the cooling platens open, the beam builder may proceed with the cutoff bay drive sequence.

Since the cutoff bay is only 60 cm long, the cap drive is energized for 17 seconds instead of 40 seconds as for a normal bay length.

The capstan brake cord tensioners are energized at the beginning of the cutoff bay drive cycle to provide sufficient time for required cord tensioning. The brakes are not released until the welding operation of the cutoff bay fabrication process is complete.

The shorter cutoff bay requires a change in sequencing of the cross-member positioner and the cord plyers. Since the bay is shorter, the cords will not be positioned correctly when the cross-members are brought in position against the caps. For this reason, the cross-member positioner pauses for 3 seconds at the 75-deg position. During this pause, the aft cord plyer is activated for 2 seconds and, after a 2-second delay, the forward cord plyer is activated for 1 second. With the cords in the proper capture position, the positioner is reactivated for 2 seconds, rotating the cross-member into position for piercing and welding. After the piercing has been completed, the cord plyer drives are reactivated and move the cord plyers to the normal ready-to-weld position. The remainder of the fabrication sequence is the sam as that of a normal bay.

After cutoff bay fabrication has been completed, one additional normal bay length must be fabricated in order to position the mid-point of the cutoff bay under the cutoff mechanism which cuts both the cap material and associated cords. The beam builder will be left with the first bay length of next beam fabricated and located within the machine.

3.3.8.2 <u>BCU Software.</u> Beam builder subsystems will be controlled by a real-time processing system. A real-time system may be defined as one which controls an environment by receiving data, processing data, and returning the results sufficiently quickly to affect the functioning of the environment at that time. The software to perform this function is divided into two groups: (1) supervisory programs and (2) application programs. Supervisory programs, also known as the Executive System, will be responsible for coordination and scheduling of the real-time system. Application programs will be responsible for processing of data transactions.

3.3.8.2.1 <u>Executive Software.</u> The BCU executive software is a set of control programs that manage the resources of the computer system and provide a logical interface between the hardware and the remainder of the software system. In addition, the executive software allocates processor time and main storage. Figure 3-60 is a block diagram which shows the general operational flow of the executive control program when external stimulus is applied. The BCU executive software will consist of the following major elements:

a. Initiation module

b. Sensor input module

c. Task scheduler

d. Clock subroutine

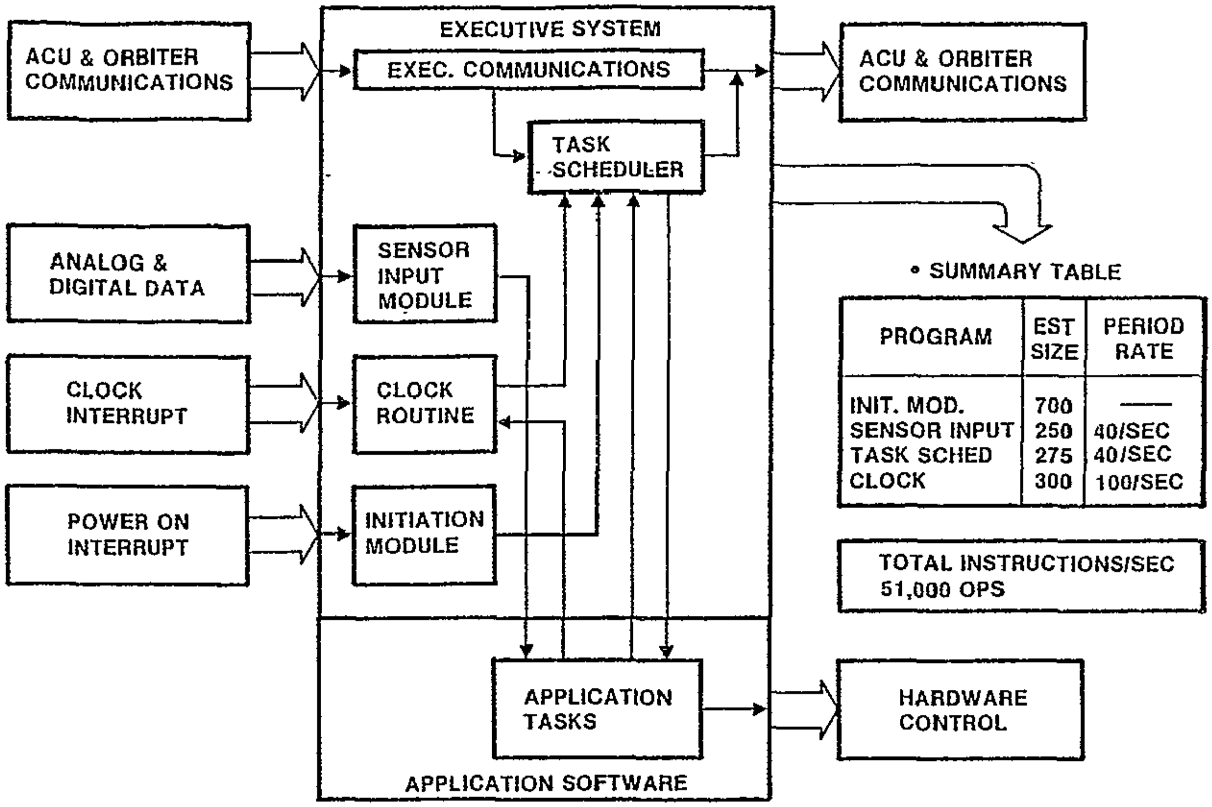

Figure 3-60. BCU software executive elements.

The summary table shown in Figure 3-60 updates earlier estimates of program size and period rates. Program size has been estimated at 1525 instructions versus the previous estimate of 1300 instructions. The rate of execution of each of the four modules was estimated, resulting in a total number of 51,000 executed instructions per second versus the previous estimate of 25,000 instructions per second. This rate is well within the memory and speed capability of currently available microprocessors. It is estimated at 10 to 15% of the BCU processing time will be allocated to executive software control programs.

Flow diagrams for the executive software module are shown in Figures 3-61 and 3-62. The operation of each module is discussed in subsequent paragraphs.

a. Initiation Module. This module is entered when the power-on interrupt occurs. System diagnostics are then executed to verify the microprocessor instruction set; the contents of Read Only Memory (ROM) are verified by a previously calculated checksum; Random Access Memory (RAM) is checked out with a variety of test patterns. The control system sensors are checked out next. At this point, any problems are reported to the ACU. The program now waits for a command from the ACU. When it is sent, it causes an interrupt of the BCU processor. The BCU processor determines which program sequence to

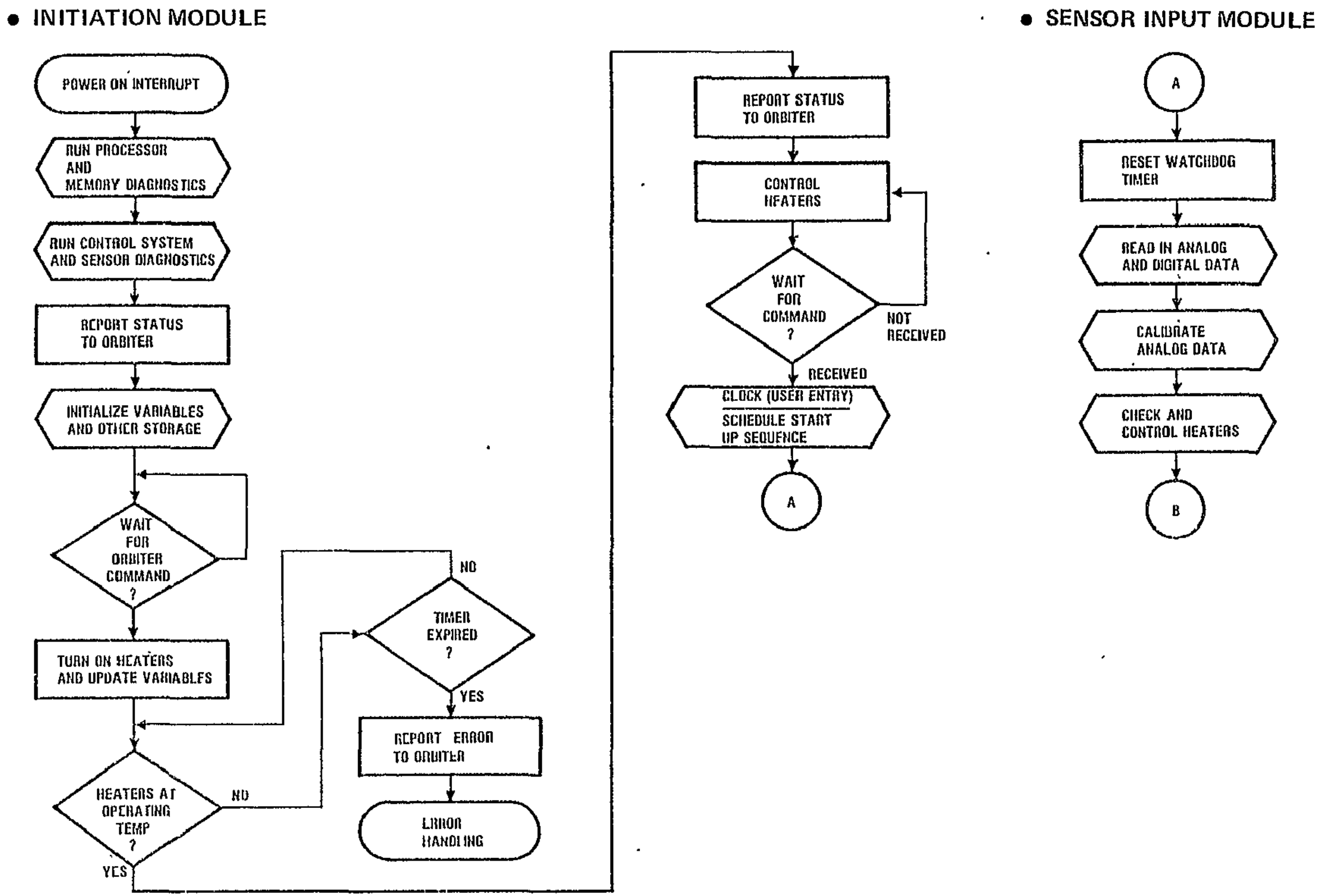

Figure 3-61. BCU executive software flow diagram I.

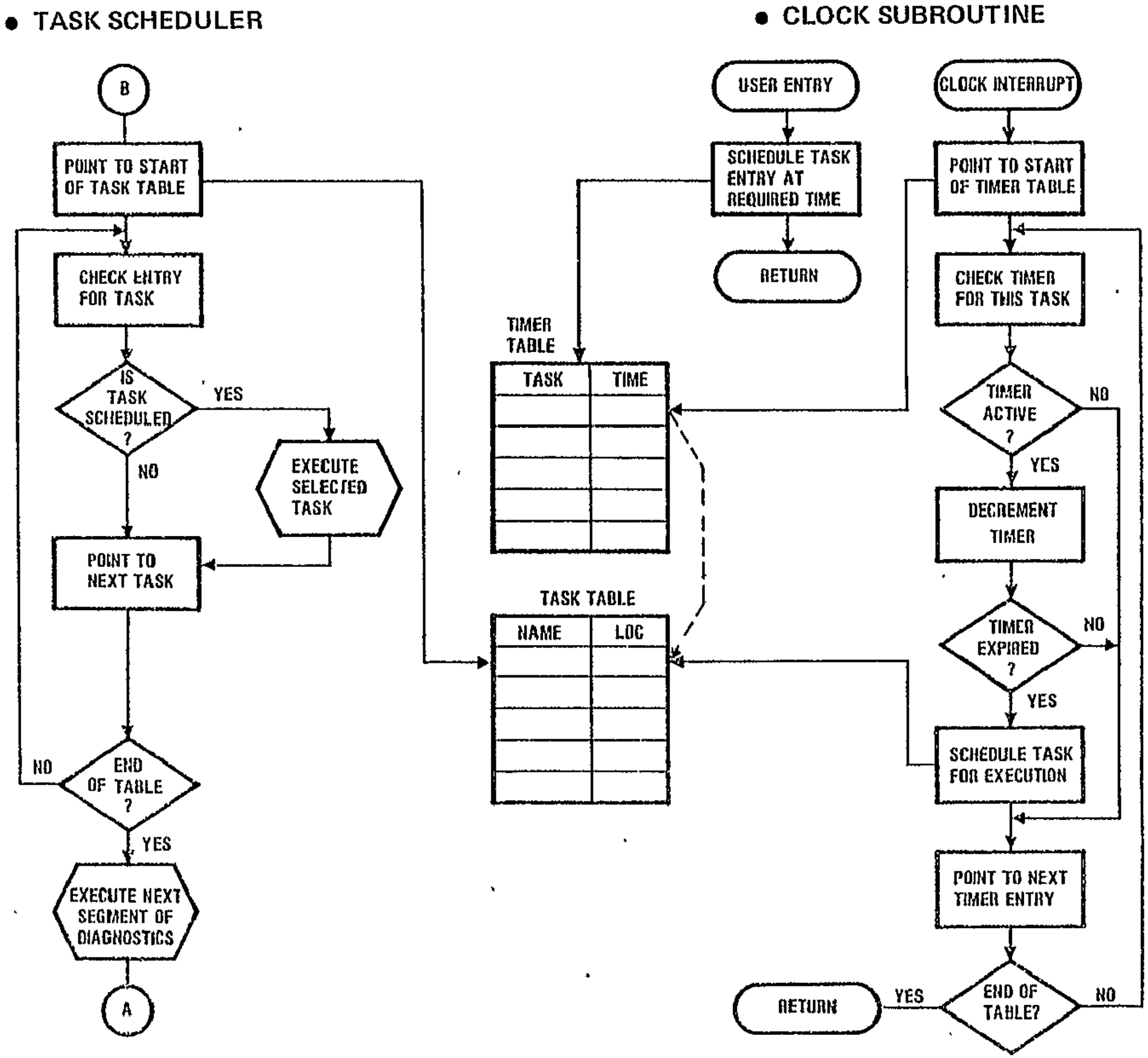

Figure 3-62. BCU executive software flow diagram II.

start and schedules that task. Ordinarily, this will be to turn on the heaters. After the preheat sequence has been completed, status is reported to the Orbiter. Heater control continues while waiting for a start command from the Orbiter. Upon receipt of a start command, the start-up sequence is scheduled, concluding operation of the initiation phase.

b. Sensor Input Module. This module is entered at the start of every scheduler cycle. First the watchdog timer is reset. If this timer is not reset within a predetermined period, it will expire and cause an interrupt. This prevents the processor from becoming "lost" or tied up in a loop, with resulting loss of control of the program. Next, the control system digital and analog data is read-in and formatted for later use by application programs. The analog data is also calibrated at that time. Control of heaters takes place before leaving this module.

c. Task Scheduler. The various functions that the BCU must accomplish can be separated into program modules called "tasks". Each task shall have space allocated in two tables:

   1. Task Scheduler Table
   2. Task Timer Table

   Entries into the task scheduler table are made by the clock routine, which is discussed below. The task scheduler looks for entries in the task scheduler table. These entries correspond to entry point addresses in the tasks themselves. When the scheduler discovers such an entry, it branches to the selected entry point and executes the task. The task, when completed, returns control to the scheduler. The scheduler continues searching the table for active tasks to process. When the bottom of the table is reached, a portion of the diagnostic routine is executed, and then the cycle begins again by resetting the watchdog time, inputting data, etc.

d. Clock Subroutine. This program consists of two parts. The first part (user entry) is used to schedule the execution of tasks. This is done by setting a time into the task timer table. There are timer table entries for each task in the system.

   The second part of the program (clock interrupt) is entered by interrupt from the BCU real-time clock. After the interrupt occurs, the task timer table is checked for active entries and their active timers are decremented. When a timer expires, an entry is made in the task scheduler table (described above) so the task will be executed during the next scheduler cycle.

3.3.8.2.2 Application Software. Applications programs carry out the processing of monitored sensor data and of control signals to the subsystem equipment. These programs, in conjunction with the executive programs, form the real-time operating system of the BCU.

The applications software programs illustrated in Figure 3-63 are grouped into two sequences: normal bay and cutoff bay. Twenty programs are required for normal bay fabrication. The same twenty programs, with a change of variables, and four unique programs are used to fabricate a cutoff bay.

• APPLICATION SOFTWARE

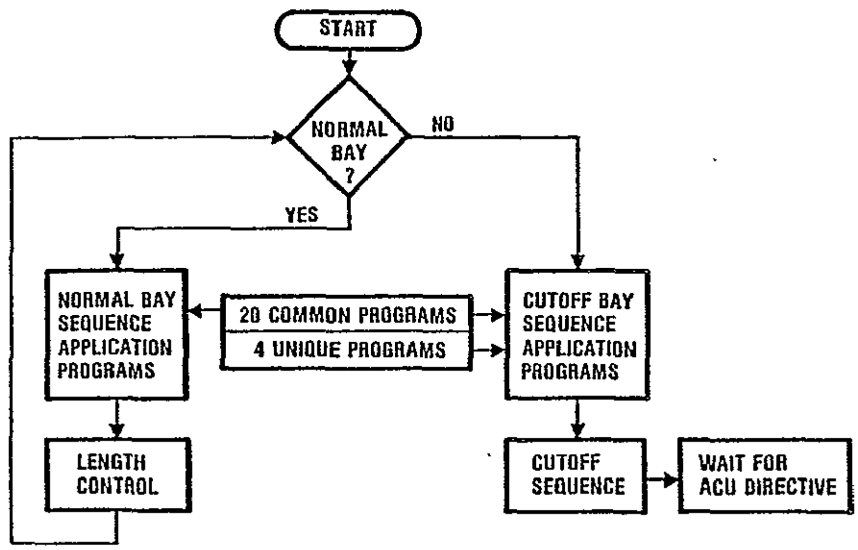

• INSTRUCTION SUMMARY

	INSTRUCTIONS	
	PART I/II	NOW
EXECUTIVE SOFTWARE	1,290	1,525
APPLICATIONS SOFTWARE	1,361	1,884
TOTAL	2,651	3,409

Figure 3-63. Applications software summary.

After a normal bay has been fabricated, a length control program will initiate the start of the next sequence. If the required number of normal bays has not been fabricated, the normal bay sequence is repeated, otherwise, the cutoff bay sequence will be initiated. After the cutoff bay has been fabricated, the beam is cut off as directed by the ACU. After cutoff is completed, the beam builder controller waits for a new ACU directive before starting fabrication of the next beam.

Application program size has been estimated at 1884 instructions versus the previous estimate of 1361 instructions. Total software quantity, executive and application, has therefore been revised to 3409 instructions from the previous total of 2651 instructions. This software effort does not include redundancy management or self-diagnosing capabilities of the BCU.

Although not required in this study contract, preliminary application program flow diagrams have been generated to shown their relationship with the executive programs, and to permit estimation of software instructions quantities. (See above.) The following paragraphs describe the applications program flows during a normal bay drive sequence.

a. Start-up Sequence. When the executive initiation module has completed its tasks, the BCU will await a start command. Upon receiving this command, the initiation module requests that the normal bay start-up sequence be scheduled. The user entry clock subroutine schedules the start-up sequences by making an entry in the timer table. When its timer expires, an entry for the start-up sequence will be made in the task scheduler table. When the scheduler discovers this entry, it will branch to the selected entry point and execute the start-up sequence.

   Figure 3-64 shows the flow diagram of the start-up sequence. Upon its execution, the start-up sequence calls for scheduling of the cap drive, forward and aft plyers, and the capstan brake tensioner application programs. The user entry clock subroutine will place entries for each of those programs in the timer table. Clock interrupts will subsequently decrement the timers and, when an application program timer has expired, an entry for this program will be made in the task scheduler table indicating it is ready for execution. Execution of application tasks will be started by the scheduler when it finds an entry in the task scheduler table.

b. Cap Drive Sequence. Figure 3-65 shows a generalized flow diagram for the cap drive application program. Upon entry into this program, the BCU will transmit an output command, starting the cap drive motors. Sensor data will be monitored and evaluated. When the cap drive process has been completed, the BCU will stop the cap drives and schedule the cooling platen, cross-member handler/positioner, and weld anvil application programs by placing entries in the timer table. Program control will then be returned to the scheduler.

   If the process has not been completed, monitor entry to the cap drive program will be rescheduled in the timer table and control will be returned to the scheduler. This will cause a periodic check on the cap drive process until completion, thereby freeing the BCU for other tasks.

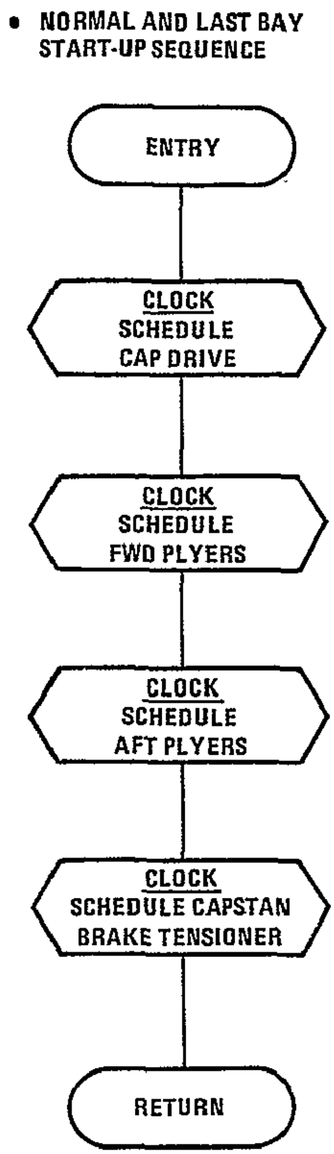

Figure 3-64. Application Software.

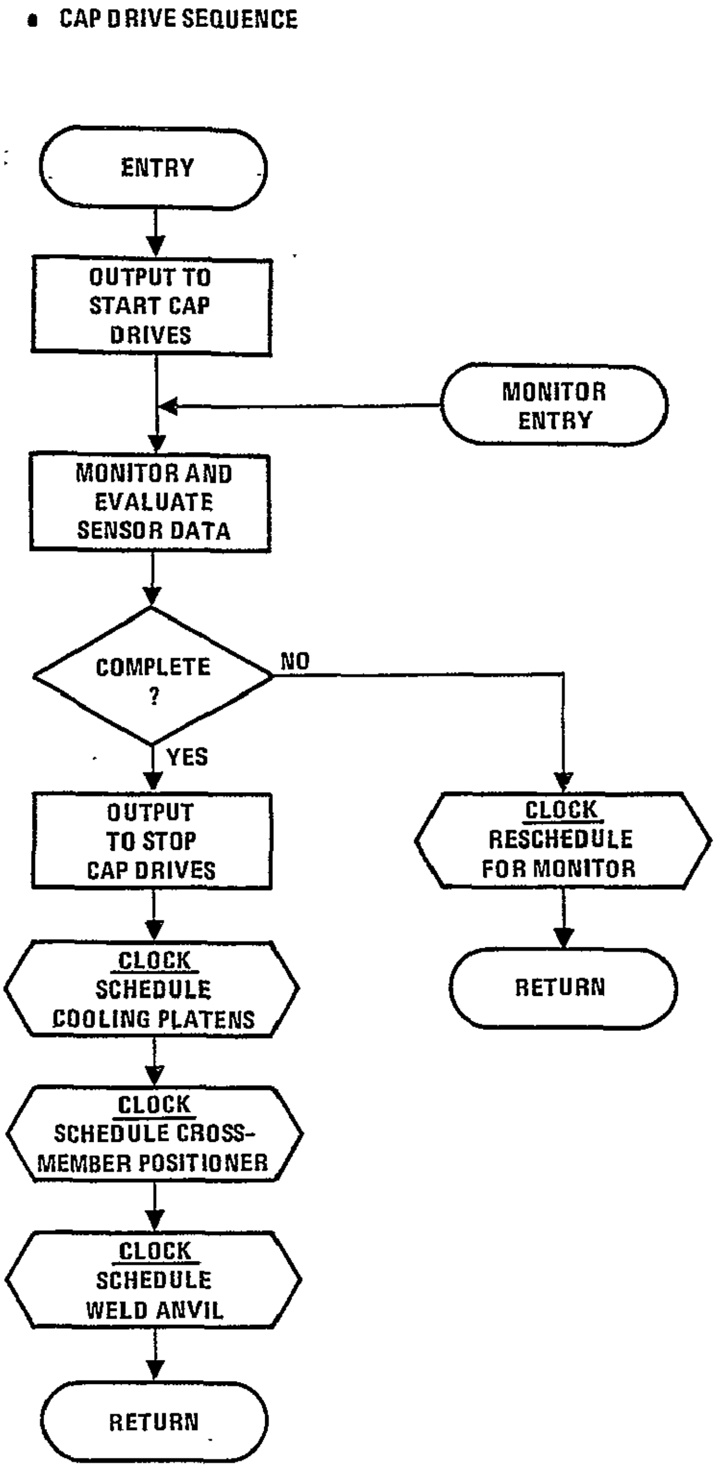

Figure 3-65. Cap drive sequence.

c. Cord Plyer Sequence. When the BCU becomes free for other tasks, the scheduler will continue to search the task scheduler table for other active entries. Since cord plyer operation will occur during the cap drive operation, the forward and aft plyer programs will be entered in the task scheduler table. These programs will be executed while the BCU is in its time-shared mode. Program flow is similar to that of the cap drive sequence and is shown in Figure 3-66.

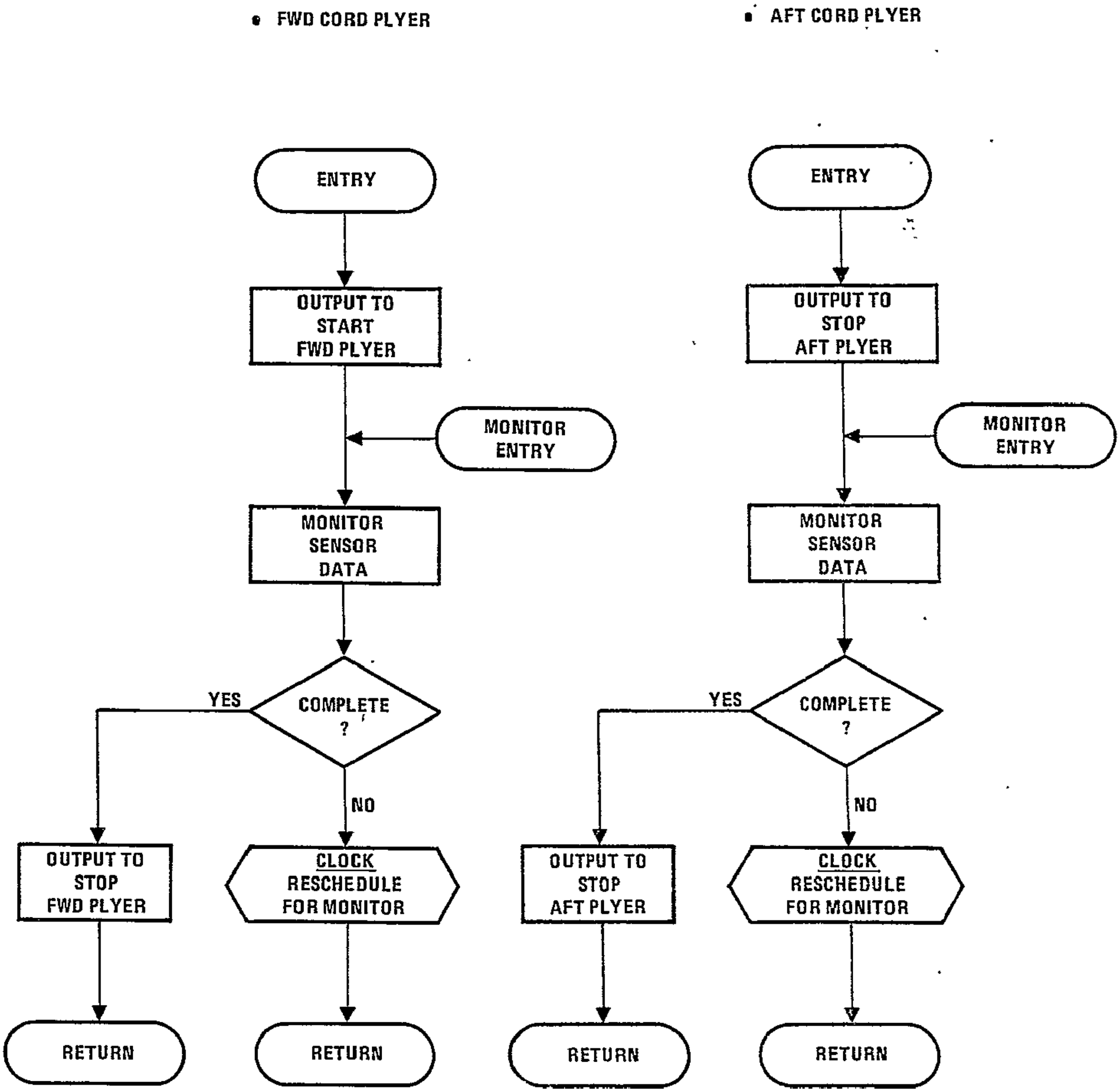

Figure 3-66. Cord plyer sequence.

d. Capstan Brake/Tensioner Sequence. The capstan brake/tensioner program will be entered into the scheduler table 23 seconds after the cap drive sequence. Figure 3-67 shows the tensioner program flow. Its execution and rescheduling of monitor entry is similar to the other application programs discussed above.

e. Other Application Programs. Additional application programs are necessary for each subsystem process. The same general philosophy of program flow will be used for the remainder of the application programs.

3.3.8.3 Avionics Equipment Arrangement. The installation of beam builder avionics and control equipment was updated to the configuration shown in Figure 3-68. The general philosophy for the avionics configuration on the beam builder is to package the controls by function, to integrate these packages with each beam builder subsystem such that each major subsystem is self-contained electrically, and to locate each functional package as near as mechanically feasible to its actuators and sensors.

Each cap forming machine is controlled by four functional control packages:

a. Heater control circuitry
b. Platen drive controller
c. Cap drive controller
d. Remote multiplexer unit, digital interface, and data acquisition system

These packages are to be installed on the bottom of each cap forming machine to allow operation and checkout of the cap forming machine before it is installed on the beam builder structure. When the cap forming machines are installed, these control packages will project into the forming section support structure envelope. Corresponding openings are provided in the adjacent structure.

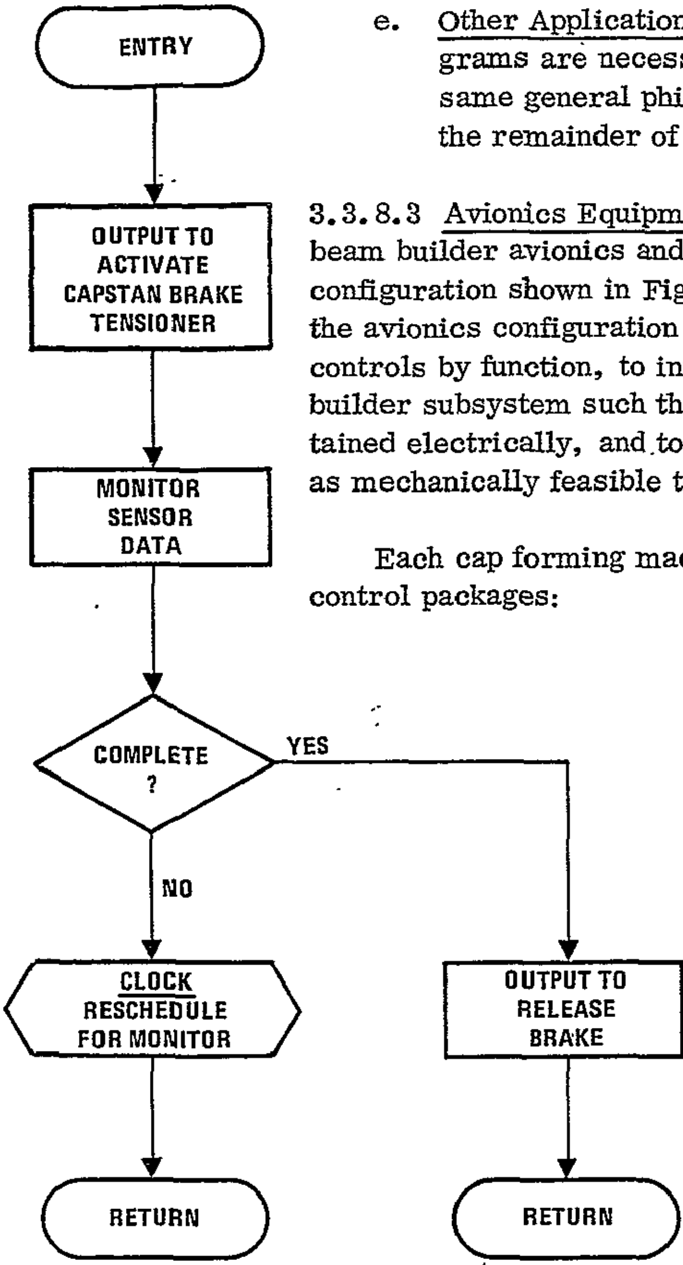

Figure 3-67. Capstan brake/tensioner sequence.

The fabrication subsystems equipment will be controlled by functional control packages installed on the assembly section support structure and on both faces of the structural spider. The weld-head controllers and electronics and the beam cutoff controllers are located in the assembly section outer support beams. The view of the spider face fromthe forming section end shows the location of the clip feed controller and the BCU. All other fabrication control packages are located on the opposite face of the spider.

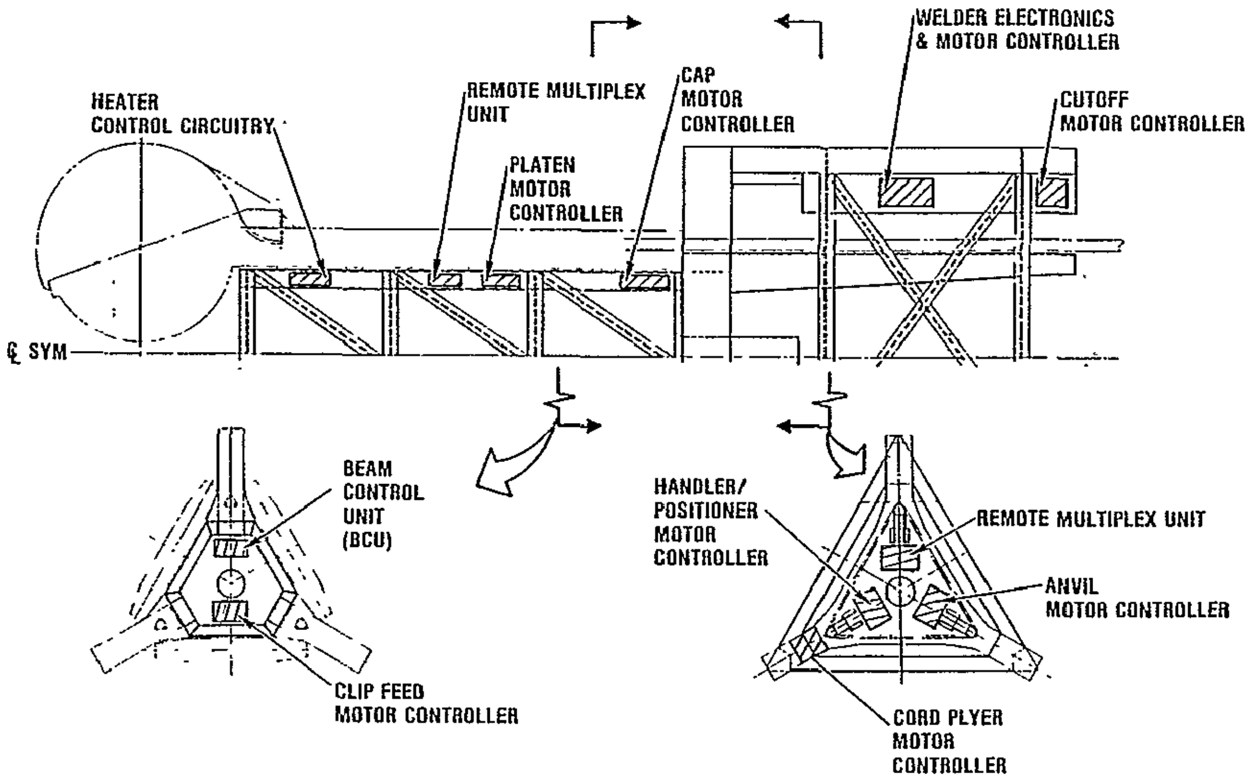

Figure 3-68. Beam builder avionics equipment arrangement.

3.4 ENVIRONMENTAL IMPACTS

3.4.1 SYSTEM HARDWARE EVALUATION. An evaluation of the impacts of the Shuttle Environmental Design Requirements on beam builder hardware design was conducted. The component operating and nonoperating design criteria were first developed and the life duty cycles were defined, based on a single SCAFE mission. These data are summarized in Table 3-14.

From the preliminary design configuration, a listing of each of the basic subsystem components was compiled and the fundamental types of devices used in the mechanical and electronic hardware were identified. Using the environmental design criteria as applied to the individual subsystem components, the principal concerns were identified and general recommendations which deal with each of these concerns were compiled. The principle environmental impacts are summarized in Table 3-15.

The evaluation of shuttle payload environmental requirements, as applied to the beam builder, did not reveal any major problems. The areas of principal concern have been dealt with effectively on spacecraft equipped with similar devices. Our recommendations are based on this source of data. The recommendations are quite general at this time and do not identify specific materials and processes to be used. Such selections are best made during the detail design where the requirements are thoroughly analyzed. Table 3-16 summarizes the recommendations.

Table 3-14. Environmental design requirements summary.

PARA	STS—JSC-07700 VOL XIV	BEAM BUILDER ENVIRONMENTAL DESIGN CRITERIA		EXPOSURE LIFE CYCLE	
4.0	SHUTTLE ENVIRONMENT	OPERATING	NON—OPERATING	OPERATING	NON-OPERATING
4.1	NATURAL ENVIRONMENTS				
4.1.1	ATMOSPHERIC	CONTROLLED ENCLOSURE	FULL/MODERATE EXPOSURE	48 HRS*	**
4.1.2	SPACE				
	PRESSURE	FULL EXPOSURE	FULL EXPOSURE	24 HRS	5 DAYS
	SOLAR RADIATION (THERMAL)	PARTIALLY SHROUDED	PARTIALLY SHROUDED		
	SOLAR RADIATION (NUCLEAR)	FULL EXPOSURE	FULL EXPOSURE		
	METEOROIDS	PARTIALLY SHROUDED	PARTIALLY SHROUDED	24 HR	5 DAYS
4.2	INDUCED ENVIRONMENT				
4.2.1	GROUND HANDLING & TRANSPORTATION	N/A NOT APPLICABLE	FULL EXPOSURE		
4.2.2	FLIGHT ENVIRONMENT				
	PRESSURE	N/A	FULL EXPOSURE		
	VIBRATION	N/A		N/A	1 FLIGHT
	ACOUSTICS	N/A			
	ACCELERATION	N/A			
	SHOCK	N/A	FULL EXPOSURE	N/A	1 FLIGHT
	RCS PLUME ENVIRONMENT	POTENTIAL EXPOSURE	POTENTIAL EXPOSURE	TBD	TBD
	THERMAL ENVIRONMENT	N/A	FULL EXPOSURE	N/A	1 FLIGHT
	EMI/EMC	FULL EXPOSURE	N/A	24 HR	N/A
	HAZARDOUS GAS DETECTION	N/A	N/A	N/A	N/A
4.2.3	RCS ANGULAR RATE & ACCEL	FULL EXPOSURE	FULL EXPOSURE	24 HR	5 DAYS
4.3	OPERATIONAL CONTAMINATION CONTROL				
4.3.1	ELEMENT CROSS-CONTAMINATION	N/A	NO IMPACT		
4.3.2	PAYLOAD BAY DESIGN	N/A	NO IMPACT		
	PAYLOAD BAY LINER	N/A	N/A		
4.3.3	PAYLOAD DESIGN	APPLICABLE	APPLICABLE		
4.3.4	OPERATIONAL CAPABILITIES				
	PAYLOAD LOADING & CHECKOUT	N/A			
	CONTAMINATION CONTROL SUBSYSTEM TO PAYLOAD LOADING	N/A			
	PREP FOR CLOSEUP OF PAYLOAD BAY	N/A			
	CLOSED PAYLOAD BAY OPERATIONS	N/A			
	LAUNCH THROUGH ORBIT INSERTION	N/A			
	ON-ORBIT	APPLICABLE			
	ENTRY PHASE	N/A			
	POST-LANDING	N/A	APPLICABLE		

*COMPONENTS ONLY

**EXPOSED TO VARYING DEGREES OF ENVIRONMENT

- WORST CONDITIONS OCCUR DURING TRANSPORTATION
- BEAM BUILDER MAINTAINED IN A CONTROLLED ENCLOSURE DURING MOST OF ITS NON-OPERATING LIFE

Table 3-15. Environmental impacts evaluation summary - mechanical and electronic elements.

MECHANICAL ELEMENTS		
TYPES OF DEVICES	OPERATING LOADS	PRINCIPLE CONCERNS
BEARINGS		
• Ball-Linear & Rotary	Light-Moderate	1. Lubrication/wear prevention
• Sleeves & Bushings	Light	2. Launch loads & vibration effects
• Rod-End Spherical	Light-Moderate	3. Corrosion
		4. Contamination
SLIDING CONTACT SURFACES	Light	1. Lubrication/wear prevention
• Cams & Followers	Light-Moderate	2. Launch vibration effects
• Chain Guides	Light	3. Corrosion
• Geneva Wheels	Moderate	
• Latches & Hinges		
POWER TRANSMISSION ELEMENTS	Light-Moderate	1. Lubrication/wear prevention
• Fine Pitch Gears	Light-Moderate	2. Launch loads & vibration effects
• Lead Screws	Light	3. Corrosion
• Ball Screws	Light	4. Contamination
• Flexible Drive Shafts	Light	
• Chains & Sprockets	Light-Moderate	
• Torque Tubes & Drive Shafts	Light-Moderate	
• Push Rods & Linkages	Light-Moderate	
• Friction Drive Rollers		
SPRINGS		1. Lubrication/wear prevention
• Helical Tension & Compression	Light-Moderate	2. Launch vibration effects
• Helical Torsion		3. Corrosion
• Negator	Light	4. Temperature effects on performance
ELECTROMECHANICAL ELEMENTS		1. EMC
• Brakes & Clutches	Light	2. Brush life in vacuum
• Motors	Light	3. Temperature/heating
OTHER		1. Launch loads
• Forming Rollers	Light	2. Wear
• Shear Blades	Light	3. Venting & repressurization
• Storage Clips/Canisters	Heavy	4. Fluid leakage
• Cooling Loop	Light	

ELECTRONIC ELEMENTS	
TYPES OF DEVICES	PRINCIPLE CONCERNS
POSITION SENSORS	1. Shock & vibration effects on LED
• Optical Encoder	2. Position shift of vane under shock or vibration
• Hall Effect (Vane Type)	
TEMPERATURE SENSORS	1. Overheating
• Thermopile	
TRAVEL SENSOR	1. Tape cleanliness & head pressure
• Magnetic Tape Head Pickup	
ELECTRONIC BOXES	1. EMI radiation
• All Types of Elements	2. Heat rejection
	3. Internal pressure
HEATERS	1. Shock & vibration effects
	2. Waste heat rejection

Table 3-16. Impacts of Shuttle environment on beam builder design - general recommendations.

• Mechanical elements	• Electrical/electronic elements
• Lubricate ball bearings & gears with low vapor pressure grease • Use hardened corrosion resistant bearing & gear metals • Use self-lubricating composite bearing materials for sleeves & journals • Apply bonded dry film lubricants to contacting metal sliding surfaces • Seal precision gears & bearings against outside contamination • Use corrosion resistant materials or surface protections on all metal parts • Minimize active cooling lines & separable fittings • Vent all large enclosures — prevent venting of contaminants into payload bay • Design forming rollers & heating elements for tolerance to launch loads	• Use brushless DC motors & clutches • Provide heat conduction paths from motors to structure • Shock mount optical encoders • Provide shielding & cooling for thermopile sensors • Rigidly mount vanes for hall effect sensors • Install pre-tape wipers & spring load magnetic tape head pickups • Pot electronic modules in sections or provide special packaging to allow heat removal • Determine pressurization/venting requirements for electronic boxes • Provide EMI vented screens & feed through filters for signal & power lines in electronic boxes.

3.4.2 BEAM BUILDER STRUCTURE SHROUD. Thermal distortions in the support structure and modular beam building subsystems can cause significant distortions in beam alignment during the assembly process. The structure shroud concept shown in Figure 3-69 eliminates this problem by completely covering the assembly process area with a multilayer insulation (MLI) blanket of aluminized mylar. Velcro strips are used to attach the MLI blanket to the external support structure. These simple attachments provide easy installation and immediate access to inspect and maintain any of the assembly subsystems. Other advantages of this concept are: it is very light weight and it needs little additional structure on the existing beam builder for support.

3.5 SPECIAL BEAM BUILDER EFFECTS

Two of the beam builder functions, design and analysis tasks, dealt with the effects of producing curved beams and scaled-up beams of beam builder design. The results of these tasks are presented in the following subsections.

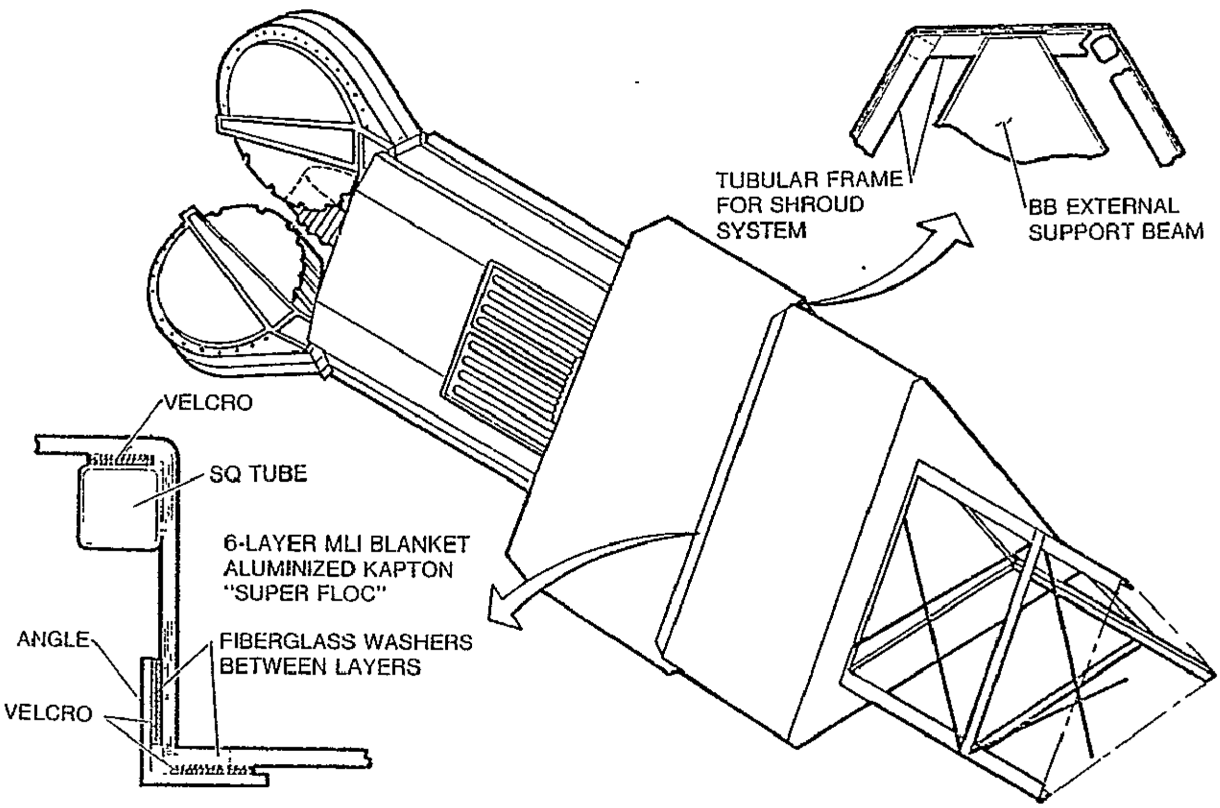

Figure 3-69. Beam builder structure shroud concept.

3.5.1 CURVED BEAM FABRICATION. An attractive approach to the construction of contoured spacecraft surfaces (e.g., antennas) is the use of curved beams, since they offer the potential for establishing the "net" contour without auxiliary standoffs. In SCAFEDS Part I, a parametric analysis investigated the effects of cumulative cap length mismatch on the tip deflection of 200-meter beam (Reference 2). At that time, the purpose of the analysis was to help drive out requirements for straight beam accuracy control, and it contributed to eventual selection of the internal-feedback/differential-cap-drive control technique. However, the analysis raised a series of new and important issues as follows:

a. If a beam, intended to be straight, can possess (unwanted) curvature, can a deliberately curved beam be produced?

b. If the answer to a. is yes, what beam builder changes are needed?

c. How do predicted and "achievable" curvature compare?

d. What is the sharpest curvature achievable?

The basis of the differential-drive control technique is the feedback and comparison of simultaneous precision length measurements made continuously on the three beam caps throughout the "run" period. To achieve identical driven cap lengths (straight beam case) in the presence of both velocity and dimensional tolerances, each cap may be differentially driven both to preclude excessive length differences during the constant-speed portion of the run period and to achieve the given "target" bay length prior to cooling platens closure. Within the accuracy of the sensing and drive components, successive precision rectangular bays are produced and a straight beam results. Conversely, if two of the three caps are driven to a nominal target length and the third cap is driven a specified additional amount, ΔL, a series of trapezoidal bays are produced and a curved beam results. This situation is shown schematically in the upper portion of Figure 3-70 for the baseline SCAFE beam.

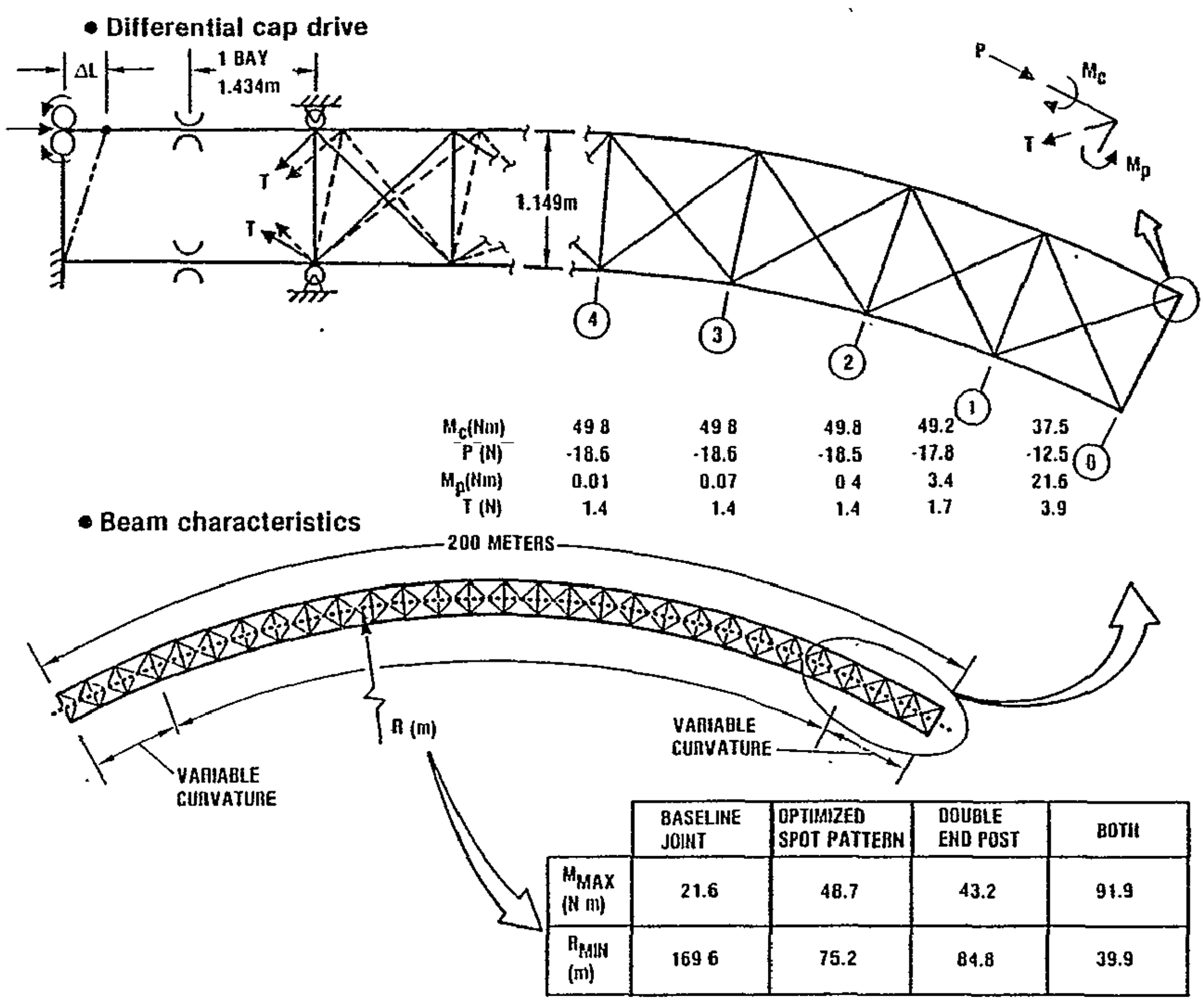

	BASELINE JOINT	OPTIMIZED SPOT PATTERN	DOUBLE END POST	BOTH
M_{MAX} (N m)	21.6	48.7	43.2	91.9
R_{MIN} (m)	169 6	75.2	84.8	39.9

Figure 3-70. Curved beam characteristics.

No physical change is required in the beam builder to produce a curved beam in this manner, only the additional software instructions and a look-up table to specify the ΔL for each bay (and even these instructions can be common for straight and curved beam manufacture, by filling the table with zeros for the straight beam case). Then, if constant (circular) curvature is desired, a constant ΔL is provided; if varying curvature (e.g., parabolic) is desired, an appropriately varying ΔL is provided.

The generation of successive trapezoidal bays forces sidesway into previously attached cross-members, generating permanent internal preload in all beam elements and joints. Consequently, the sharpest achievable curvature is governed by the weakest element. Since the baseline weld pattern will accommodate an in-plane moment of 21.5 Nm (Figure 2-6), whereas the selected cross-member can withstand 30.0 Nm (Figure 2-5), the initial analysis sought to define the radius of curvature which would produce a maximum joint moment of 21.6 Nm. A straight-beam finite element model was prepared and thermally "loaded" to produce the displacements and corresponding loads for both an upper-cap ΔL of 0.254 cm (0.10 in.), and the appropriate diagonal cord ΔL. The largest joint moment (which occurred, as expected, at the last cross-member) was then compared with the joint limit, ΔL ratioed upward accordingly, and the model rerun. Another moment comparison, further slight increase in ΔL, and model rerun produced the results shown in the lower half of Figure 3-70. A maximum moment of 21.6 Nm was achieved and the associated input ΔL "back-computed" to a predicted theoretical radius of 169.6 m. Constant internal loads were found over 96% of the arc, implying essentially circular curvature, but the loads vary significantly in the first four bays from the tip, as tabulated, for points 0 through 4, resulting in local curvature variation.

The "achieved" radius of curvature was determined by direct computation from beam joint coordinates, taken from the computer output, at selected points along the span. Somewhat surprisingly, the resulting radius was not constant but, instead, varied from 166 m to 180 m, increasing continuously toward the tip. This suggests more extensive relaxation than that implied by comparison of the internal loads, and may require a more sophisticated prediction model (i.e., ΔL look-up table) to account for relaxation and still achieve the desired curvature with sufficient precision.

In any event, further radius reduction is available as shown by adopting a higher-capability spotweld pattern (e.g., Figure 2-6, pattern U3/L2), by installing two cross-members edge to edge (at the beam ends only), or both. The weld pattern change requires new weld tips (a minor beam builder change which, if needed, could readily be used for straight beam production as well). Whereas, the dual cross-member installation is a software-only change.

In addition to curvature limitation imposed by the welds and/or cross-members, however, buckling of the beam cap side flats may also limit radius reduction. To evaluate this possible constraint, cap compressive buckling data (from privately-funded tests) were used to define critical buckling loads for combined bending plus compression for the baseline cap-shape and three material thicknesses. Global coordinate axes for the overall beam, local cap axes, and edge points on the cap flats are defined in Figure 3-71. Table 3-17 summarizes the critical point, limiting moment, and associated minimum radius of curvature for each cap and each axis of beam bending. Inspection of the table shows that, whereas the overall beam exhibits the same flexural stiffness (EI) about both global axes, it can be curved much more sharply about the X-axis due to the local buckling characteristics of the cap flats. Furthermore, although the baseline cap gage is barely adequate for the 244 m radius of the 61 m antennas, a gage increase about the 0.61 mm baseline is required to reduce R_{MIN} to the 169.6 m value the baseline weld joint can sustain.

The foregoing analyses define minimum radii of curvature assuming that limit loads are developed during the fabrication process. Clearly this is not permissible, since a substantial portion of beam strength must be reserved for construction and operational loads with reasonable safety margins. These are configuration-unique, however, and the final design of the beam structure, to provide appropriate curvature, depends on future detailed analyses of the specific project.

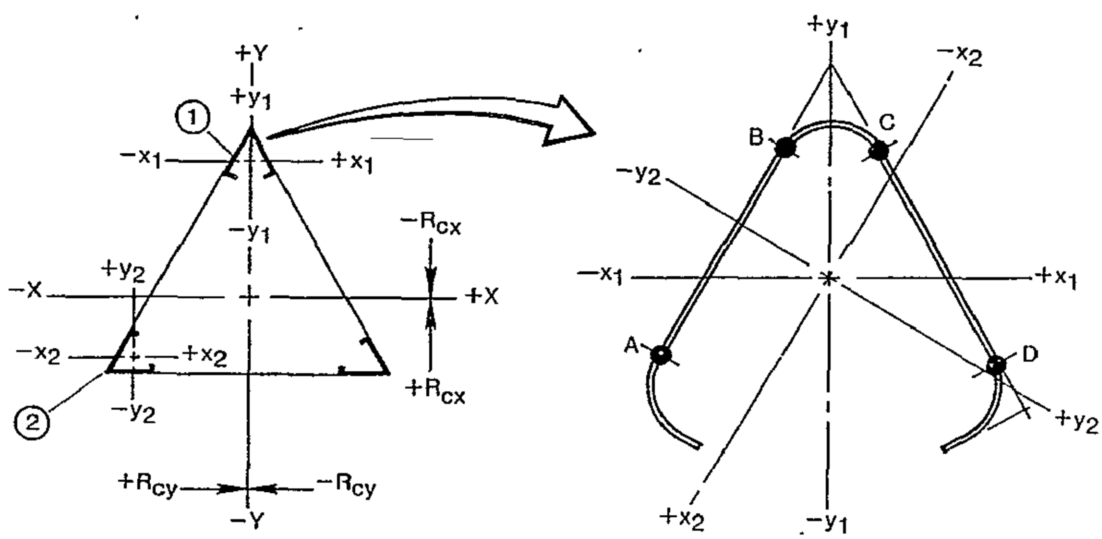

Figure 3-71. Beam/cap axes and reference points.

Table 3-17. Moment and radius limits vs cap thickness.

Curvature Direction	Item Cap	Item Point →	Cap "structural" thickness, mm (in.)* 0.610 (0.024) A	B	C	D	0.813 (0.032) A	B	C	D	1.016 (0.040) A	B	C	D
+R_{CX}	1	M_{CR} (N-m)	514	—	—	514	1218	—	—	1218	2378	—	—	2378
		R_{MIN} (m)	17	—	—	17	9	—	—	9	6	—	—	6
	2	M_{CR}	37	37	15127	—	105	105	42294	—	205	205	82606	—
		R_{MIN}	$\boxed{248}$	$\boxed{248}$	~0	—	$\boxed{140}$	$\boxed{140}$	~0	—	$\boxed{89}$	$\boxed{89}$	~0	—
-R_{CX}	1	M_{CR}	—	103	103	—	—	245	245	—	—	478	478	—
		R_{MIN}	—	82	82	—	—	46	46	—	—	30	30	—
	2	M_{CR}	—	—	—	43	—	—	—	119	—	—	—	232
		R_{MIN}	—	—	—	$\boxed{219}$	—	—	—	$\boxed{123}$	—	—	—	$\boxed{79}$
+R_{CY}	1	M_{CR}	16	58	—	—	38	137	—	—	75	218	—	—
		R_{MIN}	727	204	—	—	409	114	—	—	262	73	—	—
	2	M_{CR}	—	539	10	83	—	1086	19	167	—	2121	38	325
		R_{MIN}	—	20	$\boxed{1137}$	123	—	11	$\boxed{639}$	75	—	7	$\boxed{409}$	48
-R_{CY}	1	M_{CR}	—	—	58	16	—	—	137	38	—	—	268	75
		R_{MIN}	—	—	204	$\boxed{727}$	—	—	115	$\boxed{409}$	—	—	73	$\boxed{262}$
	2	M_{CR}	120	—	—	—	150	—	—	—	472	—	—	—
		R_{MIN}	91	—	—	—	83	—	—	—	33	—	—	—

*Excludes surface coatings.

3.5.2 BEAM BUILDER SCALE-UP. A number of guidelines were adopted in order to facilitate the beam builder scale-up task. First, a structural configuration of the scaled-up beam had to be selected. Then, guidelines governing machine storage capacity, production rate, and interfaces were required. The guidelines used for this task are summarized in Table 3-18.

Table 3-18. Beam builder scale-up approach guidelines.

- **Structure**
  - Beam geometry/details per Boeing SPS study (Source: Report D180-25037-2)
- **Machine**
  - Retain cyclic mode & 80 sec/bay rate
  - Maximize commonality of subsystem modules
  - 24 hr. material resupply cycle
  - Construction facility interfaces excluded
  - Evaluate alternative cooling approaches

3.5.2.1 Baseline Structure. The baseline structural element used for development of scaled-up beam builder concepts is taken fromcurrent Boeing SPS work, documented in Report No. D180-25037-2. Variations in beam size, bay spacing, element cross-section and thickness, and cord diameter are considered, as tabulated in Figure 3-72.

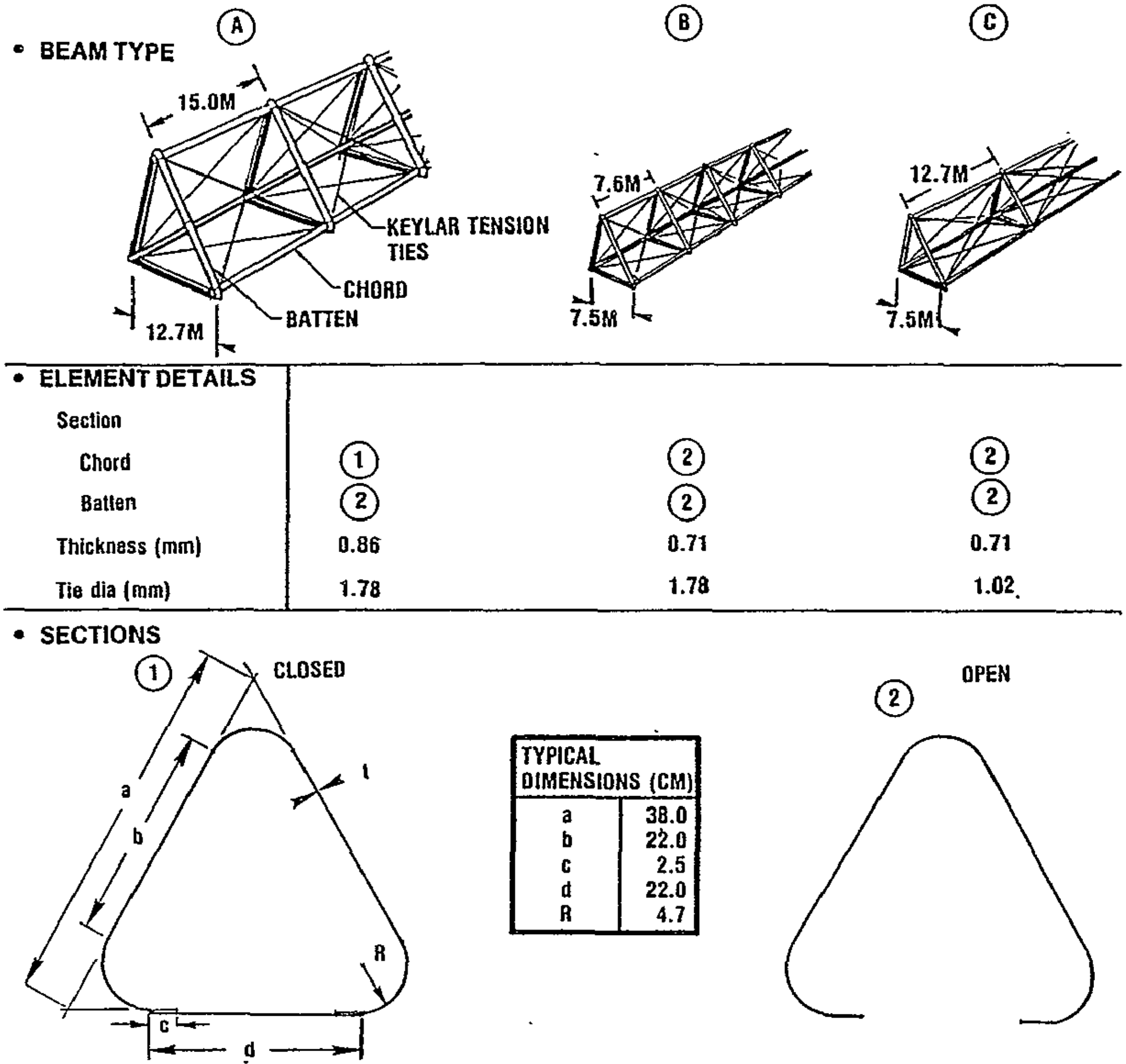

Figure 3-72. Baseline structure for beam builder scale-up.

Material variations are within the ranges considered feasible for automated fabrication using the baseline SCAFE subsystem concepts. The flat close-out strip for the closed section cap represents a simple addition in the one application where increased torsional stability is apparently needed, and its storage/feed/attachment is readily accommodated in the beam builder concepts.

3.5.2.2 Beam Builder Growth Considerations. The SCAFE beam builder has a nominal production rate of 1.08 m/min, based on a 1.434 m bay length produced every 80 seconds. The 80-second cycle time was adopted for the original SCAFE mission to meet mission timelines and is not the real machine capability. The total run and pause cycle time need only be the time required to heat the composite strip material to the forming temperature. Thus, if we assume this time to be 80 seconds, beam builder production rate will increase proportionately to the beam bay lengths as shown in Figure 3-73.

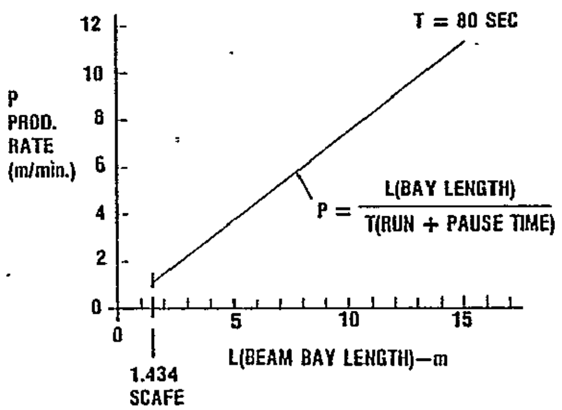

- COOLING RATE IS NOT A DRIVER
- SHORTER RUN + PAUSE TIMES ARE POSSIBLE (T <80 SEC)
- BEAM DEPTH IS NOT A DRIVER

Figure 3-73. Beam builder production rate growth capability.

Since cooling time is on the order of 10 seconds or less, it has no impact on beam production rate. Also, the depth of the beam has no effect on production rate since beam straightness (or curvature) is controlled by differential cap drive regardless of beam depth.

The effect of beam builder growth capability on cooling section length has a significant effect on overall machine length as well as variation in the length of the cap forming machines if cooling platens are used. For the Boeing SPS beam configurations there are three different bay lengths and two different cross-member lengths. If cooling platens were to be used, five different-length cooling sections would be required. To avoid this problem and retain commonality of all forming machines, an alternative cooling system is proposed, as shown in Figure 3-74. This system uses many rollers and balls to contact the material as it passes through the cooler. By assuming a nominal 10 seconds of contact cooling time, a cooling section length is determined by multiplying 10 seconds times the nominal forming rate. Further, by selecting a nominal forming rate for all cap forming machines, one cooling section length will suffice for all forming machine functions, as illustrated in Figure 3-75. The only variation in the cap forming machines is in the active length of heating and the ratio of run time to pause time.

The common cap forming machine configuration to meet all Boeing SPS beam bay length and cross-member length requirements is shown in Figure 3-74. The use of a common cap and cross-member cross-section with minor difference in material thickness makes this approach feasible. The extended heating section in the storage canister lid would be activated to the extent required for 12.7 m or 15 m stroke lengths. Other 7.5 m and 7.6 m lengths are heated in the basic heating section.

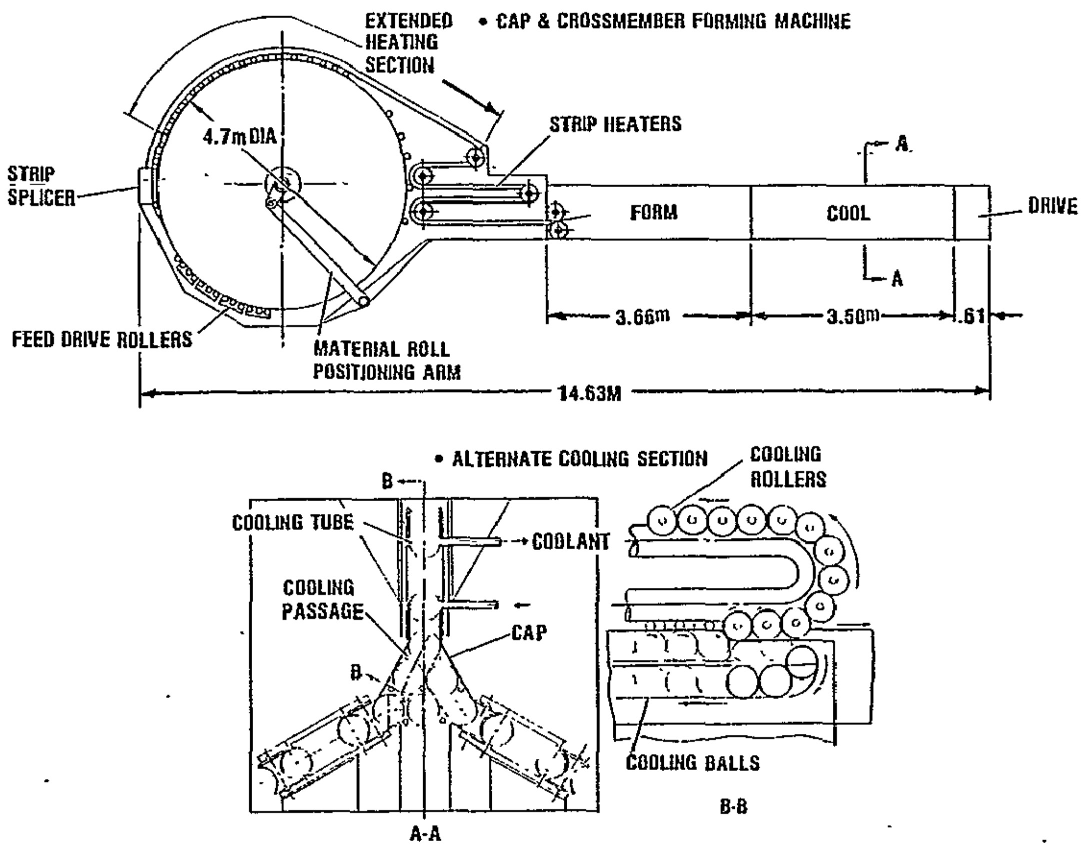

Figure 3-74. Common forming machine concept.

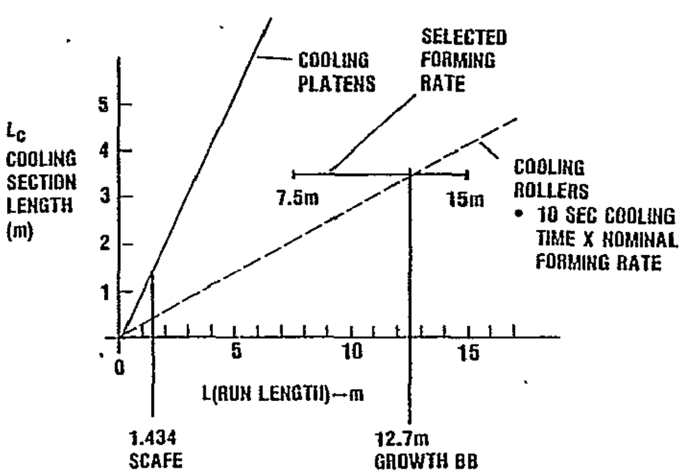

• SELECTED NOMINAL FORMING RATE

$$\bar{S} = \frac{12.7\text{m}}{40\text{ SEC}}$$

$\bar{S}$ = 0.32 m/SEC FOR ALL CAP & CROSSMEMBER FORMING MACHINES

• USE EXTENDED HEATING SECTION FOR 12.7m & 15m LENGTHS
• VARY PAUSE TIME TO MAINTAIN 80 SEC CYCLE

Figure 3-75. Selected forming rate and cooling section length.

The 4.7 m diameter strip material roll meets the criteria that the machine be reloaded in not less than 24 hours of operation for the 12.7 m nominal stroke length. Because of the mass of the roll, a feed drive is incorporated in the storage canister to provide drive and braking of the roll. A roll positioning arm is required to keep the roll in contact with the feed drive rollers. A strip splicer is incorporated in the canister lid to permit the machine to be reloaded without rethreading the strip through the machine. The tail end of the finished roll is spliced to the start end of the new roll such that no further splicing or joining is required. This splicing technique is a development item not yet defined.

The cap machine forming and drive sections increase in size proportional to the cap size. The cooling section alternate configuration works on the principal of a linear ball bearing where the strip material drives the balls and rollers to recirculate through return passages. The rollers and balls are continuously in contact with fluid-cooled surfaces to conduct the heat to the beam builder radiator for rejection to space.

3.5.2.3 Growth Beam Builder Concepts. The beam builder for the 7.5 m structure shwon in Figure 3-76 will build both the type B (7.6 m bay length) and the Type C (12.7 m bay length) beams. This requires only software variations to program the bay length and assembly timeline differences and the different cutoff bay manufacturing sequence.

The cap forming and cross-member forming machines are identical, except for software differences. The scaled-up beam builders both use forming machines to manufacture cross-members in lieu of the SCAFE concept of prefabricated cross-members stored in clips. This requires a new cross-member handler concept as described in the detailed chart. The use of prefabricated cross-members is not required in this case because a sufficiently large energy supply will be available to support on-orbit cross-member fabrication.

The basic support structure is designed along the lines of the SCAFE beam builder structure, and all of the basic subsystem functions are similar to the baseline machine as described above. The size of this machine lends itself to transportation via projected HLLVs.

The beam builder for the 12.7 m structure (Type A beam) shown in Figure 3-77 incorporates a unique subsystem to facilitate closure of the beam cap sections. This subsystem consists of three storage and feed canisters. The closure strips are each fed from a canister through a tension control roller set, then to a final feed drive which is synchronized with the cap drive. The strip is laid on the cap downstream of the cross-member-to-cap welding station. This permits the main weld anvil and cap closure anvil to be inserted inside the cap as shown. A single actuator engages the main weld anvil with the cap during the pause period, then retracts the main anvil causing the closure anvil to be engaged during the run cycle. A set of cap closure welders continuously seam welds the closure strip to the cap during the run period.

The cross-member-to-cap welds are each accomplished by a set of six welders which are engaged and retracted, as shown. The diagonal cords will be captured by one of the welds similar to the SCAFE beam builder cord capture concept.

The cord plyer subsystem is similar to the SCAFE beam builder. The major difference is that the plyers are driven along tracks on a rigid beam by a pulley/cable drive system. The beam track provides the rigidity required for the longer span on travel.

The cross-member subsystem requires new cross-member handlers to grasp the cross-members after they deploy from the forming machines. When the cross-members are cut off, the handlers rotate them 90 degrees, then drive them inboard until they contact the caps. After the cross-members are joined to the caps, the jaws of the handlers open to permit the beam to advance. The handlers then rotate and translate back in position to accept the next cross-members.

The size of the structure for this beam builder may require that the machine be partially dismantled for transportation to space, then assembled on orbit.

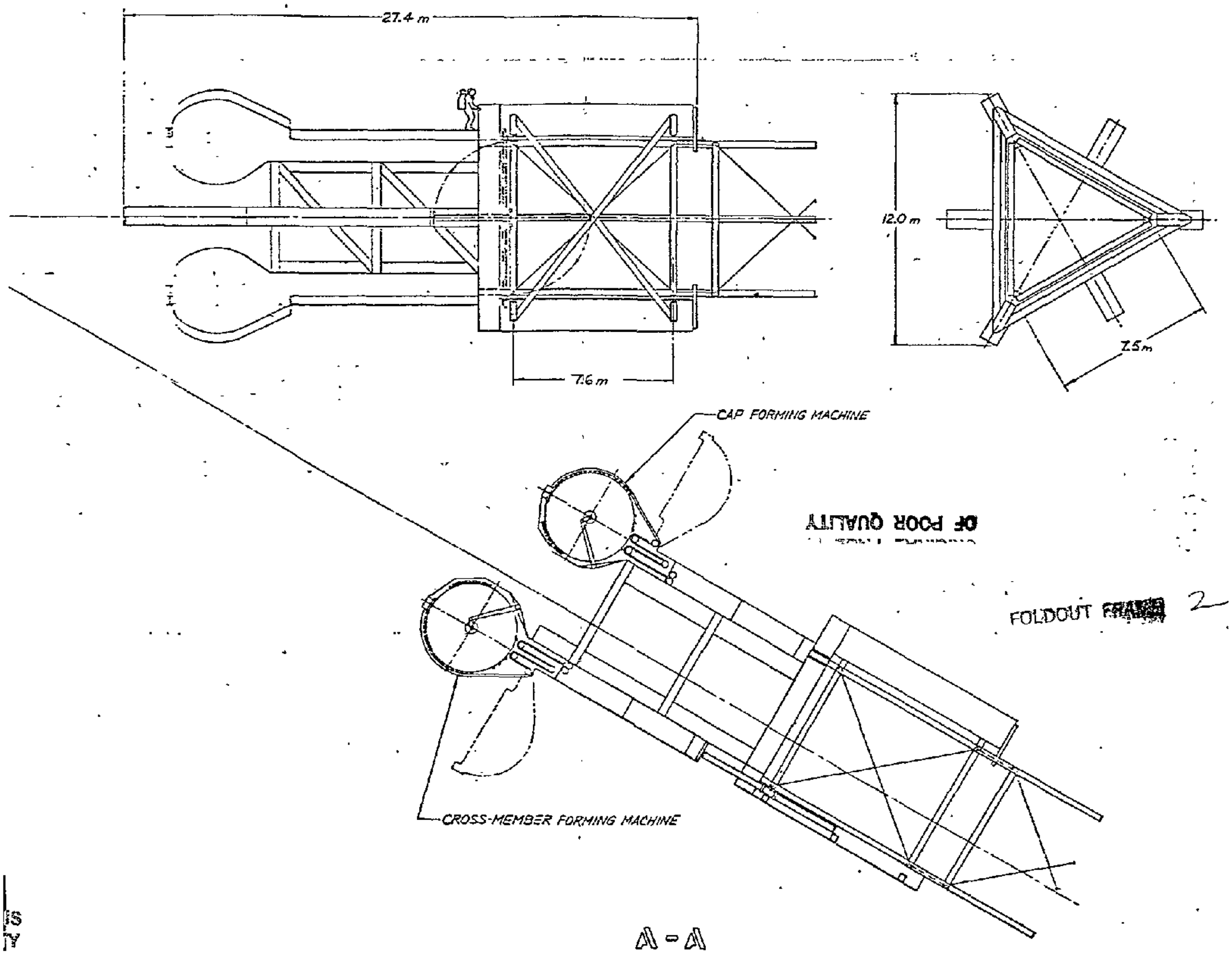

A - A

OF POOR QUALITY
FOLDOUT FRAME 2
FOLDOUT FRAME

Figure 3-76. Beam builder concept for 7.5 m structure.

4

ALTERNATIVE ASSEMBLY JIG CONCEPTS

The SCAFEDS Part I/II tasks resulted in an assembly jig concept for on-orbit fabrication of a planar ladder platform. A major task of Part III was to develop assembly jig and fixture concepts capable of constructing six alternative structural configurations using the beam builder as the basic construction tool and the Orbiter as a construction base. The SCAFE beam was the basic element to be used in building these structures. The task produced concept layouts of the structures, assembly jigs and fixtures, and superstructure installations, which were evaluated for Orbiter compatibility and mission and operation impacts.

4.1 STUDY METHOD AND ISSUES

The basic structures for which construction concepts were developed are shown in Figure 4-1. Included are:

a. An orthogonal cross consisting of two linear beams, each 100 m long

b. An open square, 100 m on a side

c. An open hexagon, 100 m on a side

d. Parabolic segment reflectors of 61 and 500 m diameters

e. A large trianglar cross-section beam 8.5 m on a side and 200 m long.

The 61 m diameter on the smaller reflector and the 8.5 m side dimension on the tri-beam were selected because these sizes in these types of structures are being used by Rockwell International in their Space Construction Systems Analysis Study (Contract NAS9-15718.

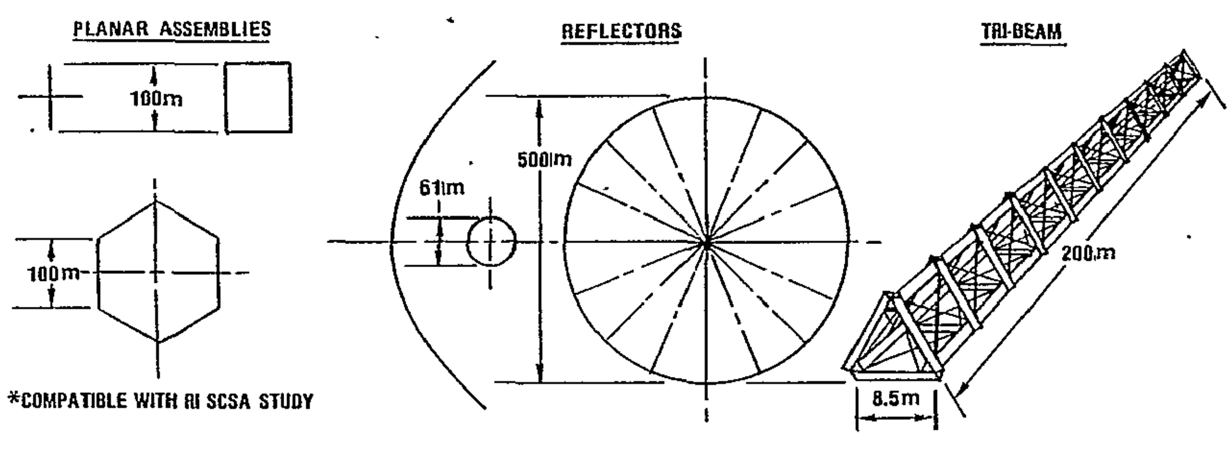

Figure 4-1. Alternative structure concepts.

The task logic flow was as shown in Figure 4-2. The structure and assembly jig design tasks build on data derived in SCAFEDS Part I/II and the curved beam beam builder data described in Subsection 3.5.1. A reference spacecraft concept was developed for each structural shape in order to facilitate the design of superstructure elements and fabrication and assembly sequences. Trade studies of various assembly jig arrangements and assembly sequences resulted in a high degree of commonality between assembly jig concepts. This included not only common subsystem modules but also common assembly jigs for some of the structures. It was found that the square and hex structures could be constructed with the same assembly jig and the cross and 61 m reflector could be manufactured with nearly identical assembly jigs.

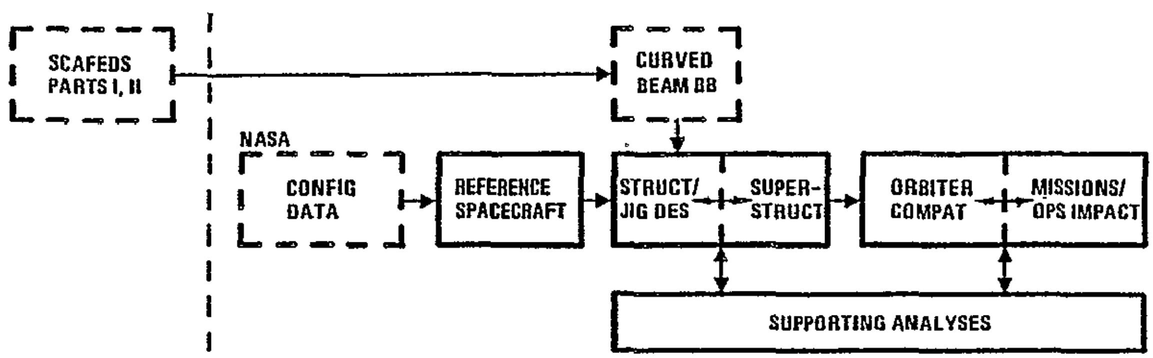

Figure 4-2. Task logic flow diagram.

4.2 CONSTRUCTION OF SQUARE AND HEXAGONAL PLATFORMS

The two open polygon structures selected for this study possessed all of the same characteristics for assembly. It was apparent that the same assembly jigs and fixtures could be used to construct the square and the hexagonal structures. Although both structures could be used to support membrane-type antennas, a different reference spacecraft application was assigned to each type of structure to provide a more complete development of superstructure installation techniques.

4.2.1 PLATFORM CONSTRUCTION TRADES. Before design of the platform structure, assembly jigs, and spacecraft systems installations could be accomplished, a basic platform construction technique had to be established. Concepts for several approaches were sketched and evaluated to determine the best approach.

Concepts 1S and 1H, shown in Figures 4-3a and 4-3b, respectively, sequentially build one side of the polygon at a time, install a corner fitting, then build the next side. This process is continued until the polygon is complete. This approach is very straightforward but has two major problems.

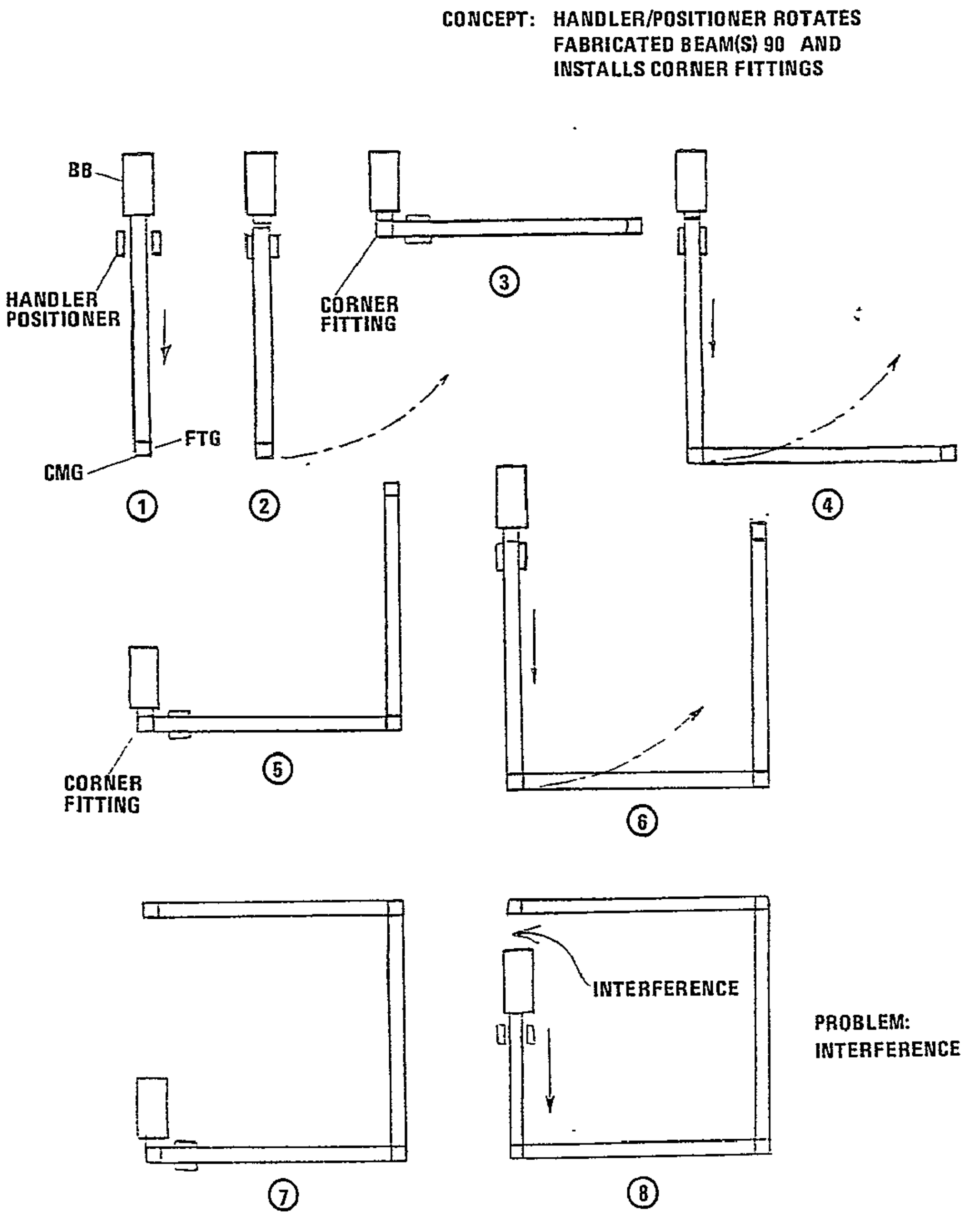

Figure 4-3a. Square platform construction, Concept 1S.

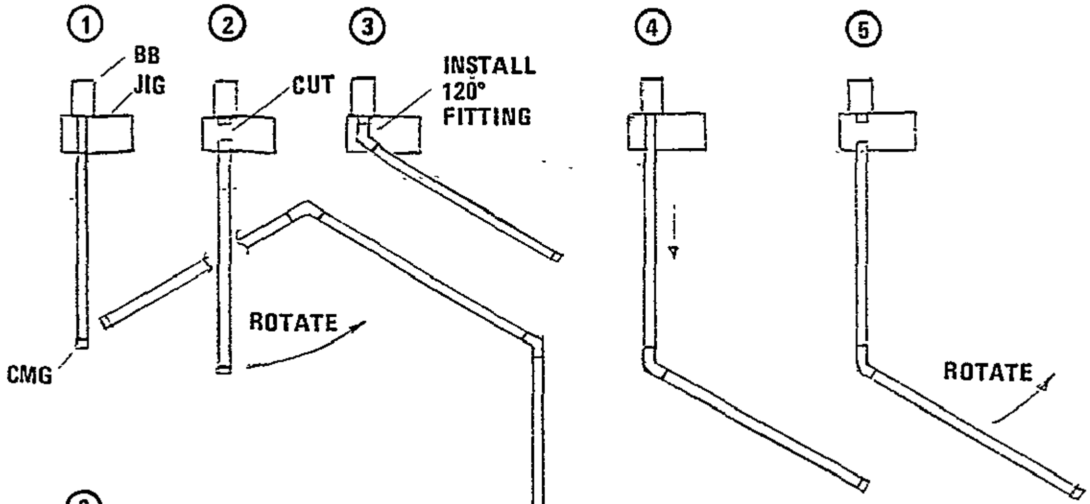

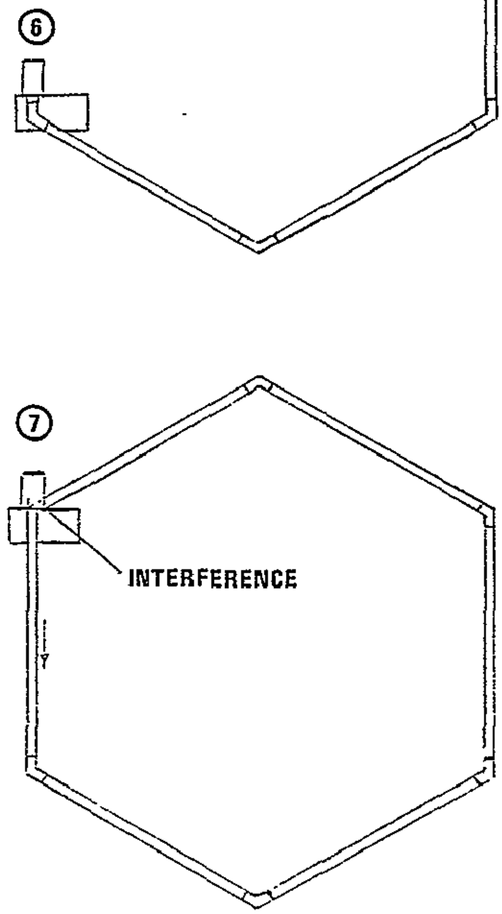

Figure 4-3b. Hexagonal platform construction, Concept 1H.

a. An active control device, such as a CMG, is required at one or several locations on the structure to minimize bending loads and deflections induced by the Orbiter and the orbit environment during construction. The CMGs must prevent the beam under construction in the beam builder from being overloaded in torsion.

b. Closure of the structure at the last corner is complicated. The end of the first beam will collide with the beam builder unless deflected and guided around the interference zone. This deflection further loads the structure in torsion.

Concept 2S, shown in Figure 4-4, is an alternative which could be used to solve the polygon closure problem. By sequential rotation of corner hinges, the polygon closure could be made after the last beam is completed and clear of the beam builder. This approach is also applicable to the hexagonal structure.

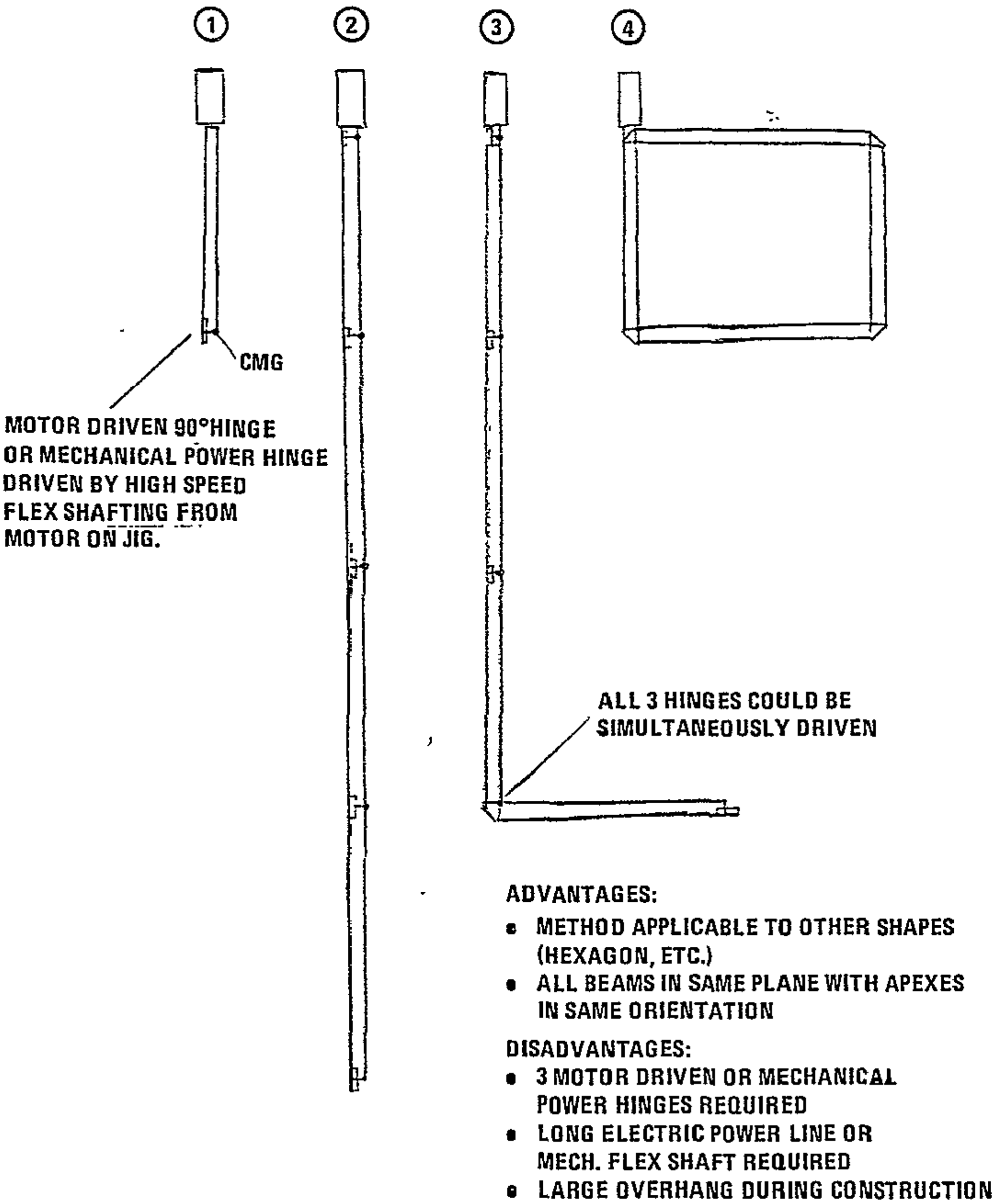

Figure 4-4. Square platform construction, Concept 2S.

Concept 3S, shown in Figure 4-5, provides a means of retaining the free end of the polygon with the assembly jig throughout the fabrication cycles. This approach is complicated by the mechanisms required to control variable geometry of the structure during the construction operations.

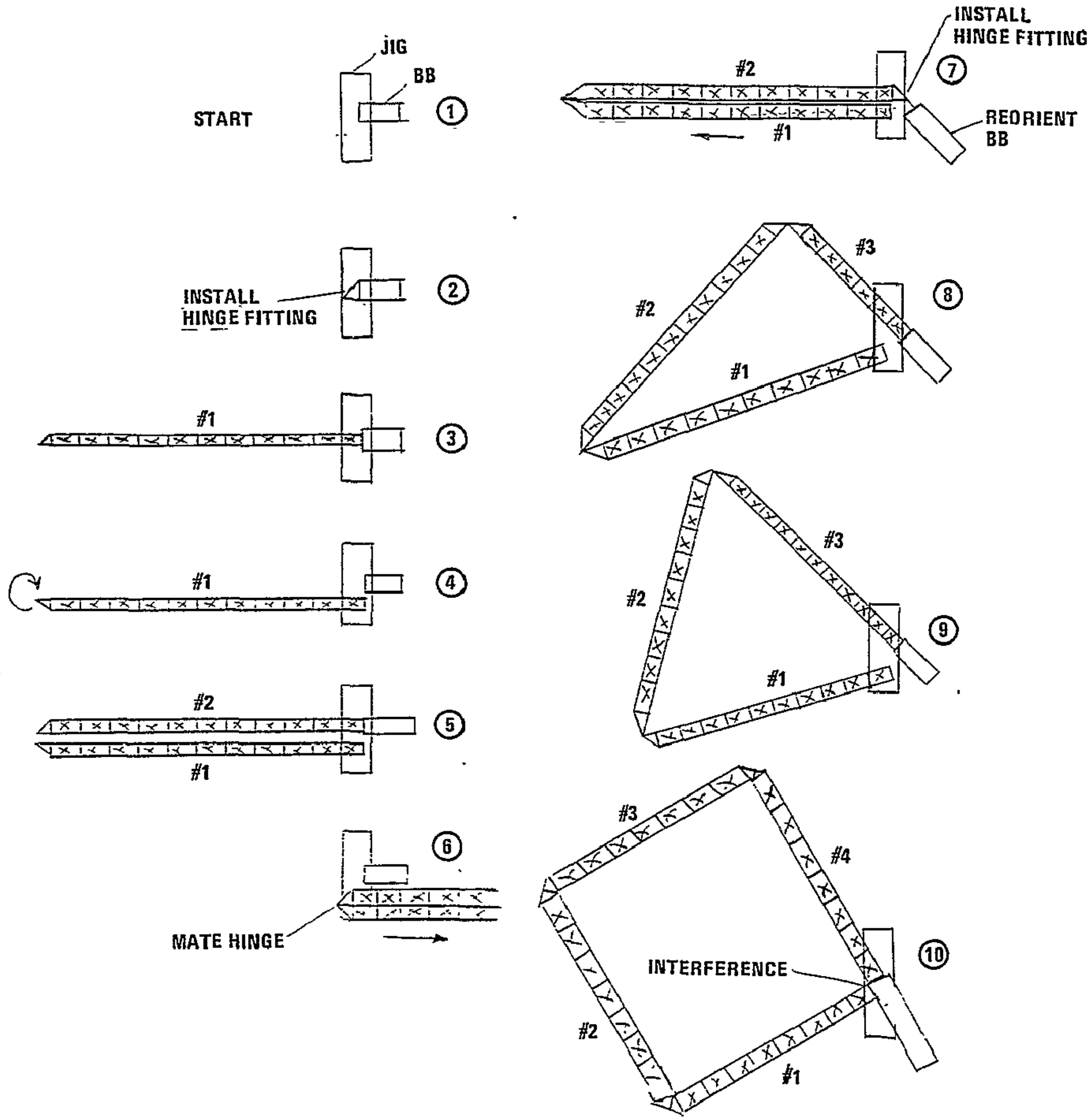

Figure 4-5. Square platform construction, Concept 3S.

Concept 4, illustrated in Figure 4-6, was finally selected as the best approach to polygon construction. The principle advantages of this technique are:

a. CMGs are not required for control of the structure because the polygon is not deployed until after construction is complete.

b. The support of the end hinge point on the jig during deployment prevents torsional loading of beam members.

c. This concept lends itself to ease of transfer and installation of spacecraft system hardware from the Shuttle payload bay prior to full deployment.

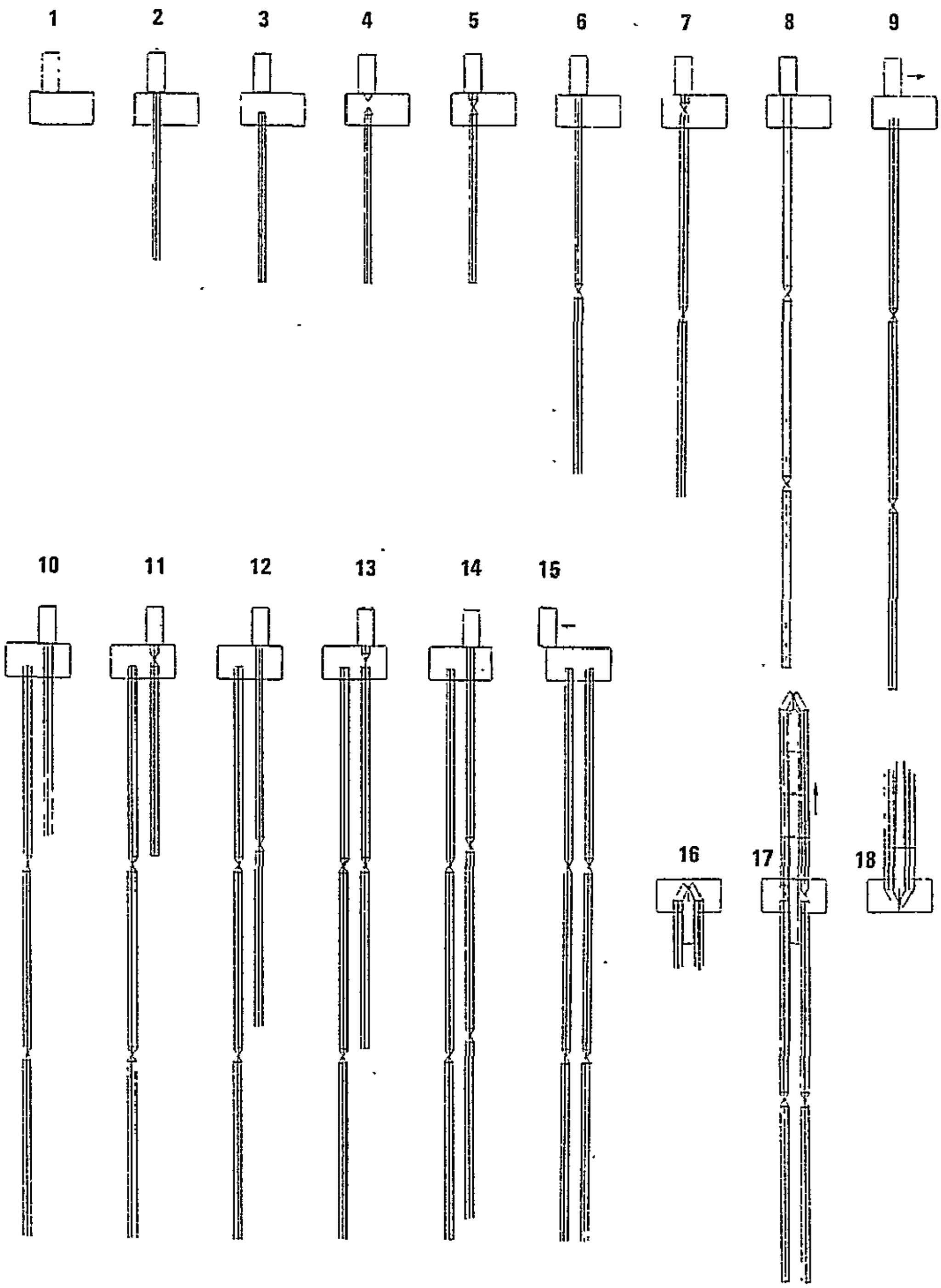

Figure 4-6. Square/hexagonal structure construction, Concept 4.

4.2.2 SQUARE/HEXAGONAL STRUCTURAL CONFIGURATION. Two structural configurations, the square and hexagonal platform, using many of the same basic structural components, have been developed for compatibility with the platform construction concept. These platforms act as rigid planar periphery frames for a variety of flat panels which require in-plane tension loads to maintan an operational tolerance.

The square platform structure shown in Figure 4-7 provides support for a solar collection system consisting of eight uniaxially tensioned blankets deployed from cylindrical canisters. The platform basic structure consists of four identical 64-bay (91.78 m) beams joined by moment-carrying corner fittings. The hexagonal structure similarly consists of six 64-bay beams joined by similar special corner fittings.

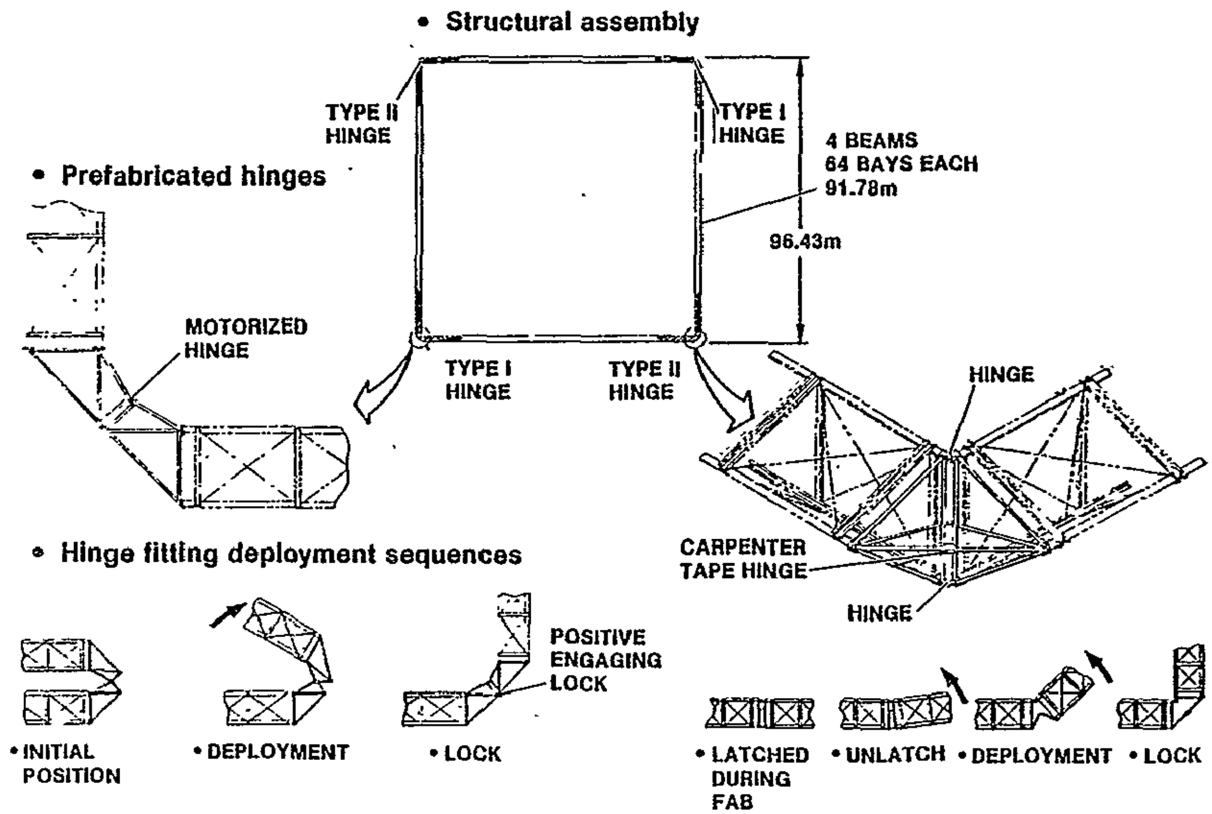

Figure 4-7. Square platform structure.

The selected fabrication and deployment sequence for the square platform requires two basic types of corner fittings to attach adjacent beams. One fitting joins two beams oriented end-to-end, and enables either one or both beams to rotate about an axis that passes through two of the beam cap intersections. This Type II hinge is shown in Figure 4-7. For the hexagonal structure, this fitting will be configured to allow only 60° rotation. The Type II hinge is a tube truss with two equilateral triangular frames that pivot about two single-degree hinges. The three vertices of each triangular frame interface with and connect to the three beam caps by means of triangular-shaped sleeves which fit inside of the beam caps as shown in Figure 4-8. Each sleeve has large radius rounded edges for easy fitting, a solid aluminum core which acts as a self anvil during ultrasonic welding, and a polysulfone coating which is necessary to ultrasonically weld the beam cap to the sleeve. A weld pattern of two 0.009 m (0.375 in) diameter spot welds on each beam cap flat provides a rigid beam cap-to-corner fitting connection. This fitting self-deploys to and positive-locks at a prescribed position (90° angle for square, 120° angle for hexagonal) by means of a carpenter tape hinge. An attachment point for the catenary cable is provided at mid-height of the interior flat side of the beam. The inclusion of a stiffening member in each triangular frame connects the load path from the catenary cable directly into the beam cap.

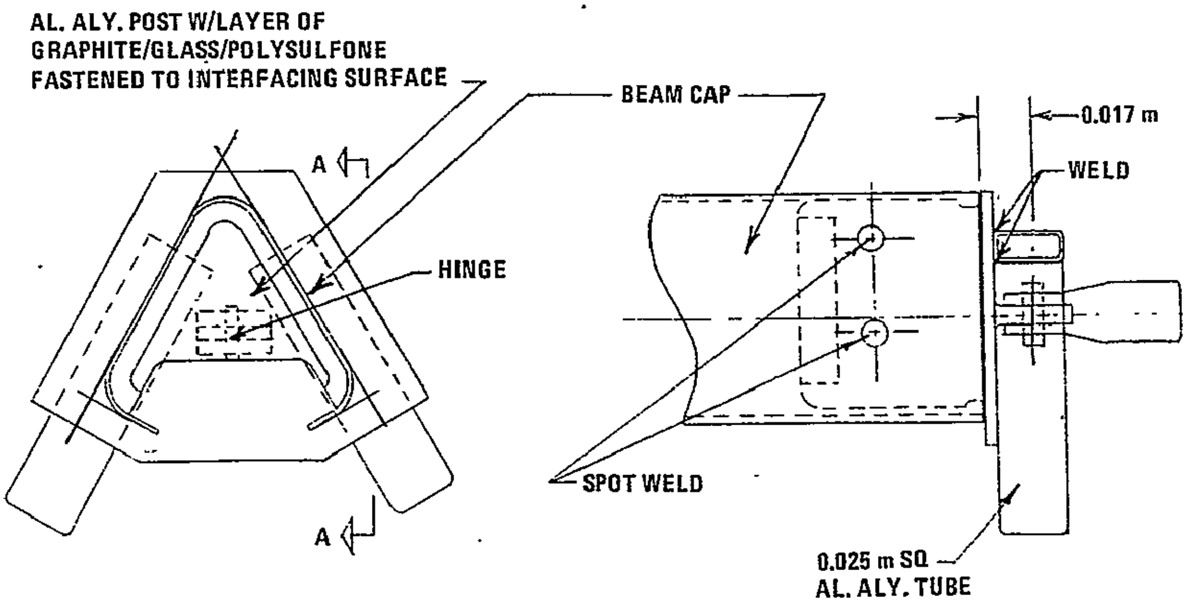

Figure 4-8. Hinge fitting-to-cap joint.

The second type of corner fitting is required to rigidly attach together two beams which are oriented side-by-side, and to be able to rotate both beams about an axis parallel to the interior flat side of each beam. It is necessary to maintain a 0.76 m (30 in) space between the two beams when they are oriented side-by-side in order to provide clearance for the solar array blanket and other equipment. This corner fitting is similar to the other fitting except that the pivot points are cantilevered 0.762 m (30 in) from each beam cap to provide clearance. Beam cap/corner fitting interfaces are the same as for the first type of corner fitting. This fitting is self-deploying by means of a drive and gear mechanism at the pivot hinges and locks in a prescribed position by means of a positive engaging lock.

Moment-carrying corner fittings, beam symmetry about the frame mid-plane, and mid-plane application of membrane tension loads all help prevent out-of-plane instability of any planar polygon. The square and hexagonal concepts include these features and preliminary analyses show adequate individual member and cap element stability under compressive loads induced in the peripheral frame by membrane tension. However, if strictly planar systems (i.e., no out-of-plane bracking by mast struts, etc.) are pursued further, detailed analyses must be performed to assure overall stability of the peripheral frame.

4.2.3 REFERENCE SPACECRAFT CONCEPTS. The reference spacecraft selected for the square platform is a planar solar array as shown in Figure 4-9. The version shown is for LEO and will provide approximately 1 MW of raw power.

For the hexagonal platform, a GEO phased-array communication satellite concept is shown in Figure 4-10. This planar array is similar to the GAC space-fed phased-array concept.

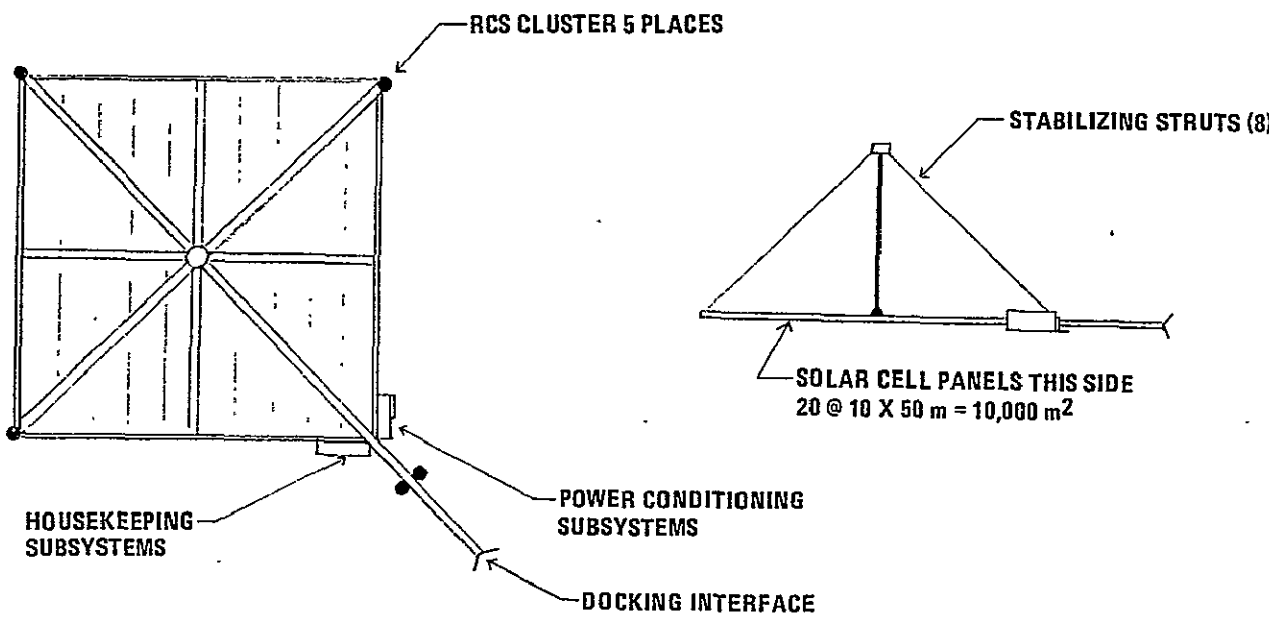

Figure 4-9. Planar solar array concept.

4.2.4 SQUARE AND HEXAGONAL STRUCTURE ASSEMBLY JIG

4.2.4.1 Assembly Jig Concept. The assembly jig concept for fabrication and assembly of the square or hexagonal structures (shown in Figure 4-11) is a common design for both. It incorporates most of the basic features of the original SCAFE "ladder" assembly jig, which include:

a. Cradle

b. Deployment actuator

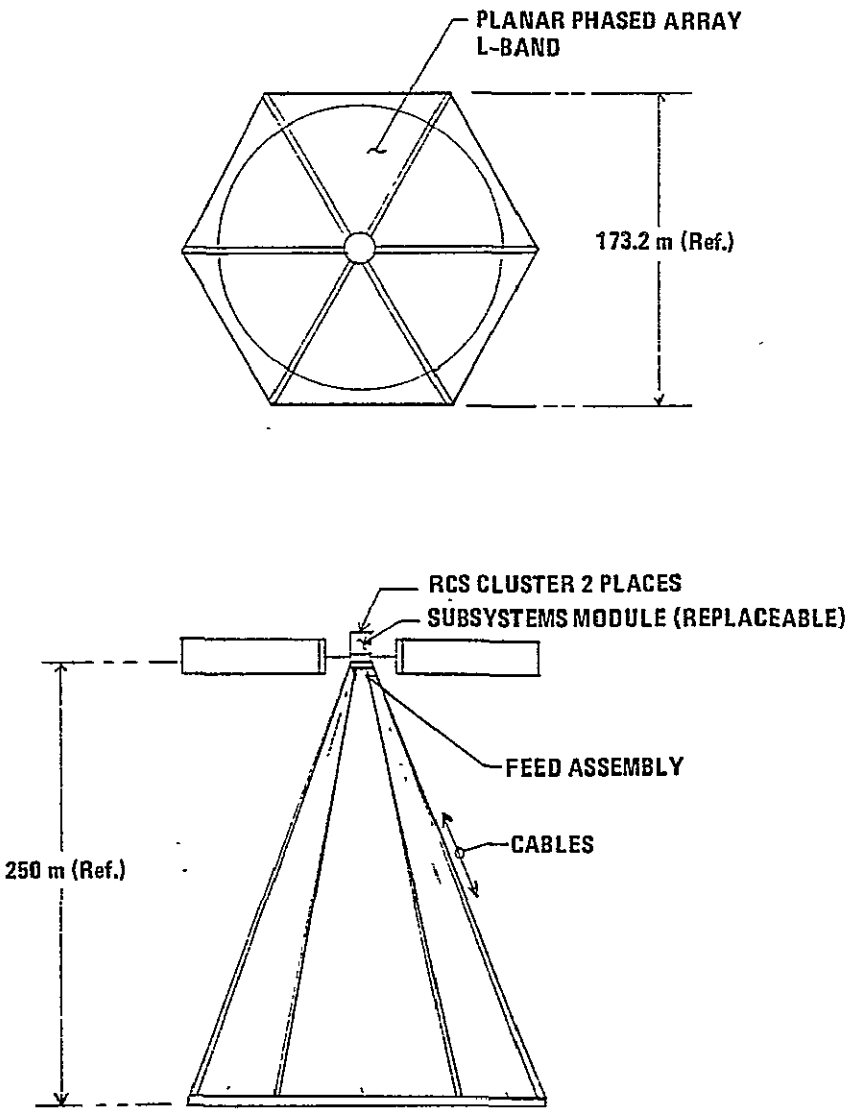

Figure 4-10. Phased-array antenna communications satellite concept.

c. Retention and guide mechanisms (RGMs) and beam drive mechanism

d. Beam builder deployment and positioning mechanisms

The unique features of this jig are the two beam fabrication stations, which make the jig shorter than the SCAFE jig, and the beam turn-in mechanisms for rotation and translation of beams as they are held by the RGMs.

The square and hexagonal structures are fabricated and assembled in the same general sequence using the same basic assembly jig. The sequence for the square structure is shown in Figure 4-12; however, for the hexagonal structure two additional beams and Type II hinges are required.

1. Beams are fabricated across the assembly jig at two stations. As one is completed, it is joined to the next through a Type II hinge by hand-held welder operations. When the required number of beams are joined in line (2 for square, 3 for hexagonal) the finished beam set is held in place by the RGMs and the beam builder is moved to the next station, where an identical set of beams is fabricated and connected by hinges.

2. The finished beam sets are turned in toward each other by the turn-in mechanisms, as shown, and a Type I hinge is installed and hand-welded in place.

3. The beam sets are driven back across the jig, during which time the superstructure and system hardware are installed.

4. At the end of the beam sets, a second Type I hinge is installed and manually welded. This hinge is secured to the assembly jig through the hinge point in preparation for deployment of the structure.

4.2.4.2 Assembly Jig Controls Concept

4.2.4.2.1 Controls Commonality. The assembly jigs baselined for the cruciform, square, hexagon, and 61-meter antenna have a significant degree of commonality. It appears achievable to develop a common control approach to accommodate most construction functions for these assemblies, with minor additions or deletions of selected configuration-unique construction equipment. The assembly jig avionics philosophy for these structures will be similar to that used for the SCAFE ladder platform, and each can be assembled in one Shuttle mission.

The basic assembly jig controls block diagram is shown in Figure 4-13. A central controller, the ACU, will be used to control and monitor the jig subsystems. The ACU will receive control signals from and send status data to the Orbiter processor. The ACU will also control and monitor the beam builder controller (BCU). Multiplexing methods, similar to those used (and presented previously) for beam builder control, will be implemented for assembly jig control.

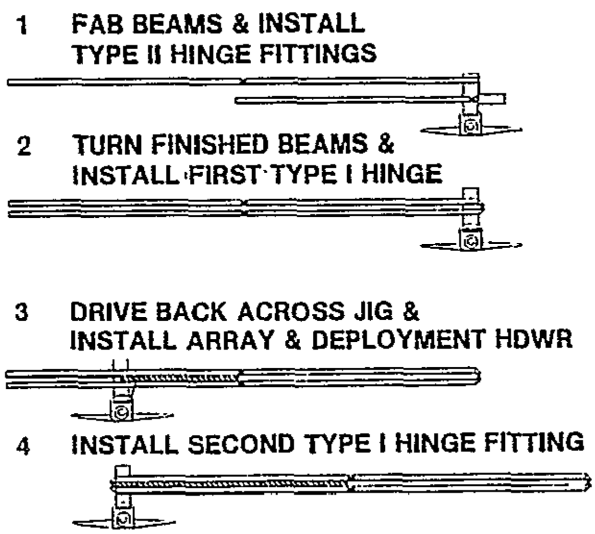

Figure 4-12. Square and hexagonal construction sequence.

The assembly jigs designed to construct the square, hexagon, cruciform, and 61-m antenna will use certain common control equipment as shown in Figure 4-14. The three basic jig mechanisms common for all structures perform:

a. Deployment of the assembly jig from the Shuttle cargo bay

b. Deployment of the beam builder from its stowed position

c. Final positioning of the beam builder on the assembly jig for beam fabrication.

This control equipment has been previously defined for the SCAFE ladder assembly jig in Part II of the SCAFED study.

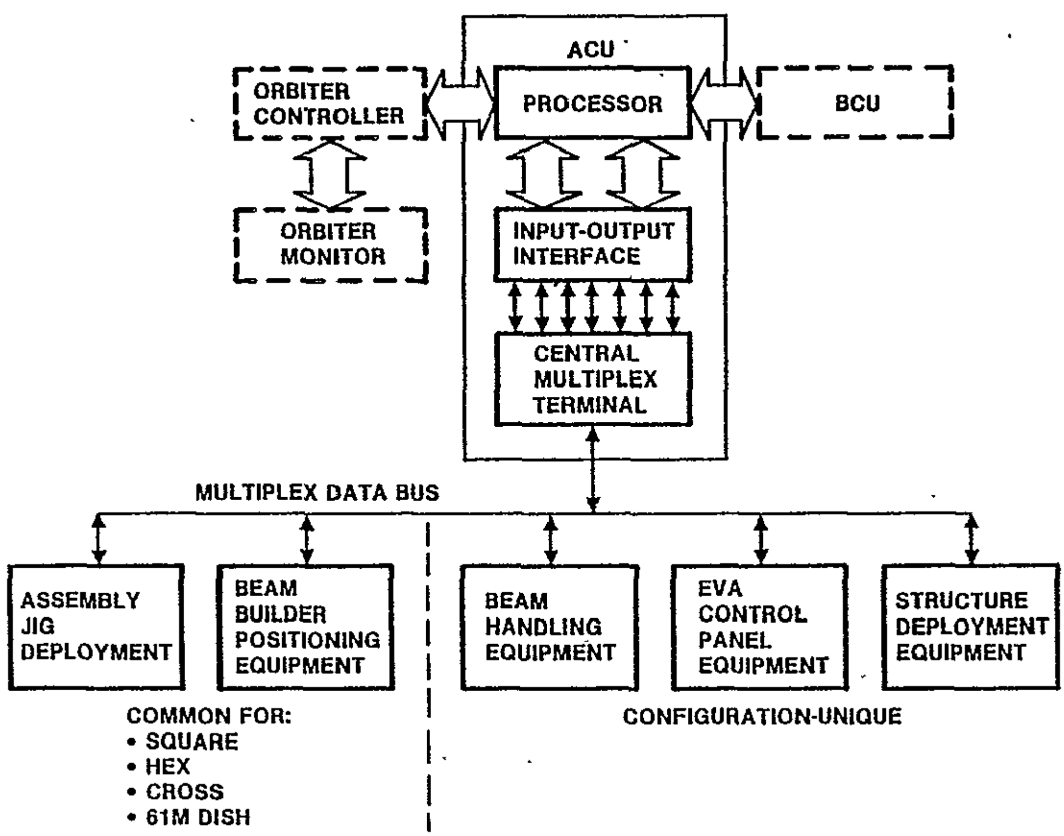

Figure 4-13. Assembly jig control system block diagram.

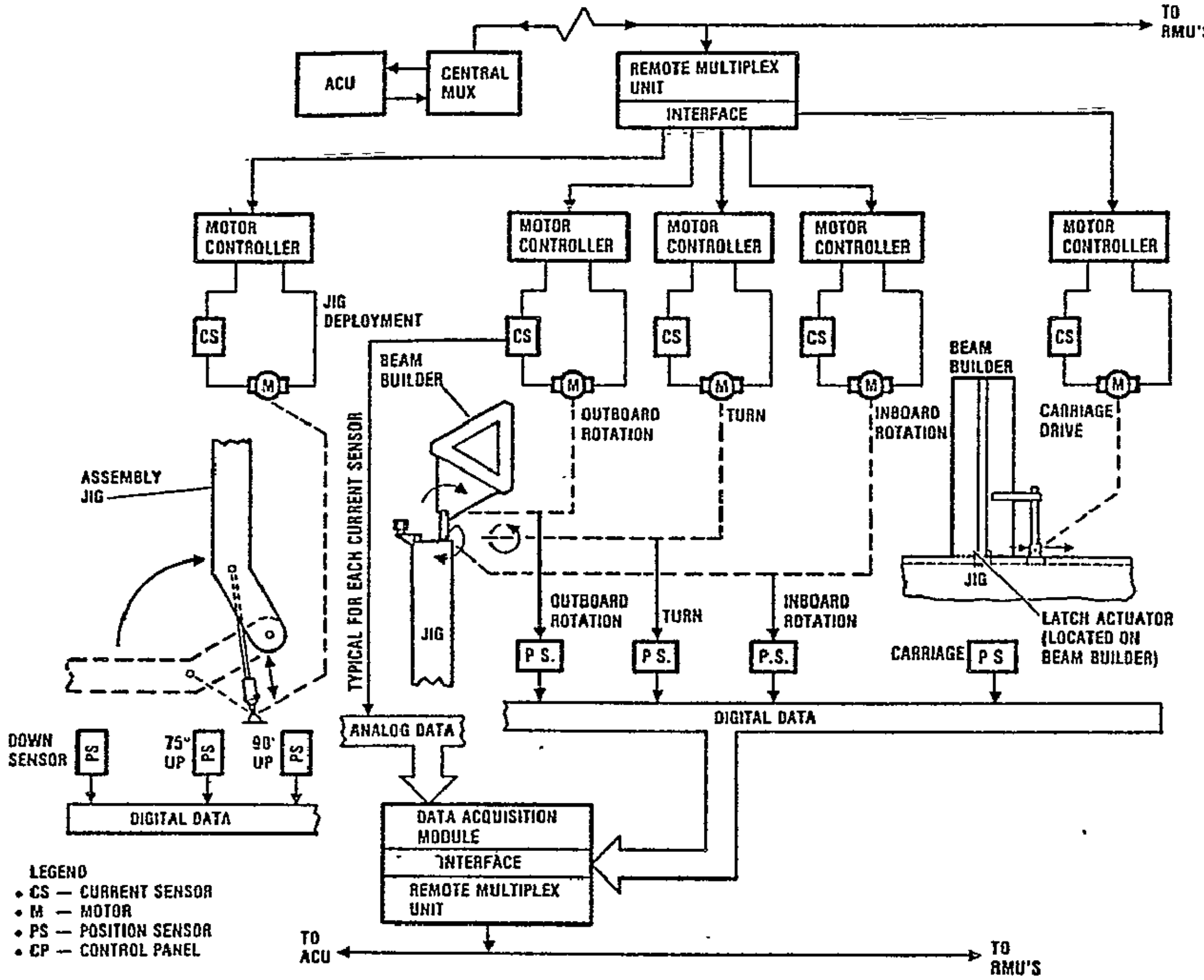

Figure 4-14. Jig/beam builder deployment control diagram.

4.2.4.2.2 Square and Hexagonal Structure Assembly Jig Control Equipment. Two beam builder fabrication stations are required on the assembly jig for the square and hexagonal structures. Two beams joined together by special hinge fittings will be fabricated by the beam builder at each station for the square structure, and three beams joined together by special hinge fittings will be fabricated at each station for the hexagonal structure. Each fabrication station will use retention and guide mechanisms (RGMs) and beam drive mechanisms for beam handling after each beam is fabricated. Figure 4-15 shows the handling, assembly, and structure deployment control equipment located on the assembly jig.

After the assembly jig has been deployed and the beam builder is located at Station I, beam fabrication is initiated by the ACU. The beam builder, under the control of the BCU, will fabricate the first beam.

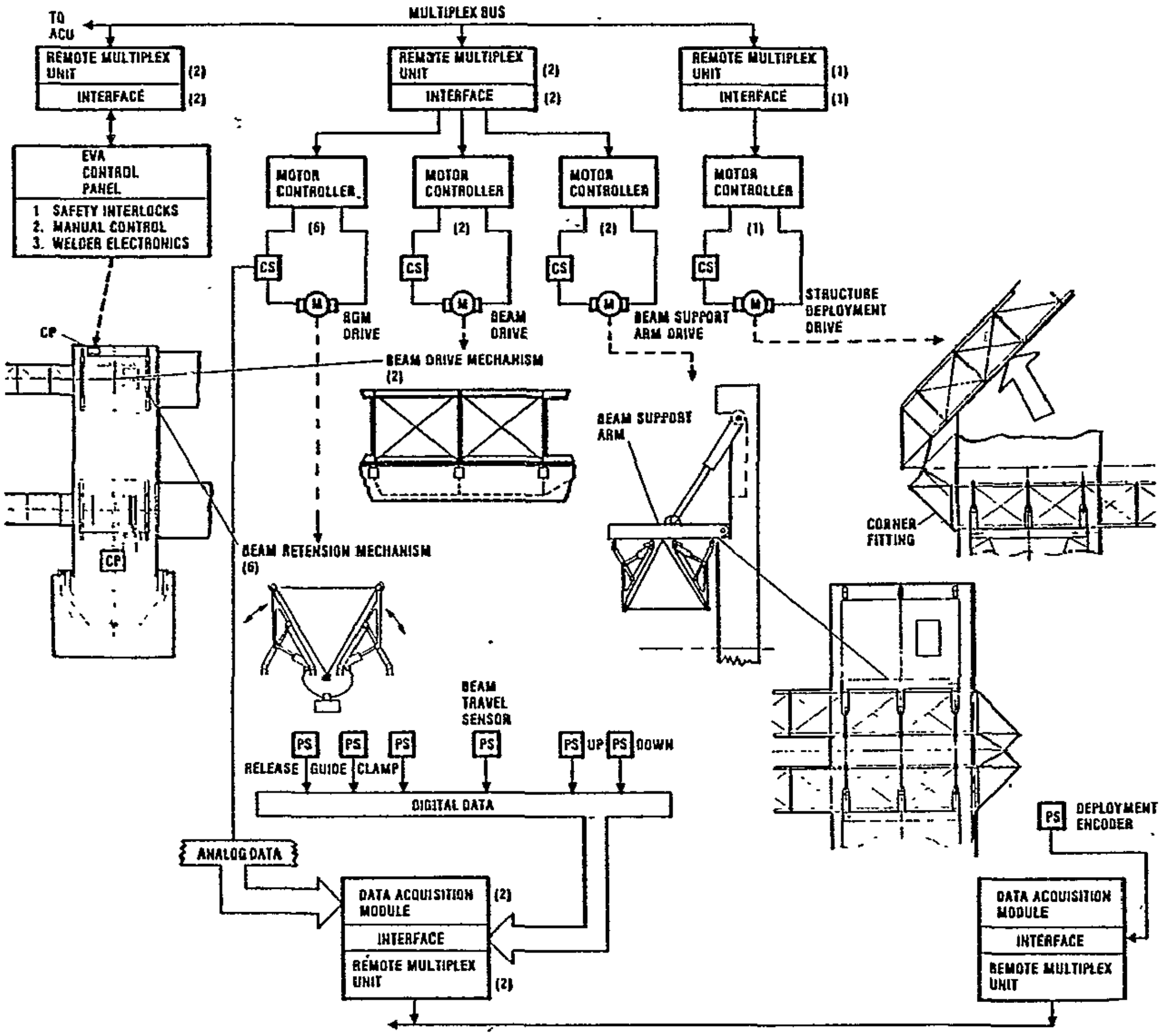

Figure 4-15. Square/hexagon jig control diagram.

Three RGMs and one beam drive mechanism are mounted on a beam support arm located at each fabrication station. During beam fabrication, the beam support arms will be collapsed into the assembly jig (down position). After the first beam is fabricated, the ACU energizes the three RGMs, which grasp the first beam. Three position sensors are used for each RGM to monitor its operation. After the beam is secured, the ACU signals the BCU to cut off the first beam. The ACU then signals the beam drive mechanism to translate the beam forward to a position where a corner fitting may be installed. A beam travel sensor is used to monitor this movement.

The hinged corner fitting is manually installed on the beam by astronauts on EVA. EVA control panels are located at each fabrication station to provide the necessary safety interlocks, beam fine positioning controls, and welder power and control interfaces. Hand-held ultrasonic welders with umbilical cords are connected to these control panels and will be used to join the hinged corner fitting to the beam. Upon completion of installation of the corner fitting on the beam, the astronaut indicates status to the ACU via the control panel.

The ACU will command the BCU to fabricate the first bay of the next beam. After one bay is fabricated, the beam builder stops the fabrication sequence. The forward end of this beam will be inserted into the corner fitting previously welded on the first beam. Using the manual fine positioning controls, the second beam is then secured to the corner fitting by the hand-held ultrasonic welder. After the welding is complete, the astronaut will once again indicate status to the ACU via the control panel.

The ACU will command the RGMs to release the first beam and then signal the BCU to complete fabrication of the second beam. After the second beam has been fabricated, the entire two-beam assembly with corner fitting is grasped by the RGMs, and the second beam is cut off by the beam builder.

For the square structure, the beam builder will be repositioned after the second beam is cut off. The two-beam fabrication and assembly sequence will then be repeated at the second (innermost) fabrication station.

For the hexagonal structure, the beam builder will remain at Station I where a second corner fitting will be installed and a third beam will be fabricated in the same sequence described above. The beam builder will then be repositioned to Station II, where the same three-beam fabrication and assembly process will be repeated.

When the two sets of beam assemblies have been completed, the ACU commands the beam support arm drives to rotate the two beam assemblies 90°. The beam builder will then be positioned, via ACU command, in its stowed position to provide clearance for final assembly operations.

Next, a hinged corner fitting will be installed across the ends of the two beam assemblies by astronauts using the hand-held ultrasonic welders. After the hinged corner fitting is installed, the beam drive mechanisms, as commanded by the ACU, will simultaneously translate the two beam assemblies until the opposite ends are positioned on the jig for installation of the second hinged corner fitting. This translation motion may be stopped periodically to allow for attachments of other equipment (such as solar blanket canisters, blanket deployment mechanisms, etc.) to the beam assemblies.

When the opposite ends are positioned on the jig, the second hinged corner fitting is installed with the hand-held ultrasonic welders. Installation of this corner fitting completes the undeployed structural assembly (square or hexagon).

A structure deployment drive on the assembly jig structure is attached to the corner fitting via a rigid shaft. The RGMs on the outermost beam support arm are released and the beam support arm is retracted into the jig. With the structure being held and supported by the RGMs on the Station II beam support arm, the structure is deployed, causing the folded assembly to open into a square (or hexagonal) structure. Latching mechanisms on all corner fittings lock the structure in its required configuration. Each latch will be energized to unlatch in the proper sequence on commands from the Orbiter control panel.

After the structure has been deployed and all spacecraft subsystems installed and verified, the RGMs will release the structure upon Orbiter command. The hinge fitting is then separated from its support shaft and the Station II beam support arm will return to its stowed position.

4.2.5 DEPLOYMENT SEQUENCES

4.2.5.1 Square Structure and Solar Array Deployment. Deployment of the square structure is accomplished by unlatching the two Type II hinges and activating the motorized Type I hinges until the structure is fully deployed and locked. This sequence, shown in Figure 4-16, requires retention of the structure at the assembly jig by one set of RGMs and a hinge support fitting. The hinge support fitting reacts bending loads on the swinging beam to prevent loading the beam held by the RGMs in torsion during and after deployment.

For this spacecraft, a solar array was selected as a reference application. With the solar panels encapsulated in canisters mounted along one beam as shown in Figure 4-17, a panel deployment drive is provided to individually deploy each panel in sequence.

4.2.5.2 Hexagonal Structure and Array Deployment. The concept for deployment of the hexagonal structure is similar to the square structure deployment, except the additional hinged joints require careful operations sequencing to ensure the stability of the structure during deployment. This sequence is illustrated in Figure 4-18, using a deployable lens array concept to show how the array is sequentially spread to its full area. This concept requires that the lens array be precisely fabricated on the ground to conform to the predetermined dimensions of the finished structure. Additional tension control devices would also be required to maintain tautness of the membrane.

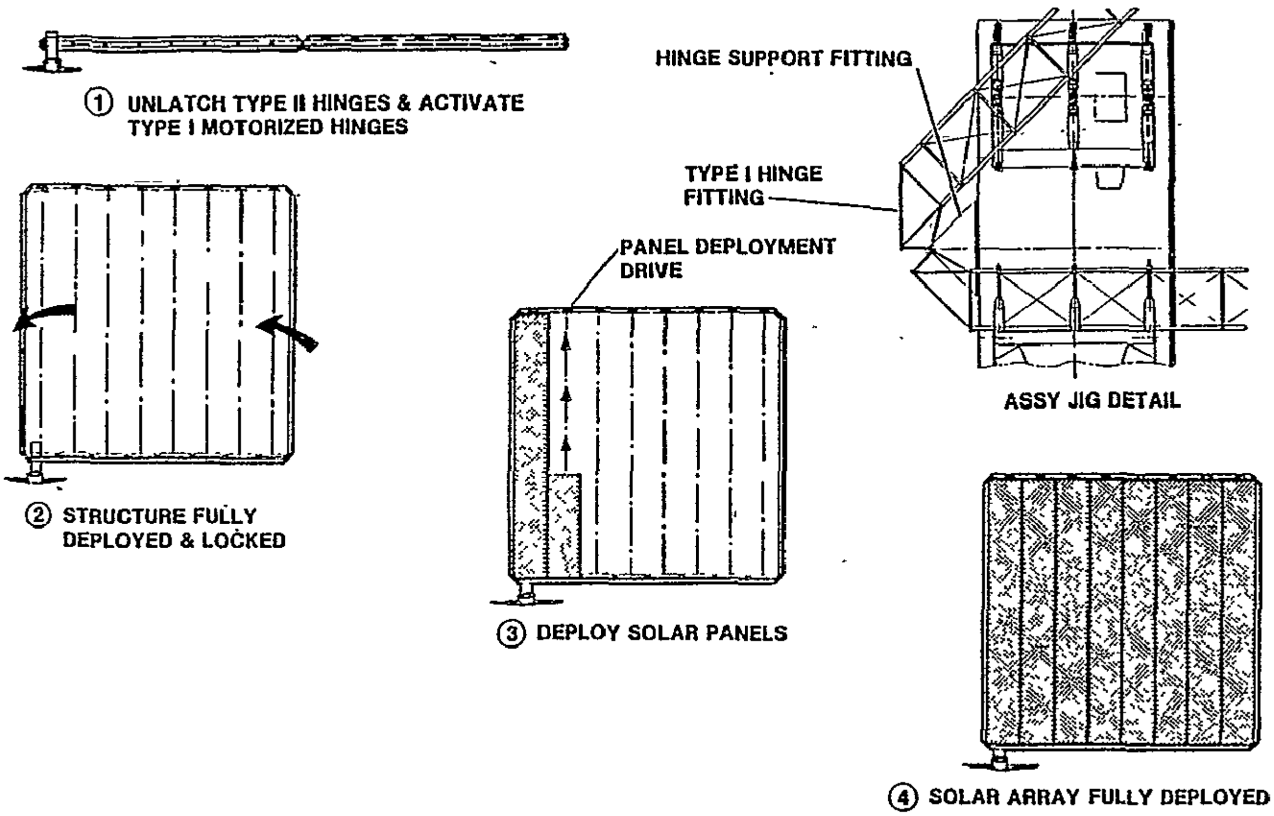

Figure 4-16. Square structure deployment sequence.

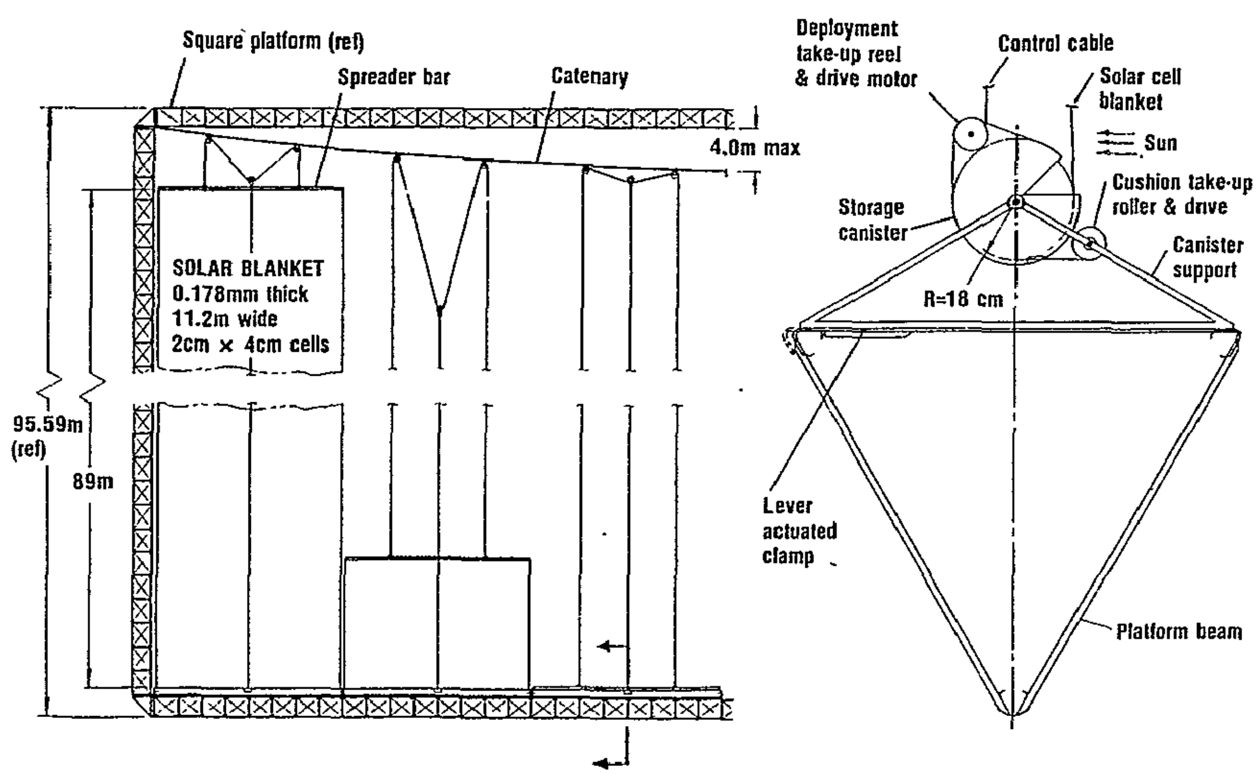

Figure 4-17. Solar blanket installation and deployment concept.

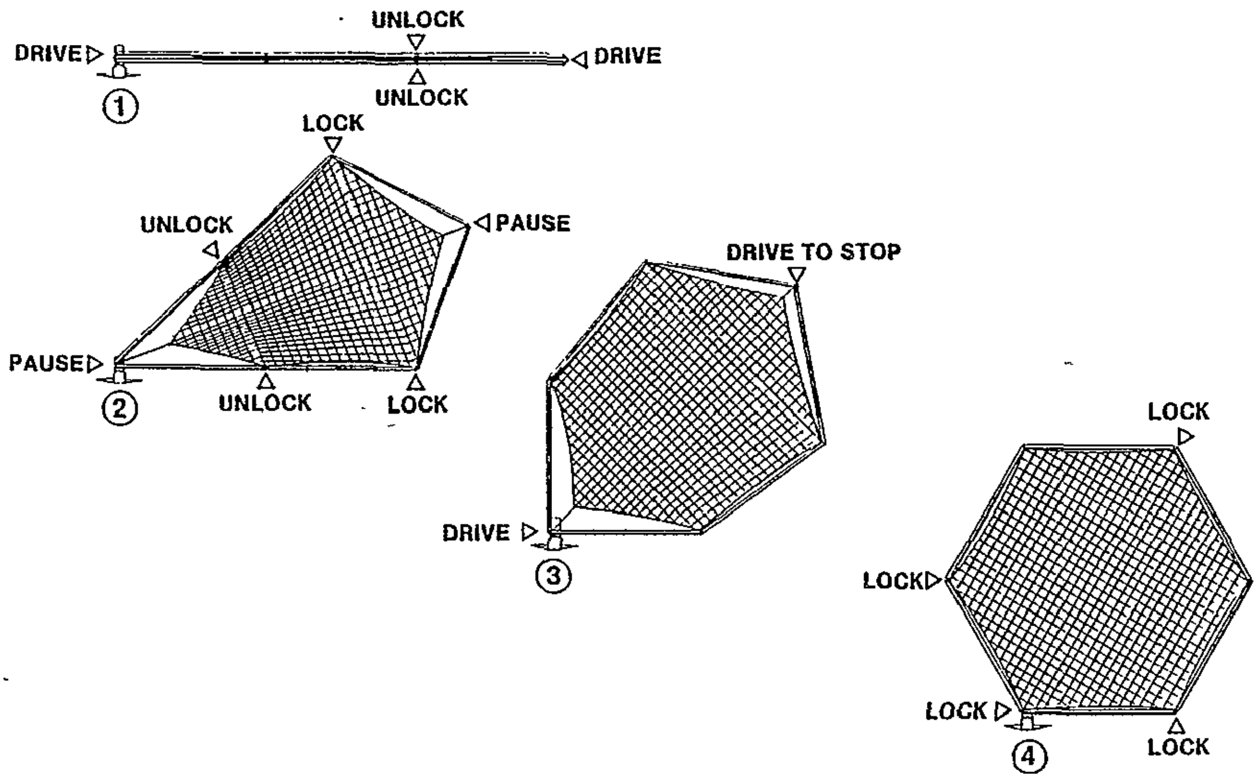

Figure 4-18. Hexagonal structure deployment sequence.

4.2.5.3 Dynamic Analysis. The hexagonal platform predeployment span exceeds the previous SCAFE ladder span by 50 percent (300 meters versus 200 meters), and its perimeter envelopes the square, cross, and small antenna. Consequently, it was selected as a worst-case configuration for modal analysis.

Four configurations representing the closed, partially opened, and fully open frame were analyzed for two support conditions: free-free, and pinned at one node (to approximate the Orbiter-attached condition). The results of these analyses are shown in Figure 4-19.

Through the combination of fitting design and the use of powered hinges for deployment, the joints are effectively rigid. Element properties, mode descriptive terminology, and results of the analyses are shown. Bending (EI) and torsional (KG) stiffnesses are the equivalent values for the baseline beam presented in Section 2. As expected, the lowest modal frequency drops significantly when the frame starts to open because the members are subjected to combined bending and twisting, and the individual member torsional stiffness (KG) is much less than EI.

• CONFIGURATION

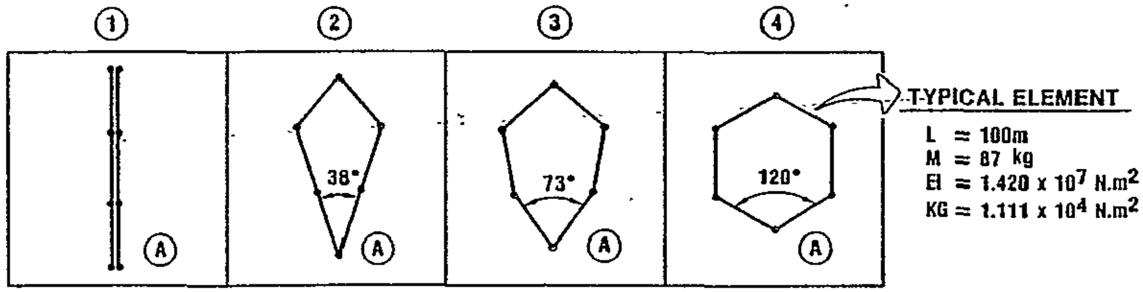

• FREQUENCIES/MODES

• PINNED AT (A)

	1	2	3	4
1	0.14 BE	0.008 BE	0.008 BE	0.008 BE
2	0.14 BE*	0.241 BR	0.019 T	0.010 T
3	0.22 BR	0.275 T	0.022 BE	0.016 BE

• FREE-FREE

	1	2	3	4
1	0.17 BE	0.009 BE	0.009 BE	0.010 BE
2	0.17 BE	0.267 BR	0.019 T	0.010 T
3	0.22 BR	0.275 T	0.026 BE	0.018 BE

MODE CODE

T

BE

BR = IN-PLANE BREATHING

BE* = IN-PLANE

• OBSERVATION

• f_1 DROPS ABRUPTLY FROM (1) TO (2)

• BEAM TWIST DOMINATES (LOW KG/EI)

Figure 4-19. Hexagonal platform modal analysis.

4.3 CROSS AND 61 m REFLECTOR CONSTRUCTION

The common characteristic of the cross and the 61 m parabolic reflector is that their structures are composed of beams radiating outward from a central point. This similarity suggested that a common assembly jig concept would be feasible for the construction of both of these structures.

4.3.1 CROSS PLATFORM CONSTRUCTION TRADES. Before selecting a final spacecraft configuration concept for the cross structure, several construction techniques were evaluated. Two possible assembly methods are: (1) non-planar assembly, where two 100 m beams are joined to each other at the center with a beam-to-beam joint such as those used on the SCAFE ladder platform; and (2) planar assembly, where the beams are joined such that one apex of each beam lies within a common plane.

Concept 1, shown in Figure 4-20, is a technique for non-planar assembly. First the beam builder fabricates one 100 m beam which is held on the assembly jig by RGMs while the beam builder is repositioned for cross-beam fabrication. The first beam is translated across the assembly jig until its center aligns with the center of the cross-beam. The beam builder then fabricates the first half of the cross-beam, the two beams are joined at their centers by ultrasonic weld joints, and the first beam is deployed along with the cross-beam by beam drive action.

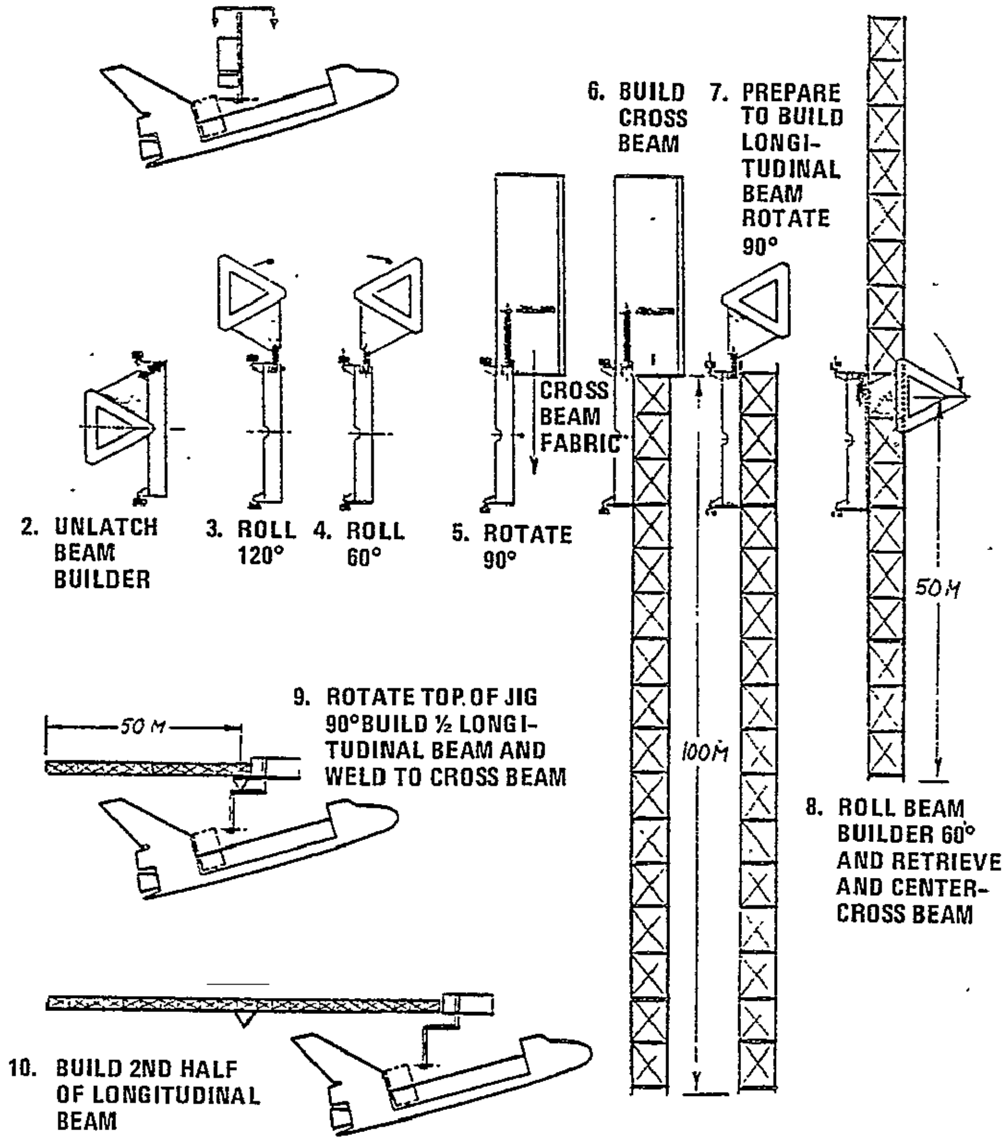

Figure 4-20. Cross platform construction, Concept 1.

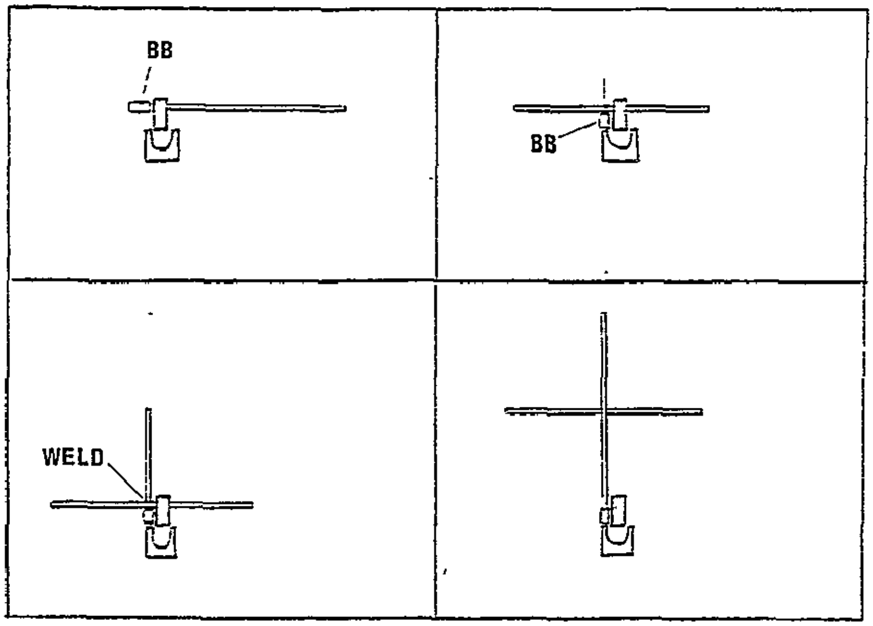

ADVANTAGES:
- SIMILAR TO BASELINE CONCEPT
- NO SPECIAL FITTING REQUIRED FOR JOINING BEAMS
- BEAM INTERSECTION JOINT ACCOMPLISHED BY ULTRASONIC WELDING

DISADVANTAGES:
- ENTIRE CONSTRUCTED PLATFORM IS CANTILEVERED FROM BEAM BUILDER BEFORE CUTOFF FROM BEAM BUILDER
- APEXES OF BEAMS NOT IN SAME PLANE

Figure 4-20. Cross platform construction, Concept 1. (Concld)

Concept 2, shown in Figure 4-21, is a technique for planar assembly. The assembly jig is similar to the Concept 1 jig, except the beam builder is not rolled after the first beam is fabricated. The beam builder turns 90° and is elevated above the plane of the first beam so the first half of the cross-beam can be fabricated. A special fixture will grasp the half cross-beam, position it in plane with the first beam, then weld it to the first beam through a special beam fitting. The beam builder is then lowered to the plane of the first beam, another beam fitting is installed, and the end of the second half cross-beam is joined to the first beam. The first beam is then deployed along with the cross-beam by beam drive action.

Concept 3, shown in Figure 4-22, is the second option for planar assembly. This technique uses a center hub fitting which is mounted on a turret mechanism. The beam builder fabricates one half length of cross-beam at a time. The beam is grasped by a positioning fixture, cut off by the beam builder, then moved into position for joining to the center hub. After the beam is joined, the positioning fixture is retracted and the hub is rotated 90°. This sequence is repeated until the cross assembly is complete.

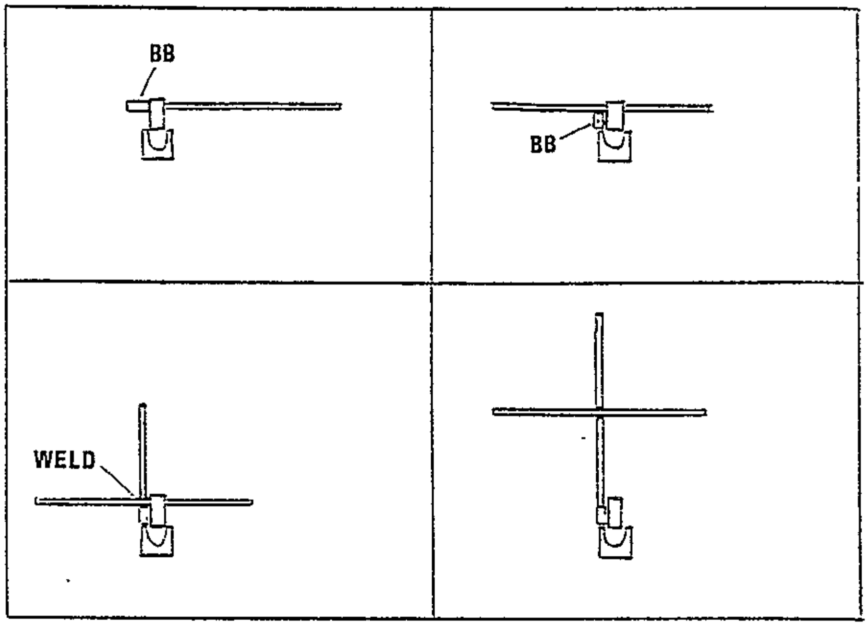

ADVANTAGES: • ALL BEAMS IN SAME PLANE WITH APEXES IN SAME ORIENTATION

DISADVANTAGES: • REQUIRES CENTER FITTINGS (2)
• ENTIRE PLATFORM CANTI-LEVERED FROM BEAM BUILDER

Figure 4-21. Cross platform construction, Concept 2.

• CROSS CONSTRUCTION/ASSEMBLY SEQUENCE

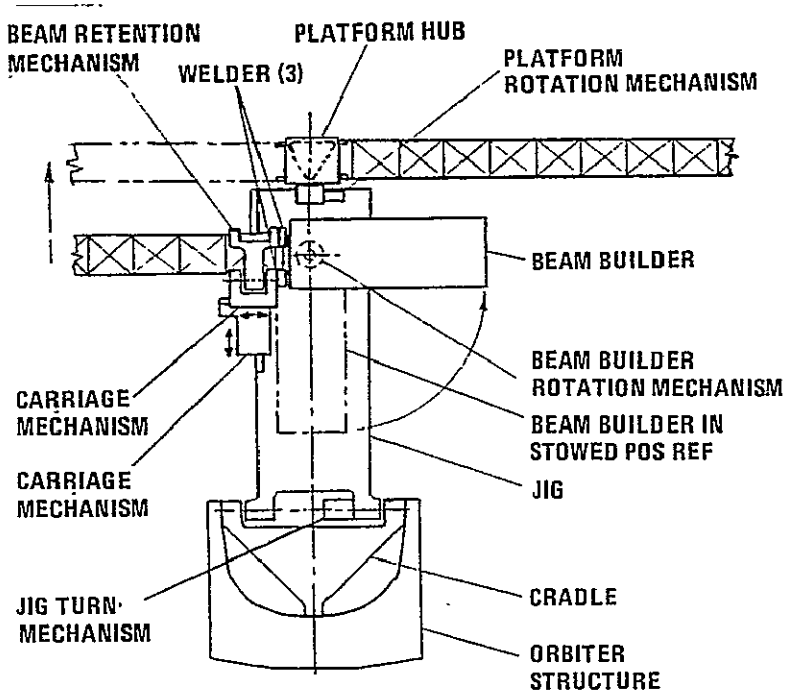

Figure 4-22. Cross platform construction, Concept 3.

• CROSS STOWAGE CONCEPT & DEPLOYMENT SEQUENCE

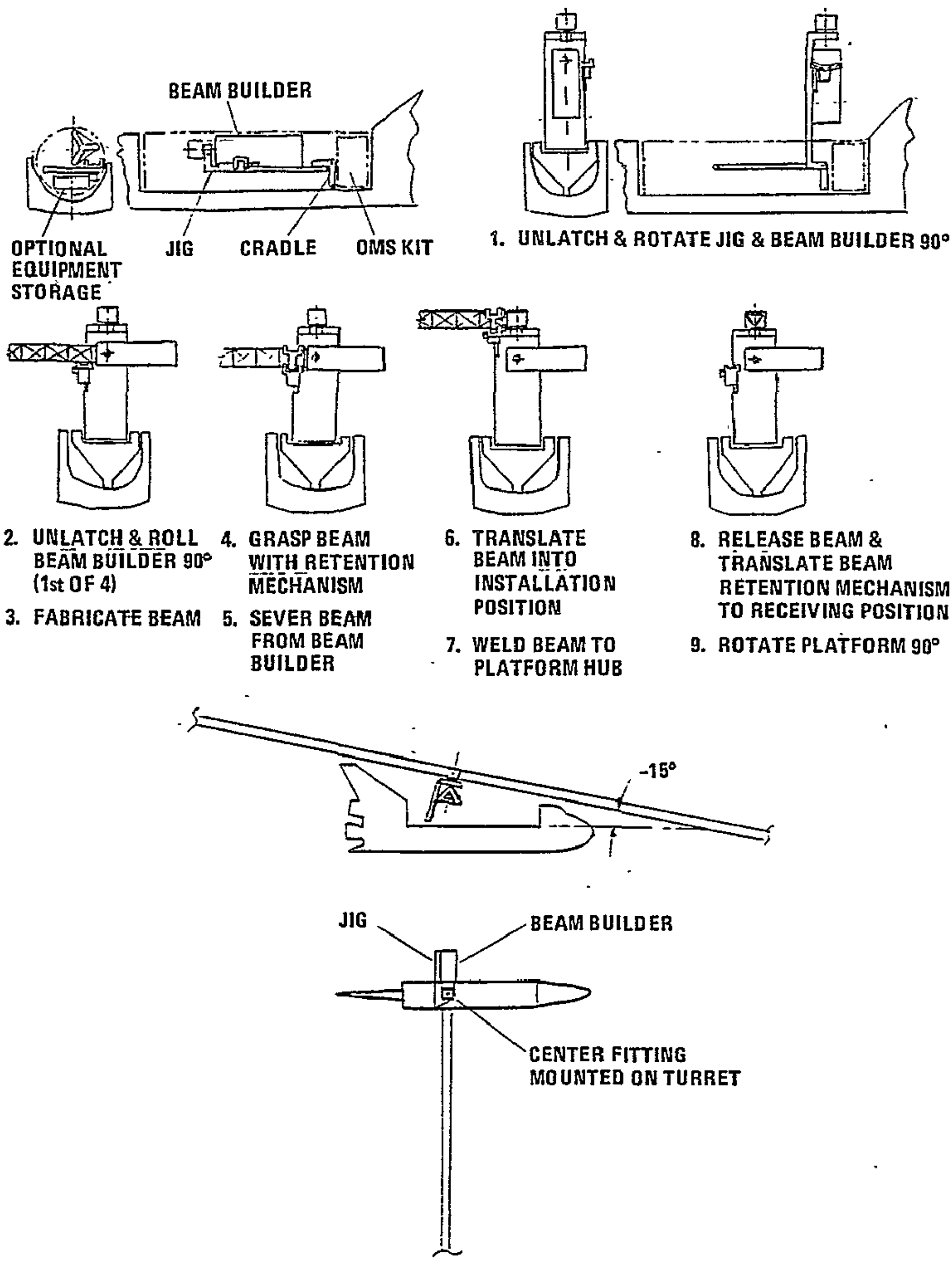

ADVANTAGES:
- SMALL CONSTRUCTION ENVELOPE (SYMMETRICAL WITH SHUTTLE)
- ALL BEAMS IN SAME PLANE WITH APEXES IN SAME ORIENTATION
- APPLICABLE FOR OTHER NUMBERS OF SPOKES
- SHORT TRANSLATION STROKE FROM BEAM FABRICATED TO BEAM INSTALLED POSITION
- EASY PLATFORM SEPARATION

DISADVANTAGES:
- REQUIRES CENTER FITTING

Figure 4-22. Cross platform construction, Concept 3. (Concld)

Non-planar assembly, Concept 1, and planar assembly, Concept 2, both have the disadvantage of moving the platform structure as far away from the Orbiter as possible. This not only creates loads at the Orbiter attach point but makes it more difficult to install system hardware. Concept 3 minimizes these problems by maintaining the center of the structure close to the Orbiter.

Concept 3 was selected because of its symmetrical orientation with respect to the Orbiter. The use of a center hub also provided an ideal interface for spacecraft subsystem module installation. It was further determined that Concept 3 provides an ideal technique for assembly of the 61 m reflector structure.

4.3.2 61-METER PARABOLIC REFLECTOR STRUCTURE AND SPACECRAFT CONFIGURATION. The reference spacecraft configuration selected for the 61-m parabolic reflector structure is a Cassegrain-type antenna. This antenna concept could be operated with multiple spot beams, electronically steerable, 1 to 6 GHz, from synchronous orbit to low power earth stations for corporate communications. The antenna assembly is illustrated in Figure 4-23.

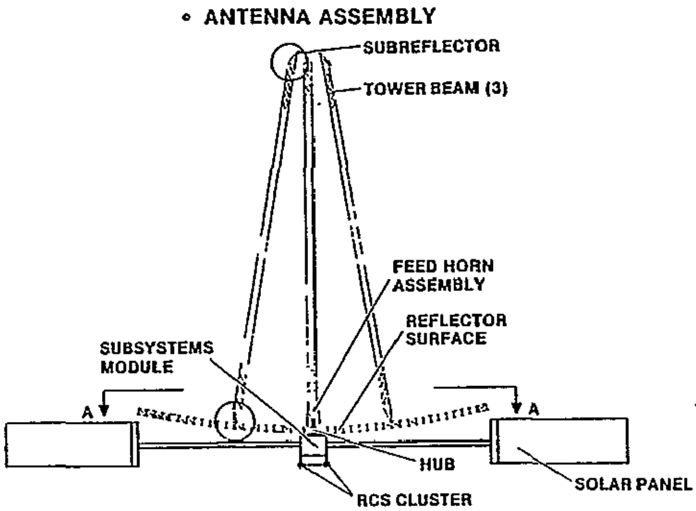

Figure 4-23. 61-meter parabolic reflector structure and spacecraft assembly concept.

A major structure of significantly higher complexity than the other planar orthogonal configurations like the square and hexagonal platforms has been developed for the 61-m parabolic reflector antenna. This structural configuration exemplifies the applicability and versatility of the beam builder to fabricate complex structures. The purpose of the 61-m antenna structure is to provide a rigid parabolic dish framework which will maintain the designed shape within a tight tolerance (3 mm) and to which a reflective mesh surface can be easily and automatically attached. This structure has the provisions to mount: (1) a tower to support a subreflector from points separated from the central hub, (2) the electronics/feed assembly module, and (3) the reflector mesh and stiffener assemblies.

The reflector dish framework has 12 parabolic curved "baseline" beams, consisting of 20 bays, oriented radially, and connected to a central hub. Overall diameter of the reflector framework is 60.7 m. Each parabolic shaped curved beam has a minimum radius of curvature of 244 m and is fabricated to the designed curvature within a low tolerance. The subreflector tower has three evenly-spaced legs which converge to the subreflector and are attached to three of the curved beams at the 8th bay. Each tower leg is an 80-bay "baseline" beam which supports the subreflector at a height of 122.0 m.

The central hub shown in Figure 4-24 is a hollow, circular spool with 3.25 m diameter flanges on the top and bottom. It has three functions. First, it provides a central assembly to which all of the beams can be mounted. Each beam is attached to the hub at two points, one for each beam on the top and bottom flanges, with expansive pin joints. The interface between the three beam cap vertices of the equilateral triangular beam and the 2-point attachment to the hub is bridged by a tubular frame hub/beam fitting. This fitting positions the beam in a single-vertex-on-the-concave-surface orientation. It also attaches to the adjacent fittings with a pin joint at the convex surface beam cap-to-hub fitting interface to provide a rigid truss frame interacting with the central hub for easier handling during assembly. The beam/hub fitting can be folded to a packaged size of approximately 1.5 m × 1.1 m × 0.25 m (5 ft × 4 ft × 7 in) and is self-deploying by means of a carpenter tape hinge and six single-degree hinges.

Each beam interfaces with the beam/hub fitting at the three beam caps. The three vertices of each triangular beam-to-hub fitting frame interface with and connect to the three beam caps by means of triangular shaped sleeves which fit inside of the beam caps as shown in Figure 4-8. Each sleeve has large-radius rounded edges for easy fitting, a solid aluminum core which acts as a self anvil during ultrasonic welding, and a polysulfone coating. A weld pattern of two spot welds on each beam cap flat provides a rigid beam cap-to-corner fitting connection.

The subreflector tower consists of four basic elements. First, the subreflector is a precision manufactured surface prefabricated and stowed in the Orbiter payload bay fully assembled. Second, the tower support structure consists of three straight beams fabricated by the beam builder. The third element is the beam end fittings which connect the end of the beams to the subreflector and the reflector. They converge the three beam cap vertices of the beam to a single point/single axis of rotation joint by means of a tubular frame fitting, shown in Figure 4-25. This fitting is similar to the beam-to-hub fitting described previously, except it converges to a single point rather than two points. It is also self-deployable and self-stowable in a 1.5 m × 1.1 m × 0.25 m package.

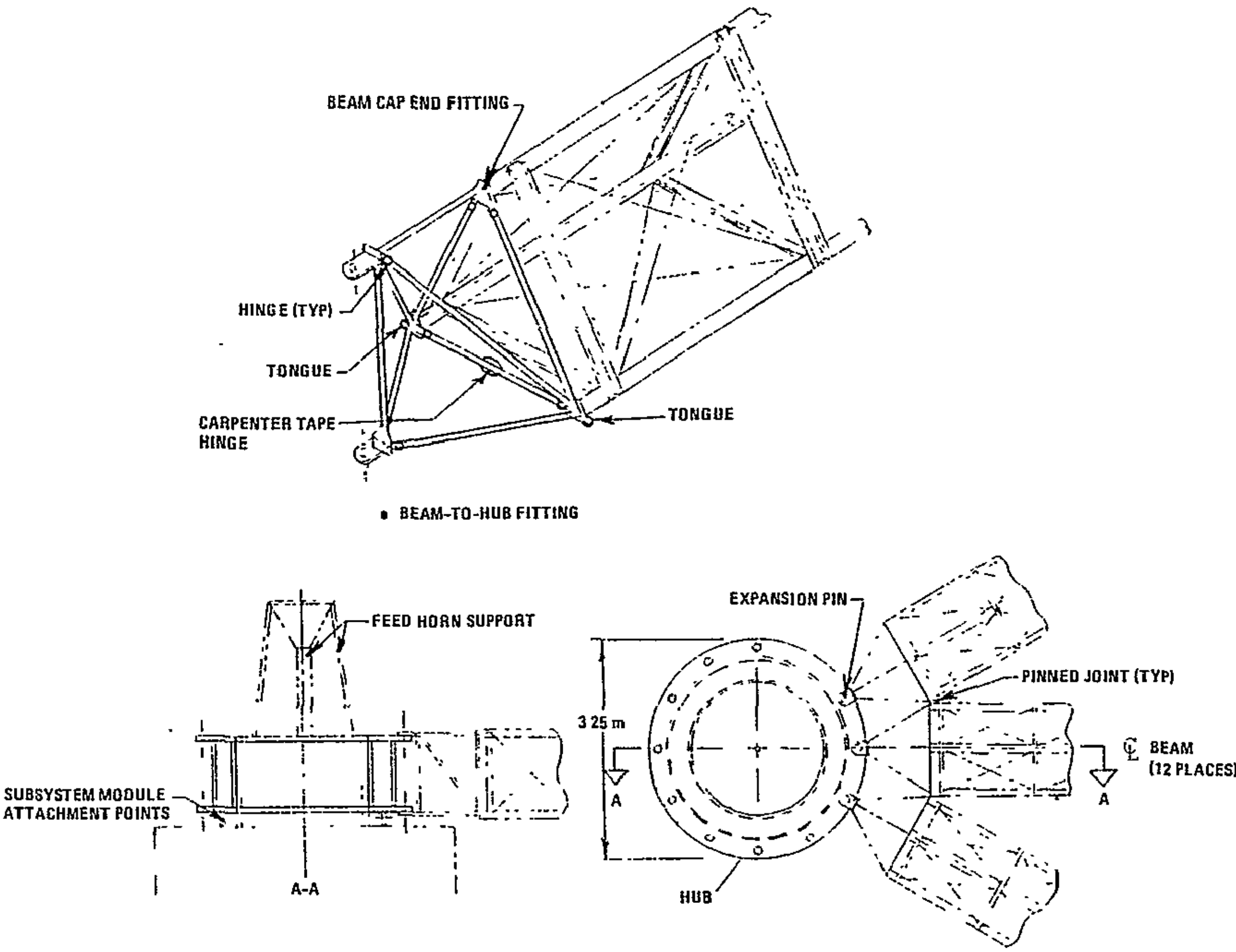

Figure 4-24. - Hub and attach fitting concepts.

Finally, the fourth element is the tower mounting fitting shown in Figure 4-25. This fitting is a single axis pivot hinge mounted on the concave surface beam cap at a beam cross-member intersection. It is secured to the radial curved beam caps by lever-engaged clamps, similar to the superstructure attachment device described for the cross structure in Figure 4-6.

Electronic equipment such as the feed assembly, subsystem module, and solar panel is assembled on the ground and packaged as a single unit to be mounted to the central hub. A 2.0 m diameter hole in the center of the hub provides clearance for the feed assembly to be positioned on the concave surface of the reflector while the remaining electronic equipment is located on the convex surface. This allows for an unobstructed area on the reflective surface of the antenna and eliminates all wiring during fabrication since the electronic equipment is a single unit.

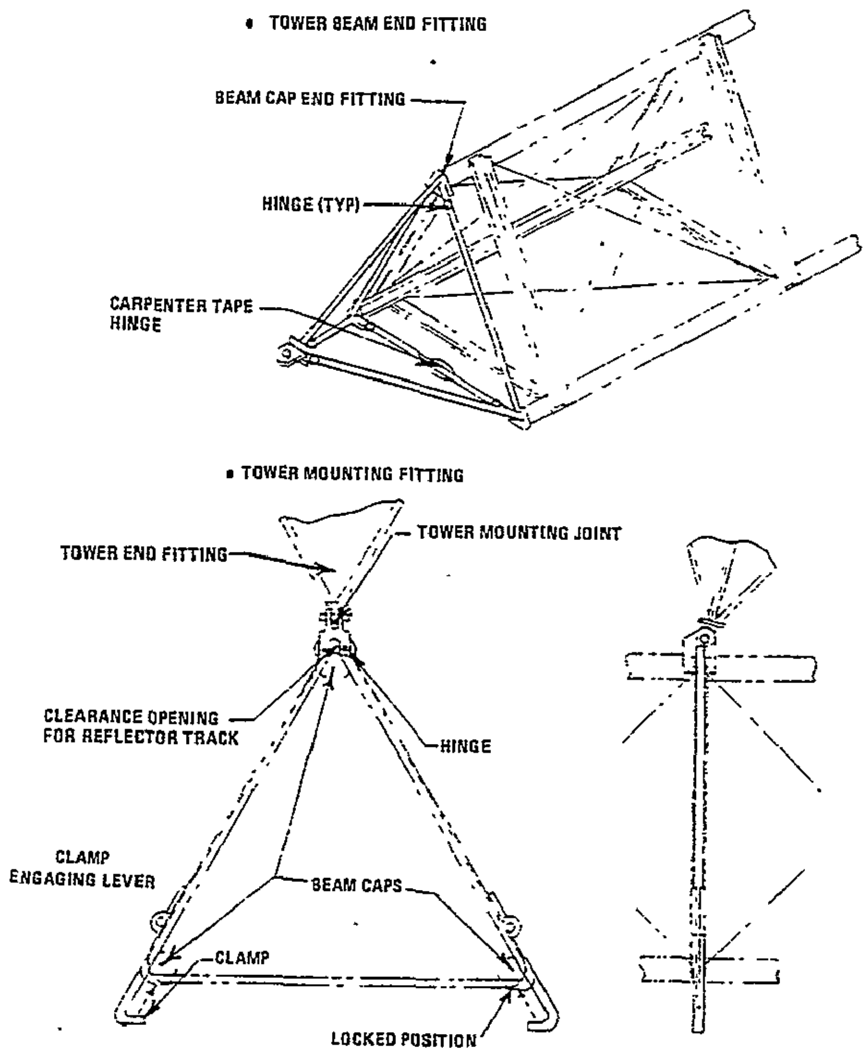

Figure 4-25. Tower support beam end fitting and mounting fitting concept.

The antenna's reflective surface is a mesh system consisting of 12 gore sections that attach to and span between the 12 radial beams. In the tangential direction, the mesh is supported by circularly arranged intermediate graphite tube ribs which span between the radial beams. They are contoured to the reflective surface shape and spaced to maintain the designed shape within an allowable tolerance (3 mm). The reflective mesh is attached to the contour tubes during ground assembly and deployed with the contour tubes after the radial curbed beam structure has been completely assembled. Deployment of the mesh/contour tube reflector assemblies is accomplished by attaching the mesh and rib end fittings to a series of 2.8 m track sections located end-to-end. These are tack welded along the beam cap apex during beam fabrication and form a continuous track. This attachment is detailed in Figure 4-26. As the rib end fittings slide outward along the track, the reflector is unfolded as discussed in Subsection 4.3.3.1 until one complete gore segment is completely deployed. The mesh and contour tube end fitting rides in the continuous track by means of a system of rollers that minimize friction between the rib end fittings and the track. This prevents the reflective-mesh system from binding during deployment. Each mesh gore section contour tube folds at both its midspan and end points for easy stowage and deployment.

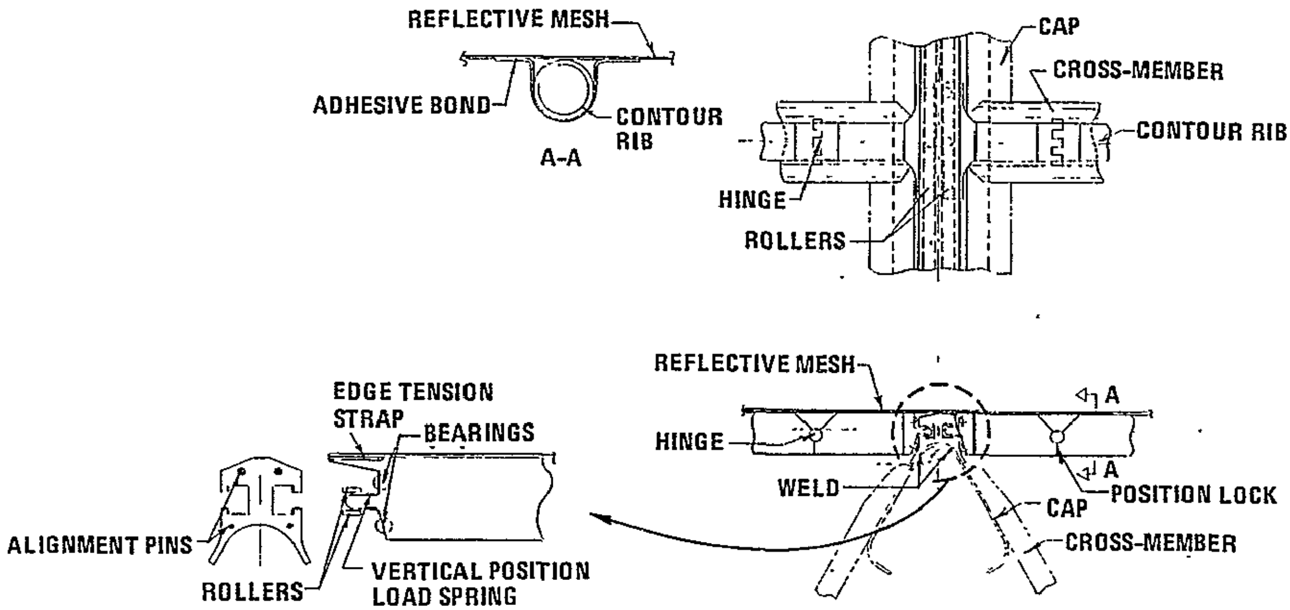

Figure 4-26. Reflector installation concept.

4.3.3 61-METER REFLECTOR ASSEMBLY JIG

4.3.3.1 Assembly Jig Concept. The assembly jig for the 61-m reflector assembly, shown in Figure 4-27, is similar to the assembly jig proposed for the erection of the cross structure. It contains many features of the original SCAFE assembly jig including:

a. Cradle

b. Deployment actuator

c. Stowage, deployment, and translation of beam builder on jig

d. Beam retention and guide and drive mechanism.

The assembly jig is first rotated 75 degrees from its stowed position. This provides a minimum of 1.56 m clearance between the Shuttle's tail and cockpit and the reflector's structure. If appropriate, greater clearance is achievable by increasing jig length.

The assembly of the 61-m reflector assembly is accomplished in the following sequence:

a. The beam builder fabricates the first beam past the two retention and guide mechanisms (RGMs). Next, the finished beam is grasped by the RGMs and cut off by the beam builder cutters. The RGM then moves the beam away from the beam builder to provide room for installation of the beam/hub attach fitting.

b. The beam/hub attach fitting is removed from its stored location, positioned on the beam, and manually welded to it using a hand-held ultrasonic welder. This step has not been automated due to the relatively small number of weld joints to be made.

c. The beam positioner/handler is rotated 90 degrees to bring the beam assembly to the level of the hub.

d. The RGM drive mechanism then translates the beam assembly toward the hub until the two beam fitting attach holes line up with the corresponding holes on the hub. Local controls are provided to permit manual control of beam positioning and alignment.

e. Two expansion pins are installed to secure the beam to the hub and, to provide in-plane rigidity, the beam is secured to the adjoining beam with an expansion pin through the pin joint. (A swing-out strut, preassembled to the hub, performs the stabilizing function for the first beam.)

f. The RGM is retracted and the beam positioner/handler rotated 90 degrees to its stowed position. The hub can now be indexed 30 degrees and the assembly sequence repeated until completion of the structure.

g. As each beam is being built, the mesh track used to deploy and fasten the contour ribs to the curved beams is applied to the beam cap apex on the concave side in 2.74 m (9 ft, 2-bay length) sections. They are fastened to the beam cap by spot welds. During this operation, a continuous cable is threaded through both the track guide and back to the central hub inside the beam cap.

h. After the 12 curved beams have been fabricated and assembled to the central hub, a stowed mesh/contour rib gore package is positioned by EVA at the inboard end of the tracks and attached to the track guide cords. The stowed mesh package has automatic guide feed features. The mesh is deployed along the track by a motor on the stowed package which reels in the cord through the track guide and inside the beam cap. See Figure 4-28. This procedure is repeated for all 12 gores.

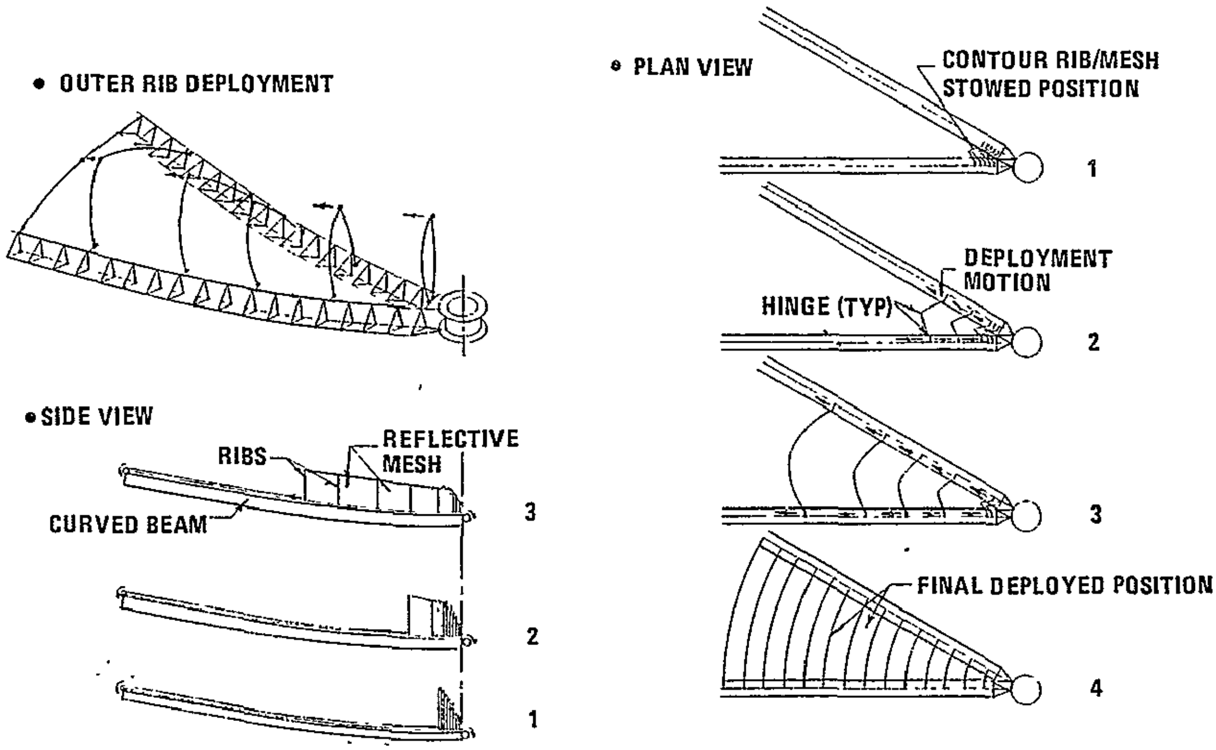

Figure 4-28. Mesh/contour rib deployment sequence.

4.3.3.2 61-Meter Antenna Assembly Jig Control Equipment. Assembly jig and beam builder deployment and positioning control equipment is the same as that described in Subsection 4.2.4.2.1. The configuration-unique assembly control equipment is diagrammed in Figure 4-29.

When the assembly jig and beam builder have been positioned, the ACU commands the hub support arm to rotate 90° to its assembly position. Two sensors are used to monitor position of the hub support arm.

After the hub support arm has been deployed, the ACU will command the hub extension arm to rotate into the hub assembly position. Two sensors will monitor the hub extension arm position. A circular assembly hub with attachment points for 12 beams is stored in the Shuttle bay. This assembly hub is picked up by the RMS arm and transported to the hub extension arm for installation. Installation of the hub to the extension arm is performed by astronauts on EVA.

After the hub has been installed, the ACU will command the BCU to start curved beam fabrication. When a beam of required length has been fabricated, two RGMs located on the beam support arm are energized by the ACU, grasping the beam. The ACU will command the BCU to cut off the beam and will then energize the beam drive mechanism, translating the beam forward to a position where an end fitting may be installed.

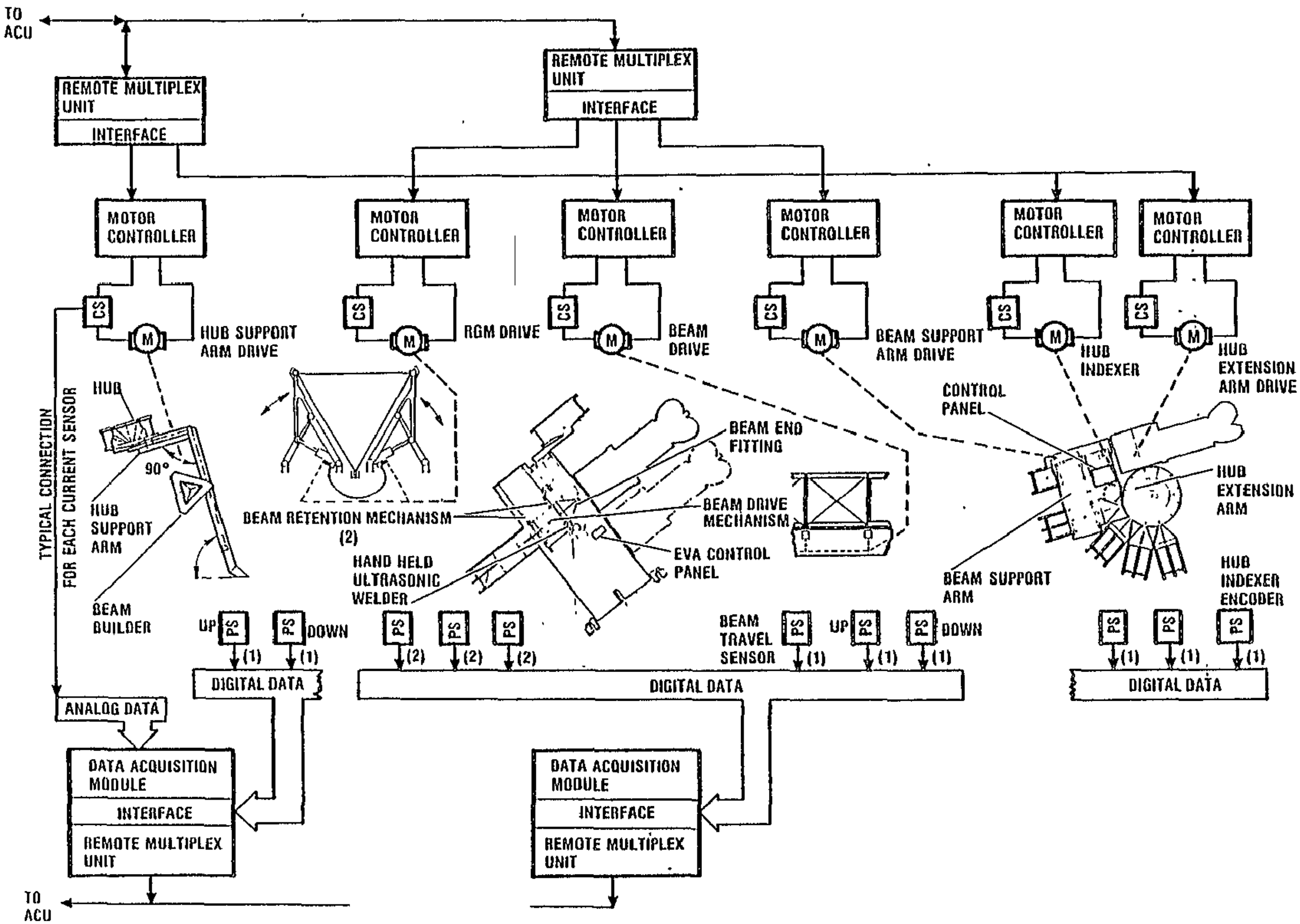

Figure 4-29. 61-meter antenna jig control diagram.

An astronaut will install the end fitting to the beam with a hand-held ultrasonic welder. An EVA control panel will be supplied at this work station to provide the astronaut with fine positioning and welder controls. The hand-held welder to be used will be connected to this control panel by umbilical cord. After the end fitting is installed, the astronaut will report status to the ACU via the control panel. The ACU then commands the beam support arm to rotate 90°, placing the fabricated beam with end fitting in its final assembly position.

Final assembly of the beam to the hub will be accomplished by EVA. A control panel will be provided on the hub support arm to allow the astronaut to position the beam onto the hub. When the beam is aligned properly on the hub, a mechanical locking pin is inserted by the astronaut securing the beam to the hub. Additional locking pins required between adjacent beam end fittings are also installed. After this installation is completed, the astronaut will report status to the ACU via the control panel.

The ACU will command the RGMs to release the beam, and the beam support arm to rotate back to the beam fabrication position. The ACU will energize the hub indexer causing the hub assembly to rotate 30°, clearing the final assembly position for the next beam.

Eleven additional curved beams will be fabricated and attached to the assembly hub in the sequence described above, resulting in an assembled 61-m antenna structure.

4.3.4 CROSS STRUCTURE AND SPACECRAFT CONFIGURATION. The reference spacecraft selected for the cross structure is a microwave interferometer. This spacecraft concept is shown in Figure 4-30.

A cruciform platform structure, using four coplanar baseline beams attached to a central hub, has been conceptually designed for this satellite application. Satellite systems include helicone antennas, electronic modules, an MMS module, a propulsion system, and solar collectors. The structure has an overall span of 99.82 m along both axes. Each leg is a 34-bay baseline beam with a standard 0.30 m cutoff at the outer end and a special 0.10 m cutoff at the hub interface end. The applications for this spacecraft could include position location of emergency locator transmitters, tracking of buoys, animal herds, icebergs, etc.

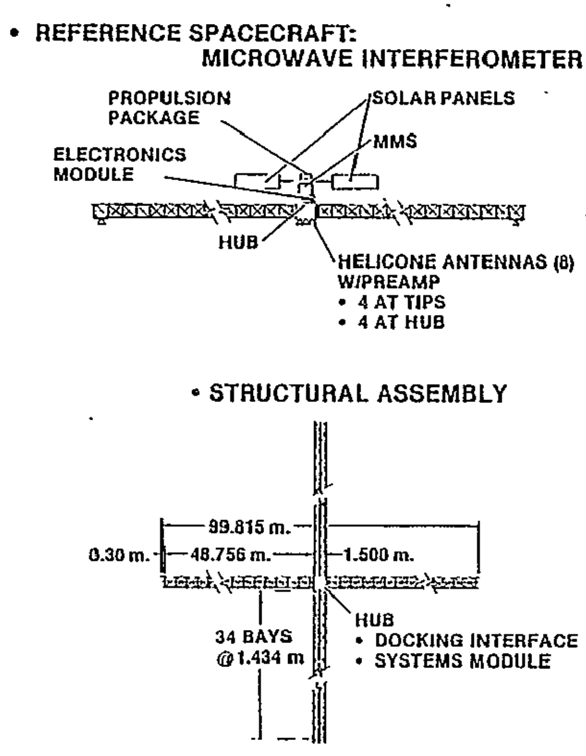

Figure 4-30. Cross structure and spacecraft assembly.

Several reasons made it more advantageous to design this structure using four separate beams connected to a central hub, rather than the concepts of two long beams crossing or one long beam and two short beams attached to it at mid span. The central hub is convenient for handling the spacecraft during fabrication. A central hub also provides a simple, rigid connector for the beam intersections, and a good mounting base for electronic and controls modules. The selected concept also orients all of the beam apexes in the same plane. This allows the use of universal fittings for attaching systems hardware at any point along the beams.

The central hub, shown in Figure 4-31, is a preassembled graphite/epoxy cube with attachment interfaces on four sides for the four triangular beams, and on the top for the electronics module. The beam-to-hub interface connection is a triangular-shaped sleeve which fits inside of a beam cap. Each sleeve has large radius rounded edges for easy mating, a solid aluminum core which acts as a self anvil during ultrasonic welding, and a polysulfone coating which is necessary to weld the beam cap to the sleeve. A weld pattern of two 0.009 m diameter spot welds on each beam cap flat provides a rigid beam cap-to-hub connection, also shown in Figure 4-31.

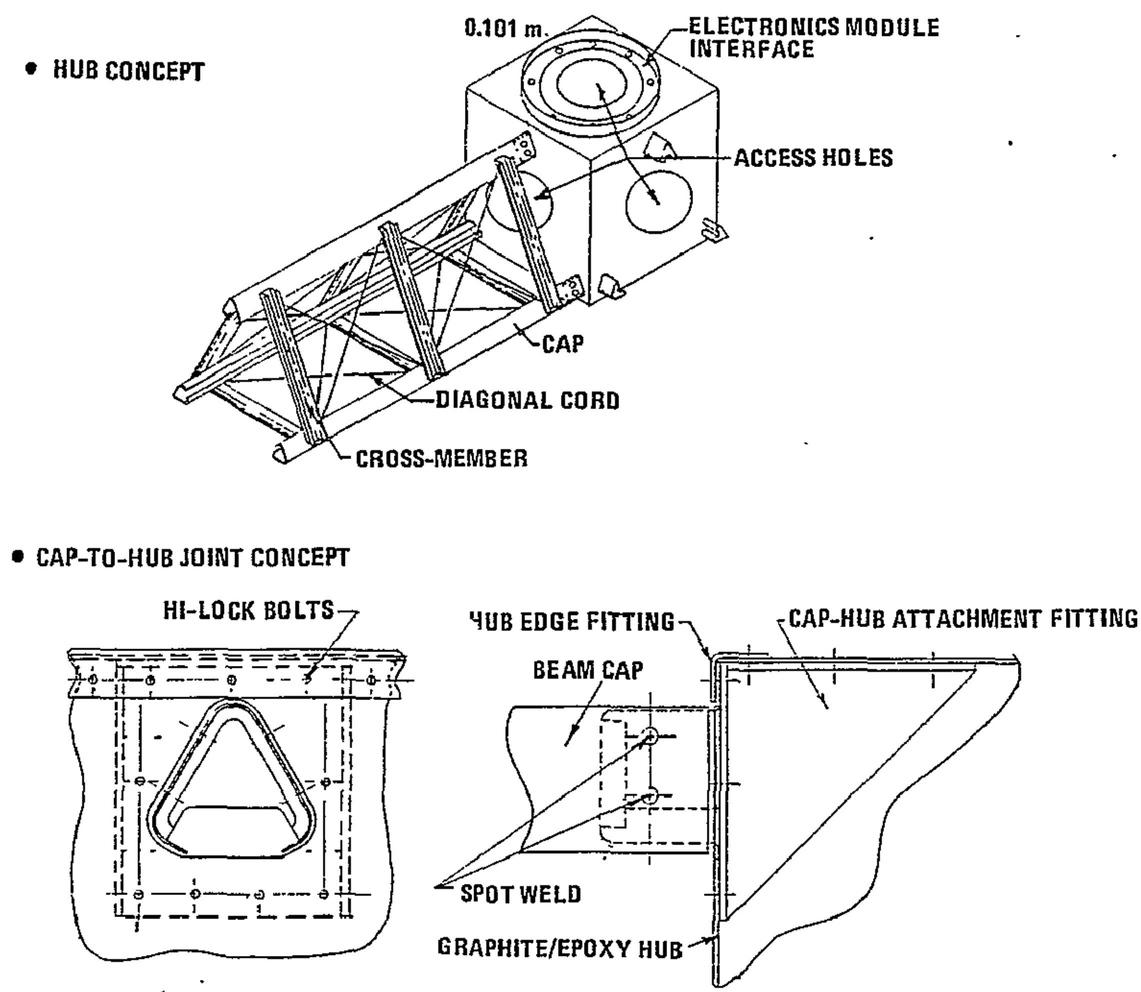

Figure 4-31. Beam-to-hub joint concept.

A circular sleeve is mounted on the top face of the hub cube. This sleeve interfaces with a slightly larger sleeve on the electronic module for easy installation with spear pins. Access holes are provided for hub fabrication purposes. Titanium hi-lok fasteners are used to connect the cap-to-hub fittings and the electronics module attachment fittings to the hub.

Helicone antennas are attached at the extreme outside bay of each beam by means of a lever-engaged flat platform, which connects to two of the beam caps and spans a full bay length. The antenna (or other equipment) is mounted on the platform by conventional methods (welded, bolted, etc.). Antenna cables are routed along the beam caps to the central hub.

4.3.5 CROSS STRUCTURE ASSEMBLY JIG

4.3.5.1 Assembly Jig Concept. The assembly jig for the cross structure shown in Figure 4-32 is similar to the assembly jig concept for the 61-m reflector structure. It differs in the hub design and the hub joining process. No beam hub attach fittings are required since the beams can be welded directly to the hub. Again, the welds are made manually because only a small number of joints are required. The operating sequence is described below.

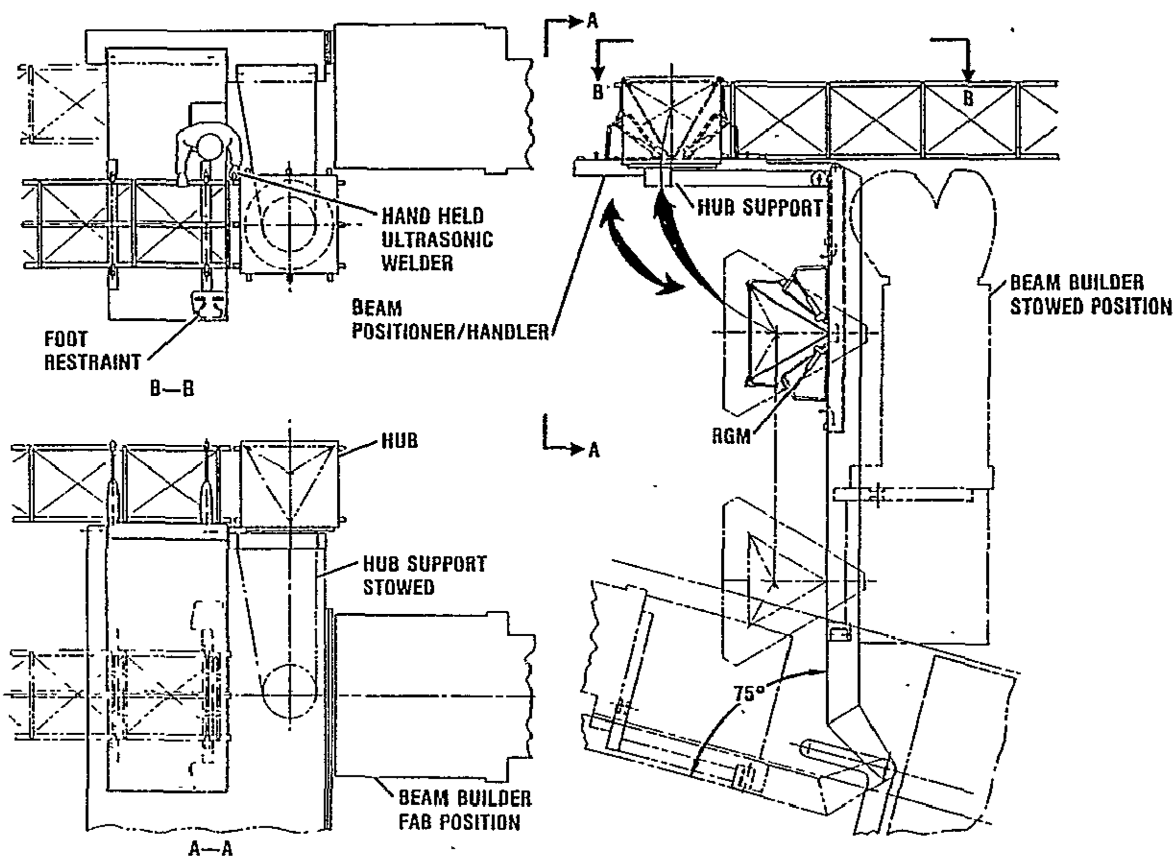

Figure 4-32. Cross structure assembly jig concept.

4.3.5.2 Assembly Jig Controls Equipment. Assembly jig deployment and beam builder positioner equipment is the same as that described in Subsection 4.2.4.2.1. The configuration-unique assembly control equipment is diagrammed in Figure 4-33.

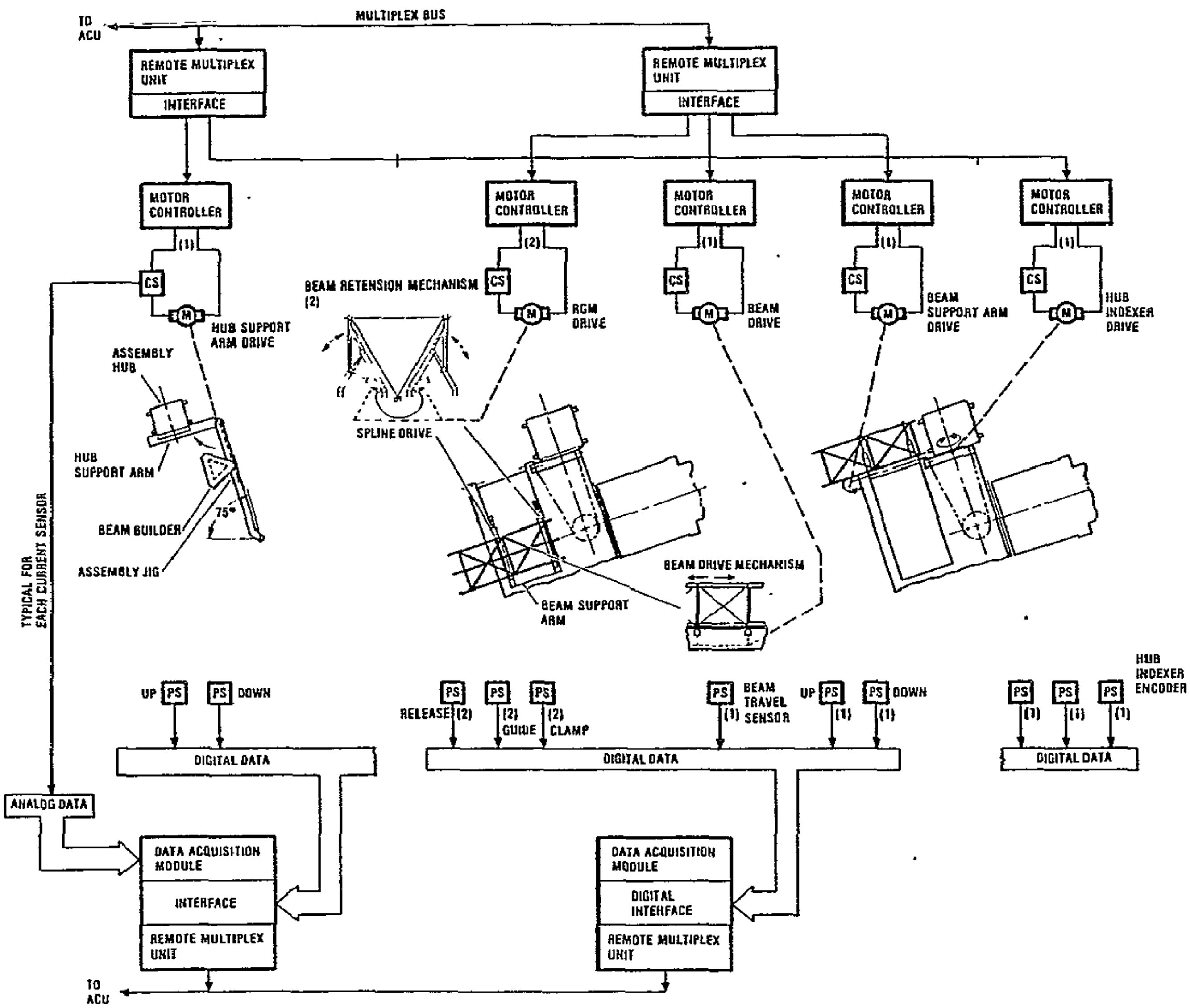

Figure 4-33. Cross structure assembly jig control diagram.

After the assembly jig and beam builder have been positioned, the ACU commands the hub support arm to rotate 90° to its assembly position. The assembly hub, which is stored in the Shuttle bay, is picked up by the RMS arm and transported to the hub support arm for installation. Two installation methods are possible, automatic "snap-in" or EVA assembly by astronauts. Further analysis is required to select the optimum method.

The ACU will then command the BCU to start beam fabrication. After a beam of required length has been fabricated, two RGMs located on the beam support arm are energized by the ACU. These RGMs grasp the fabricated beam. Position sensors will be used to monitor RGM operation.

The ACU will command the BCU to cut off the beam and then energize the beam drive mechanism, translating the beam forward. A beam travel sensor will be used to monitor beam movement. Beam travel is stopped at a predetermined position which will allow for proper clearance between the beam and assembly hub. After the beam has stopped, the ACU commands the beam support arm to rotate 90°, placing the fabricated beam in its final assembly position.

Astronauts will be required to attach the beam to the assembly hub. An EVA control panel will be supplied to provide the astronaut with limited beam positioning controls and welder controls. A hand-held ultrasonic welder, connected to this control panel by umbilical cord, will be used to attach the beam to the assembly hub mounting stubs.

The astronaut will signal the ACU via the control panel when the assembly task has been completed. The ACU will then command the RGMs to release the beam and rotate the beam support arm back to the beam fabrication position. The ACU will energize the hub indexer, causing the hub assembly to rotate 90°, clearing the final assembly position for the next beam.

Three additional beams will be fabricated and attached to the assembly hub in the sequence described above, resulting in an assembled cross structure.

4.4 TRI-BEAM CONSTRUCTION

Large complex structures can be designed and developed for space using the same fabrication methods employed on the simple cross and square platform structures. Just as the basic beam cap and cross-member components are assembled to develop a beam, a larger tri-beam can be fabricated using "baseline" beams as the beam cap and cross-member components.

The large tri-beam structure is sufficiently unique to warrant a special assembly jig for automated fabrication and assembly. The selected assembly jig concept, however, incorporates many of the subsystems developed for the SCAFE platform jig.

4.4.1 TRI-BEAM CONSTRUCTION TRADES. The tri-beam assembly jig options considered are shown in Figures 4-34 through 4-36. In Concept 1, the assembly jig is a collapsible configuration which allows the beam builder to be stowed in the same position used on all the other assembly jig concepts. The jig would be initially elevated on four swinging linkages. The central support structure would then be elevated along four fold-up beams while the beam builder was set aside using the RMS. The beam builder and cross-beam positioner/welder would then be installed on their respective handler arms using the RMS.

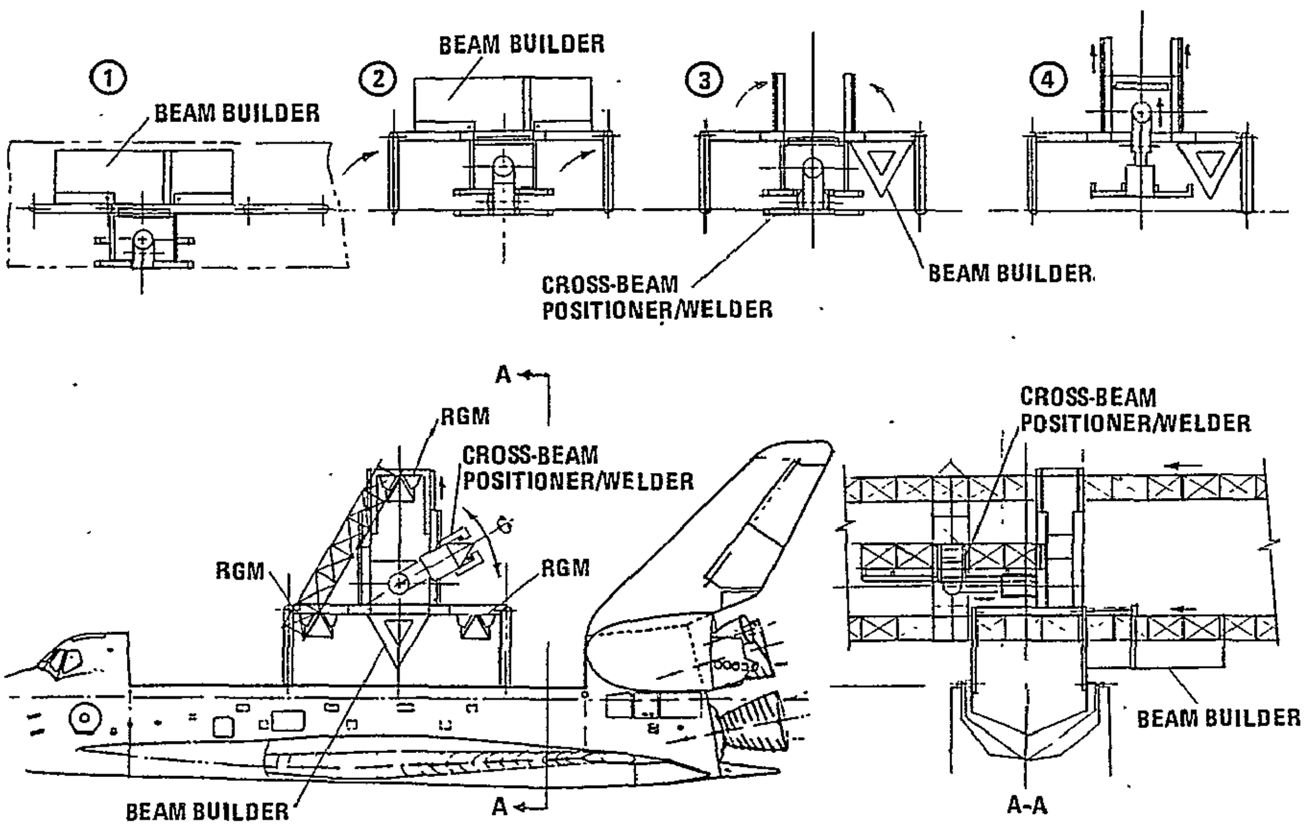

Figure 4-34. Tri-beam assembly jig, Concept 1.

The Concept 1 assembly jig first builds the three longitudinal beams. These three beams are translated back to their opposite ends by the RGM/beam drive mechanisms. The beam builder then builds cross-beams, which are handed off to the positioner/welder for attachment to the longitudinal beams.

Concept 2 uses a turntable with RGMs to hold and position the longitudinal beams. The beam builder is then positioned to build cross-beams in a direction perpendicular to the longitudinal beams. The turntable rotates the entire structure for each cross-beam installation sequence. Portions of the turntable would be assembled on-orbit.

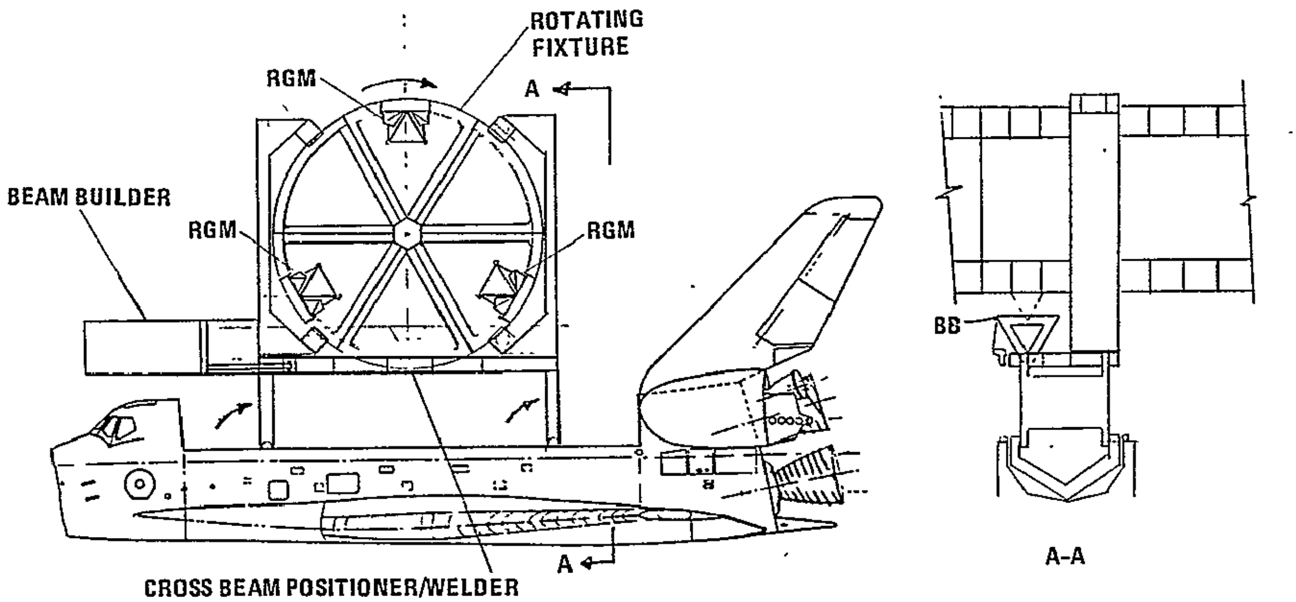

Figure 4-35. Tri-beam assembly jig, Concept 2.

Concept 3 uses a box structure for the assembly jig with fold-out platforms with RGMs to handle two of the longitudinal beams. The beam builder is nested in the box structure on one side and the positioner/welder on the other side for stowage. The assembly jig, beam builder, and positioner/welder all deploy automatically from their stowed positions.

Concept 3 was selected because of its capability for completely automatic deployment and stowage. This precludes time lost and potentially hazardous operations associated with assembly of the assembly jig. Concept 3 also represents the minimum stowage length of all of the concepts.

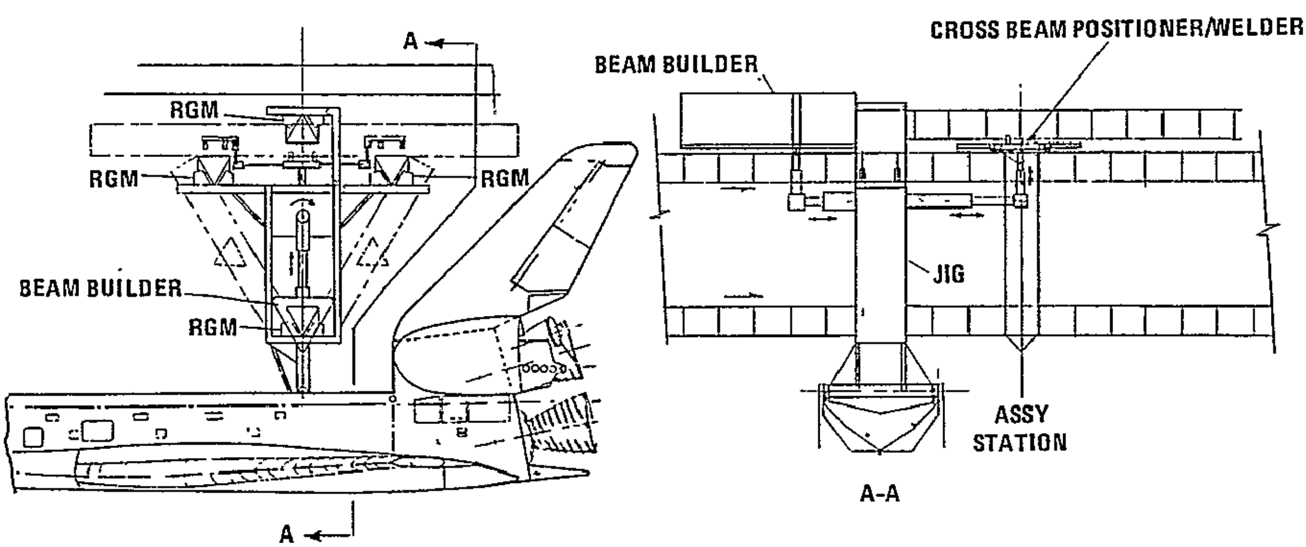

Figure 4-36. Tri-beam assembly jig, Concept 3.

4.4.2 TRI-BEAM STRUCTURE AND SPACECRAFT CONCEPT. The large tri-beam structure can provide a large rigid platform capable of supporting a multi-user communications system fabricated in a low earth orbit (LEO) and transferred to a geosynchronous earth orbit (GEO). This reference spacecraft concept is shown in Figure 4-37.

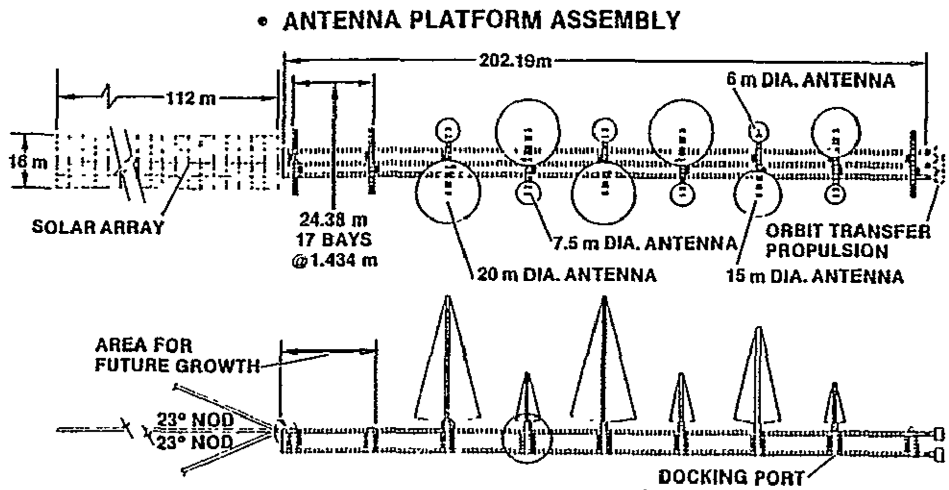

Figure 4-37. Tri-beam structure and spacecraft assembly.

The overall length of the tri-beam platform is 202.2 m with a 112 m × 16 m solar array attached at one end. All tri-beam components are baseline beam builder beams. The tri-beam platform has a cross-section consisting of three cap beams fixed in an equilateral triangle cross-section arrangement by three cross-member beams six bay lengths long, as shown in Figure 4-38. One of the three cross-members has an additional four bay lengths cantilevered beyond the beam cap on each side of the tri-beam resulting in a total platform width of 20.7 m. Twelve antennas of four different sizes are arranged on the platform areas: (1) four 20 m diameter antennas, (2) two 15 m diameter antennas, (3) four 7.5 m diameter antennas, and (4) two 6 m diameter antennas. An area for future antenna system growth is included on the platform.

The fabrication plan for the tri-beam uses baseline beams for cross-member components, but a staggered cross-beam arrangement is necessary to eliminate any overlapping or interference problems at the tri-beam cap apexes. This staggered arrangement places each cross-member in adjacent cap beam bays so that they are in three planes parallel to each other and normal to the tri-beam longitudinal axis. Structural analysis indicates no significant stress risers are developed in the staggered arrangement components when compared to similar components in a non-staggered cross-member arrangement which has all three cross-members in the same plane. For example, the maximum stress increase incurred in any of the beam components due to transverse bending moments applied to the tri-beam is 11%. In most cases, the stress level is decreased by the staggered cross-member effect. In the tri-beam caps, stress response to beam torsion loads increases by a maximum of 184% due to the staggered

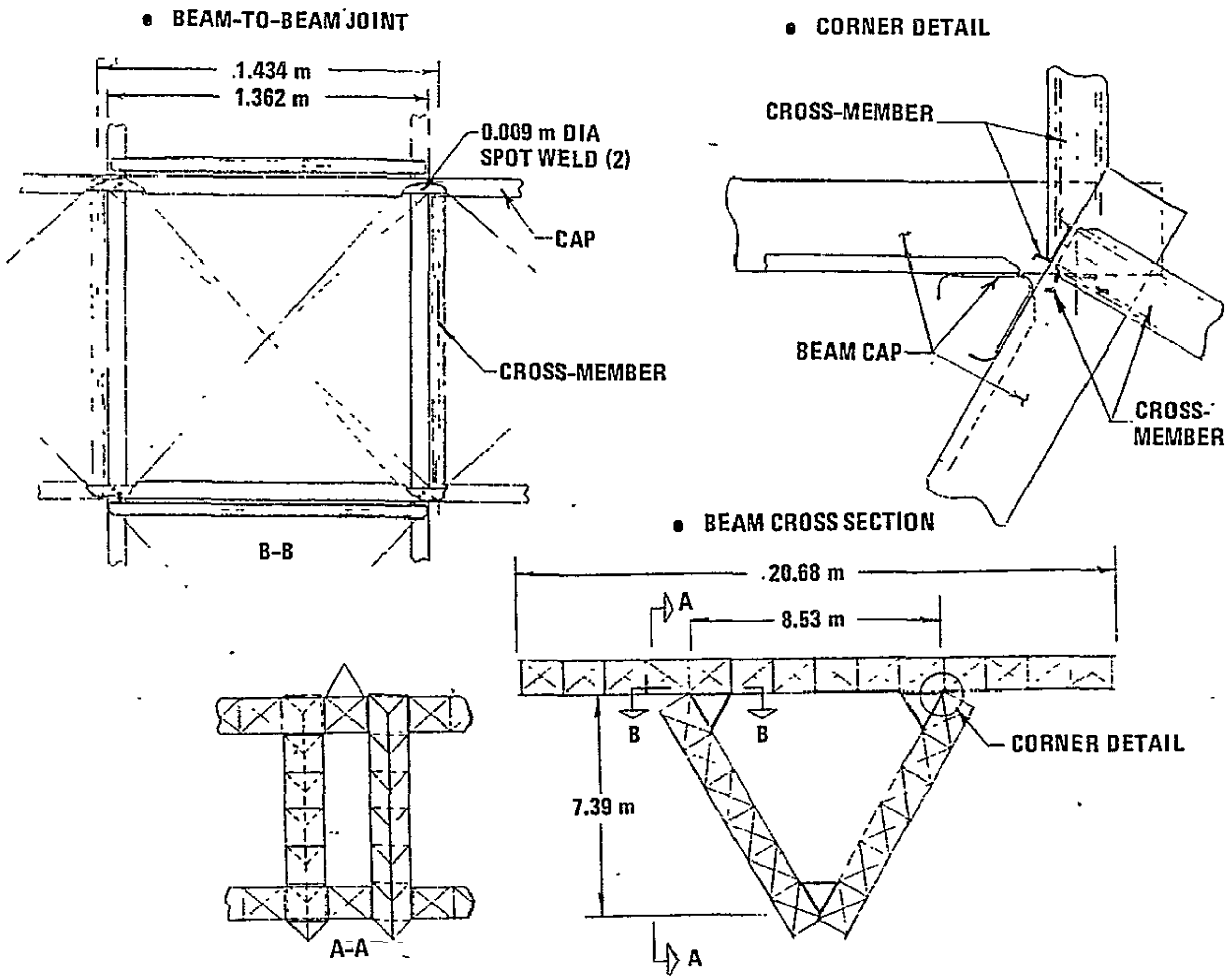

Figure 4-38. Tri-beam assembly details.

arrangement effect. But torsional loading on the tri-beam is at a significantly lower level than the bending moment loads, thus making the torsional stress risers of insignificant proportion to the bending moment increases. Standard dimensions for bay length and height of the SCAFE beam allow for a 0.011 m clearance between the beam caps and cross-members at the intersection of the tri-beam longitudinal and cross-beam components. The typical tri-beam longitudinal beam-to-cross-beam connection consists of two 0.009 m diameter spot welds at each of the four cap-to-cap joints as shown in Figure 4-38. The welded connections at the four beam cap intersections provide a moment-resistant joint that precludes the requirement for diagonal cords in the tri-beam.

All antenna superstructures are mounted on the cantilevered tri-beam cross-members using hardware described in Figure 4-32. The superstructure beam fitting platform is mounted on two adjacent beam cross-members on the beam cap apex and is supported from the platform edges to the lower beam caps by four lever engaging clamps similar to the superstructure attachment device described for the cross structure. Hinge joints allow the platform supports to be folded for easy stowage. The spring lock detent is a positive-locking device in the deployed position.

Other functional systems are also attached to the tri-beam. An orbit transfer propulsion unit is attached to the end of the tri-beam to transfer the tri-beam communication system from a LEO to a GEO after fabrication. During the fabrication sequence, Shuttle maneuvers require undocking and redocking facilities to be implemented into the structure design. A docking port has been included. To provide a sustained source of power, a solar array has been developed that has the capability of rotating 360° about the tri-beam longitudinal axis and nodding up or down 23° to position it in the most advantageous orientation with the sun.

4.4.3 TRI-BEAM ASSEMBLY JIG

4.4.3.1 Assembly Jig Concept. The tri-beam assembly jig, shown in Figure 4-39, represents a significant departure from the basic SCAFE platform assembly jig; however, most of the basic jig subsystem modules are also used in this concept. These include:

a. RGMs and beam drive mechanisms

b. Jig deployment actuator

c. Cross-beam handler mechanism

d. Beam-to-beam automatic welders

The unique subsystem elements required for this concept are:

a. Cross-beam positioner/welder mechanism

b. Beam builder positioner mechanism

c. Beam handling fixture deployment mechanism

d. Forward equipment cradle

e. Jig structure

The beam assembly sequences are described in the subsequent controls section. The long cross-beam handling fixture is included in this concept to permit the fabrication and installation of long cross-beams to be used for antenna mounts. For tri-beams without overhanging cross-beams, this fixture is not required.

4.4.3.2 Assembly Jig Controls Equipment. Fabrication and assembly of the tri-beam structure requires a different assembly jig controls concept than described in the previous sections. Although the jig equipment has changed and the deployment and assembly sequence is unique to the tri-beam, the assembly jig avionics philosophy will be the same as that implemented for the other structures.

Figure 4-40 shows the tri-beam assembly jig controls block diagram. The amount of assembly equipment has increased; however, the same multiplexing methods, previously discussed, are used to interface control equipment to the ACU.

The following paragraphs describe the assembly jig equipment, sequence of operation, and controls.

4.4.3.2.1 Jig Deployment. After the cargo doors have been opened, the Orbiter initiates tri-beam construction by commanding the ACU to deploy the assembly jig. The ACU energizes the jig deployment drive motor, causing the jig to rotate 90° out of the cargo bay. The jig platform drive motors are then sequentially energized, causing the platform leaves to unfold to their deployed positions. Position sensors monitor platform leaf deployment.

After the platform leaves are in position, the beam builder is deployed from its stowed position on the assembly jig. Position encoders are used to monitor beam builder positioning. Control equipment for jig and beam builder deployment is shown in Figure 4-41.

4.4.3.2.2 Beam Handling. Three fabrication stations are required to fabricate and handle the three longitudinal beams used in the construction of the tri-beam. Two of these stations are located on the platform leaves extending from the sides of the jig structure. The third station is located on the bottommost portion of the assembly jig. Each fabrication station will incorporate two RGMs and one beam drive mechanism for beam handling and translation. Beam handling control equipment is shown in Figure 4-42.

After the beam builder has been deployed, it is positioned adjacent to one of the fabrication stations. Beam fabrication is initiated by a command to the BCU from the ACU. After a beam of proper length has been fabricated, the RGMs are energized to grasp the beam. After the beam has been secured, the beam is cut off and the beam builder is repositioned at the other fabrication stations, where two more beams are fabricated.

After three beams have been constructed, the beam builder is repositioned to one of the three cross-beam fabrication positions. The beam drive mechanisms are then energized, translating the beams into position for cross-beam attachment.

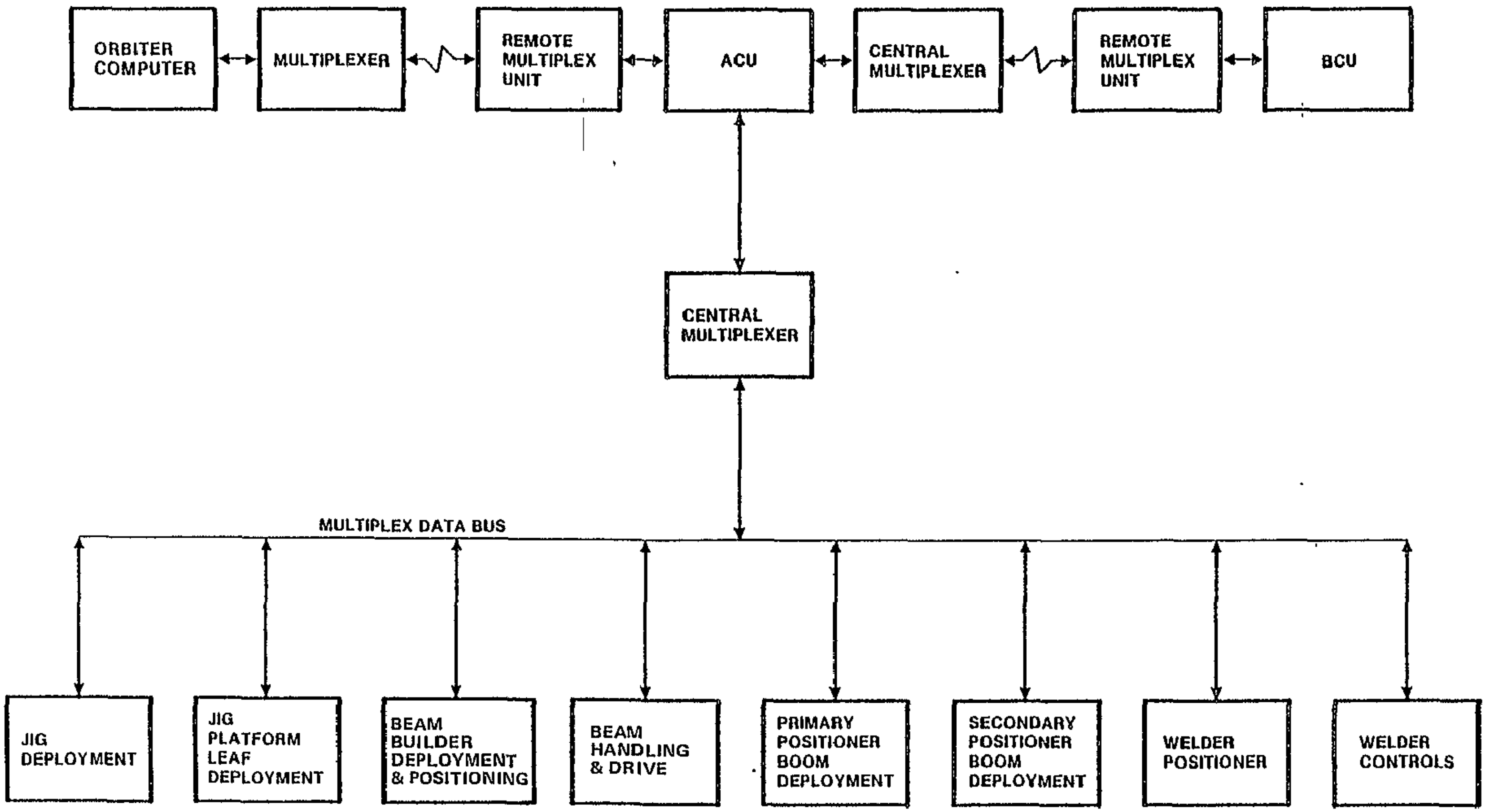

Figure 4-40. Tri-beam jig control block diagram.

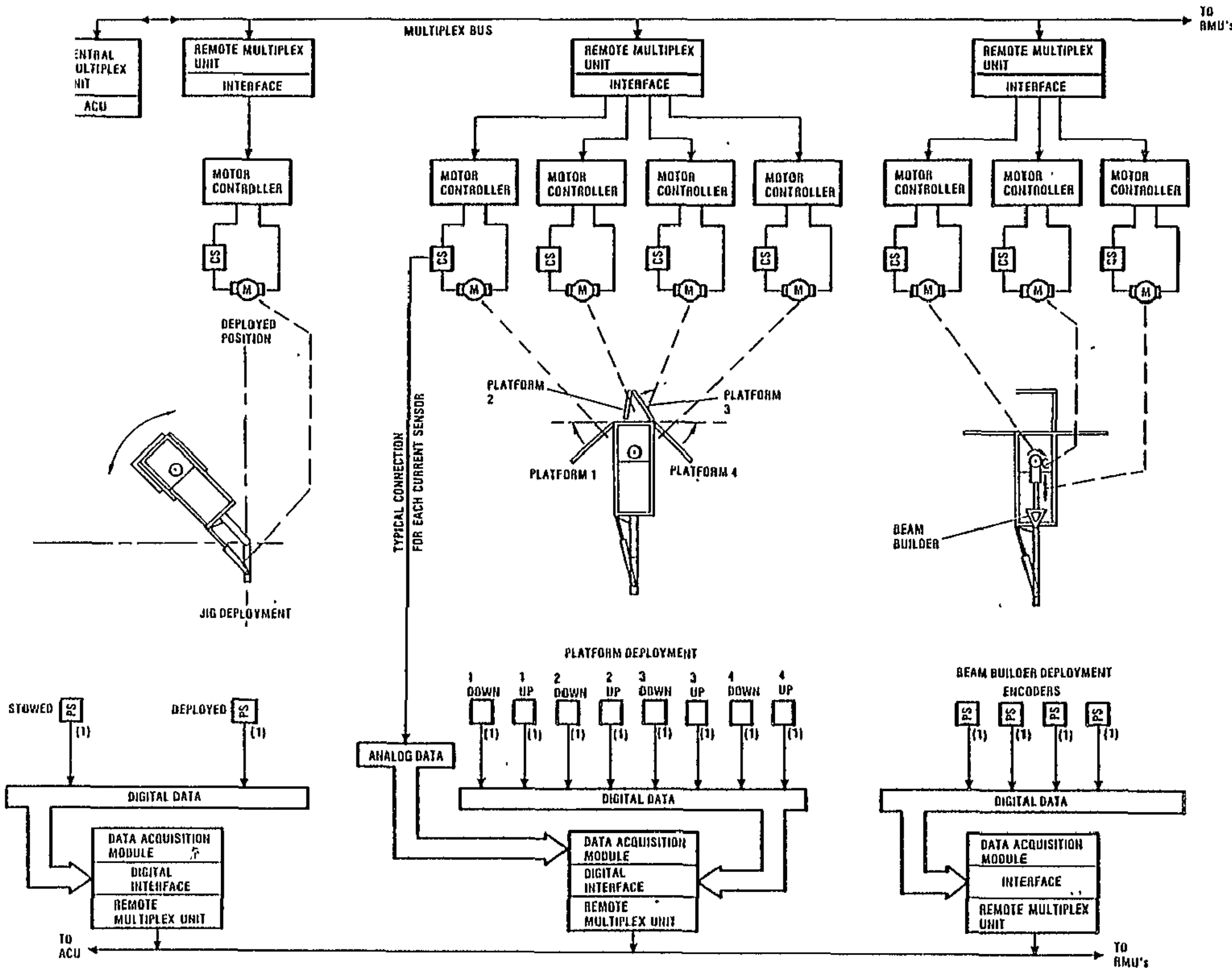

Figure 4-41. Tri-beam jig control diagram, Part 1.

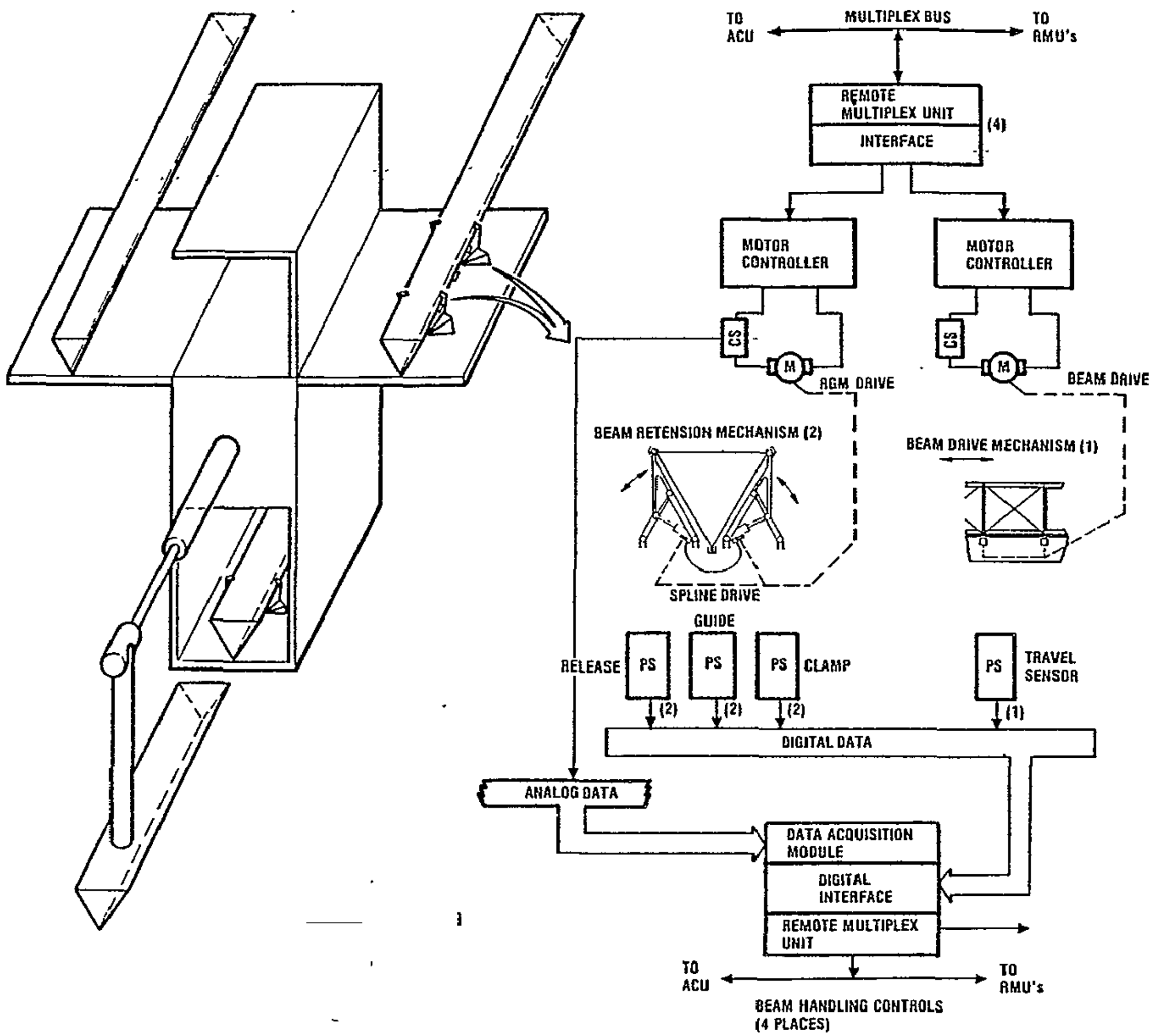

Figure 4-42. Tri-beam jig control diagram, Part 2.

4.4.3.2.3 Cross-Beam Fabrication, Handling, and Final Attachment. The cross-beam fabrication positions are located on an imaginary circle circumscribed through the longitudinal beam fabrication positions and equidistant from the positions of each adjacent pair.

Cross-beam handling equipment (RGMs and beam drive mechanism) is provided on the uppermost platform leaf extending from the top of the main jig assembly. Cross-beams fabricated at this position are longer than those fabricated at the other two positions and will be attached to the top of the tri-beam assembly. When attached, the top cross-beam will provide "outriggers", allowing room for attachment of mission-peculiar equipment on the completed tri-beam. The handling equipment will properly position the top cross-beam for pickup by the cross-beam positioner. The cross-beams fabricated at the other two positions will be of the length necessary to form the bottom sides of the tri-beam.

After the cross-beams have been fabricated, they will be picked up by the cross-beam positioner/welder, which is brought into proper position by a series of rotational and translational boom movements. Control equipment for the cross-beam positioner/welder is shown in Figure 4-43.

When in position, a cross-beam holder will grasp the fabricated cross-beam. The positioner will then rotate and translate the cross-beam into position for attachment to the longitudinal beams. Attachment of the cross-beams is accomplished with eight ultrasonic welders, which are rotated and translated into position under direction of the ACU. After welding is completed, the welder positioner arms retract and the cross-beam positioner is directed to pick up the next cross-beam. After three cross-beams have been attached, the entire tri-beam assembly is translated by the beam handling equipment located on the assembly jig to a position where the next series of three cross-beams is to be attached.

4.5 500-METER REFLECTOR CONSTRUCTION

Construction of a 500 m diameter reflector, using the SCAFE baseline beam builder and beam as the basic construction elements, is a large and complex task that requires multiple missions using the Shuttle Orbiter for transportation of material and equipment and to support construction operations. The best means of minimizing total construction time and number of missions is to fully automate construction operations and equipment. This subsection describes a concept for the construction of a 500 m diameter reflector in a minimum of eight missions.

4.5.1 500-METER REFLECTOR STRUCTURE AND SPACECRAFT CONCEPT. The 500-m reflector structural assembly concept, shown in Figure 4-44, is made almost entirely from curved beams produced by the beam builder. Twenty-four radial parabolic curved beams establish the basic dish contour. These radial beams are joined together by circular rib beams through special node joint fittings. The circular rib beams are spaced 25 meters apart. Slip-on end caps are placed on the end of each rib beam. The rib beam is positioned at the installation station established by the node fittings. The end cap is then automatically welded to the node fitting and the beam caps.

Construction of the dish requires that a construction platform first be assembled. This platform consists of two special tri-beam assemblies for construction arms, joined together through a central equipment and control hub. The construction arms provide support for traveling assembly crawlers used to fabricate and install rib beams. They also support solar panels that power the fabrication equipment and ultimately provide power for antenna operation.

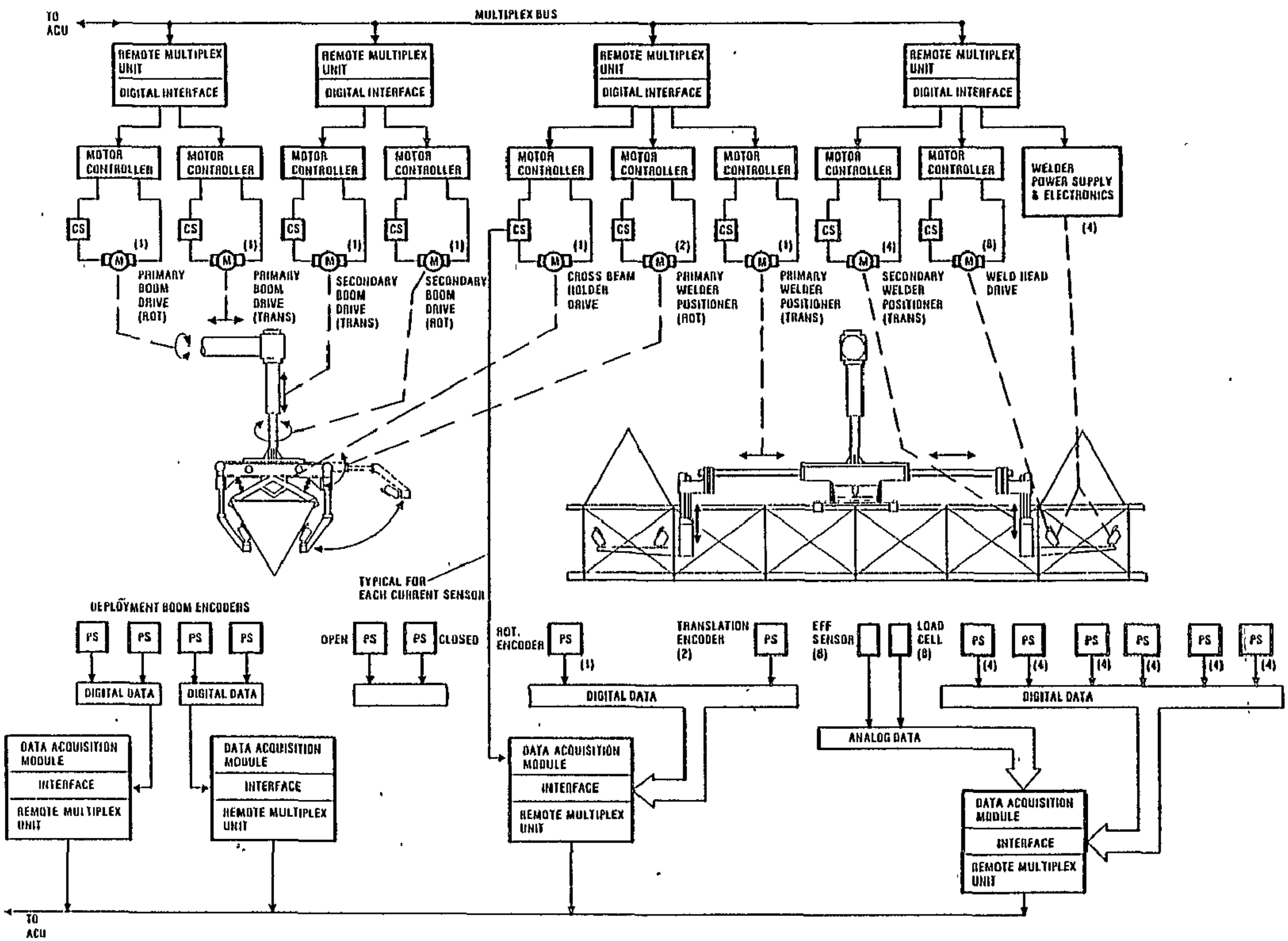

Figure 4-43. Tri-beam jig control diagram, Part 3.

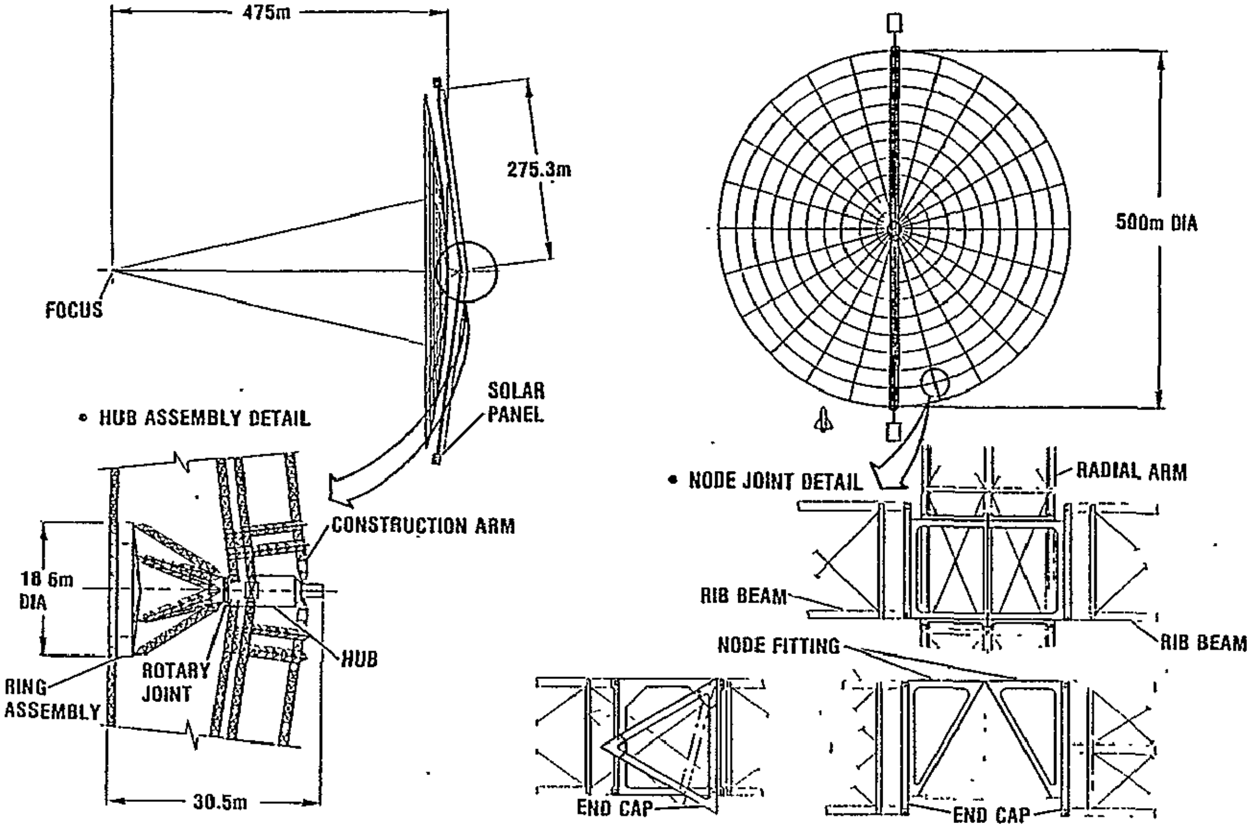

Figure 4-44. 500-meter parabolic reflector structural assembly concept.

The hub also supports a center ring assembly through a rotary joint. The ring assembly provides the mounting structure for the radial beams and supports the radial beam fabrication equipment during construction.

The dish is baselined as a large aperture space antenna facility for radio astronomy and communications; however, details of the antenna system hardware are not defined. The high f/D, 0.95, was selected to produce a large radius of curvature to maintain close proximity of the dish structure to the construction arms.

4.5.2 500-METER REFLECTOR CONSTRUCTION TRADES. A trade study was performed to determine the optimum number of construction arms required. More construction arms would reduce the time required to assemble the antenna structure and install the reflector. Structure fabrication and assembly rates were estimated based on the nominal beam builder production rate and assumed times for automated assembly operations. Reflector installation time was based on an assumed installation rate for each construction arm. The results of this evaluation are shown in Table 4-1.

Table 4-1. Assembly platform trade.

Factor	Construction Platform Option		
	2 Arm	3 Arm	4 Arm
Time to build assembly platform	15 days	25 days	30 days
No. of missions to build assembly platform	3	5	6
Time to assemble antenna dish	18 days	12 days	9 days
Time to install antenna reflector	15 days	10 days	7 1/2 days
Time to build mast	3 days	3 days	3 days
Time to install and checkout system	10 days	10 days	10 days
No. of missions to construct and activate antenna	8	9	9
Total construction days	61 days	60 days	59 1/2 days

The evaluation showed that the time advantage gained in reflector construction using more construction arms was lost to construction time and number of missions required for fabrication of the additional arms. It was concluded that a two-arm system was the optimum approach.

4.5.3 500-METER REFLECTOR CONSTRUCTIONS CONCEPT

Mission profiles for the eight missions required to construct the 500 m parabolic reflector antenna are summarized in Table 4-2.

Each construction arm assembly will require one full seven-day mission to fabricate and assemble, and part of another mission to complete the equipment installation and checkout. One beam builder reload is required to complete one arm structure.

The first step is to construct the special tri-beam using a modified version of the tri-beam assembly jig, as shown in Figure 4-45. The two additional longitudinal beams will act as tracks for the crawler, which transports the rib beam fabrication and installation equipment. The completed tri-beam is separated from the Orbiter and a ladder-style cross platform is fabricated as shown.

Through a series of docking maneuvers, the tri-beam assembly jig is dismantled and installed on the tri-beam. Special RGMs are deployed from the central jig and engaged with the track beams. This element of the jig thus becomes a crawler and support structure for the beam builder. The cross-beam positioner/welder is modified by removing the welders so it can be used as a rib beam positioner. The fold-out jigs are attached through RGMs to the cross platform and become traveling jigs complete with a rib beam installer and rib beam end cap installer. Finally, the solar panel and stationkeeping equipment are installed on the tri-beam. Note that the maximum rib beam span and height above the crawler are illustrated in Figure 4-45.

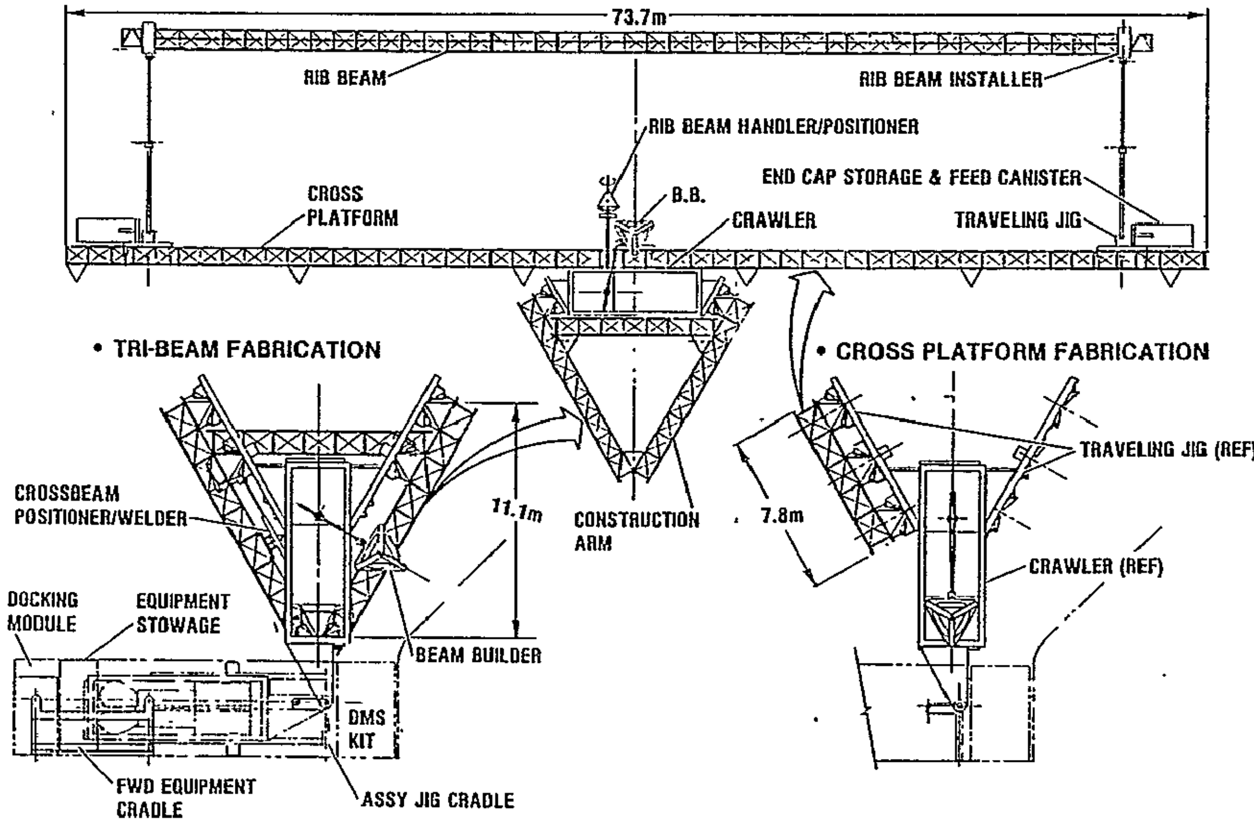

Figure 4-45. 500-meter reflector construction arm assembly concept.

Table 4-2. Mission profiles for 2-arm assembly platform system.

Mission		Payload	Task
No.	Duration		
1 & 2	7 days	• Assy jig & beam builder • Beam materials • Power bus cables/connector stations • Arm docking fitting • RCS package • OMS kit • Docking module	• Fabricate and assemble construction platform arms and subsystems
3	7 days	• Rib beam installers • Rib beam end cap storage & feed canisters • Docking module • Solar arrays (2) • OMS kit	• Install rib beam installers • Install end cap storage & feed canisters • Install solar arrays • Complete all arm equipment electrical hookups

Table 4-2. Mission profiles for 2-arm assembly platform system. (Contd)

Mission No.	Mission Duration	Payload	Task
4	7 days	• Center hub support, control & docking module • Center hub ring segments • Beam attachment fittings • Beam materials • OMS kit	• Join construction platform arms to center hub support, control & docking module • Assemble center hub ring structure • Fab, assemble, & install beam struts to join hub ring to hub support module • Connect & check out controls & power system • Check out construction platform equipment & subsystems • Reload beam builders
5	15 days	• Center hub assy jig, beam builder, & fixtures • Center hub ring interior structure • Center hub power & controls equipment • Center hub docking fitting • Beam materials	• Install hub docking fitting & dock to hub ring • Install hub ring interior structure • Install hub assy jig, beam builder, & fixtures • Install, connect, & check out hub construction equipment controls & power system • Start dish fab & assy operations • Monitor & control fab & assy operations
6	15 days or more	• Beam materials, rolls, & spools • Antenna reflector materials • Beam node & joint fittings • Antenna feed horn • Spare parts as required • Some antenna system hardware	• Relieve or overlap Mission No. 5 • Replenish beam builder & assy fixtures • Perform maintenance as required • Complete dish structure fab & assy • Fab & attach mast struts • Install feed horn • Install portions of antenna system hardware • Off-load & stow reflector matls • Monitor & control fab & assy operations • Remove hub assy jig, beam builder, & fixtures & stow in Shuttle for return to Earth

Table 4-2. Mission profiles for 2-arm assembly platform system. (Concld)

Mission No.	Mission Duration	Payload	Task
7	15 days or more	• Remainder of reflector matl • Reflector installation fixtures • Reflector attachment hardware • Spare parts as required • More antenna system hardware	• Relieve Mission No. 6 • Start reflector installation • Perform maintenance as required • Monitor & control reflector installation operations • Install portions of antenna system hardware • Supply reflector matls to the traveling assembly platforms • Dismantle traveling assembly platform No. 1 • Stow jig, beam builder, & fixtures in Shuttle for return to Earth
8	10 to 15 days	• Remainder of antenna system hardware • Boost package	• Overlap Mission No. 7 • Complete reflector installation • Complete antenna system hardware installation • Checkout antenna system • Dismantle traveling assembly platform No. 2 • Stow jig, beam builder, & fixtures in Shuttle for return to Earth • Install & check out boost pkg. Prep all systems for orbit change.

After fabrication and assembly of the two construction arms, an equipment and control hub is transported by a fourth Shuttle mission. The hub is joined to the two construction arms by end fittings welded to the ends of the tri-beam longitudinal beams, as shown in Figure 4-46. The beam builders on the crawlers are then used to fabricate support struts for the center ring assembly, which is transported inside the hub in segments and assembled in place.

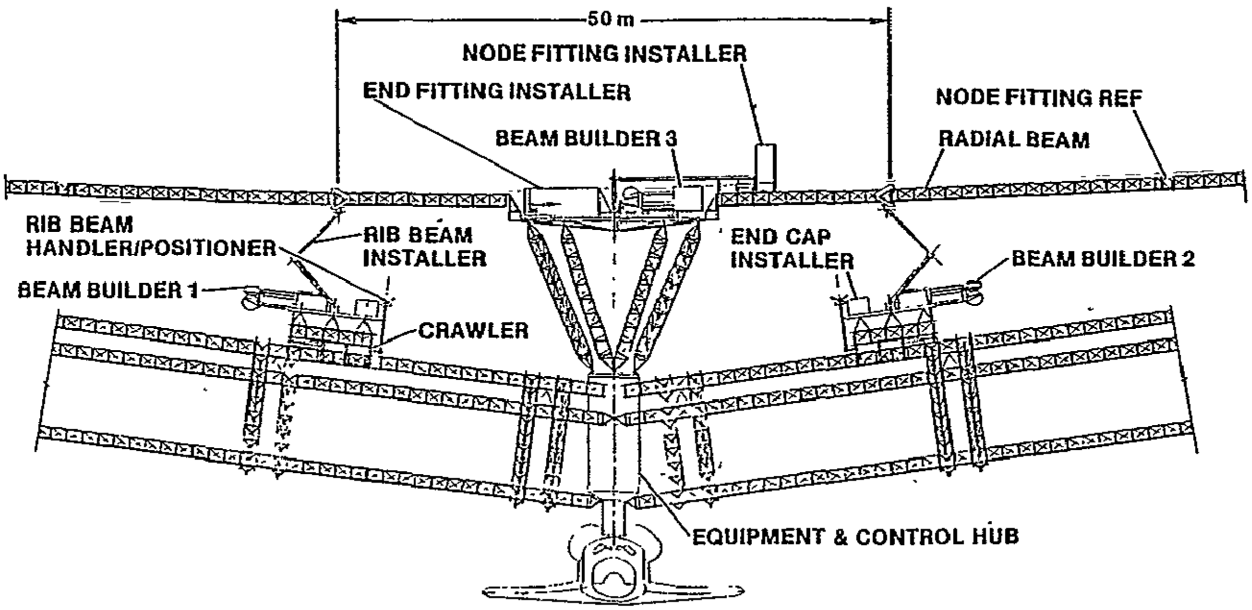

Figure 4-46. 500-meter reflector construction detail.

The next mission transports the radial beam fabrication and installation equipment, which is installed in the center ring assembly as shown. The power and control distribution system is installed and all equipment is checked out prior to the start of reflector structure fabrication.

The dish structure fabrication sequence starts with the fabrication of the first four radial beams. The radial beam fabrication sequence is described in Figure 4-47. The central hub and construction arms are rotated with respect to the dish until the arms are centered between two radial beams. Starting with the innermost rib beam, as shown, the rib beams are fabricated and installed by the crawler and traveling jigs in sequence until the outermost rib is installed. During this period, the next two radial beams are fabricated and installed.

The crawler then returns to the innermost rib beam position, the dish is rotated 15 degrees to center the construction arm on the next segment to be completed, and the process continued until the entire dish structure is complete.

Fabrication and installation of radial beam assemblies is accomplished with a beam builder mounted on a turntable opposite a beam end fitting installer. A special swing arm jig provides beam node fitting installation, beam handling and positioning, and beam-to-end fitting welding functions.

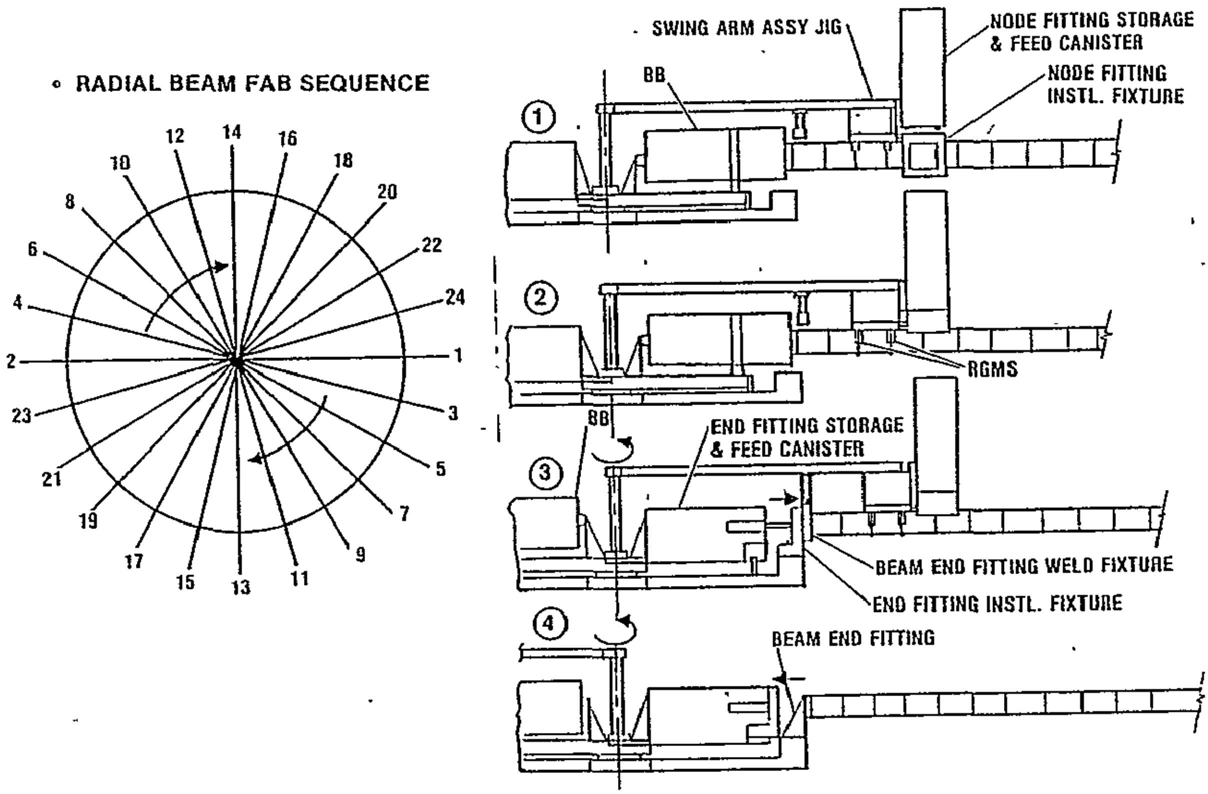

Figure 4-47. 500-meter reflector radial beam fabrication sequence.

As the radial beam emerges from the beam builder, the fabrication sequence is interrupted at predetermined lengths and a pair of node fittings is automatically moved into position from a storage canister by rotating installation fixtures equipped with automatic welders.

When the beam is complete, RGMs grasp the beam and the beam is cut off at the beam builder. The RGM beam drive mechanism then moves the beam into position for installation as the beam builder rotates 180 degrees and the beam end fitting installer is brought into position.

An end fitting installation fixture removes an end fitting from a storage and feed canister, places it on the end of the beam, and automatically welds it to the ring structure. A beam end fitting weld fixture is rotated into position and automatically joins the beam caps to the end fitting. The swing arm jig is then rotated to the next radial beam fabrication station and the process is repeated.

After the structure is completed, the reflector surface will be installed using the construction arm crawler and traveling jigs. Table 4-2 schedules this task for Missions 7 and 8. It is assumed that the reflector surface will be in deployable prefabricated sections which can be automatically attached to the structure, using the manipulator arms and special installation fixtures on the traveling jigs.

The two construction arms and central hub remain as an integral part of the antenna after construction. The arms continue to function as supports for the solar power panels. The central hub houses the controls and instruments for the antenna system and also serves as the mounting structure for a LEO-to-GEO transfer vehicle.

The remainder of the construction equipment is removed and either returned to earth via Orbiter or attached to the cross platforms and maintained in LEO for future use.

4.5.4 <u>500-METER REFLECTOR CONSTRUCTION SYSTEM CONTROLS.</u> The construction base for the 500-meter antenna will be automatically controlled by a distributed computer system arranged per the block diagram shown in Figure 4-48.

Local controllers will be used by each of 13 equipment subsystems for process control. A central hub computer (HCU) will orchestrate the activities of the 13 subsystems during the antenna fabrication sequence. The HCU will provide status data to the Orbiter or ground control for monitoring purposes.

A direct hardware link is provided between the HCU and Orbiter computer when the Shuttle is docked at the construction base; otherwise, an RF link will be used. Communication between the HCU and crawler controllers (CCUs) will be achieved either by RF or light beam links eliminating the need for traveling data cables. Similar data links will be used between the CCUs and the traveling jig controllers (TCUs).

All power required to operate subsystem equipment will be generated by two solar collector panels located at each end of the construction base. A power distribution controller (PCU) will provide solar collector attitude control and power distribution management functions.

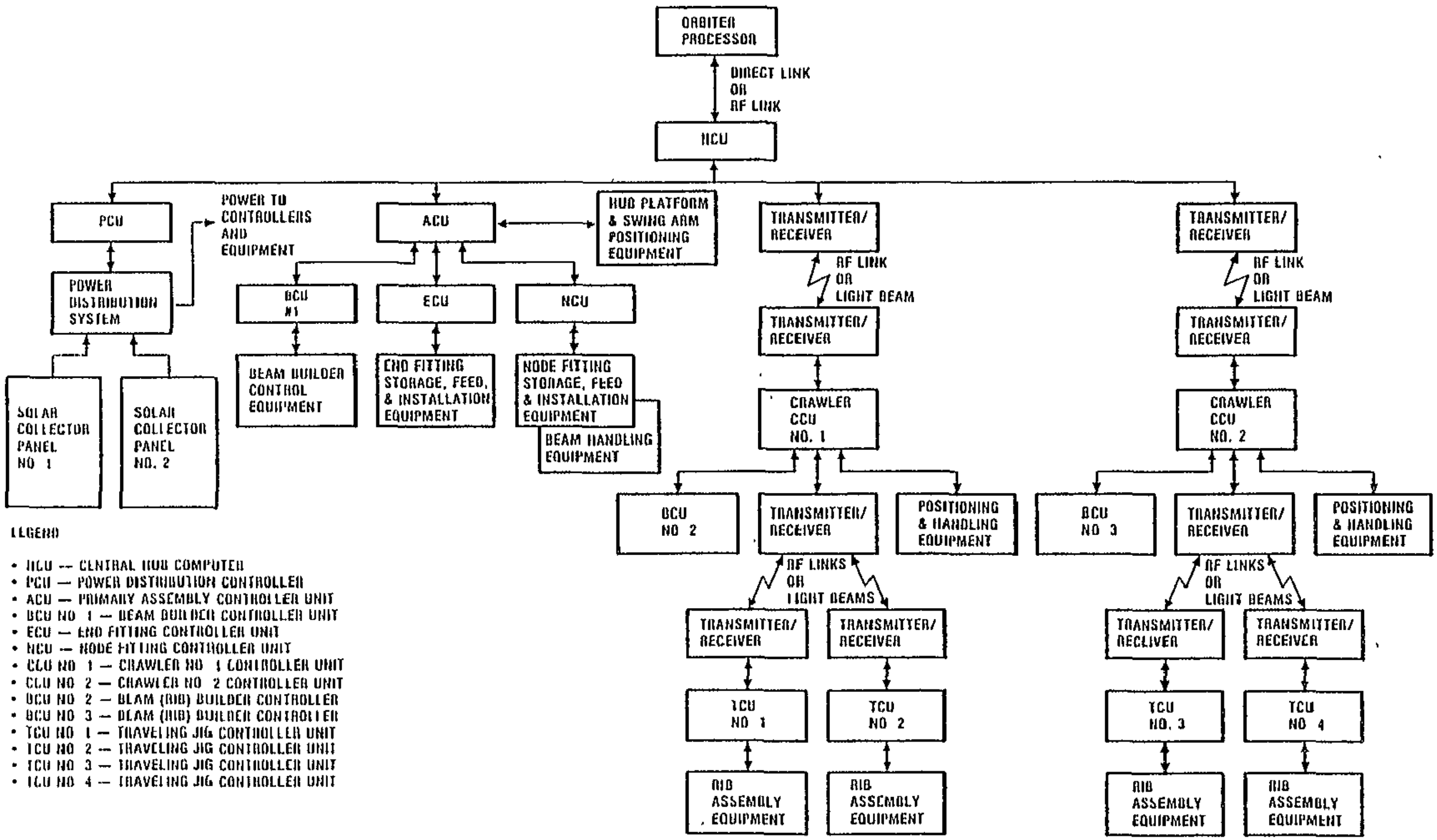

Figure 4-48. 500-meter antenna assembly controls block diagram.

5

DEVELOPMENT EXPERIMENTS

5.1 ULTRASONIC WELDING

All large space structures will require joining together numerous truss members to produce the final structure for support of large space systems in orbit. The process by which structural members are attached together must be efficient, repeatable, verifiable, and reliable in the environment of space. Ultrasonic welding has proven to be the most likely candidate for joining structures fabricated from composite material which contain thermoplastic resins. Experiments and studies have shown that ultrasonic spot welding is highly efficient and capable of being fully automated with in-process quality control monitoring of welds.

The following paragraphs describe an ultrasonic welding apparatus designed to operate in space environment. Development and testing of this type of device is required to establish a firm technology base leading to complete evaluation of capabilities and performance. Ultrasonic welding apparatus is capable of automatically performing numerous welds inside a vacuum chamber or as a flight experiment to provide the necessary weld specimens and functional data required to complete the evaluation of ultrasonic welding performance characteristics.

5.1.1 APPROACH. The ultrasonic welder experiment has been designed to serve as a Space Shuttle "suitcase" experiment and can operate with only minor Shuttle interfaces for power and support. Only a nominal amount of EVA assist is required as explained in Subsection 5.1.2.3. Requirements include various design features as follows:

a. Fully automated

b. In-process monitoring and controls

c. Various weld heads and transducers

d. Operate in vacuum and zero-g

e. Temperature independent/self compensating

5.1.2 MECHANICAL DESIGN AND OPERATION. The welder, shown in Figure 5-1, is designed to automatically perform a series of spot welds in flat, two-piece test specimens of composite material. It will perform the following operations for each weld specimen:

a. Acquire a test specimen from the removable coupon magazine.

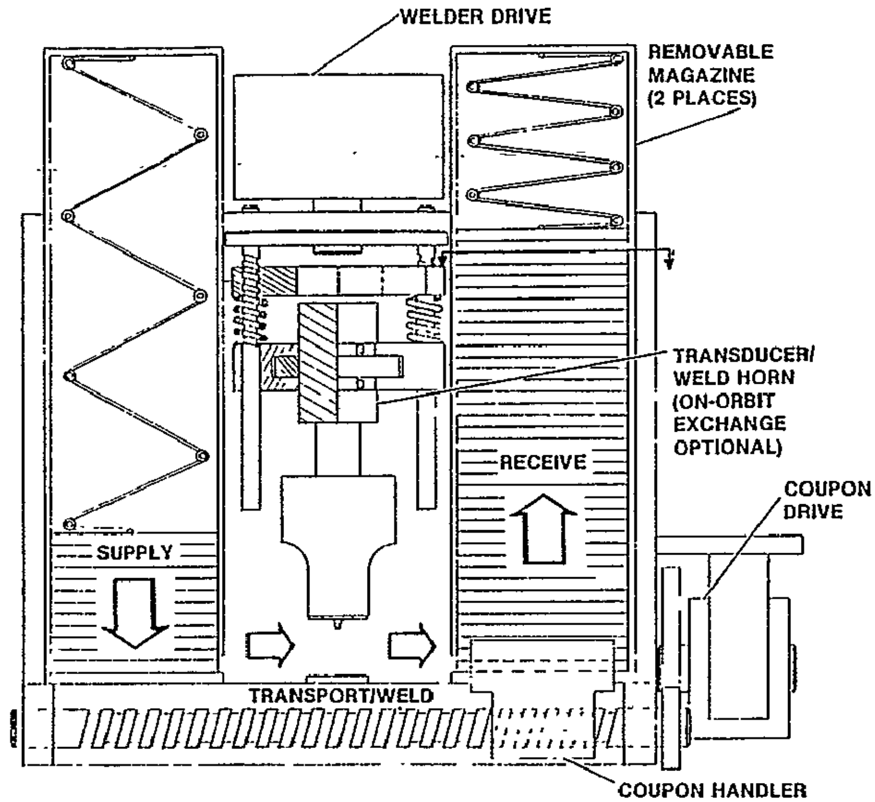

Figure 5-1. Ultrasonic welding experiment concept.

b. Position the specimen under the weld tip and hold it in place.

c. Engage weld tip, pierce, and weld the specimen.

d. Monitor the weld cycle and modify it to optimize weld quality.

e. Retract the weld tip.

f. Place the test specimen in the receiving magazine.

g. Position the next test specimen.

h. Repeat operations/sequences.

i. Provide weld schedule data on each specimen.

The two drive motors are brushless dc motors. The weld transducer is a standard off-the-shelf, 20 kHz transducer designed for a magnitude of oscillation of 0.00191 cm (0.00075 in.). The horn is exactly as intended for the beam builder application and produces the same spot weld configuration. The flight version of the ultrasonic welding experiment (Figure 5-2) is attached to a mission-unique Shuttle bridge beam which will have the same profile as the normal bridge beam at the (TBD) support location. A shelf attached to the bridge beam holds the experiment package, power supply/control electronics, and the air-tight coupon magazine storage cabinet.

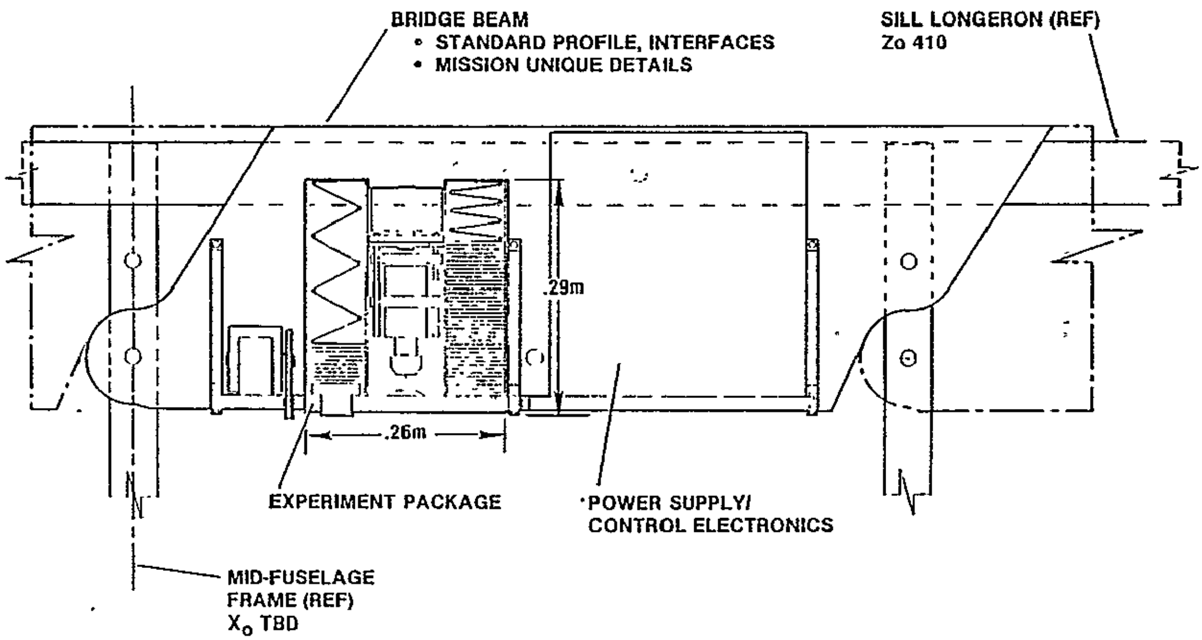

Figure 5-2. Welding experiment installation concept.

5.1.2.1 Test Coupons. The test coupon specimen is designed to simulate the actual weld site of a cap and cross-member. Fiber directions at the area of interface, polysulfone content, and protective coating are identical to that of the beam and cross-member interface.

A test coupon is shown in Figure 5-3 including the coupon holder. This bracket performs four important functions for the welder. The first is to hold the two pieces of composite firmly aligned and in contact with each other. The second is to provide firm attach points for transporting and holding the coupon from sending magazine to weld site to receiving magazine. Third, it provides the ramped surfaces necessary to slide the coupon from one magazine and into the other. And, fourth, it provides ease of handling and identification of each weld specimen before and after weld tests.

The coupon bracket has two pockets that provide the alignment and locking points for the spring-actuated bearings in the coupon drive mechanism. These provide a firm grip of the test coupon to remove the specimen from the magazine during weld operations and while stacking it in the receiving magazine

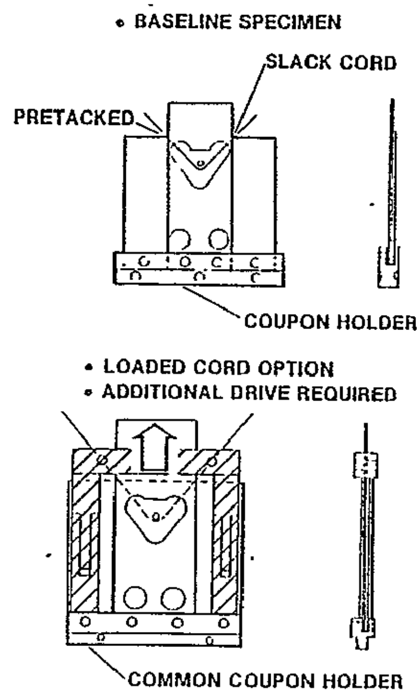

Figure 5-3. Ultrasonic welding experiment test specimen concepts.

5.1.2.2 Welder Operations. When the drive is actuated, the mechanism slides over the outer edges of the bottom coupon bracket (coupon cannot slide to the left due to the wall of the magazine). When the position of the bracket is verified by sensors, the coupon drive will reverse direction, sliding the coupon from the magazine and placing it over the weld anvil. (Sensors again verify position.) At this point the welder drive mechanism is actuated. A brushless dc motor drives the main gear of the welder drive mechanism, shown in Figure 5-1. This gear turns two synchronized and threaded drive shafts. As these turn, the upper pressure plate is forced down, moving the lower pressure plate, which carries the transducer and weld horn. The springs, attached to both pressure plates, are designed to produce the correct force (as determined by previous ground tests) required for optimum weld pressure at the weld surface. The lower pressure plate is designed for ease of removal and replacement of transducer/horn (for different weld configurations and/or frequencies). The springs can also be changed easily for testing different weld pressures. (Flight version would use the optimum weld pressure, frequency, and horn configuration, as determined on ground tests.)

As the weld tip contacts the weld specimen, pressure is sensed in the weld anvil (pressure sensor). When the force required to pierce the specimen is obtained, the drive mechanism is shut off and the welder power supply is activated. The motion of the lower pressure plate as the pierce point moves into the coupon is verified by a sensor on the pressure plate and by a lowering of the pressure on the anvil.

The drive is again activated to obtain the proper weld pressure. When this is verified, the welder is again activated and the specimens are welded together.

Ultrasonic inspection to verify weld quality would be performed at this point in the process using the same horn and transducer. However, further testing is required to determine frequency, direction of ultrasonic impulses, and point and method of sensing for ultrasonic inspection of thin composite materials.

The weld being completed and the quality verified, the welder drive motor is reversed and retracts the horn from the specimen. The position sensor verifies horn position and the coupon drive is activated to move the coupon to the receiving magazine where it is trapped in the magazine with a one-way "trap door". The coupon dirve then moves across the experiment package passing the weld site and gripping the next weld specimen bracket.

The welding process can be summarized in a flow chart as shown in Figure 5-4. This diagram shows a point for removing and replacing the coupon magazines. Sensing of an empty sending magazine can be accomplished by any one or a combination of the methods listed below.

a. Counting of weld cycles (50).

b. Direct sensing in the magazine.

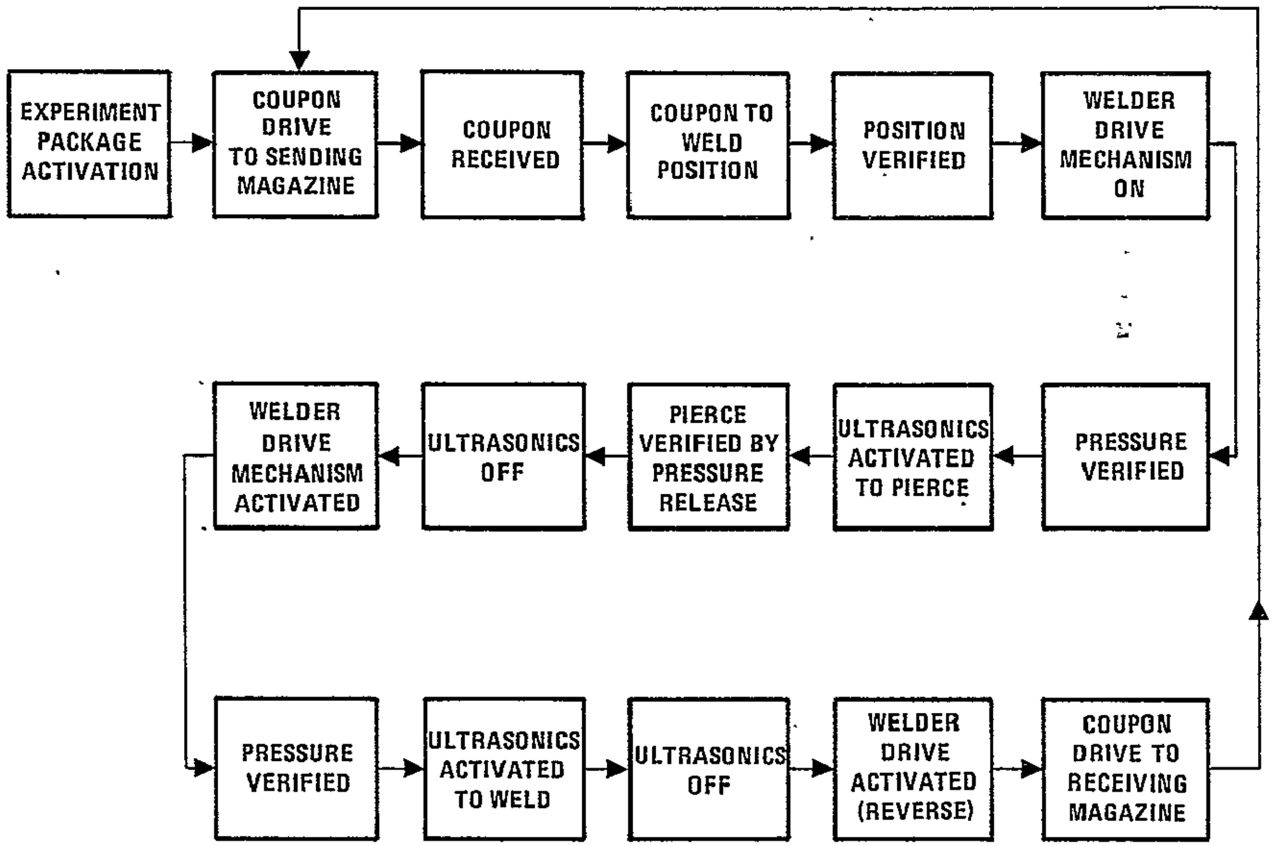

Figure 5-4. Welder major operations flow diagram.

c. Sensing "No Coupon" on the coupon drive mechanism.

d. Sensing "Full Receiving Magazine"; therefore empty sending magazine.

When an empty condition exists, the coupon drive moves to the "weld" position out of the way of both the sending and receiving magazines.

5.1.2.3 Coupon Magazine Storage. The test coupons are held in magazines large enough to carry up to 50 test specimens. The number of magazines required will depend on the total number of specimens desired in the flight test.

Each magazine is designed to perform both the sending and receiving functions. In the flight test, the astronaut will not be required to monitor the welder constantly. His only duty during the experiment will be to remove the full magazine of welded specimens and store it under the welder electronics package. Then move the now empty sending magazine to the receiving position on the right and place a full magazine in the sending position. The welder can then be reactivated to resume the welding operations.

5.1.3 ELECTRONICS AND SENSOR SYSTEMS. The ultrasonic welder control electronics are shown in block diagram form in Figure 5-5. These systems are designed to monitor, and in some areas self-correct, the weld sequences and weld schedules. The only interfaces required with the Orbiter consist of the 28 Vdc input and possible system status indicators, (i.e., operational status, alert for any electromechanical problem, or indication of no coupons in the sending magazine). The welding experiment control system consists of a small microprocessor, a data acquisition module, ultrasonic welder electronics and power supply, weld head positioning controls, test coupon storage/feed controls, and a data recorder.

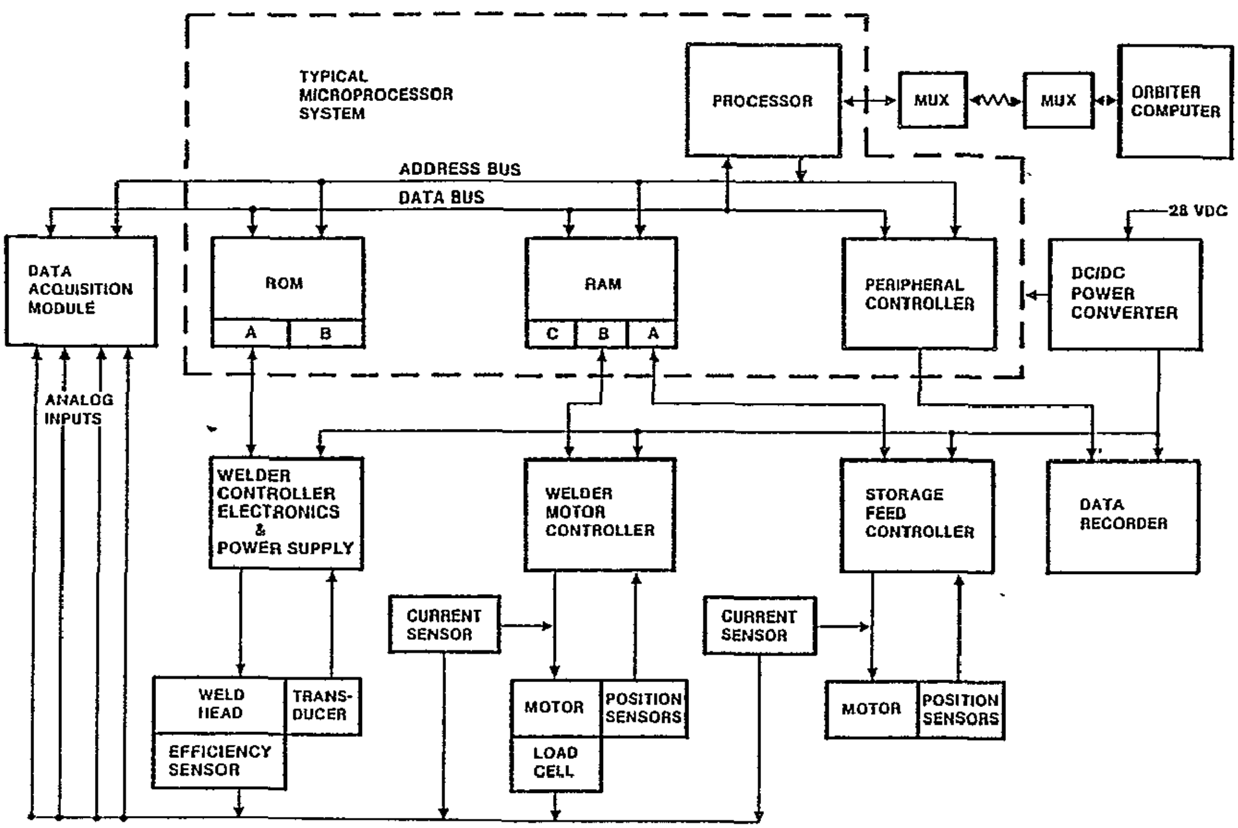

Figure 5-5. Welding experiment control diagram.

The microprocessor is interfaced to the Orbiter computer via the Orbiter multiplex system. The microprocessor directs operation of the control equipment and monitors analog and position sensor data. A data acquisition module is provided to digitize the analog sensor data for processing by the microprocessor. This module is interfaced directly onto the microprocessor bus system. Sensor data and weld inspection results for each test coupon are recorded on the data recorder for future analysis.

5.1.3.1 Power Supply and Controller Electronics. The power supply consists of three major components: the oscillators, amplifier, and efficiency analyzer. These components work together to produce the required frequency and for the precise length of time to produce consistent weld results.

The oscillator sets up the initial oscillations (approximately 20,000 Hz) in the amplifier. It is only activated long enough to create oscillations of approximately the correct frequency for the weld transducer and horn. The transducer and horn system will oscilate at their own natural frequency. This natural frequency is a function of system temperature. (Temperature fluctuations not only effect the length over which the sonic impulses must travel but also the speed at which they travel.)

The power supply is a 300-watt amplifier which changes the Shuttle's 28 Vdc signal to a 300-watt ac signal at approximately 20,000 Hz.

The efficiency analyzer portion of the welder controller will "read" the natural frequency of the system through a sensor located at the top of the horn. The analyzer then becomes an oscillator for the amplifier and reproduces the exact natural frequency for the system. This method of frequency compensation results in the horn essentially becoming its own oscillator and nearly independent of minor temperature fluctuations during operating cycles.

The efficiency analyzer will also compare wattage input to that reflected from the horn tip. The difference is the power input (absorbed) to the parts to be welded. The analyzer will then shorten or lengthen the weld time to ensure optimum wattage to each weld. This assures that each weld receives an equal, and correct, amount of energy, which results in very uniform and consistent welds.

5.1.3.2 Sensors. The position sensors work on the Hall effect principle, i.e., a disturbance in a magnetic field creates a small electric current. Pressure sensors and load cells are located under the weld anvil and on the hold ring of the transducer, respectively. Efficiency sensing can be accomplished by either mechanical or electrical systems incorporated into the welder controller.

5.1.4 VARIABLES IN ULTRASONIC WELDING. Ultrasonic welding can be affected by a relatively large number of variables. Each must be controlled or fixed by design to a very narrow "range" of acceptability in order to obtain consistent weld results for a given material. These variables and the electromechanical methods by which they are held within those very strict limits are listed in Table 5-1.

5.1.5 WELD SCHEDULE DATA. The weld schedule will vary slightly from part to part due to in-process correction systems. Therefore, a necessary part of the weld experiment will be to record these schedules for comparison with the weld specimen produced by that schedule. A numerical code will be applied to each weld specimen bracket, which can be referenced to the weld schedule used to produce that specimen. In this way, minor

Table 5-1. Variables in ultrasonic welding can be eliminated by mechanical design and/or electronic self-correcting systems.

Variable	Approx. Value	Tolerance	Held to Tolerance by	Comments
Frequency	20,000 Hz	±50 Hz	Frequency analyzer portion of power supply	
Watts	300 watts	±5%	Efficiency analyzer	
Pressure/Force	172.36 kN/m^2 (25 psi)	±1.72 kN/m^2 (±0.25 psi)	Spring constant	Optimized by ground tests
Weld Time	1 sec	±.05 sec	Efficiency analyzer	Optimized approximated by ground tests ±0.02 sec
Weld Area	6.45 cm^2 (1 $in.^2$)	—	Design of weld tip	
Magnitude of Oscillations	0.00191 cm (.00075 in.)	—	Design of transducer and horn	Optimized by ground test
Material Variations	—	—	Quality control during manufacture	Polysulfone surface thickness 0.010 ± .005 cm for optimum weld strength
Moisture Content	—	—	Test coupons must be dried to eliminate moisture	

variations in weld strengths can be analyzed as a function of weld schedule variations. Weld pressure weld time, efficiency (watt-sec), hold time, and pressure curves during each weld can then be compared to the strength of the weld. After sufficient test coupons have been tested and data comparisons completed, a large and reliable data base will exist on which confidence in the ultrasonic welding processes can be based.

5.1.6 GROUND TESTS. The variables in ultrasonic welding not fixed by design can be investigated in three steps. Step one should use a standard production type ultrasonic welder to prove tip configuration, magnitude of oscillations, weld pressure, and approximate weld time. Step two should be conducted with the actual configuration of power supply and hardware needed for the flight test. This will include tests to investigate transducer/horn configurations, holding mechanisms, weld schedules, and electronic systems. Step three in the ground tests should be to certify all electromechanical systems and run a large number of test specimens with the actual flight hardware. The data base developed from a large number of test specimens will include running the welder at the various temperatures anticipated in space and in a vacuum chamber.

5.1.7 FLIGHT TESTS. Provisions for varying the weld schedule for the in-space environment should be included in the electronics. Ground tests can not reproduce the combination of temperature and vacuum conditions which exist in space. Weld time and hold time will be longer due to the pre-weld temperature of the specimens and the rate at which the weld areas cool down. The weld schedules used in space will, therefore, be unique to that environment. Ground tests will only prove the electromechanical systems and weld strengths anticipated from the flight tests, and the flight tests will determine the actual weld schedule required for optimum weld strength and reliability.

5.1.8 POST FLIGHT TESTS. Additional weld test specimens made after flight will add to the data base and increase confidence in the total system. Environmental effects of space on the piezoelectric crystals in the transducer and all sensor systems can be checked, as well as wear on the weld tip, horn, and pierce point.

5.2 CAP FORMING EXPERIMENT

An in-space investigation of forming of graphite/polysulfone composite materials may be necessary to evaluate the performance of the beam builder cap forming section. Since the combined environmental effects of zero g, vacuum, and expected operating temperatures cannot be simulated on earth, testing of the cap forming system under space conditions is advisable prior to completion of the full-scale beam builder for space flight.

5.2.1 APPROACH. The cap forming experiment should be designed as a "suitcase" package requiring limited interface with the Orbiter. The functional mechanisms should be identical to the beam builder cap forming machine. This provides two advantages: (1) it will prove a system in-space identical to that of the beam builder, and (2) much of the same hardware and software could be incorporated into the flight version of the beam builder to save on development costs. Minor modifications are necessary in order to support additional sensing systems and ability to cut off test lengths as desired.

The machine should also produce multiple cap specimens, approximately 16 ft long, to permit postflight column element tests, plus assembly and test of three-bay beam segment(s). Specimen storage provisions shall preclude potentially adverse environmental effects (atmosphere/humidity) during deorbit/postflight removal.

5.2.2 CAP FORMING ELECTROMECHANICAL DESIGN. The cap forming machine shown in Figure 5-6 uses the full-size canister of composite material. A smaller canister designed to supply just the quantity necessary for flight tests could be substituted

• ARRANGEMENT

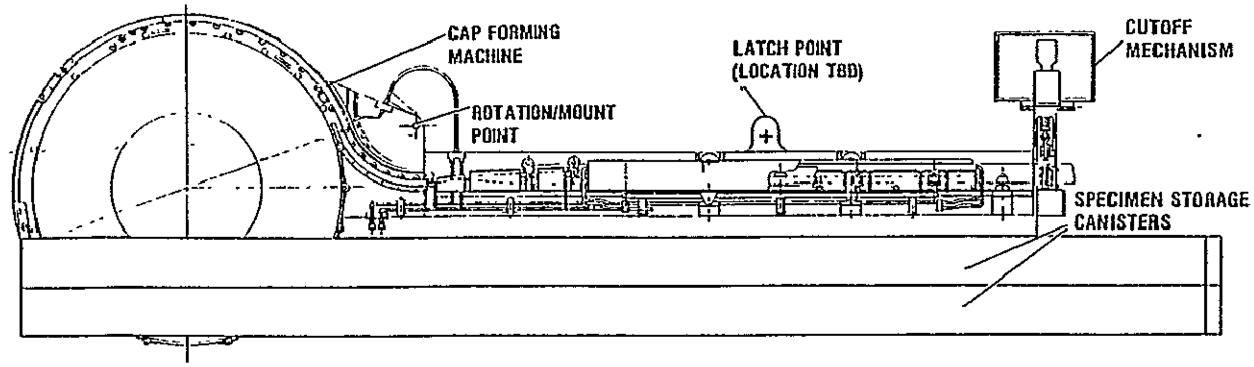

Figure 5-6. Cap forming experiment concept.

to save space and weight. The full-size version, however, has the added advantage of testing the characteristics of the coiled composite strip material while unwinding from the canister.

The heating, forming, and cooling areas of the cap forming machine are identical to the beam builder and are detailed in Figure 3-13 of Section 3. This design mounted on the end of the cap former. The cutoff mechanism is illustrated in Figure 3-55 of Section 3 and shown attached to the cap forming machine in Figure 5-6.

5.2.3 CARGO BAY POSITION TRADES. Assumptions made in determining possible locations in the Shuttle bay of the cap forming machine include: (1) little or no movement of the mechanism from storage to operating positions; (2) 16-foot cap specimens when being formed must clear the Shuttle bay and/or other mechanisms; and (3) minimum EVA assist to deploy and operate the experiment.

Figure 5-7 illustrates three positions where the cap forming machine could be mounted on a single pivot point near the center of mass. Three options exist, with several variations of each, for installation of the cap forming experiment in the Shuttle cargo bay. Options 1 and 2 use bridge beams and can be moved forward or aft to accommodate prime payload requirements. Degree of rotation, if needed, is also dependent on other payload requirements. The rotation option would be necessary only if a clear path in front of the cutoff mechanism could not be provided. If a small rotation (~15°) is found possible, the experiment package could be mounted permanently in that position to eliminate the necessity of manual deployment in orbit. Figure 5-8 illustrates positions 1, 2, and 3 in more detail to show the pivot point location, and three manual/automatic latch points and other details required to mount and operate the mechanism. Payload envelope limitations and the strip material storage canister envelope require the cap forming experiment to be mounted at least 16.5 cm (6.5 inches) from the bridge beam.

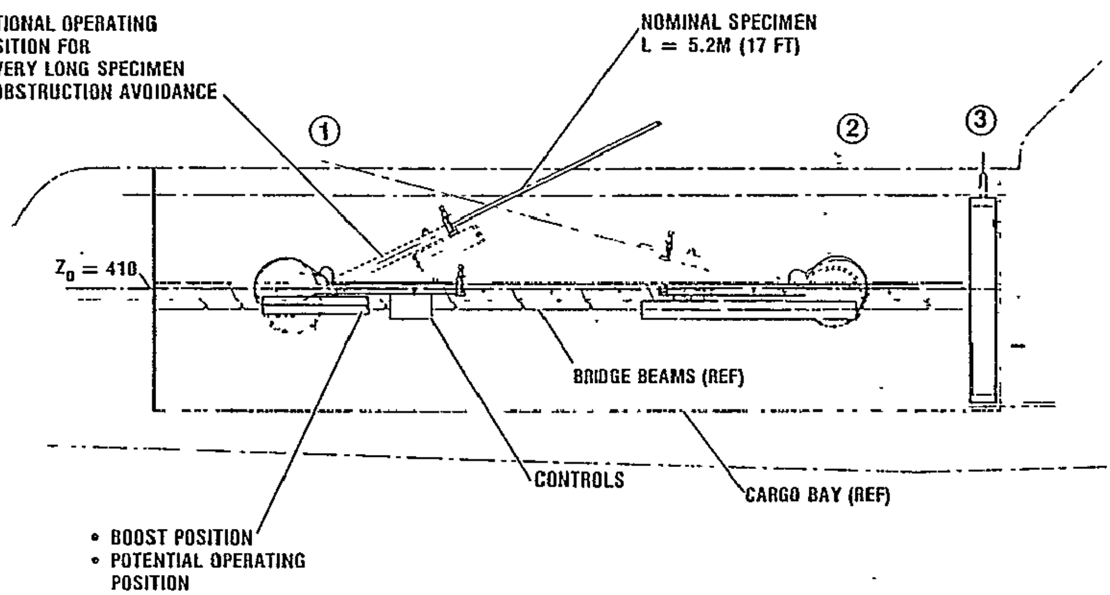

Figure 5-7. Cap forming experiment installation options.

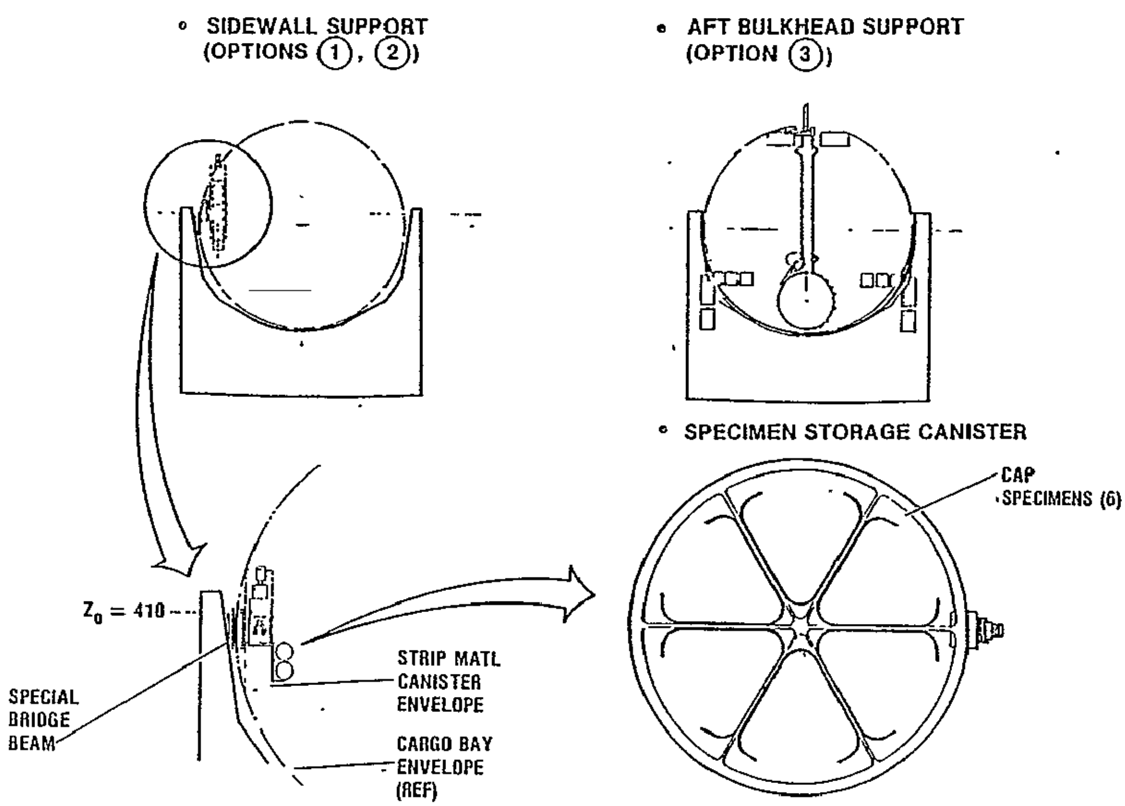

Figure 5-8. Orbiter installation options.

The aft bulkhead position (3) would have the added advantage of a permanent mount; therefore, no EVA assist would be required to reposition the mechanism for operation. This position would require the beam builder to be shortened by 10 inches if the full-size spool proved desirable (e.g., attach points could be isolated from the heating section and insulated to decrease heat transfer from the machine to the aft bulkhead). Electronic controls would also be more remotely mounted.

5.2.4 CAP FORMING ELECTRONICS. The electronic control systems package (Figure 5-9) is similar to that of the full size beam builder. Simplifications can be made due to the fact that only one cap forming section is controlled and monitored. A data recorder can be added to store temperature data as a function of length so that a complete comparison of material condition versus forming temperature can be made when specimens are returned to earth.

The electronics package is a separate assembly mounted near the cap forming machine. All major controls and monitoring can be operated from the Shuttle bay. Interfaces with the Shuttle include power supply and operational status readouts through the Orbiter controller and Orbiter monitor.

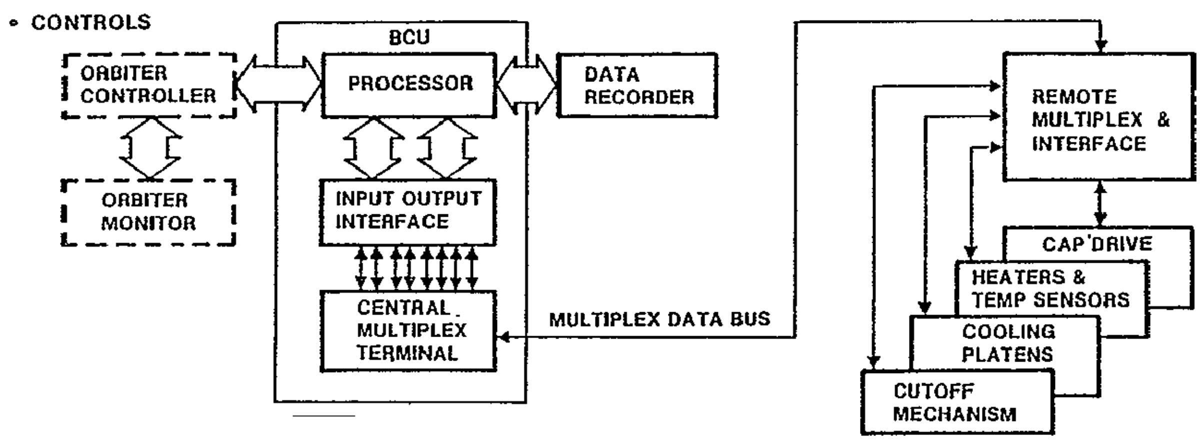

Figure 5-9. Cap forming controls block diagram.

5.2.5 SPECIMEN STORAGE. The shape of the caps to be formed offers a variety of storage configurations, as shown in Figure 5-10. In selecting the best storage configurations, several ground rules were assumed: (1) maximum use of space; (2) ease of storage in weightless conditions; and (3) storage system designed to include capability of returning specimens in vacuum. (This will facilitate testing of cap specimen similar to the as-formed condition with limited degradation due to earth atmosphere.)

The canister method of storage of Figure 5-10 satisfies these criteria with the added advantage of ease of handling when returned to earth. This method will also offer a numerical storage system so that data records in the system memory will correspond to a certain specimen and area on that specimen.

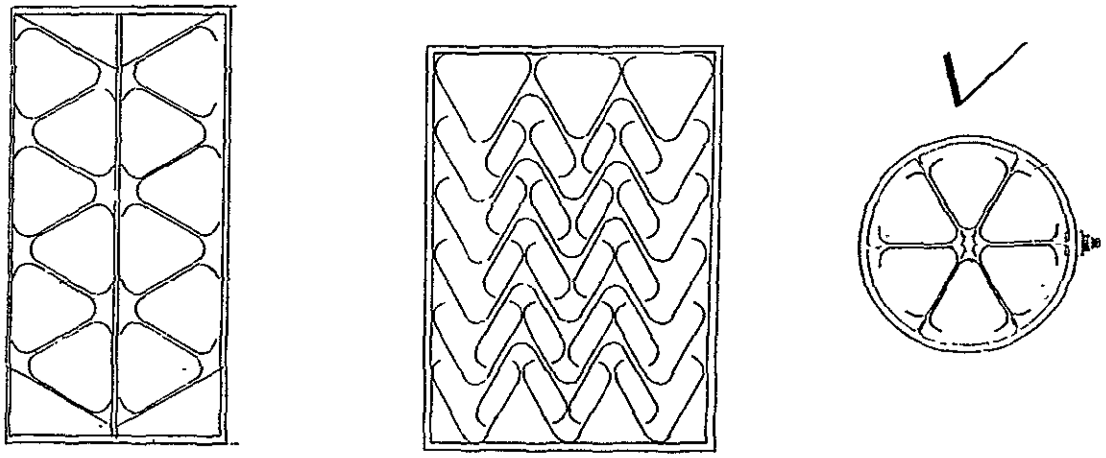

DISADVANTAGES
- SPACE NOT UTILIZED EFFECTIVELY
- DIFFICULT TO MANUFACTURE
- DIFFICULT TO SEAL
- HIGH WEIGHT WITH SUFFICIENT STRENGTH

ADVANTAGES
- SEPARATE COMPARTMENTS
- NUMERICAL STACKING
- EASY INSTALLATION OF SPECIMENS

DISADVANTAGES
- HIGH PROBABILITY OF SPECIMEN DAMAGE
- DIFFICULT TO SEAL
- NO NUMERICAL STACKING
- INSUFFICIENT STRENGTH

ADVANTAGES
- HIGHLY COMPACT
- LIGHT WEIGHT
- EASY TO MANUFACTURE

DISADVANTANGES
- SPACE NOT UTILIZED AS EFFECTIVELY

ADVANTAGES
- EASY TO SEAL
- NUMERICAL STACKING
- SEPARATE COMPARTMENTS
- EASY INSTALLATION OF SPECIMENS
- VERY STRONG FOR WEIGHT
- EASY TO MANUFACTURE

Figure 5-10. Cap forming experiment specimen storage canister trade options.

The cap section storage canisters have been designed with check valves to vent internal pressure during boost and to provide two vacuum seals during reentry to prevent atmospheric degradation of the cap sections and to preserve the as-formed condition.

6

BEAM BUILDER DEVELOPMENT

6.1 BEAM BUILDER DEVELOPMENT ARTICLE

This section summarizes the study effort directed toward the preliminary design of a Ground Test Beam Builder (GTBB), definition of a test plan to guide its development, and formulation of an overall development plan and associated cost estimate to ultimately employ the beam builder (and associated construction equipment) in a baseline flight experiment mission.

6.1.1 GTBB PRELIMINARY DESIGN. The dominant ground rule guiding beam builder design and development is:

The initial flight experiment shall be a "one-machine" program.

This requires that, as development and qualification progress, the GTBB must evolve into the Flite Test Beam Builder (FTBB). This, in turn, requires that, from the outset, the GTBB must be treated as a flight qualifiable machine. Therefore, a major issue must be addressed:

What is meant by "Flight Qualifiable?"

Clearly the GTBB cannot be totally designed and manufactured from the start to meet all requirements for flight test, since this implies the mandatory use of flight quality items throughout the machine, even during early development. In some cases it may well be advantageous to use less expensive and readily available components to build a particular subsystem to verify the design concept in the development phase. Then, if further changes and refinements are needed to achieve top performance for flight, the rework and retrofit would be far less expensive than they would be if flight quality components were used originally, only to be superseded by other flight quality components as early development progressed. A reasonable goal, then, is to design and select system parts, elements, and components to the following sequence of standards, listed in their order of preference:

a. Fully capable of use for flight test as determined by past qualification test data acceptable for Shuttle.

b. Capable of being upgraded to meet quality and qualification requirements for flight based on: (1) only partial requalification required to meet Shuttle standards and/or (2) material changes required to meet Shuttle standards.

c. Capable of being qualified for flight based on: (1) analysis, (2) design evaluation, and (3) test data.

d. Capable of meeting requirements for ground test but requiring redesign, modification, or replacement with a qualifiable item in order to meet Shuttle flight qualification requirements.

The key to achieving unimpaired flight qualifiability, as development progresses, lies in the execution of a design whose weight, physical/functional interfaces, clearances, and equipment space allocations result in a well integrated flight machine which nevertheless accommodates substitution of non-flight items where appropriate. Accordingly, the following additional ground rules and assumptions were developed to govern GTBB/FTBB development.

a. The integrated beam builder system shall include the following subsystems, which shall be modular to the maximum extent practicable:

   1. Cap Forming Subsystem
   2. Joining Subsystem
   3. Cross Member Subsystem
   4. Cord Subsystem
   5. Cutoff Subsystem
   6. Controls Subsystem
   7. Structure

b. The system shall automatically fabricate a beam which conforms to the configuration established by SCAFEDS Part III.

c. Material storage capacity for the system shall be designed to meet the following criteria:

   1. Storage capacity for cap strip material shall be sufficient to prove the functional capability of the cap material storage & feed concept.
   2. Storage capacity for cross-members shall be sufficient to prove the functional & mounting capability of the corss-member clip feed mechanism.
   3. Modular storage clips & canisters shall be considered to allow storage capacity to be varied conveniently.

d. All materials and components shall be selected for compatibility with space environment or for their suitability for spacecraft applications. Substitutions for space-compatible materials and components may be made where future retrofit is feasible and the following conditions prevail:

1. The preferred material or component is too costly or requires too much time to procure such that the program budget & schedule cannot be maintained.
2. The substitute material or component is adequate to allow the beam builder to be tested and evaluated on the ground in air and vacuum.
3. The substitute component is functionally and physically similar to the preferred component such that major differences in performance or interfacing hardware are avoided.

e. The degree of redundancy in systems design required to achieve the optimum safety and reliability for the flight article may be reduced for the development article under the following conditions:

1. Implementation of the redundant system element would significantly affect program budget and schedule.
2. The redundant system element is a passive device requiring no active monitoring and control.
3. Development considerations dictate the use of simple devices initially to prove system capability.
4. Omission of the redundant system element does not significantly affect the cost of implementing it on the flight qualification article.

f. General requirements for achieving optimum safety and reliability for the flight article are outlined as follows:

1. Redundant system elements shall be provided as follows:

   (a) Wherever the failure of a system element will result in damage to the beam or beam builder equipment if the failed element is not backed up by a redundant element or redundant operating mode.

   (b) Wherever the manual replacement of a failed system element in space is either not feasible or would require so much time and effort that the mission objectives cannot be achieved.

   (c) Wherever the failure of a system element compromises Orbiter or flight crew safety during any mission phase.

2. Condition monitoring and fault detection (CMFD) provisions shall be incorporated as follows:

   (a) The failure of any critical system element which will cause damage to the beam or beam builder equipment shall be detected automatically.

   (b) The control subsystem shall diagnose the failure and initiate corrective action before damage occurs. The control subsystem shall either stop the beam builder process in a safe mode or allow the process to continue uninterrupted by automatic switch-over to a redundant element.

The substitution of non-flite items will, therefore, be made on an item-by-item basis during early development and the GTBB shall otherwise be identical to the FTBB, as discussed in detail in Section 3, except for the few differences illustrated in Figure 6-1. The machine configuration will be similar to the flight test article in size, function, and general arrangement, but will use a facility source of coolant and will, therefore, not require a self-contained cooling system or radiator. (The radiator is shown here for reference to illustrate the new location selected for the flight article.) It will be comprised of the subsystem modules (SSMs) listed in Table 6-1.

Table 6-1. Subsystem modules.

- Forming Subsystem
  - Cap forming machine (3)
- Joining Subsystem
  - Welder assembly (3)
  - Welder control module (3)
  - Weld anvil positioner installation
    - Drive package
    - Anvil assembly (3)
- Cross-member Subsystem
  - Cross-member storage and feed clip (3)
  - Clip feed drive installation
    - Feed drive unit
    - Feed drive shafts (3)
  - Cross-member handler positioner
  - Cross-member subsystem control module
- Cutoff Subsystem
  - Cap Cutter (3)
  - Cap cutoff control module (3)
- Structure
  - Machine structure
  - Ground handling pallet
- Cord Subsystem
  - Forward and aft cord plyer installations
    - Master cord plyer
    - Slave cord plyer (2)
    - Flexible drive coupling (3)
    - Cord plyer control module
    - Cord plyer cord tensioner unit (3)
    - Cord storage and feed module (3)
- Avionics and Control Subsystem
  - BCU
  - Central MUX
  - Remote MUX for assembly subsystem
  - Power distribution and control module
  - Data and control link
  - Power harness
  - Data and control harness
- Software
  - Applications programs
  - Executive programs
  - Test and checkout programs
  - Diagnostic programs

Since full cross-member storage capacity is not required for ground test, a set of short clips will be used. The clip length will allow the clip storage/feed concept to be full develope The cap material storage canisters will remain full size, in spite of the greatly reduced beam length demand expected of the GTBB, to permit the full-size roll-in-a-can concept to be fully evaluated.

The structure and ground handling pallet shown in Figure 6-2, will provide the basic support for all subsystems, and the structure will act as the test bed for all integrated subsystem tests.

6.1.2 GTBB TEST PLAN. Testing of the beam builder will be conducted per the top level flow of Figure 6-3. The test program has four major phases. In keeping with the "one-machine" ground rule, elements will be "refurbished and updated" as required for each test phase. Objectives of the phases are:

a. Breadboard Testing. To prove concepts or support the basic design activity.

b. Developmental Testing (DET). Builds on breadboard test experience to evaluate system performance and the effect of environments on flight qualifiable hardware. DET = Design Evaluation Test.

c. Qualification Testing (DPT). Uses DET experience to qualify the beam builder for flight testing. DPT = Design Proof Test.

d. Flight Test. To conduct a beam builder flight experiment and to obtain flight-assembled specimens for later evaluation.

The heat rejection subsystem will not be developed during the GTBB program. Heat rejection during DET and DPT will be performed with facility systems. The heat rejection subsystem required for the flight phase will be developed during the preflight test phase and its need and characteristics will depend on the flight program requirements. Control during DET will be accomplished using a software development control computer system which uses the same language as the BCU. The Beam Control Unit (BCU) will be finalized based on the results of the DET program and will be available for component qualification. Test plans and test procedures will be written and approved for each test phase.

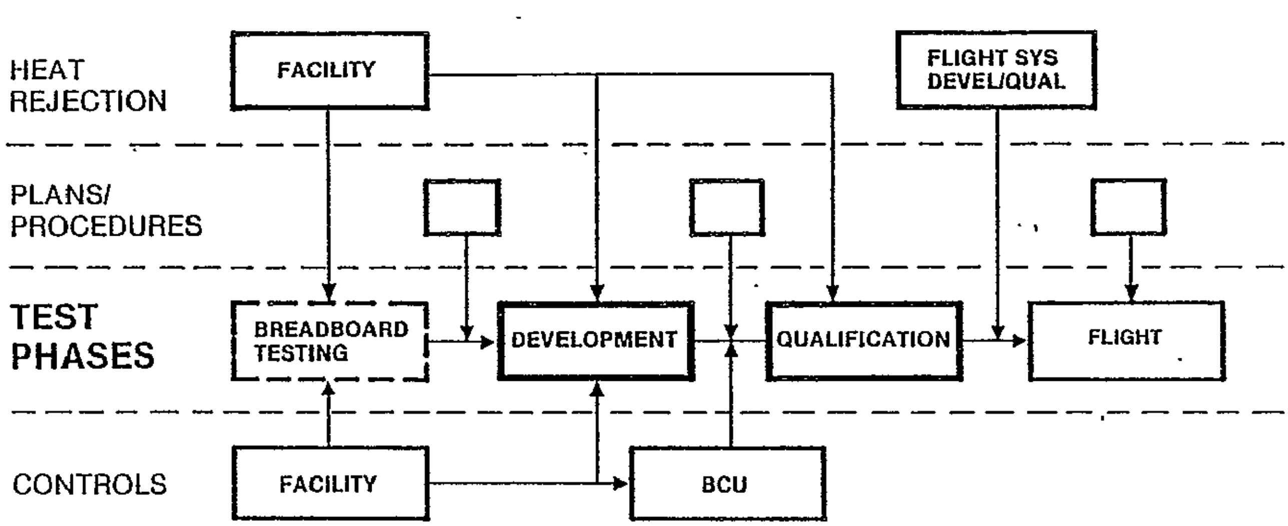

Figure 6-3. Test program flow.

Developmental testing proceeds in a linear flow with increased test article complexity at each step, as illustrated in Figure 6-4. The qualification test phase, shown in Figure 6-5, involves the following three levels of testing:

a. Component Testing. To flight-qualify beam builder components. These components will be updated, refurbished, or replaced, based on data derived from the DET program. Testing, where possible, will be performed by the vendor. GDC inspection will monitor all testing. The vendor will submit a procedure for GDC approval and a test report on the testing. All remaining testing will be performed at GDC. Where it is economically and technically more advantageous to do so, the components will be qualified at the subsystem module (SSM) level rather than individually.

b. Subsystem Module Testing. To flight-qualify the major beam builder subsystems modules.

c. Integrated System Testing. To flight-qualify the full-scale beam builder using all the components, modules, and subsystems tested in the previous DET and DPT programs. Following assembly and ambient checkout at GDC, the beam builder will be forwarded to JSC where it will be subjected to the environments required to demonstrate flight qualification.

A tabulation of the units requiring test during each major test phase, based on a preliminary identification of the environments considered to be the most critical for each individual unit, has been accomplished as illustrated in Figure 6-6.

The complete test plan is included as Appendix A of this volume.

6.2 BEAM BUILDER DEVELOPMENT PLAN

Current planning activity has focused on an update of SCAFE requirements and formulation of both a nominal (baseline) and an alternative development plan for the SCAFE mission. The ground rules guiding these activities and the subsequent cost analysis are given in Table 6-2.

Table 6-2. Baseline development plan/cost analysis ground rules.

- Technology development and program definition prior to phase C/D
- One machine program: GTBB → FTBB
- GTBB is flight qualifiable
  - Modular subsystem development
  - Contains all machine functions
  - Non flight type components where no compromise to function, fit, or safety
  - No redundancy
- Costs in current constant FY79 dollars with no prime contractor fee
- Total program costs include pre-phase C/D and phase C/D development/production/operations costs through first flight

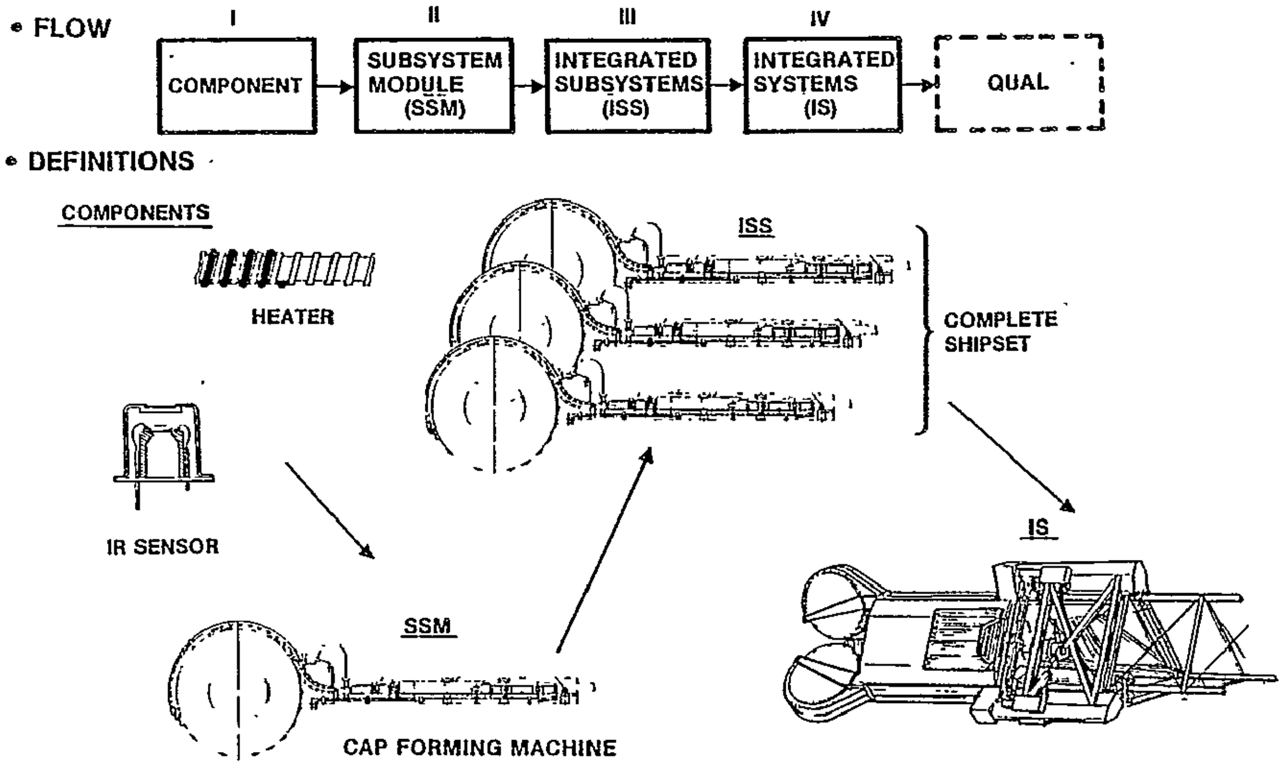

Figure 6-4. Developmental testing.

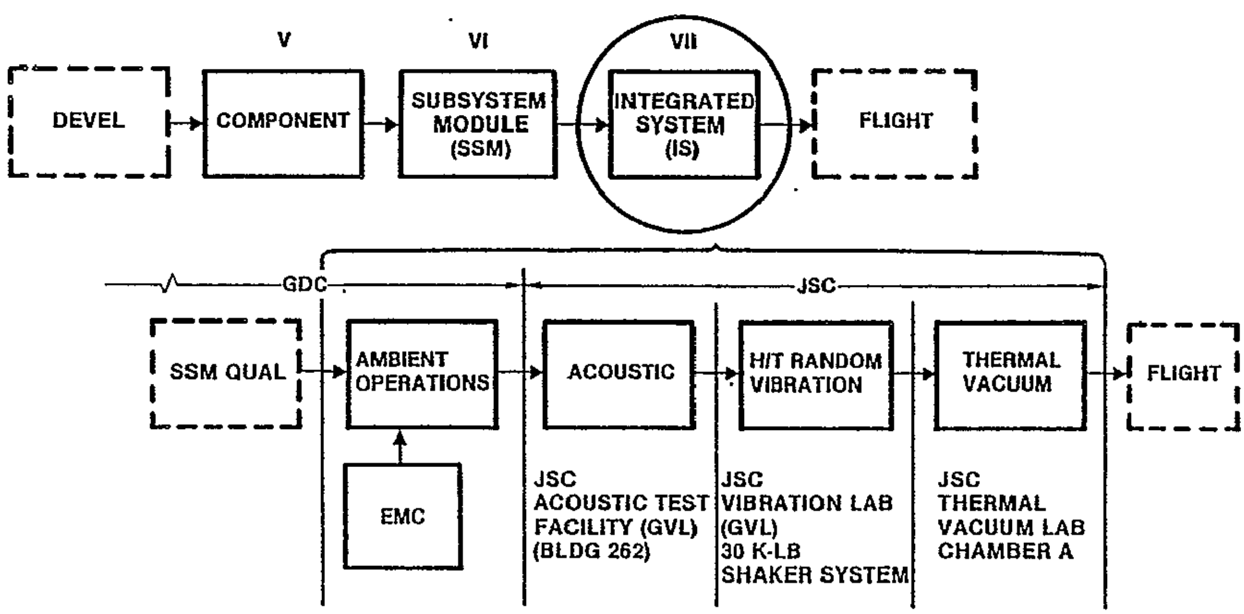

Figure 6-5. Qualification testing.

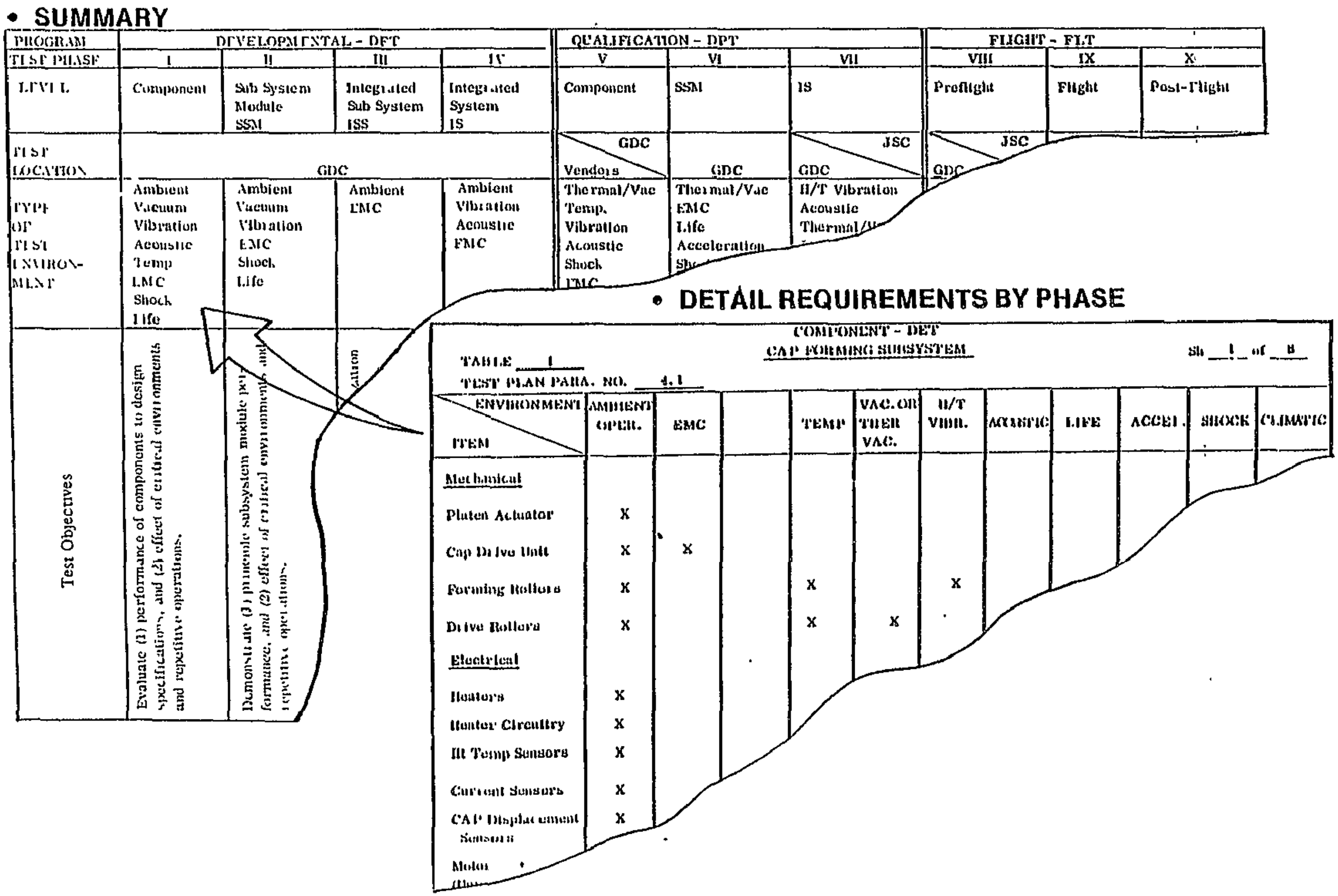

Figure 6-6. Test requirements.

6.2.1 REQUIREMENTS UPDATE. As summarized in Figure 6-7, the Part III requirements analysis task involves updating and expansion of requirements initially defined in Part I/II and collected in the May 1978 Requirements Document (Volume III of the Part I/II Final Report). Changes and additions have resulted from three sources: (1) work performed in Part III study tasks; (2) updated ground rules and assumptions; and (3) revision of the Space Shuttle System Payload Accommodations document.

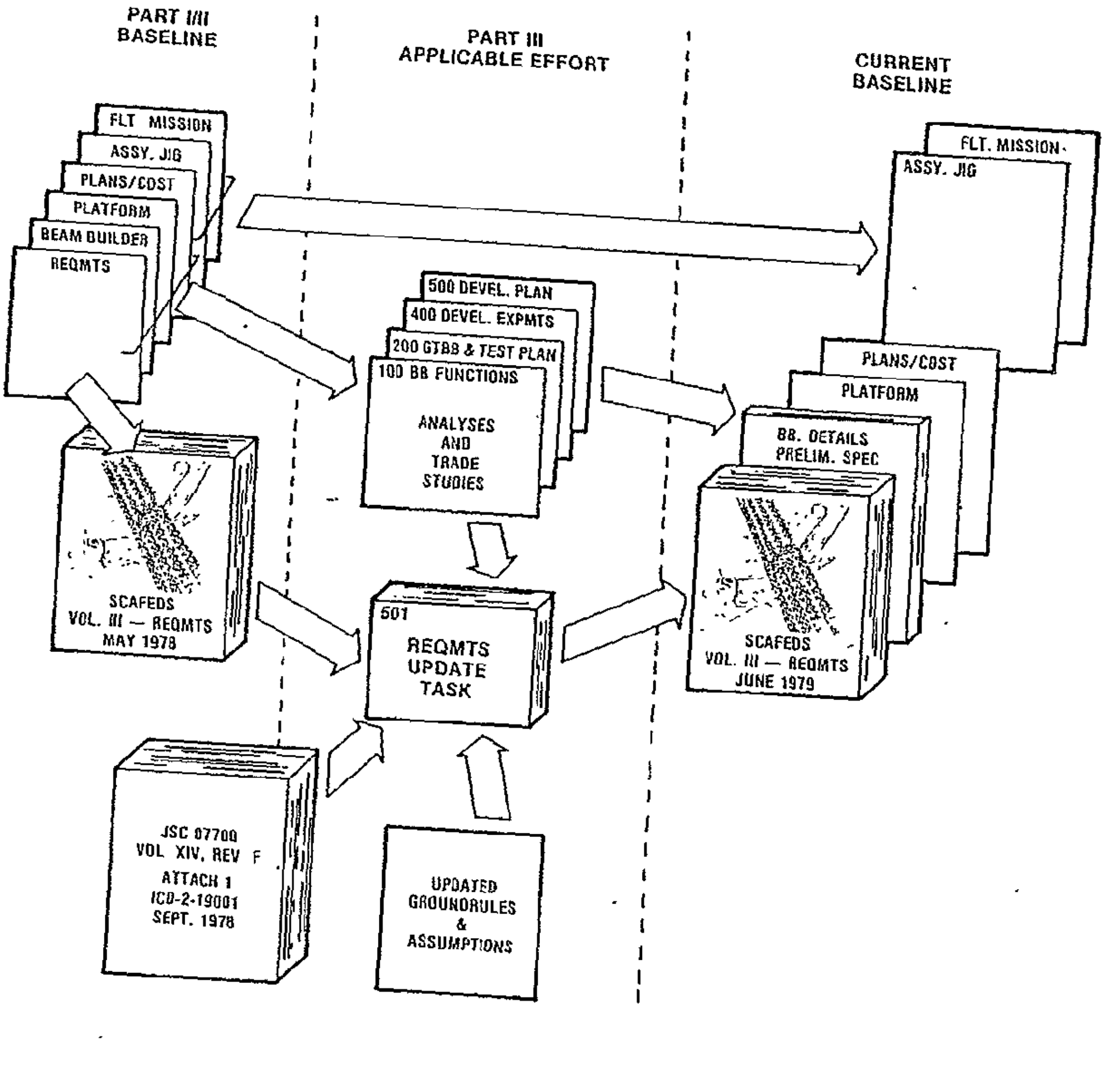

Figure 6-7. SCAFE requirements update.

Continuing programmatic analyses, by both NASA and GDC, have led to ground rule changes. Target first mission flight dates have slipped and a decision has been made to develop only one beam builder end item that will first serve as the ground test development article and will then be updated and refurbished for qualification testing and again for the flight mission. Program schedules have been modified accordingly, as discussed in following subsections.

The major September 1978 "F" revision of JSC-07700, Vol. XIV, produced the greatest number of changes. Many functional requirements were deleted from Vol. XIV proper, and included instead in ICD-2-19001. Most of these changes are of a bookkeeping rather than a technical nature, however.

Certain elements of the Part I/II program baseline - specifically the flight mission spacecraft, assembly jig, and in-orbit operations/time lines - remain unchanged from Part I/II. As before, SCAFE detail requirements are published as a separate volume (III) of the Final Report.

6.2.2 <u>BASELINE DEVELOPMENT PLAN.</u> Formulation of a reasonable and complete program schedule involved three steps: (1) preparation of a detailed GTBB development plan; (2) definition of a nominal Phase C/D schedule, unconstrained by artifically imposed flight dates; and (3) integration of these into an overall schedule.

A typical development approach for a single subsystem in a program such as the GTBB is shown in the upper portion of Figure 6-8. It is a low-risk approach predicated on the desirability of developing components and a single subsystem module first, and then revising the design as necessary before committing funding for fabrication and testing of the remaining modules in the shipset. It is also desirable to stagger the development of the individual subsystems so that simultaneous testing is reduced. This minimizes the peak build-up of manpower and efficiently spreads the demand on test facilities. The lower portion of the figure shows the recommended schedule to develop the GTBB and demonstrate it per this philosophy. Individual subsystem modules are developed first and their testing time is staggered. Then the remainder of the modules are fabricated, verification tested, and combined into a shipset for integrated subsystem testing. Subsystems are then integrated for the first full-machine demonstration at the start of integrated system testing.

The baseline Phase C/D approach to SCAFE system development is shown in Figure 6-9. The major categories of tasks per the WBS (presented in detail in subsection 6.3) are shown with their assigned time spans and their relationships to one another. This is a relatively tight schedule, but one which can be met, provided initial development work is done on the beam builder and a Phase B definition study has been performed to define the assembly jig, the instrumentation for the SCAFE, and the interfaces with the scientific experiments to be carried by the space platform.

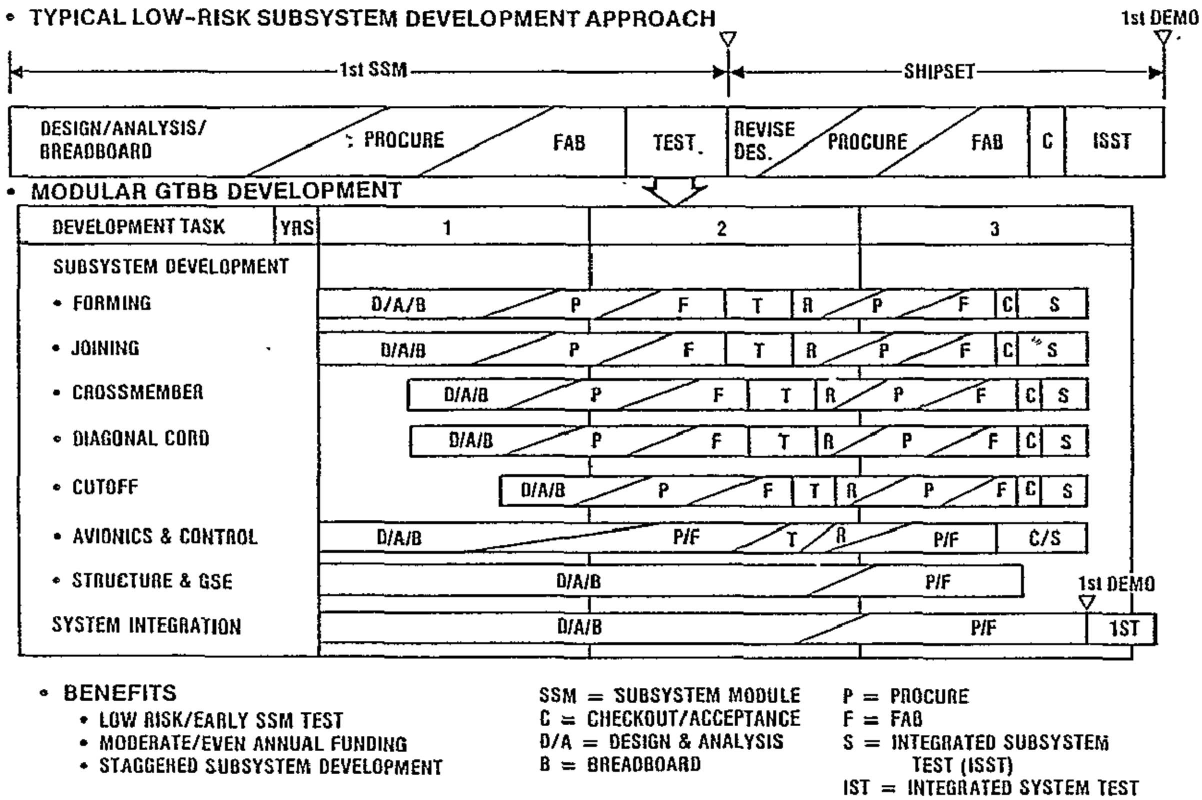

Figure 6-8. Baseline GTBB development plan.

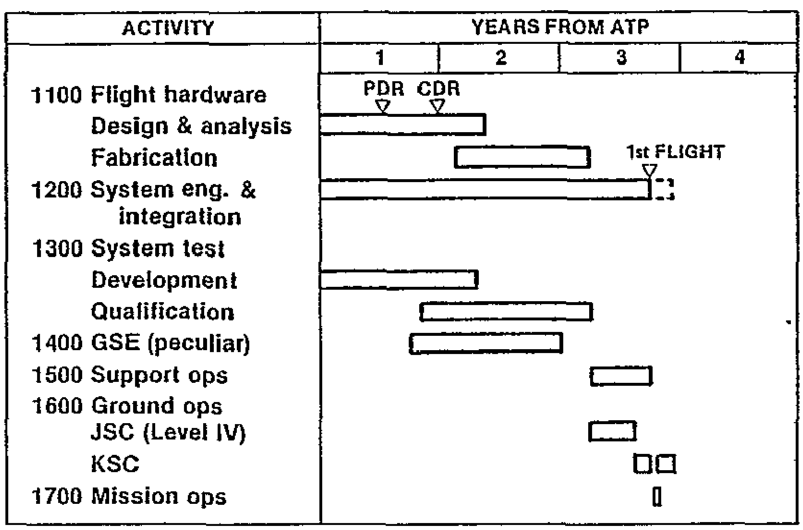

Figure 6-9. Baseline phase C/D schedule.

The total development process, from the present to flight, for the baseline approach is shown in Figure 6-10. Following completion of this current study, a Beam Builder Technology program would be conducted in parallel with a program to generate a GTBB specification. The results of these activities would support preparation of a competitive RFP for the flight program, with source selection/program start in late 1980.

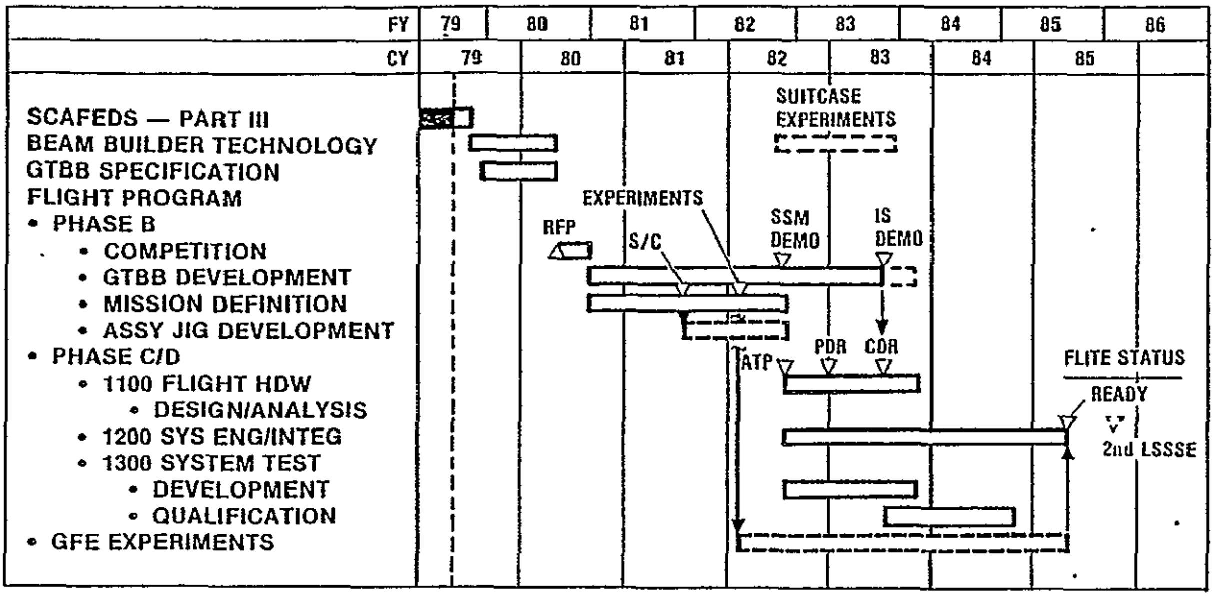

Figure 6-10. Baseline program schedule.

Combining the baseline GTBB development program and Phase C/D schedule (above) shows that developmental testing of all subsystem modules can be completed before Phase C/D start, that the GTBB demonstration will occur concurrent with CDR, and that the system can be ready for flight somewhat before the second LSSSE flight mission milestone shown in current NASA planning.

In addition to the GTBB development, a Phase B study must be performed to define the spacecraft configuration for the mission, the attendant assembly jig, and the selected scientific experiments. The schedule allows for a three-year development time for the flight experiments, which is moderately tight but attainable based on recent experience.

6.2.3 <u>ALTERNATIVE DEVELOPMENT PLAN.</u> In the baseline development plan, ATP for Phase C/D requires successful demonstration of each SSM and integration of beam builder subsystems then parallels other flight hardware design/development, with demonstration of the complete machine in support of CDR. By adopting a higher level of risk, GTBB development can be shortened such that demonstration of the complete machine is accomplished prior to Phase C/D ATP.

The alternate approach to development of a single GTBB subsystem is shown in the upper portion of Figure 6-11. It requires that the full shipset of components and subsystem modules be developed simultaneously. The lower portion of the figure shows the associated schedule to develop the integrated machine and demonstrate it. The complete shipsets of subsystem modules are developed at one time and virtually all of the testing of the different individual subsystem modules is also performed simultaneously. The major effects of this approach are higher risk and increased funding rates but potentially lower total cost.

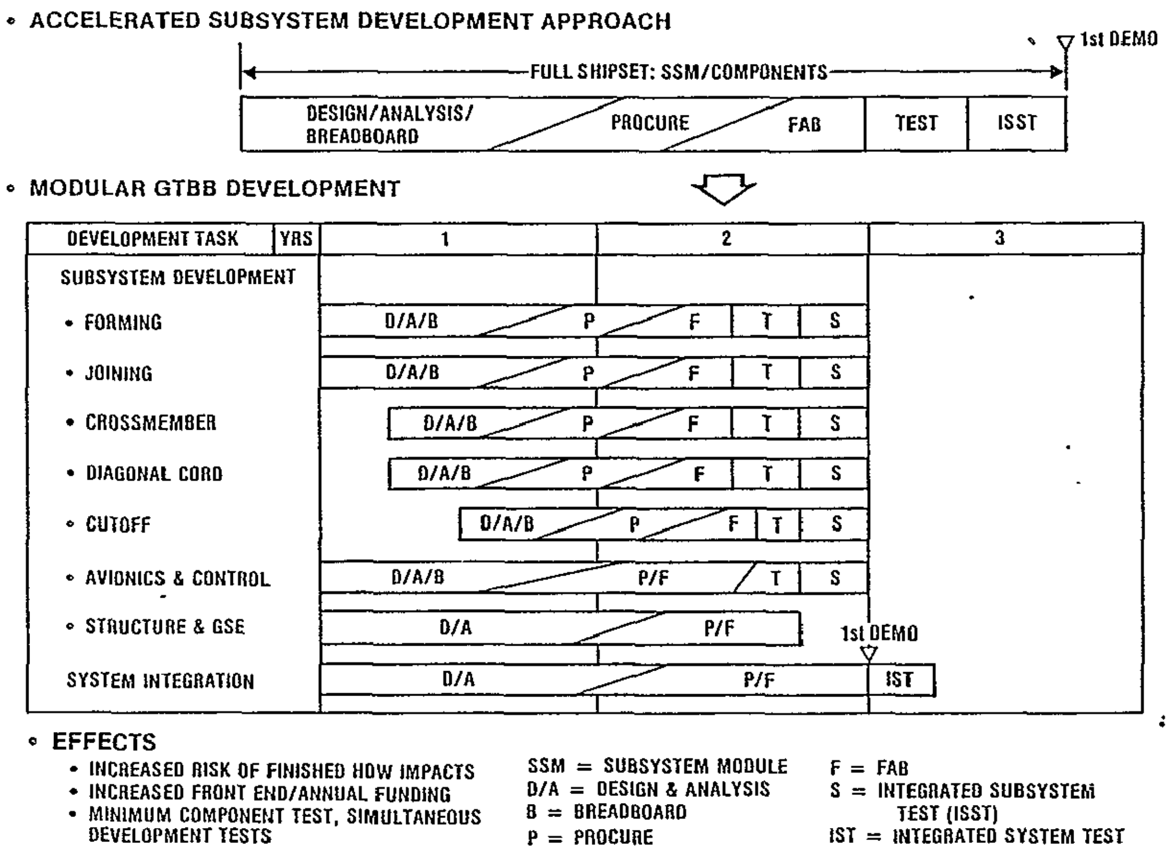

Figure 6-11. Alternative GTBB development plan.

In the alternative total program, shown in Figure 6-12, the activity prior to the start of the GTBB development is identical to the baseline plan. Substituting the alternative GTBB development approach permits demonstration of the GTBB prior to the start of Phase C/D. All other activities are the same as the baseline plan, but the margin between flight readiness and the LSSSE milestone is reduced from five months to three months.

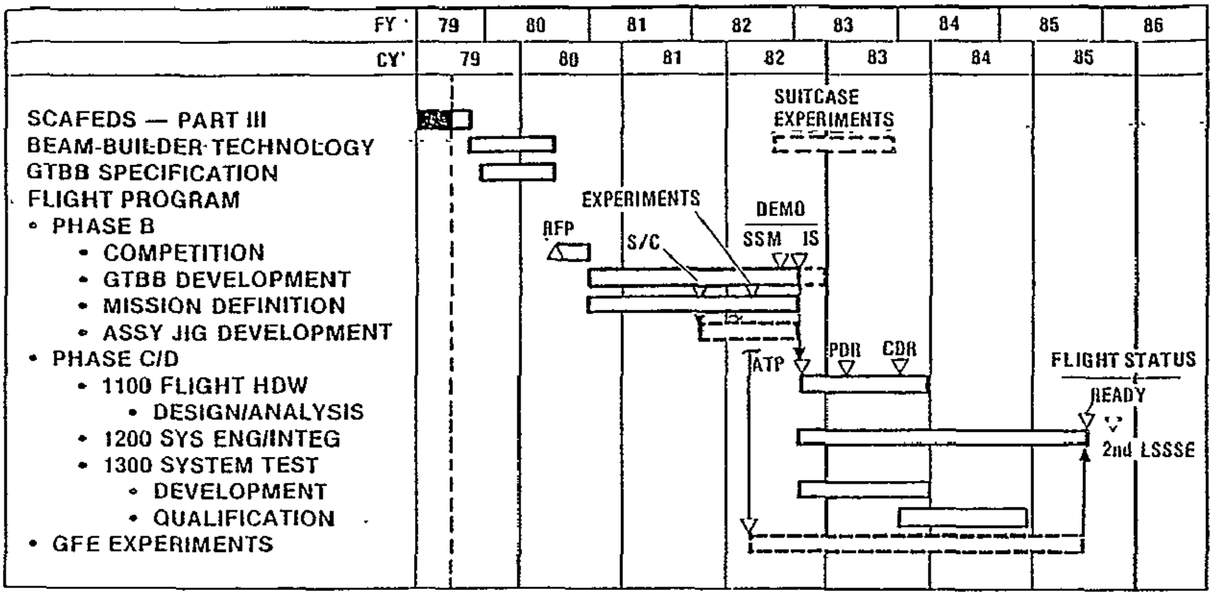

Figure 6-12. Alternative program schedule.

6.3 COST ANALYSIS

A cost analysis of the SCAFE has been conducted and the results are presented herein. This section includes the WBS, the cost analysis methodology and ground rules, program definition and assumptions, and the program cost estimates themselves, including annual funding requirements.

These data represent preliminary top level estimates that can only reflect the program definition work performed to date and, therefore, cannot be considered complete or final. They do, however, represent a reasonable estimate based on information available at this time and are usable for planning purposes. As the program proceeds and more detailed definition of specific hardware becomes available, increased accuracy of individual cost element estimates can be attained.

6.3.1 WORK BREAKDOWN STRUCTURE. A preliminary Phase C/D work breakdown structure (WBS) for the SCAFE program is presented in Figure 6-13. This WBS is based on the program defined in Section 6.2.2, Baseline Program Development Plan wherein a GTBB Technology Development phase has been accomplished to the point of subsystem module demonstration prior to ATP for Phase C/D. Phase C/D will include all additional development and hardware fabrication as well as the actual flight demonstration. The GTBB hardware produced prior to Phase C/D will eventually be converted to the flight article (FTBB) by refurbishment and updating following development tests. The WBS element definitions reflect such a program.

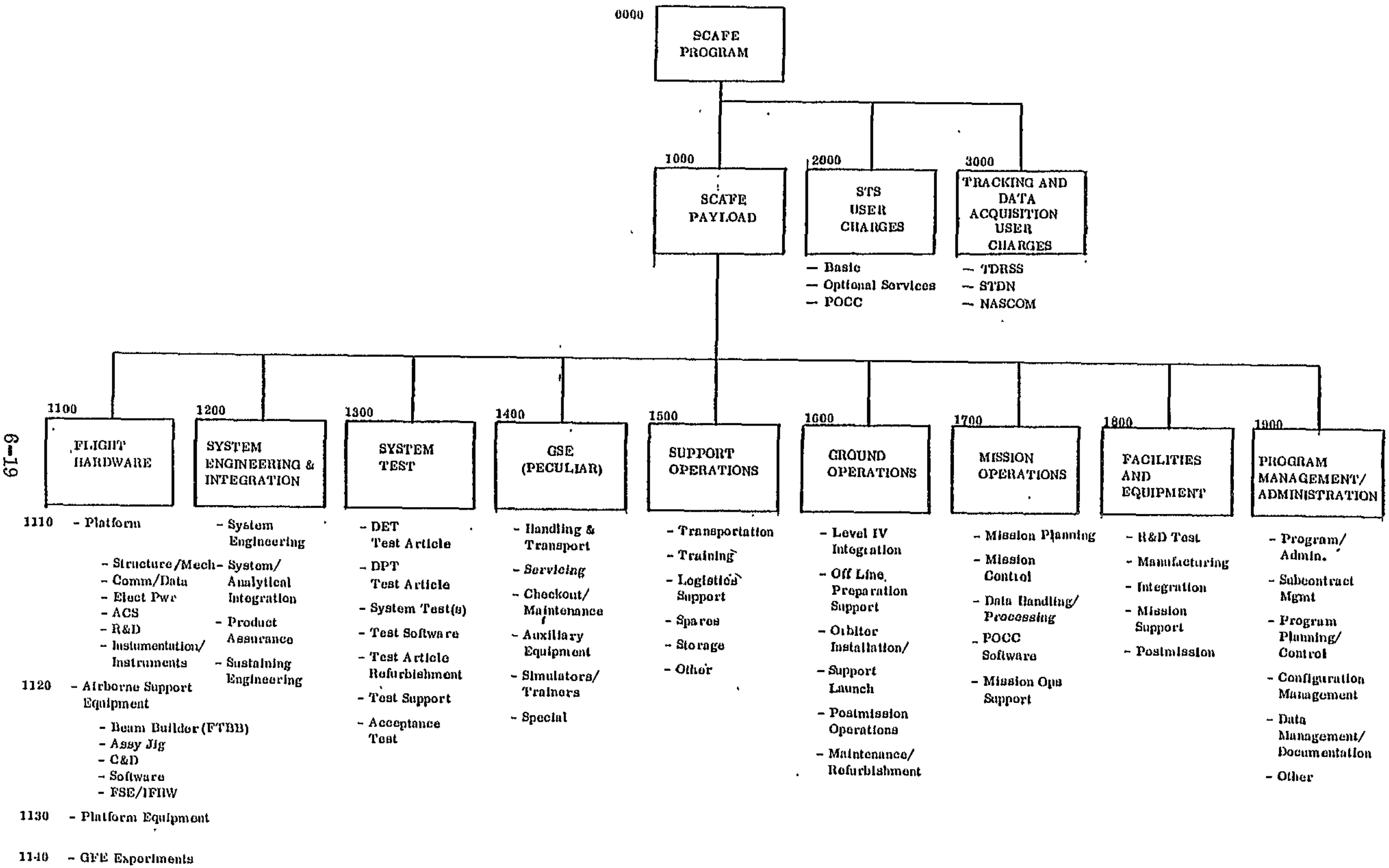

Figure 6-13. SCAFE phase C/D program work breakdown structure.

The WBS serves to identify all of the cost elements to be included in the cost analysis task. This WBS contains all of the hardware and tasks associated with program Phase C/D development and test, the refurbishment, modification, and fabrication of the flight hardware, and the operations activities incurred during the first flight. It is assumed that the Shuttle user charge includes all Shuttle-related activities such as on-line payload installation (OPF), MOC activities, flight crew costs, and other common ground operations/mission operations and activities. Other Shuttle-related services such as OMS kits, RMS, and other optional services are added to the Shuttle user charge for the basic transportation. Potential user charges for tracking and data acquisition (TDRSS, etc.) are carried as separate program level items.

The nonrecurring development portion of the C/D phase includes the one-time tasks and hardware to design and test the SCAFE demonstrations. It includes the required design and analysis for all ground and flight hardware, including structural analysis, stress, dynamics, thermal, mass properties, etc. This phase also includes all software development. The nonrecurring category includes component development and test through component qualification as well as all component development test hardware. In addition, this phase includes: system engineering and integration; system level test hardware and system test; GSE design, development, test, and manufacture; facilities; and, lastly, overall program management and administration.

The production portion of the C/D phase (unit cost estimate) includes all tasks and hardware necessary to provide one complete set of flight hardware equipment. It includes all material and component procurement, parts fabrication and hardware refurbishment, subassembly, and final assembly. In addition, this category includes the required quality control/inspection task, an acceptance test procedure for sell-off to the customer, and program management and administration activities accomplished during the manufacturing phase.

The operations phase includes all preparation, launch, and on-orbit operations associated with the SCAFE experiment. It includes all ground operations, Shuttle system integration (including postmission activities), and the mission operations (ground) activities themselves, including mission control, data handling, support, etc., together with program management and administration during the operations period.

The individual cost elements are discussed below.

<u>1000 SCAFE Program</u>

This summary cost element includes all labor, hardware, and services necessary for the engineering development, production of the flight article, and the first flight operations of the SCAFE. The development phase, in addition to the design analysis and test activities, includes the fabrication of all additional hardware necessary to update and modify the GTBB to the desired configurations level for all Development Evaluation Test (DET) and the subsequent Development Proof Test (DPT) activities.

It also includes all necessary GSE. The production cost includes the refurbishment of the DPT test article to flight configuration and status, including the fabrication of all required new hardware, and the flight article acceptance tests. The operation phase includes: the preparation, integration, and installation of the SCAFE flight unit into the STS Orbiter; the on-orbit beam construction operations; the return, removal, and disposition of the SCAFE equipment; and the on-orbit test and monitoring of the free-flyer space platform for three months. The revisit flight and all GFE experiments and equipment are excluded. It is assumed for this estimate that maximum use is made of developed available off-the-shelf components for both the platform spacecraft and the beam builder and assembly jig. The only component development costs incurred are those of the truly unique new-design components required. System (or subsystem) level design, analysis, and test are included in all cases, however.

1100 Flight Hardware

This element includes all labor materials and services necessary for the platform spacecraft (WBS 1110), and the airborne support equipment (WBS 1120), which includes the beam builder and assembly jig. Costs are not included in this estimate for GFE experiments and equipment (WBS 1140).

1110 Platform Spacecraft

Includes the platform structure or beam itself together with such subsystems as are assembled to the beam and remain in orbit when the Orbiter returns to earth. These subsystems include communications/data management, electrical power, attitude control and stabilization, and rendezvous and docking.

1111 Beam Structure

The beam structure unit cost consists of the composite material (hybrid laminate with fabric of single-ply Pan 50 fiber woven with glass in polysulfone P1700 resin) used in the cap forming machine, the preformed composite cross-members, miscellaneous hardware such as the "docking" fixture for the manipulator, and equipment attachment provisions.

No beam structure fabrication/assembly labor costs are included for on-orbit fabrication by the flight crew during flight operations. The composite cross-members and the miscellaneous hardware such as alignment sensor reflectors are fabricated on the ground.

Material development, and production nonrecurring costs are included.

1112 Communications/Data Management

The communications/data management subsystem installed in the free-flying beam will consist of standardized, off-the-shelf components, such as an applicable standard MMS CDHS module. This equipment will include a computer, a telemetry transceiver/tracking transponder, and a data recorder and auxiliary interface equipment. In addition, unique antennas tailored to the free-flyer configuration will be necessary.

1113 Electrical Power

An electrical power system is required to provide power for the structural response instrumentation and the communications/data handling system (as well as other GFE experiment equipment). It consists of a solar array and secondary batteries, and charge controllers and power conditioning (voltage regulators). In addition, all wiring and cable harnesses are also included in this cost element.

It should be noted that this subsystem is sized to include the capability of providing power for the GFE experiments, and full subsystem costs are included.

1114 Attitude Control Subsystem

The majority of the active attitude control system is considered to be GFE and required for the GFE experiments, and is, therefore, not defined at this time. Only the passive elements, specifically the magnetic dampers, are required for the structural response tests and, therefore, they are the only costs included herein.

1115 Rendezvous and Docking

The rendezvous and docking subsystem for the free-flying beam consists of a rendezvous transponder and a "docking" grappling fixture for use by the RMS. This latter item is included under the beam structure/mechanical cost element.

1116 Experiments/Instrumentation

This element includes the components and equipment on the free-flying beam necessary to conduct the planned structural response experiments and measurements. These items include a sun shade, accelerometers, temperature sensors, reflectors, laser reflectors, laser beacon and detector array, vibrators, and an orbiter-to-beam telemetry transceiver and battery pack. Certain other proposed experiments are assumed to be GFE and not included in the current estimate; however, a cost element (WBS 1140) is provided, but not estimated at this time because of lack of definition.

1120 Airborne Support Equipment

Includes the beam builder and the assembly jig, necessary controls and display (located in the aft flight deck), software required by the beam builder and assembly jig, and all other flight support equipment (FSE) or interface hardware necessary to interface with the Orbiter or other STS systems.

The production cost for this element is limited to the refurbishment and additional new hardware necessary to bring the DPT article to flight configuration.

1121 Beam Builder

This cost element includes the basic structure of the beam builder, all mechanical and mechanism hardware, process controls, sensors and instrumentation, wiring (cables and harnesses), and the system control computer. It includes the cap forming machine subsystem, the coolant subsystem, the cross-member subsystem, the cord application subsystem, the joining (beam welding) subsystem, the beam cutoff subsystem, and the basic structure.

1122 Assembly Jig

This cost element includes the basic structure of the assembly jig, all mechanical and mechanism hardware, all machine and process controls, sensors and instrumentation, all wiring (cables and harness), and the system control computer. It includes the basic structure, the beam builder positioning subsystem, flight support subsystem, longitudinal beam handling subsystem, the cross-beam handling subsystem, the platform assembly subsystem, and the EVA support subsystem.

Equipment associated with experiments and performance test instrumentation (WBS 1124) are excluded from this cost element.

1123 Controls and Displays

The SCAFE will use Orbiter baseline aft flight deck control and display equipment, including the CRT and keyboard at the MSS, and RMS and TV controls and displays at the OOS. In addition, redundant SCAFE control panels (2), redundant SCAFE positioning panels (2), and 2 additional SCAFE TV (CRT) displays will be required.

1124 Software

Software is required for: (1) the beam builder, (2) the assembly jig, and (3) SCAFE/ Orbiter interface. The POCC software required during the mission operations phase is included in WBS 1740. Software for the beam builder and assembly jig is estimated at 4000 instruction words each. A preliminary estimate for the Orbiter interface is approximately 10,000 words. Total flight software is, therefore, estimated at 18,000 words.

1125 Flight Support Equipment/Interface Hardware

The Flight Support Equipment (FSE) and Interface Hardware (IFHW) cost element includes all equipment items necessary for interface between the SCAFE experiment itself and the Orbiter payload bay, aft flight deck, and all associated systems. It is assumed that the majority of the interface hardware requirements will be satisfied by the basic design and only a minimum of interface equipment will be required. The principal interface hardware identified at this time is the experiment support cradle and deployment mechanism.

STS/Orbiter FSE such as EVA aids, MMU, etc., is excluded from this element and included in WBS 2000.

1126 Experiments/Instrumentation

This cost element includes the components and equipment on the beam builder and assembly jig necessary to conduct the planned structural response experiments and measurements. These equipment items include a fixed black and white TV camera with a zoom lens and a spotlight illumination source. A small development allowance is included but the principal experiment design and development cost is carried in WBS 1116.

1130 Not used (Reserved for Flight 2 Hardware)

1140 GFE Experiments/Equipment

Several GFE experiments and supporting hardware are being considered for inclusion in the free-flying beam for Flight 1. They include a geodynamics experiment, an atmosphere composition source, and an active attitude control system. Costs for these items are excluded from the current estimate because of lack of definition.

1200 System Engineering and Integration

This cost element includes all labor, hardware, and services necessary for system engineering and integration (SE&I) during the development phase of the program.

The SE&I activities include the overall integration activities during the SCAFE development phase, the integration into the STS system (analytical integration), and product assurance functions.

1210 System Engineering

This element includes all system level engineering and integration to ensure that all subsystems and all other aspects of the total experiment are compatible and properly integrated. Any sustaining engineering activities required during the production phase are assumed to be satisfied by system engineering activities during the concurrent development phase.

1220 System Integration/Analytical Integration

This element is defined as those tasks necessary to ensure the compatibility of the SCAFE with all components of the STS and other external systems with which the experiment must interact. It includes such activities as mission planning analysis, flight operations analysis, ground operations analysis, Orbiter/payload integration analysis, and experiment requirements analysis.

1230 Product Assurance

This cost element includes the functions of quality assurance, reliability, safety, and parts-material-processes (PMP) control.

1300 System Test

This cost element includes all labor, test articles and other hardware, and services necessary to accomplish the all-up system level testing activities. The category excludes lower level subsystem and component development testing included under the individual hardware development elements.

The program development phase includes two system level testing phases, the design evaluation tests (DET) and the design proof tests (DPT). The DET will provide the development and engineering tests to demonstrate functional performance. The DPT will provide for flight qualification. Fabrication of all new DET hardware and modification and refurbishment of the GTBB are included, as are fabrication of new DPT hardware and refurbishment of the DET article. The preparation for and conduct of the various system level development and qualification tests are included under System Test Operations, Test Support, and Test Software. Test article refurbishment to the flight article is excluded and included in WBS 1120 (Production). Also included is acceptance test of the production flight unit as a production (unit) cost.

1310 DET Test Article

This complete test article is a prototype using prototype subsystems and components which will be functionally accurate but will not necessarily be flight rated. This test article will be used for all early development testing and feasibility demonstration of the basic function and processes of the SCAFE. It will include refurbished and updated GTBB components and subsystems from the GTBB Technology Development Phase.

1320 DPT Test Article

This complete test article will be made up of flight-qualified subsystems and components and will be used to accomplish the flight qualification testing. It will consist of refurbished and updated DET test articles. A portion of this testing will be conducted in the thermal vacuum chamber at JSC (Space Environment Simulation Chamber A). Any user charge for this facility is excluded and TBD.

1330 System Test Operations

This element includes system level test activities associated with both the all-up integrated DET beam builder/assembly jig as well as the DPT article during the development phase. Individual component or subsystem testing is excluded and included under the nonrecurring cost element for the beam builder (WBS 1121) and assembly jig (WBS 1122). This element also includes cost of the test operations associated with thermal vacuum testing of the qualification article in the JSC environmental simulation chamber. For the purposes of this estimate, no user charges for use of the JSC facility are included.

A minimum allowance is also made for engineering analysis support during the three-month period following platform fabrication and Orbiter return when the platform is free-flying and is being monitored.

This element includes preparation of test planning and procedures, test preparation, the test operations themselves, and test analysis, evaluation, and documentation.

1340 Test Software

In addition to the beam builder and assembly jig process control software, an allowance estimate of 500 words of ground test software is made for interface functions, etc., during development system level tests, thermal vacuum tests, etc.

1350 Not Used

1360 Test Support

The test support category includes all tasks and hardware necessary for the direct support of the system level test operations. It includes such items as design, fabrication, and installation of instrumentation, special test fixtures, instrument calibration, and all other supporting equipment and services not accounted for in other cost elements.

1370 Acceptance Test

This cost element includes the activities for the test and checkout of the flight article necessary to satisfy NASA acceptance procedures. This item is included as a production phase cost.

1400 Ground Support Equipment (GSE)

This cost element includes all hardware, labor, and services required to define, design, develop, test, and fabricate new or modified ground support equipment for the SCAFE program. This element includes deliverable GSE for support of the flight experiment through its lifetime. It includes all necessary unique handling, shipping, and transportation equipment, servicing equipment (fluids, batteries, pneumatic, etc.) checkout and maintenance equipment, and other auxiliary equipment items such as auxiliary power and ground heat exchanger. POCC (mission control) equipment is excluded.

1500 Support Operations

This cost element includes all labor, material, and services necessary for support operations activities. Support operations are defined to include transportation, logistics support, spares, storage, training and all other peripheral activities. Transportation of the SCAFE payload between Convair and JSC and KSC was not analyzed in detail; however, for purposes of the study, a dedicated C5A aircraft was assumed both for: (1) the qual article (San Diego to JSC and return) and (2) the flight article (San Diego to JSC to KSC and return to JSC). Minimum spare and repair parts are assumed. Components will be repaired and, during launch preparation, parts will be available from the backup unit.

1600 Ground Operations

This cost element includes all material, labor, and services necessary for the preflight ground operations phase of the program. It includes the equivalent of Level IV integration at JSC, off-line preparation, Orbiter installations, launch, and postmission operations at KSC, and postflight maintenance and refurbishment (excluded from this estimate).

1610 Level IV Integration

These activities will be accomplished at JSC with the primary flight article and include the flight article test and functional checkout, EVA/IVA operations verification, training simulation and training, integration of GFE experiments, and the potential functional operation of the flight article in the thermal-vacuum chamber (Space Environment Simulation Chamber A).

1620 Off-Line Preparation

These activities, equivalent to Level III/II integration, will be accomplished at KSC, primarily by KSC personnel, to prepare the flight unit for Orbiter installation. Costs are estimated only for SCAFE-related personnel who provide monitoring and standby support to KSC personnel.

Functions to be accomplished include payload receiving and inspection, installation in Cargo Integration and Test Equipment (CITE) simulator and simulated Aft Flight Deck (AFD), conduct of a complete interface verification and compatibility check, conduct of an Orbiter mission sequence test, and removal from CITE.

1630 Orbiter Installation/Launch

These activities, equivalent to Level I integration, are accomplished primarily by KSC personnel. Costs are estimated only for SCAFE payload personnel providing monitoring and standby support for KSC crews. The functions include moving of the payload to the OPF, installing in the Orbiter payload bay and aft flight deck, connecting the interfaces and verifying the Orbiter integrated test, Shuttle buildup and move to launch pad, and the countdown and launch.

1640 Postmission Operations

These activities will be accomplished at KSC and involve payload safing at Orbiter landing, removal of the SCAFE payload from the Orbiter bay and aft flight deck at the OPF, moving of the payload to the O&C building for postmission processing, including equipment disassembly, storage, or shipping, as appropriate. Only SCAFE support personnel are included in the estimate.

1650 Maintenance and Refurbishment

This element includes all postflight SCAFE payload maintenance and refurbishment undertaken prior to storage or reflight. The location of this activity depends on payload disposition. For purposes of the current cost estimate, maintenance and refurbishment are excluded.

1700 Mission Operations

This cost element includes all labor and services required for mission control, data handling/processing, and mission operations support. The identification and definition of any unique POCC hardware (consoles, etc.) is TBD and not included in the current estimate. POCC user charges are excluded from this element and are included in WBS 2000.

1710 Mission Control

The SCAFE orbital flight is designed for full autonomous on-board control. The POCC in this concept will only provide monitoring and quicklook data functions and standby fault diagnosis assist. The POCC operation includes a six-week preparation period (POCC reconfiguration, preparation, integration, test, crew familiarization, and training), a one-week flight support (launch and orbital operations), a one-week retrieval, disassembly, and cleanup, and a three-month free-flyer data acquisition monitoring activity prior to revisit (Flight 2).

1720 Data Handling/Processing

This cost element covers data reduction and tape or hard copy data preparation, as well as data handling processing associated with POCC quick-look data activities.

1730 POCC Software

In addition to available standard POCC and data processing software routines, it is estimated that an additional 2000 words of payload-unique software will be required for data display, data formatting, etc.

1740 Mission Operations Support

This item covers all backup and support personnel necessary to support WBS cost elements 1710, 1720, and 1730.

1800 Facilities

This cost element includes all facilities or related services during development, test, or manufacturing, integration at JSC, integration at KSC, or mission support (POCC).

1810 Development, Test, and Manufacturing Facilities

It is currently estimated there are no new customer-funded capital facilities required for the development, test, or manufacturing of the SCAFE. It is anticipated that thermal vacuum tests will be conducted in the JSC Space Environment Simulation Chamber A. (User charges for this facility are not included in the current estimate. Other associated costs are included under System Test cost element 1300.)

Other development or operations training facilities are also assumed available such as a simulator for development or training with the RMS, simulator for flight operations docking, and buoyant tank facility or other EVA training simulators.

1820 Integration Facilities (JSC)

None.

1830 Integration/Post Mission Processing Facilities (KSC)

None.

1840 Mission Support Facilities (POCC)

None.

1900 Program Management/Administration

This cost element includes all labor, services, and materials necessary for program management/administration for all three phases of the program. It includes program administration, subcontract management, program planning and control, configuration management, data management, and documentation and other services necessary for the overall conduct of the program.

2000 Shuttle Transportation User Charges

This cost element includes all user charges associated with the STS for preparation, launch, on-orbit activities, and return to earth. It includes the basic transportation charge plus all additional charges for optional supporting services, such as energy kits, EVA, second RMS, MMU, etc., and any user charges related to the POCC operations. It is assumed that the basic Shuttle user charge includes all Shuttle-related activities such as on-line payload installation (OPF), MDC activities, flight crew costs, and other common ground operations/mission operations and activities.

3000 Tracking and Data Acquisition

This cost element includes all necessary related user charges associated with the NASA tracking and data acquisition facilities and services, including TDRSS, STDN, NASCOM, etc., not included in the basic STS user charge, both during the Shuttle on-orbit phase as well as the SCAFE platform free-flying phase. Data processing of returned data is not included.

6.3.2 COST ANALYSIS METHODOLOGY. The economic analysis approach and cost estimating methodology is discussed in this subsection.

Initially a cost work breakdown structure (discussed above) was developed that includes all elements, chargeable to the SCAFE program for each of the program phases, i.e., development, production, and operations. This cost WBS then sets the format for the estimating model, the individual cost estimating relationships (CERs), cost factors or specific point estimate requirements, and, finally, the cost estimate output itself. Cost estimates are then made for each element, either at the WBS breakdown level shown or one level below in certain cases. These estimates are then accumulated according to the WBS to provide the required development, flight article production, and first flight operations costs.

The estimating methodology varies with the cost element and with the availability of historical data or vendor quotes. For new non-off-the-shelf hardware, parametric CERs are used. These CERs have been derived for various categories of hardware and many subcategories representing differing levels of complexity or technology families. These CERs are derived from available historical cost data or detailed estimating information and relate cost to a specific driving parameter such as weight, area, power output, etc. For example, the various SCAFE structural items, mechanisms, control systems, etc., were estimated using such CERs.

Point estimates were used for specific pieces of equipment where the definition data was sufficiently detailed or the hardware item was existing equipment and cost data was available. Certain electronic equipment and instrumentation were estimated in this manner. In another example of point estimates, several task areas in ground and mission operations consist of all labor and, therefore, manloading estimates were made and converted to cost.

The remaining "floating item" cost elements such as system engineering and integration, program management, etc., are estimated using simple cost factors consisting of appropriate percentages of the applicable related program effort.

The following general ground rules and assumptions were used in estimating the SCAFE program costs presented herein. Specific assumptions and definitions for individual cost elements are discussed in Subsection 6.3.1.

a. Costs are estimated in current/constant FY 1979 dollars.

b. Costs are estimated for nonrecurring, recurring production, and recurring operation phases. The costs include all SCAFE payload-related costs incurred from the start of Phase C/D (development phase) through a single (first) launch of the SCAFE, including three months of experiment orbital monitoring and data acquisition.

c. In addition to the costs of Phase C/D, the costs of SCAFE follow-on activities, the Ground Test Beam Builder Technology Development Program, and certain Phase B activities are estimated.

d. The estimate presented represents total cost to the customer; however, NASA IMS and Program Office support (salaries, travel, etc.) are excluded.

e. The flight will occur in 1985.

f. The Shuttle user charge will be included in the estimate.

g. The program estimated is defined in Reference 1, Section 5.1. Programmatic data as updated per Subsection 6.2. Weights are defined in Reference 1, Section 4.1 as updated per Section 3.1.

h. This cost data are provided for planning purposes only.

6.3.3 SCAFE PROGRAM COST ESTIMATE. The preliminary cost estimate for the complete SCAFE program is summarized in Table 6-3 and in more detail in Table 6-4. Costs are presented for the Pre Phase C/D phases and for Phase C/D, including the nonrecurring or development phase, recurring production (flight hardware), and the operation phase including the experiment flight test. These estimates represent total cost to customer incurred by the overall program, not just SCAFE prime contractor costs. The costs are estimated in current constant FY 1979 dollars, and prime contractor fee is not included.

Table 6-3. SCAFE program cost summary.

	(Millions of 1979 Dollars)		
	Nonrecurring (Development)	Recurring-Production	Recurring-Operations
Flight Hardware			
Platform Spacecraft	2.43	.98	-
Airborne Support Equipment	18.12	1.22	-
GFE Experiments	-	-	-
System Engineering & Integration	3.62	-	-
System Test	2.55	.28	.03
GSE (Peculiar)	.91	-	-
Support Operations	.11	-	.70
Ground Operations	-	-	-
Mission Operations	.06	-	-
Facilities	0	0	0
Program Mgmt/Admin	1.39	.12	.07
	29.19	2.60	1.42
Phase C/D Total		33.21	
Shuttle User Charge		23.60	
Prephase C/D		3.51	
Program Total		60.32	

Table 6-4. Total SCAFE program cost estimate.

COST - 1979 M $

PRE PHASE C/D

	Nonrecurring (Development)		Recurring Production (Manufacturing)	Recurring Operations
Phase B Definition Study and Tecnnology Development	3.51			
Mission Definition		(.30)	-	-
GTBB Development (Design/Analysis/Test)		(2.04)	-	-
GTBB Test Hardware (DET)		(1.17)	-	-
Total		3.51		

PHASE C/D

		Nonrecurring (Development)		Recurring Production (Manufacturing): Refurb DPT	All New * Unit	Recurring Operations	
1100	SCAFE Flight Hardware						
1110	Platform Spacecraft	2.43		.98	.98		
1111	Structure/Mechanical		(.48)		(.14)		-
1112	Communication/Data Mgmt		(.20)		(.22)		-
1113	Electrical Power		(.79)		(.39)		-
1114	Attitude Control and Stabilization		(.18)		(.02)		-
1115	Rendezvous and Docking		(.06)		(0)		-
1116	Experiments/Instrumentation		(.72)		(.21)		-
1120	Airborne Support Equipment	18.12		1.22	3.28		
1121	Beam Builder		(7.27)	(.46)	(1.56)		
1122	Assembly Jig		(7.08)	(.41)	(1.37)		-
1123	Controls and Displays		(.07)	(.04)	(.04)		-
1124	Software		(1.47)	-	-		-
1125	FSE/IFHW		(2.22)	(.28)	(.28)		-
1126	Experiments/Instrumentation		(.01)	(.03)	(.03)		-
1140	GFE Experiments/Equipment	-				-	
1200	System Engineering & Integration	3.62		-		-	
1210	System Eng/Sustain Engineering		(1.80)		-		-
1220	System Integ/Analytical Integ		(1.10)		-		-
1230	Product Assurance		(.72)		-		-
1300	System Test	2.55		.28	.21	.03	
1310	DET Test Article (Assy Jig)		(1.03)		-		-
1320	DPT Test Article (BB & Assy Jig)		(.88)		-		(.03)
1330	System Test Ops (DPT)		(.42)		-		-
1340	Test Software		(.01)		-		-
1360	Test Support		(.21)		-		-
1370	Acceptance Test		-	(.28)	(.21)		-
1400	GSE (Peculiar)	.91		-		-	
1500	Support Ops	.11		-		.70	
1600	Ground Ops	-		-		.42	
1610	"Level IV" Integration (JSC)		-		-		(.317)
1620	Off Line Preparation (KSC)		-		-		(.074)
1630	Orbiter Installation/Launch (KSC)		-		-		(.011)
1640	Post Msn Ops		-		-		(.021)
1650	Maintenance/Refurb (Post Flt)		-		-		TBD
1700	Mission Operations	.06		-		.20	
1710	Mission Control		-		-		(.066)
1720	Data Handling/Processor		-		-		(.065)
1730	POCC Software		(.06)		-		-
1740	Support		-		-		(.070)
1800	Facilities	0		-			
1810	Dev/Test/Mfg		0		-		-
1820	Integration (JSC)		0		-		-
1830	Integration/Post Msn Ops		0		-		-
1840	Mission Support		0		-		-
1900	Program Management/Admin.	1.39		.12	.22	.07	
	Subtotal	29.19		2.60	4.69 *	1.42	

	Phase C/D Project Total	33.21
2000	Shuttle Transportation	23.60
3000	Tracking & Data Acquisition	TBD
	Pre-Phase C/D	3.51
	Grand Total	60.32

The estimate includes all payload-incurred costs through the first launch (1985) of the fabrication experiment, including three months of experiment orbital monitoring and data acquisition. The program estimated is essentially a one-machine program. The GTBB hardware produced during the Pre Phase C/D technology development phase will be updated, refurbished, and provided with all new additional hardware necessary so as to serve as the integrated DET article in Phase C/D. Similarly, the DET will be converted to the DPT article for qualification tests and, in turn, to the flight article for the experiment flight. The flight hardware article, therefore, consists of the DPT ground test article refurbishment to flight configuration and standards. The costs for updating of this test article are included as the recurring production cost. In addition to this production cost, the cost of an optional completely new flight article is also estimated and presented for additional information in Table 6-4. The cost of the refurbishment of the flight unit upon its return from the first flight is excluded. All flight platform avionics, electrical power, and their associated GSE were assumed essentially off-the-shelf, and little or no component development is necessary.

Annual funding requirements for the SCAFE program are illustrated in Figure 6-14. These funding estimates are shown individually for: (1) the Pre Phase C/D period, which includes program definition and the GTBB technology development phase (beam builder subsystem DET); (2) Phase C/D, which includes completing the development (assembly jig DET and combined beam builder/assembly jig DPT), refurbishment of the DPT test article to flight configuration, and flight experiment prep and operations; and (3) the STS user charge. These funding requirements were obtained by accumulating the costs for each of the WBS elements spread over time in accordance with the program development schedule. STS user charges are spread according to the STS User Handbook (Jun 1977).

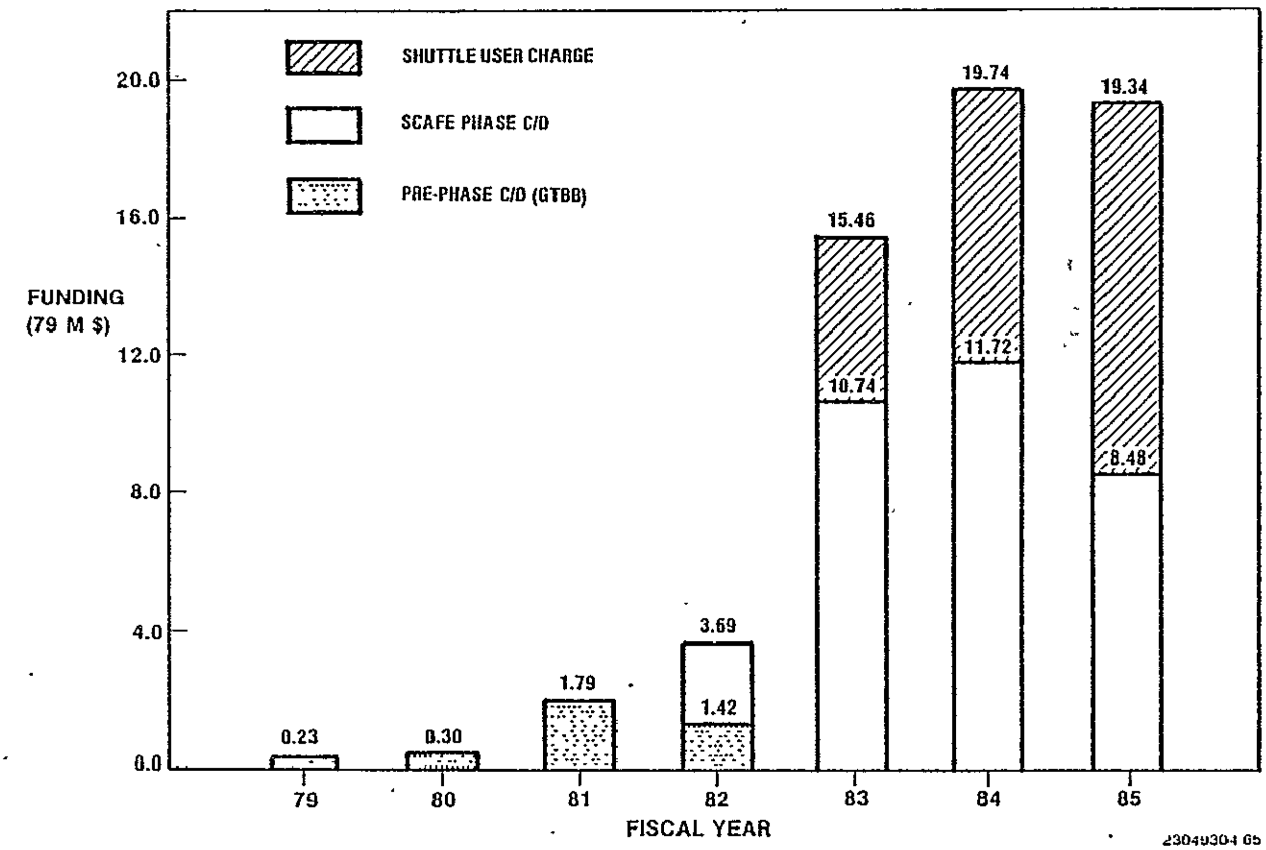

129

Figure 6-14. SCAFE program annual funding requirements.

7

CONCLUSIONS AND RECOMMENDATIONS

This section summarizes the noteworthy conclusions drawn from the Part III SCAFED Study effort and provides recommendations for subsequent program effort to implement the development plan.

7.1 CONCLUSIONS

Conclusions are presented in the same groupings/sequence as preceding text.

7.1.1 STRUCTURE/MATERIALS

a. Overall beam dimensions are unchanged.

b. Replacement of the previous multi-ply laminate with a new woven glass graphite single-ply strip material improves raw material processing, retains key physical/mechanical properties, and permits cap gage reduction.

c. Beam weight is significantly reduced by the cap gage reduction. Mechanical properties revised by incorporating the new material include increased stiffness, small but acceptable reduction of frequency parameter, and an insignificant decrease in local stability.

d. During heating the through-thickness ΔT of the new strip material is small (3 to 6 C), enhancing temperature control.

e. A new "lipped channel" cross-member improves handling by the beam builder and greatly increases the permissible limit load due to sidesway during differential drive.

f. Caps and cross-members now use identical material.

g. The spotweld pattern is slightly modified for cross-member compatibility; higher capability options are readily available if dictated by future higher load applications.

7.1.2 BEAM BUILDER DESIGN.

a. The evaluation of shuttle payload environmental requirements, as they apply to beam builder design, revealed no major problems. The potentially detrimental effects of environments on subsystem elements and components are avoidable through use of known techniques and processes.

b. A thermal shroud enveloping the beam builder assembly section will prevent thermal distortion of the aluminum support structure during on-orbit operations. It will also maintain an acceptable thermal environment for externally mounted subsystem elements in the assembly section.

c. The definition and selection of sensors for control and monitoring of beam beam builder functions indicates the following types are preferred:

   1. Temperature/Heater Control - thermopile
   2. Linear Position - Hall effect
   3. Rotary Position - optical rotary encoder
   4. Cap Displacement - encoded tape with reader head
   5. Current - Hall effect
   6. Force - load cell

d. Brushless dc motors are preferred for all beam builder mechanical drives. One baseline motor configuration can be used in each of the mechanical drive applications. Commonality of drive components is maximized by application of a universal drive unit (UDU) to all driven mechanisms except the cooling platens. The dual motor UDU with mechanism-unique gear reduction will provide the necessary redundant drive capability and potentially useful dual power backup capability.

e. The new cooling platen positioning drive mechanism is failure tolerant. Although the drive uses dual baseline motors, the use of the UDU is precluded by space limitations inside the cap forming machine.

f. Detail timelines for both normal and cutoff bays indicate adequate time in the baseline 80-sec cycle for execution of all functions; cycle speedup appears possible, the extent depending on material capability to accommodate increased heating rates.

g. Definition of executive and applications software modules, including four cutoff-bay-unique programs, results in a minor increase in total instructions (from 2651 to 3409).

h. The new arrangement of avionics and control equipment improves subsystem modularity by allowing controls packages to be located in close proximity to the mechanical modules which they operate. This minimizes the number of control and power interfaces and enhances checkout and maintenance of individual subsystems.

i. The cap forming machine update has shown that a high degree of modularity is possible within the machine, i.e., the forming section, cooling section, and drive sections can each be designed as modular units. Dual wire redundant heater elements are feasible and permit the machine to operate in air and in vacuum. Potential temperature overshoot control problems can be solved through power modulation of the heaters. The overall cap forming machine length was increased 45.7 cm to accommodate the revised forming and drive section configurations.

j. The original cross-member subsystem design concept used too many drive motors and actuators, and the handler did not ensure positive gripping action of the individual cross-members. The new design has only two central drives and provides improved cross-member feed, handling, and positioning characteristics.

k. Incorporation of optical rotary encoders in the cord plyers provides total flexibility in position control and monitoring. It further precludes the use of numerous discrete position sensors along the path of each cord plyer. The additional flexible drive shaft for coupling cord plyer lead screws together ensures reliability of operation of each set of three lead screws driven by a single UDU.

l. Preliminary sizing of the ultrasonic weld heads for the beam builder joining subsystem shows that relatively small envelopes are readily achievable and that further size and weight reductions are possible through use of higher operating frequencies and/or integration of weld tips into the transducer. Cost and reliability considerations will ultimately establish optimum beam builder welder size.

m. The ultrasonic welding process is capable of providing completely automated process control and in-process quality control. By monitoring and controlling the critical weld parameters of pressure, frequency, and energy, the quality of each weld joint is ensured.

n. The joining subsystem modules for welder positioning and weld anvil positioning are now defined in more detail. Incorporation of the UDU and modular packaging of these modules have simplified and enhanced their maintainability and replaceability.

o. The cap cutoff mechanism is revised to incorporate the UDU. This update provides improved modular packaging for the cap cutter assembly.

p. The beam builder basic structure has lengthened to accommodate mechanism requirements and to reduce material canister overhang; bolt-on ground handling provisions permit use of the basic structure as a test bed for subsystem module development and integration.

q. The overall machine cross-sectional envelope is unchanged, but length has increased by 0.55 m to accommodate increased cap forming machine length and to provide clearance for the new cross-member handler/positioner.

r. Mass of the fully loaded machine has decreased from 3618 kg to 3404 kg.

s. The baseline beam builder can build curved beams by deliberately programming differential length(s) among the three beam caps; the degree of curvature is limited first by buckling of the cap flats, next by in-plane weld joint moment, and lastly by cross-member sidesway; increased curvature is easily achievable. by increased material gage and increased weld area.

t. The baseline beam builder concept can be scaled up to produce 7.5 m and 12.5 m beams configured for solar power satellite (SPS) construction. Beam production rate will increase in proportion to the beam bay length to be produced. Although the time selected to produce one bay length of beam, regardless of size, is 80 seconds, material heating characteristics may permit speedup. Cap closure requires the addition of another modular subsystem, which is readily integrated into the machine to store/feed/join the flat closing strip.

u. A common cap and cross-member cross-sectional geometry permits the highest degree of beam builder commonality for SPS applications. A common forming machine for caps and cross-members is feasible for all three SPS beam configurations. These scaled-up forming machines are similar to the baseline, except for their size, extended heating section, and new cooling section design. Cooling rollers are required in lieu of cooling platens to minimize overall machine length and achieve commonality of forming machines. A technique and mechanism is required for splicing strip material. This will permit uninterrupted flow of material from the storage canister to the fabrication process after reloading the canister.

v. In-process forming of cross-members for SPS beam fabrication is preferred to use of clip-fed prefabricated cross-members as used on the baseline beam builder. This is because there is ample power available for cross-member forming and material handling, and replenishment is simplified.

w. A major element of large-scale beam builder operation will be a system for reloading the material canisters.

7.1.3 ALTERNATIVE ASSEMBLY JIG CONCEPTS.

a. The baseline SCAFE assembly jig and platform construction system concept provides a basic model for a wide variety of Shuttle-borne automated space construction systems. The alternative assembly jigs defined for this phase of the study were readily derived from the baseline concept through the maximum use of common subsystems and common stowage and deployment concepts.

b. Construction of open polygons, such as the square and hexagonal structures, can be accomplished with nearly identical construction systems regardless of the assembly sequence selected.

c. The assembly sequence selected for the square and hexagonal structures completes the end-to-end joining of all beams and installs the system hardware before expansion to final shape. This approach is considerably faster, and simpler to control and accomplish than alternative concepts whereby the structure is deployed as it is being fabricated and assembled.

d. Construction of structures having radial beam elements, such as the cross and the 61 m antenna can also be accomplished with nearly identical construction systems.

e. Construction of the cross and 61 m antenna using a central jig-mounted hub is a fast, efficient method of construction. It is also probable that in any user application the central hub is required for hardware and system module interfaces. This technique also maintains the cg of the structure near the shuttle for ease of control. All elements of the structure are also equally accessible from the Orbiter.

f. It is feasible to develop a family of beam end fittings and clamp-on beam attachment fittings which are convenient to stow, simple to install, and provide a wide variety of beam-to-beam, equipment-to-beam or beam-to-structure joining techniques.

g. Fully automated fabrication of tri-beams is possible using the derived construction system concept. This system is greatly simplified by the staggering of cross-beams and the elimination of diagonal cord members from the tri-beam structure.

h. The selected tri-beam fabrication system is a significant departure from the baseline concept in that it requires new subsystems for the beam builder positioner, cross-beam positioning mechanism, RGM support platform deployment, and a new forward cradle assembly. This system can be expanded, within the limits of Orbiter payload bay stowage space, to produce larger tri-beams. A variation of this tri-beam construction system is also possible using the concept derived for building the construction arms for the 500 m antenna.

j. The construction system concept for the 500 m antenna is very preliminary and would require a much more thorough study to fully develop its feasibility and optimize the various construction techniques and equipment which were identified.

k. The construction of very large space structures such as the 500 m antenna requires operation of the space shuttle to its maximum capacity and capability. To make every mission count, the shuttle must deliver the maximum amount of equipment and material and remain on station throughout the period of maximum utilization of its payload. The construction equipment must be designed for multi-purpose operation in order to minimize the total number of missions required to complete the spacecraft, e.g., the assembly jigs and beam builder which fabricate the construction arms are also used as functional elements of the construction arm crawler and traveling assembly jigs.

7.1.4 DEVELOPMENT EXPERIMENTS.

a. An automated "suitcase" experiment on an early Shuttle flight can prove the reliability, repeatability, and physical characteristics of ultrasonic welding in combined vacuum/zero-g with no impact on other payloads.

b. The baseline design fits on a single bridge fitting and requires only power and minimal control interfaces with the Orbiter.

c. Cord capture and weld experiments can be performed with minor additions to the baseline design.

d. The optional EVA-assisted interchangeability of specimen canisters, horns, and transducers permits welding experiments to be performed with various thermoplastic materials, gages, and spotweld patterns.

e. The welder controls can record all weld parameters to facilitate complete evaluation of weld strength vs. weld schedule upon return of the specimens to earth.

f. A cap forming suitcase experiment can be performed on an early Shuttle mission to verify the operational characteristics of the cap forming section in the combined space environment prior to completion of the Flight Test Beam Builder (FTBB).

g. Various options exist for mounting the cap forming experiment in the Shuttle bay to avoid conflict with other Shuttle payloads; sidewall support from two bridge beams (with EVA-assisted tilt-up, if needed); vertical support on either end-bulkhead.

h. The cap forming experiment hardware is identical to the beam builder cap forming section with a cap cutoff mechanism added; postflight integration into the FTBB is planned.

i. Storage of 5.2 m (17 ft) formed cap specimens in vacuum sealed canisters permits both postflight data acquisition on the as-formed condition of the material and construction of 3-bay beam specimens for structural test.

7.1.5 BEAM BUILDER DEVELOPMENT.

a. SCAFE equipment is state-of-the-art but a nominal development period is needed to ensure that the equipment components will operate properly and can be combined into an effective total system.

b. The baseline GTBB Development Program provides a low risk program approach by developing individual subsystem modules first, and then revising the design as necessary before committing funding for fabrication and testing of the remaining modules in the shipset.

c. The GTBB Development Program is scheduled such that the development testing of all subsystem modules can be completed before initiation of Phase C/D, thus proofing the concept before committing C/D funds.

d. To meet the potential 1985 flight date, in addition to the proposed GTBB Development Program, a Phase B mission definition study must be performed to define spacecraft configuration, the attendant assembly jig, and the selected scientific experiments.

e. With the proposed GTBB Development Program and a competitive Phase B System Study, a noncompetitive Phase C/D of less than three years can be accomplished which will meet the 1985 flight date with 3 to 5 months margin.

f. Total program costs, excluding Shuttle user charges, are estimated at $37.7M including $3.5M for Pre-Phase C/D technology development work.

g. The ability to accomplish all fabrication/assembly/equipment installation/test activities on a single Shuttle flight saves $23.6M in Shuttle user charges for the now unneeded revisit mission.

7.2 RECOMMENDATIONS

Based on the SCAFE program work completed to date, further near-term effort is indicated in several categories. Recommended continuation of beam builder technology, preparation of a GTBB Specification, and initiation of study activities leading to a space fabrication proof-of-concept flight experiment are summarized in the following subsections.

7.2.1 BEAM BUILDER TECHNOLOGY.

a. Evaluate and optimize the functions of the cap forming machine, including sensitivity to variations in operating parameters using the existing bench model. Demonstrate ability to produce operational-quality caps (section, length, and straightness).

b. Develop and evaluate variations of theSCAFEDS graphite thermoplastic composite strip material. Using the existing bench model, evaluate samples of material variations for compatibility with the machine.

c. Investigate and evaluate ultrasonic welding by investigating weld heat buildup and dissipation during the welding operation in a thermal vacuum simulation.

d. Investigate and evaluate the flow of an ultrasonic weld in a zero-g environment by determining the effect of gravity on the molten weld. Investigate gravity effects by welding with the weld plane oriented at different angles to horizontal.

e. In connection with welding process, investigate the problem of high voltage in LEO and determine the value which will prevent excessive losses into the plasma.

f. Manufacture a prototype triangular truss segment using the existing bench model of the cap forming machine to form the cap members. Weld cross-members and cord members ultrasonically to the cap members. Use the SCAFEDS-developed truss configuration for the truss segment fabrication. Base the cap members and the welding operation on the results of the above tasks. Also assess the effects of end constraint on the prototype truss.

g. Prepare a test plan for the structural test of the prototype truss which, as a minimum, defines procedures for determining individual cap section strength properties and truss stiffness, dynamic damping, and strength characteristics. Perform these tests on a prototype truss segment.

h. Determine individual cap section mechanical properties by preparing short column cap test specimens and load testing the specimens. Perform associated non-linear finite element analysis and correlate test/analysis results.

i. Prepare materials and welding samples for testing in a NASA/LaRC material space environment testing program. Perform comparative testing and analysis after exposure of the samples to the simulated space environment.

7.2.2 GROUND TEST BEAM BUILDER DEVELOPMENT.

a. Prepare detailed procurement specifications for a GTBB. The baseline configuration shall be that established in SCAFEDS Part III. The environmental design criteria shall be based on the baseline SCAFE mission. The baseline assembly jig concept shall be used to identify and determine load and installation interface requirements applicable to the GTBB. GTBB specifications shall include GSE/STE requirements.

b. Defer development of the heat rejection subsystem (radiator, circulation package) to the flight system development program.

c. Use an executive control and software development system for GTBB development in lieu of a prototype BCU but using the language proposed for the BCU. The BCU would be manufactured and tested as part of the flight system development program, based on data derived from using the development system.

d. Use a staggered subsystem development approach to minimize risk and maintain reasonable annual funding levels.

7.2.3 FLIGHT EXPERIMENT.

a. Initiate a flight experiment program for space fabrication proof-of-concept.

b. Establish planning ground rules and a nominal schedule.

c. Conduct GTBB hardware development such that flight hardware design and analysis is supported and conversion of the GTBB to a flight configuration can be accomplished with minimum cost and within schedule constraints.

d. Perform mission definition studies to define a baseline spacecraft, select a construction approach and all necessary construction equipment, and perform preliminary mission and systems integration.

e. Conduct assembly jig development.

8

REFERENCES

1. Browning, D. L., Space Construction Automated Fabrication Experiment Definition Study (SCAFEDS), Final Report, Vol. II, CASD-ASP77-017, 26 May 1978.

2. Springer, G. S., Thermal Conductivity of Unidirectional Materials, Journal of Composite Materials, Volume 1 (1967), P. 166.

3. Carslaw, H. S. and J. C. Jaeger, Conduction of Heat in Solids, Oxford University Press, 1950.

4. Hottel, H. C. and A. F. Sarofim, Radiative Transfer, McGraw Hill Book Co., 1967.

APPENDIX A

TEST PROGRAM FOR DEVELOPMENT AND QUALIFICATION OF SPACE CONSTRUCTION AUTOMATED FABRICATION EXPERIMENT BEAM BUILDER

C-4

TEST PLAN
CONTENTS

1.0 INTRODUCTION AND PURPOSE

1.1 INTRODUCTION

The beam builder is an automatic machine carried in the space shuttle for the purpose of building space structure beams from prepackaged raw materials.

This test plan presents the developmental and qualification testing concepts associated with the evolution of the beam builder following prototype/breadboard developmental testing.

1.2 PURPOSE OF THE TEST PLAN to define the planning, test objectives, test flow, test environments, test facilities, and locations required during the beam builder test program.

1.3 GROUND RULES FOR THE BEAM BUILDER TEST PROGRAM

1.3.1 PROTOTYPE OR BREADBOARD TESTING of components and subsystems is not included within the scope of this test plan. The above test phase will be conducted to prove concepts or support of the basic design activity.

1.3.2 Only one beam builder machine is planned for all developmental phases. Elements will be "refurbished and updated" as required for each test phase.

1.3.3 Components and various machine elements shall be flight qualifiable in order to comply with the one machine ground rule.

1.3.4 Each major subsystem shall be modular to permit independent development and test.

1.3.5 The heat rejection subsystem will not be developed during the GTBB program. Heat rejection during DET and DPT will be performed with adequate but inexpensive non-flight qualifiable systems. The heat-rejection subsystem required for the Flight Phase will be developed during the pre-flight test phase and will depend on the flight program requirements. Use of the shuttle coolant system may be a feasible alternative depending upon the nature of the mission.

1.3.6 Avionics components will be manufactured utilizing parts from the contractors preferred parts list. Components utilized that are not on this list must be evaluated for acceptability when exposed to the worst case environment. These components will be identifiable during the developmental program.

1.3.7 Control for the BB subsystem modules and integrated system testing, during DET, will be accomplished using the executive control and software development system. The Beam Control Unit (BCU) configuration will be finalized based on the results of the DET program. The BCU will be available for the qualification test program.

1.3.8 DET and DPT testing shall be accomplished at the highest level of assembly deemed appropriate, e.g. component, module, subsystem or system level.

1.3.9 All vacuum testing during developmental DET will be performed at the component or subsystem module level.

2.0 ACRONYMS/DEFINITIONS

1. BB - Beam Builder
2. DET - Design Evaluation Test
3. DPT - Design Proof Test (Flight Qualification)
4. SSM - Sub System Module (i.e. cap forming system, welding system, etc.)
5. ISS - Integrated Subsystem (i.e. (3) cap forming subsystems, (3) cord plyer systems, etc.)
6. GTBB - Ground Test Beam Builder (non-flight structure)
7. IS - Integrated System (completed BB machine)
8. EMC - Electromagnetic Compatibility
9. W/H - Weldhead
10. BCU - Beam Control Unit
11. UDU - Universal Drive Unit
12. Subassembly is defined as an integral unit comprised of components and which is part of a subsystem.
13. Subsystem module (SSM) is defined as an assembly of functionally related components and subassemblies that perform one or more prescribed functions. Each subsystem is a major element of the integrated beam builder system. Subsystem modules are defined in ~~Figure~~ Table 6-1.

3.0 SUMMARY OF TEST PROGRAM PHASES

The test plan is summarized in the following table and figures. These show how the program has been divided into the DET, DPT, and Flight phases. The major objectives associated with each test phase has been outlined in the table. The DET test phase of the program is pictorially presented in the following figure for definition of the various development tasks.

Figures 1 through 4 feature a detailed graphic presentation of the test phases of the test program flow. These diagrams emphasize the timing associated with the various test phases.

PRECEDING PAGE BLANK NOT FILMED

TABLE 3.1. SUMMARY OF TEST PLAN PHASES

PROGRAM	DEVELOPMENTAL - DET				QUALIFICATION - DPT			FLIGHT - FLT		
TEST PHASE	I	II	III	IV	V	VI	VII	VIII	IX	X
LEVEL	Component	Sub System Module SSM	Integrated Sub System ISS	Integrated System IS	Component	SSM	IS	Preflight	Flight	Post-Flight
TEST LOCATION	GDC	GDC	GDC	GDC	Vendors / GDC	GDC	GDC / JSC	GDC / JSC	JSC Shuttle	JSC
TYPE OF TEST ENVIRONMENT	Ambient Vacuum Vibration Acoustic Temp EMC Shock Life	Ambient Vacuum Vibration EMC Shock Life	Ambient EMC	Ambient Vibration Acoustic EMC	Thermal/Vac Temp. Vibration Acoustic Shock EMC Climatics Life	Thermal/Vac EMC Life Acceleration Shock Climatics	H/T Vibration Acoustic Thermal/Vac EMC	EMC Vibration Ambient Thermal/Vac	Orbital	Ambient Thermal/Vac
TEST OBJECTIVES	Evaluate (1) performance of components to design specifications; and (2) effect of critical environments and repetitive operations.	Demonstrate (1) principle subsystem module performance; and (2) effect of critical environments and repetitive operations.	Demonstrate subsystem control and synchronization with multiple subsystem module operations.	Demonstrate the full scale operation and control of the BB before, during, and after exposure to critical environments. Establish final configuration of the BCU.	Qualify the selected BB components for flight operations in critical environment.	Qualify selected subsystem modules for flight operations in critical environments.	System level qualification demonstrates BB performance, before, during and after the required environmental spectrum.	Checkout operation and performance of the refurbished DPT BB.	Demonstrate BB performance during orbital flight operations.	Demonstrate BB post flight operation, accuracy, and reliability. Compare pre flight test, orbital, and post flight test performance. Conduct tear down inspection of selected critical modules and components.

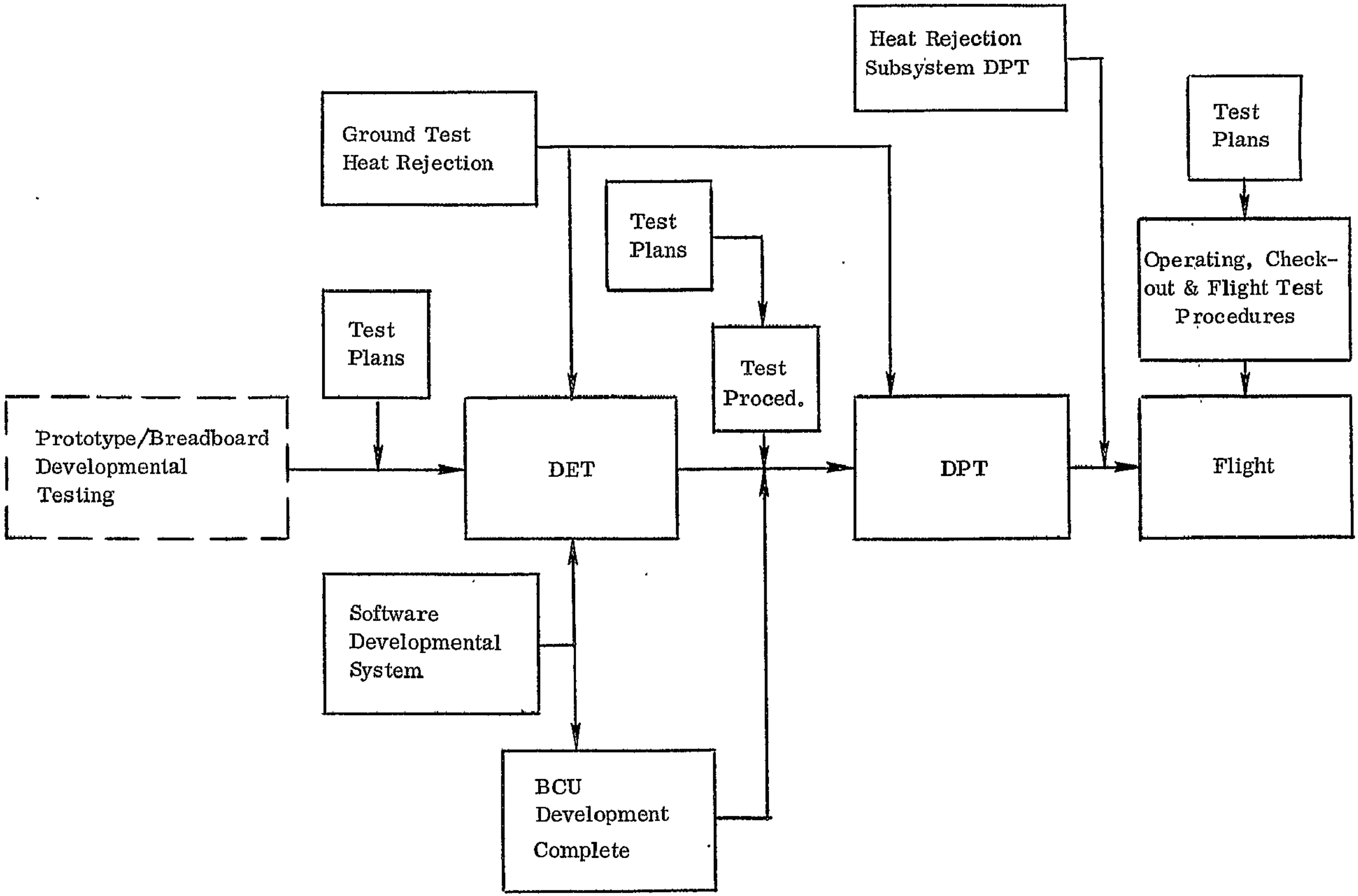

Figure 1. Test program flow.

3.0

Test Phase

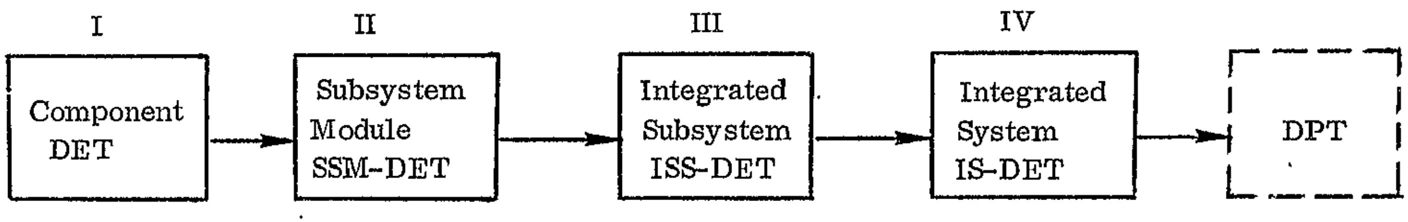

Figure 2. Developmental Test Phase.

3.0

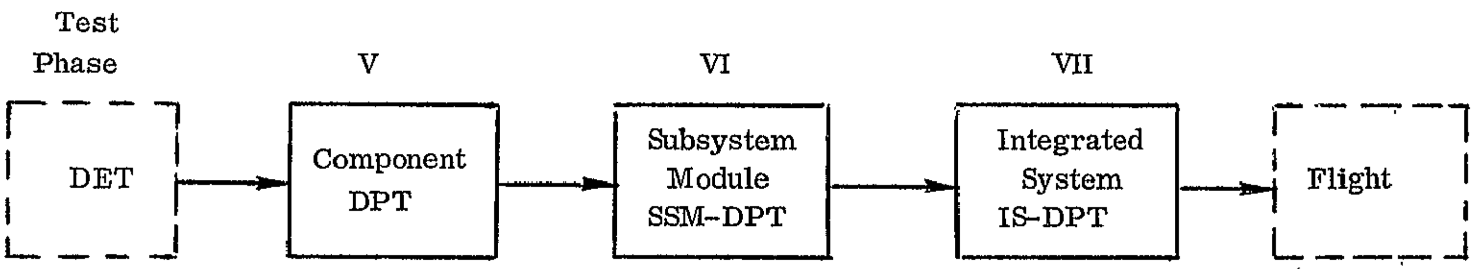

Figure 3. Qualification Test Phase.

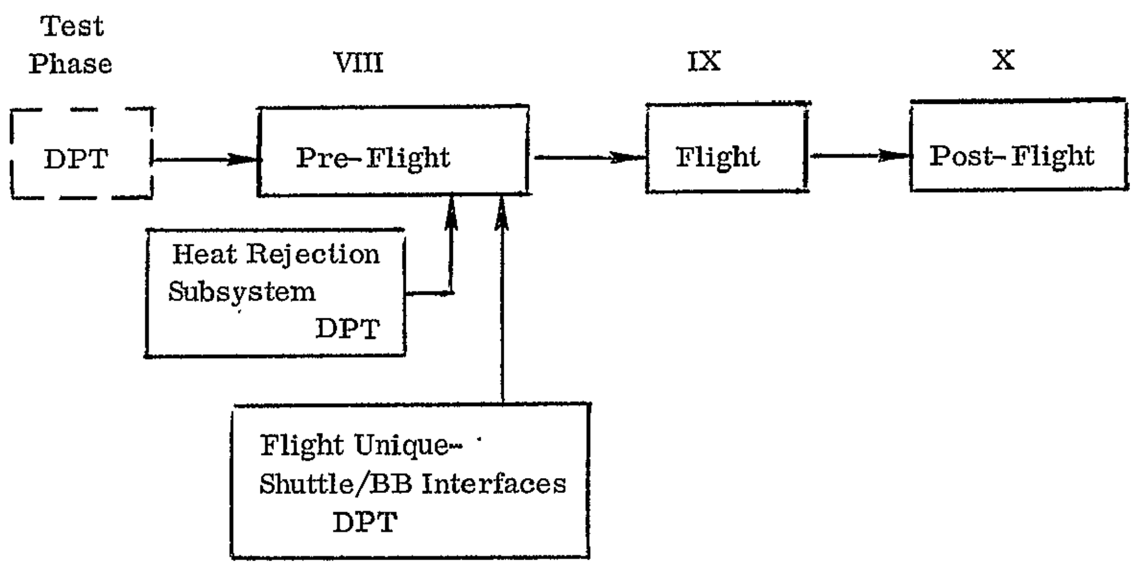

Figure 4. Flight Test Phase.

4.0 TEST PLAN

4.1 COMPONENT - DET

A. Components = designs and selections will be based on prototype studies and prototype developmental testing.

B. Components will be flight qualifiable except alternative hardware will be utilized only if schedule or substantial cost impact would occur.

C. The required testing is tabulated in Table I for components requiring DET operations. Testing will be performed at GDC or selected subcontractor facilities.

D. When appropriate, components will be tested as part of a sub-assembly rather than as individual components.

E. Objectives

1. Evaluate performance of each component for compliance to design specifications.
2. Evaluate the most critical environmental effects on performance of specified components.
3. Evaluate the electromagnetic environment produced by selected componts.
4. Verify no deleterious effects of operating various components (i.e. outgassing, debris, deterioration, etc.).

4.2 SUBSYSTEM MODULE - DET

A. One of each subsystem major assembly shall be assembled per the existing design and subjected to the DET prescribed herein.

B. Knowledge gained during component DET shall be incorporated into this subsystem design.

C. The Ground Test Beam Builder structure shall be utilized as the basic test fixture for subsystems and subassemblies which would otherwise require a special test fixture for support.

D. The Ground Test Hot Bench shall be used to provide control system support during subassembly testing.

E. Testing shall be performed per Table II.

COMPONENT - DET

CAP FORMING SUBSYSTEM

TABLE I

TEST PLAN PARA. NO. 4.1

ENVIRONMENT / ITEM	AMBIENT OPER.	EMC		TEMP	VAC. OR THER VAC.	H/T VIBR.	ACOUSTIC	LIFE	ACCEL.	SHOCK	CLIMATIC
Mechanical											
Platen Actuator	X										
Cap Drive Unit	X	X									
Forming Rollers	X			X		X				X	
Drive Rollers	X			X	X			X			

COMPONENT - DET

CAP FORMING SUBSYSTEM

TABLE I

TEST PLAN PARA. NO. 4.1

ENVIRONMENT / ITEM	AMBIENT OPER.	EMC		TEMP	VAC. OR THER VAC.	H/T VIBR.	ACOUSTIC	LIFE	ACCEL.	SHOCK	CLIMATIC
Electrical											
Heaters	X				X	X				X	
Heater Circuitry	X				X					X	
IR Temp Sensors	X				X					X	
Current Sensors	X										
CAP Displacement Sensors	X			X	X	X					
Motor * (Universal Drive Unit)	X	X			X						
Position Sensors	X										
Cap Drive Motor Controller	DET will be performed on these modules at the subsystem module level.										
Platen Drive Motor Controller											

* The motor utilized in the cap forming subsystem will be the same basic unit used as the motor on other subsystems, and therefore is included as a component DET only in this table.

COMPONENT - DET

DIAGONAL CARD SUBSYSTEM

TABLE I

TEST PLAN PARA. NO. 4.1

ENVIRONMENT / ITEM	AMBIENT OPER.	EMC		TEMP	VAC. OR THER VAC.	H/T VIBR.	ACOUSTIC	LIFE	ACCEL.	SHOCK	CLIMATIC
Mechanical											
Storage & Tensioner Subassembly	X	X		X	X	X	X				
Card Plyer Unit	X				X	X	X				
Electrical											
Capstan Brakes	X										
Magnetic Clutches	X										
Cord Plyer Drive Motor Controller		DET will be done on this unit at the subsystem module level									

COMPONENT - DET
JOINING SUBSYSTEM

TABLE I

TEST PLAN PARA. NO. 4.1

ENVIRONMENT / ITEM	AMBIENT OPER.	EMC		TEMP	VAC. OR THER VAC.	H/T VIBR.	ACOUSTIC	LIFE	ACCEL.	SHOCK	CLIMATIC
Mechanical											
Anvil Drive Unit *											
Electrical											
Welder Pressure Sensors	X										
Welder Efficiency Sensors	X										
Position Sensors											
Welder Electronics *											
Welder Power Supply *											
Welder Drive Motor Controller *											
Weld Anvil Motor Controler *											

* DET will be performed on these components at the subsystem module level.

COMPONENT-DET

CROSSMEMBER SUBSYSTEM

TABLE I

TEST PLAN PARA. NO. 4.1

ENVIRONMENT / ITEM	AMBIENT OPER.	EMC		TEMP	VAC. OR THER VAC.	H/T VIBR.	ACOUSTIC	LIFE	ACCEL.	SHOCK	CLIMATIC
<u>Mechanical</u>											
Feed Drive Unit	X					X					
Handler/Positioner Drive Unit	X	X				X		X			
Storage Clip	X										
<u>Electrical</u>											
Handler Positioner Motor Controller	X				X						
Clip Feed Motor Controller	X				X						

COMPONENT-DET
CUTOFF SUBSYSTEM

TABLE I

TEST PLAN PARA. NO. 4.1

ENVIRONMENT / ITEM	AMBIENT OPER. *	EMC *		TEMP *	VAC.* OR THER VAC.	H/T VIBR. *	ACOUSTIC *	LIFE *	ACCEL.	SHOCK *	CLIMATIC
Mechanical											
Cutoff Drive Unit		These units will be evaluated at the Subsystem module level.									
Electrical											
Cutoff Drive Motor Controller											

* The motor utilized in the cap forming subsystem will be the same basic unit used as the motor on other subsystems, and therefore is included as a component DET only in this table.

COMPONENT-DET

HEAT REJECTION SUBSYSTEM

TABLE I

TEST PLAN PARA. NO. 4.1

ENVIRONMENT / ITEM	AMBIENT OPER. *	EMC *		TEMP *	VAC.*OR THER VAC.	H/T VIBR.	ACOUSTIC *	LIFE *	ACCEL.	SHOCK *	CLIMATIC
Coolant Power Package	This subsystem is not part of the GTBB program. The coolant subsystem will be developed during the Pre-Flight phase of the flight program or utilize the shuttle coolant system. The GTBB head rejection subsystem will be non-Slight qualifiable.										
Coolant Radiator											

* The motor utilized in the cap forming subsystem will be the same basic unit used as the motor on other subsystems, and therefore is included as a component DET only in this table.

COMPONENTS - DET
AVIONICS & CONTROL SUBSYSTEM

TABLE I

TEST PLAN PARA. NO. 4.1

ENVIRONMENT / ITEM	AMBIENT OPER.	EMC		TEMP	VAC. OR THER VAC.	H/T VIBR.	ACOUSTIC	LIFE	ACCEL.	SHOCK	CLIMATIC
Encoders	X										
Load Cells	X										
Signal Conditioner	X				X						
Remote MUX, Interface & Data Acquisition Module	X				X						

F. Objectives

1. Demonstrate subsystem performance to design specification using flight qualifiable hardware.
2. Evaluate environmental effect on subsystem operation.
3. Evaluation subsystem reliability by performance of repetitive duty cycle operations.
4. Evaluate the effects of various phases of subsystem testing on the material properties and condition of beam caps, crossmembers and cords.
5. To develop the necessary knowledge to establish the prototype controls concept required by each individual subsystem using the Software Development Control Computer System.

4.3 INTEGRATED SUBSYSTEM — DET

A. Incorporate the knowledge obtained from the subsystem testing into the design, and assemble a shipset of each of the subsystems and install them on the GTBB Structure.

B. Subject these shipset subsystems to functional testing (reference Table III).

C. Testing shall consist of operational demonstrations at ambient environmental conditions and will be performed at GDC.

D. Objective

1. Demonstrate the operation, control, and synchronization necessary to function at the full scale system level.
2. Demonstrate the accuracy required during multiple beam builder subsystem operations.
3. Study the integrated avionics controls concepts developed during the subsystem DET.
4. Develop the preliminary concepts associated with the BCU.

4.4 TEST PLAN

A. Incorporate any changes resulting from the integrated subsystem testing.

TABLE II

TEST PLAN PARA. NO. 4.2

SUBSYSTEM MODULE - DET

ENVIRONMENT / ITEM	AMBIENT OPER. *	EMC *		TEMP *	VAC. OR THER VAC.	H/T VIBR. *	ACOUSTIC *	LIFE	ACCEL.	SHOCK	CLIMATIC
Cap Forming SS	X	X			X	X					
Joining SS	X	X			X	X				X	
Crossmember SS	X	X									
Diagonal Cord SS	X	X									
Cutoff SS	X	X			X	X		X		X	
Avionics/Control SS Modules	(This subsystem will be included as integral parts of the above subsystem modules.)										

TABLE III

TEST PLAN PARA. NO. 4.3

INTEGRATED SUBSYSTEM - DET

Sh 1 of 1

ITEM \ ENVIRONMENT	AMBIENT OPER.	EMC		TEMP	VAC. OR THER VAC.	H/T VIBR.	ACOUSTIC	LIFE	ACCEL.	SHOCK	CLIMATIC
(3) Cap Forming Assemblies	X	X									
(3) Joining Assy's	X	X									
(3) Crossmember Assys	X	X									
(3) Diagonal Cord Assys	X	X									
(3) Cutoff Assys	X	X									
Avionics & Control Subsystem	X	X									

B. Add all remaining subsystems/hardware to the GTBB structure at GDC.

C. Perform the first full scale demonstration of the BB at ambient conditions.

D. Test the resulting beam structure for compliance to the structural and beam properties specified below:

<u>Beam Properties Determination/Verification</u> (full beam requirements).

1. Geometry Verification

   Cap: Cross-section shape; straightness (curvature, twist); free edge waviness

   Cross-Member: Perpedicularity to cap ℄; "vertical position" (Offsets of EOP from cap apex equal?);

   Weld-Joint: Pattern ℄ vs. cross-member ℄

   Beam Assembly: Spans between adjacent caps; bay spacing; straightness (curvature, twist)

   Cutoff: Square; free of ragged edges

2. Structural integrity verification (strength, stiffness)

   Axial: Compression; tension

   Bending: About 2 axes

   Torsion

   Cord Tension vs time

3. Environmental behavior characteristics (correlation of measured behavior vs analytical prediction)

   a. Thermal: Temperature distribution, distortion, Thermal Loads (?), transient behavior in sun/shadow transit

   b. Dynamics: Modal survey (as a function of length)
   Damping
   Effects of support softness while supported by Beam Builder

E. Subject the BB to the testing required in Table IV.

F. Evaluate the beams made during or after each environment for compliance to the requirements of Step D above.

TABLE IV
TEST PLAN PARA. NO. 4.4

INTEGRATED SYSTEM - DET

ITEM / ENVIRONMENT	AMBIENT OPER.	EMC		TEMP	VAC. OR THER VAC.	H/T VIBR.	ACOUSTIC	LIFE	ACCEL.	SHOCK	CLIMATIC
Full Scale Beam Builder *	X	X				X	X				

*DET testing will utilize the Software Development Computer Control System during the above testing. The BCU Configuration will be finalized based on this testing and will be utilized during the DPT test phase.

G. Objective

1. Demonstrate full scale operations and control of the BB either during and/or after exposure to various environments.
2. Demonstrate the structural integrity and producability of the resulting beams.
3. Demonstrate readiness to proceed to qualification testing of the BB.
4. Demonstrate the prototype avionics control elements.
5. To finalize all concepts associated with development of the BCU.

4.5 COMPONENTS - DPT

A. Components will be updated, refurbished, or replaced, based on evaluation derived from the DET program.

B. Testing, where possible, will be performed by the vendor. GDC inspection will monitor all testing. The vendor will be responsible to submit a procedure for GDC approval and a test report on the testing. All remaining testing will be performed at GDC.

C. The required testing is tabulated in Table V.

D. Where it is economically and technically more advantageous to do so the components will be qualified at the sub-assembly level or subsystem module rather than as individual components.

E. Objective

1. To fully qualify for flight operations all components or component subassemblies.
2. Demonstrate the upgraded performance capabilities of the components resulting from the developmental DET program.

4.6 SUBSYSTEMS - DPT

A. As a goal the components and subassemblies from the DET, and component DPT test program will comprise the subsystems during DPT.

B. The subsystem qual testing shall be limited to operational demonstrations and to those environments considered critical to the BB operation.

TABLE V

TEST PLAN PARA. NO. 4.5

COMPONENT - DPT

CAP FORMING SUBSYSTEM

ENVIRONMENT / ITEM	AMBIENT OPER.	EMC		TEMP	VAC. OR THER VAC.	H/T VIBR.	ACOUSTIC	LIFE	ACCEL.	SHOCK	CLIMATIC
Mechanical											
Platen Actuator	X				X	X		X			
Cap Drive Unit	X	X			X	X		X			

TABLE V

TEST PLAN PARA. NO. 4.5

COMPONENT - DPT

CAP FORMING SUBSYSTEM

ENVIRONMENT / ITEM	AMBIENT OPER.	EMC		TEMP	VAC. OR THER VAC.	H/T VIBR.	ACOUSTIC	LIFE	ACCEL.	SHOCK	CLIMATIC
Electrical											
Heaters	X			X	X	X		X		X	
Heater Circuitry	X			X	X	X				X	X
IR Temp Sensors	X			X	X	X		X		X	
Current Sensors	X			X	X	X		X		X	
Cap Displacement Sensors	X			X	X	X		X		X	
Motors*	X	X		X	X	X		X		X	
Electronic Components	X			X	X	X		X		X	
Position Sensors	X			X	X	X		X		X	
Cap Drive Motor Controller	DPT will be performed on these modules at the subsystem level.										
Platen Drive Motor Controller											

*The motor utilized in the cap forming subsystem will be the same basic unit used as the motor on other subsystems and therefore is included as a component DET only in this table.

TABLE V

TEST PLAN PARA. NO. 4.5

COMPONENT - DPT

DIAGONAL CORD SUBSYSTEM

ITEM \ ENVIRONMENT	AMBIENT OPER.	EMC		TEMP	VAC. OR THER VAC.	H/T VIBR.	ACOUSTIC	LIFE	ACCEL.	SHOCK	CLIMATIC
Mechanical											
Storage & Tension Subassy	X	X		X	X	X	X				
Cord Plyer Unit	X				X	X	X				
Electrical											
Capstan Brakes	X	X		X	X	X		X		X	
Magnetic Clutches	X	X		X	X	X		X		X	
Cord Plyer Drive Motor Controller	DPT will be done on this unit at the subsystem level.										

TABLE V

TEST PLAN PARA. NO. 4.5

COMPONENT - DPT
JOINING SUBSYSTEM

ENVIRONMENT / ITEM	AMBIENT OPER.	EMC		TEMP	VAC. OR THER VAC.	H/T VIBR.	ACOUSTIC	LIFE	ACCEL.	SHOCK	CLIMATIC
Mechanical											
Anvil Drive Unit	X	X			X	X					
Electrical											
Welder Pressure Sensors	X			X	X	X		X		X	
Welder Efficient Sensors	X			X	X	X		X		X	
Position Sensors	X			X	X	X		X		X	
Welder Electronics	DPT will be performed on these components or modules at the subsystem level.										
Welder Power Supply											
Welder Drive MTR Controller											
Weld Anvil Motor Controller											

TABLE V

TEST PLAN PARA. NO. 4.5

CROSSMEMBER SUBSYSTEM

ENVIRONMENT / ITEM	AMBIENT OPER.	EMC		TEMP	VAC. OR THER VAC.	H/T VIBR.	ACOUSTIC	LIFE	ACCEL.	SHOCK	CLIMATIC
<u>Mechanical</u>											
Feed Drive Unit	X					X					
Handler/Positioner Drive Unit	X	X				X		X			
Storage Clip	X										
<u>Electrical</u>											
Handler/Positioner Motor Controller	X			X	X	X				X	X
Clip Feed Motor Controller	X			X	X	X				X	X

COMPONENT - DPT

CUTOFF SUBSYSTEM

TABLE V

TEST PLAN PARA. NO. 4.5

ENVIRONMENT / ITEM	AMBIENT OPER.	EMC		TEMP	VAC. OR THER VAC.	H/T VIBR.	ACOUSTIC	LIFE	ACCEL.	SHOCK	CLIMATIC
Mechanical											
Cutoff Drive Unit											
	DPT ON THESE UNITS WILL BE CONDUCTED AT THE SUBSYSTEM LEVEL.										
Electrical											
Cutoff Drive Motor Controller											

TABLE V

HEAT REJECTION SUBSYSTEM

TEST PLAN PARA. NO. 4.5

ENVIRONMENT / ITEM	AMBIENT OPER.	EMC		TEMP	VAC. OR THER VAC.	H/T VIBR.	ACOUSTIC	LIFE	ACCEL.	SHOCK	CLIMATIC
Coolant Power Package Coolant Radiator	THIS SUBSYSTEM IS NOT PART OF THE GTBB PROGRAM. THE COOLANT SUBSYSTEM WILL BE DEVELOPED DURING THE PRE-FLIGHT PHASE OF THE FLIGHT PROGRAM OR UTILIZE THE SHUTTLE COOLANT SYSTEM. THE GTBB HEAT REJECTION SUBSYSTEM WILL BE NON-FLIGHT QUALIFIABLE.										

COMPONENTS - DPT

AVIONICS AND CONTROL SUBSYSTEM

TABLE V

TEST PLAN PARA. NO. 4.5

ENVIRONMENT / ITEM	AMBIENT OPER.	EMC		TEMP	VAC. OR THER VAC.	H/T VIBR.	ACOUSTIC	LIFE	ACCEL.	SHOCK	CLIMATIC
Encoders	X			X	X	X		X		X	
Load Cells	X			X	X	X		X		X	
Signal Conditioner	X			X	X	X				X	X
Remote MUX, Interface & Data Acquisition Module	X	X		X	X	X				X	X
Electronic Components	X			X	X	X		X		X	
BCU and MUX Components	X			X	X			X			

C. Testing is depicted in Table VI and will be performed at GDC.

D. Objective

1. To qualify the subsystems for flight.

4.7 INTEGRATED SYSTEM - DPT

A. As a goal the beam builder will utilize all of the components, sub-assemblies, and subsystems tested in the previous DET and DPT program.

B. Any modifications or improvements resulting from the component or subsystem DPT will be incorporated.

C. Perform a full scale demonstration at GDC of the BB. Testing shall be as depicted in Table VII. The thermal vacuum shock, and (H/T vibration) will be conducted at JSC. Figure 5 describes the testing flow.

D. Test the resulting beams for compliance to the structural and beam properties specified in Paragraph 4.4D.

E. Objective

1. Qualify the full scale beam builder for flight operations.

2. Certify the beam structures produced during the DPT.

4.8 PREFLIGHT OPERATIONS

A. The flight BB shall be prepared for preflight operations by refurbishing the DPT test article.

B. The heat rejection subsystem shall be designed based on the beam builder flight program. The shuttle coolant system may be utilized if possible. A DPT on this subsystem will be performed before installation on the BB.

C. Flight unique shuttle/beam builder interfaces will be designed and qualification tested before installation on the BB.

D. Components shall be replaced or refurbished based on the accumulated data obtained from the DPT test programs.

E. Following article assembly the testing depicted in Table VIII shall be conducted. The ambient demo shall be performed at GDC following refurbishment. All remaining test operations shall be at JSC.

SUBSYSTEM MODULE - DPT

TABLE VI

TEST PLAN PARA. NO. 4.6

ENVIRONMENT / ITEM	AMBIENT OPER.	EMC		TEMP	VAC. OR THER VAC.	H/T VIBR.	ACOUSTIC	LIFE	ACCEL.	SHOCK	CLIMATIC
Cap Forming SS	X	X			X				X	X	X
Joining SS	X	X			X			X	X	X	X
Crossmember SS	X	X									
Diagonal Cord SS	X	X									
Cutoff SS	X	X			X			X	X	X	X
Avionics/Control SS	(THIS SUBSYSTEM WILL BE AN INTEGRAL PART OF EACH OF THE ABOVE SUBSYSTEMS. EACH OF THOSE SUBSYSTEMS WILL QUALIFY THE AVIONICS ELEMENTS OR MODULES AS A SUBSYSTEM.)										

TABLE VII

TEST PLAN PARA. NO. 4.7

ENVIRONMENT / ITEM	AMBIENT OPER.	EMC		TEMP	VAC. OR THER VAC.	II/T VIBR.	ACOUSTIC	LIFE	ACCEL.	SHOCK	CLIMATIC
Full Scale Beam Builder	X	X			X	X	X				

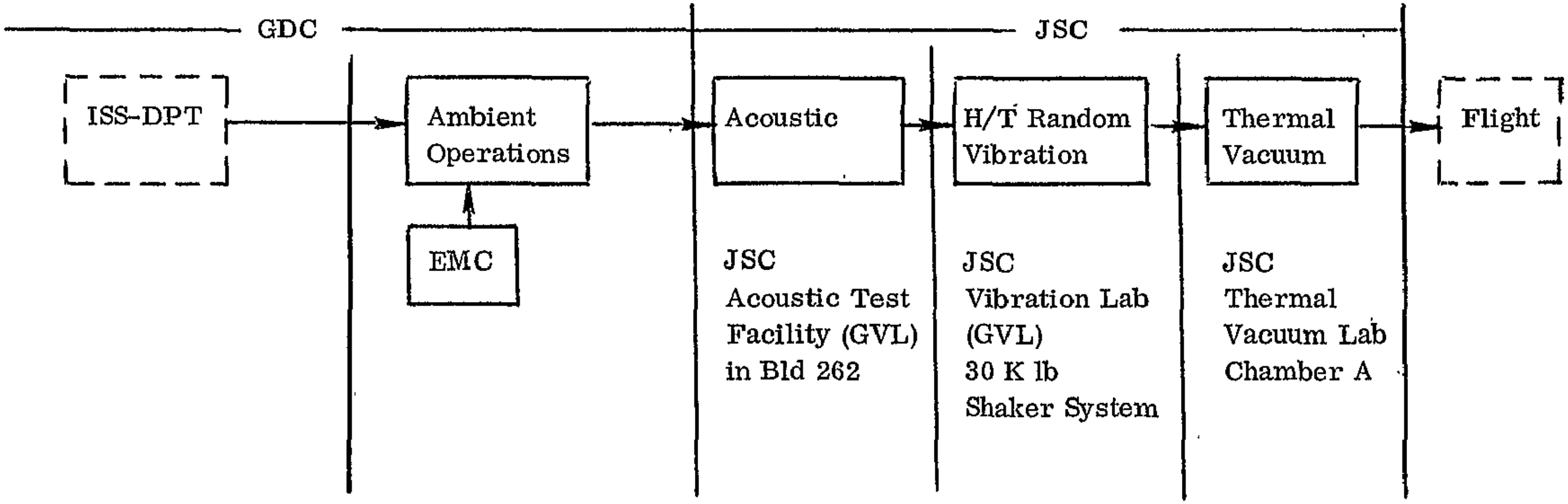

Figure 5. Integrated Systems - DPT.

TABLE VIII

TEST PLAN PARA. NO. 4.8

ENVIRONMENT / ITEM	AMBIENT OPER.	EMC		TEMP	VAC. OR THER VAC.	H/T VIBR.	ACOUSTIC	LIFE	ACCEL.	SHOCK	CLIMATIC
Full Scale BB	X	X			X	X					
Heat Rejection Subsystem-DPT	X	X			X	X	X	X	X	X	X
Shuttle/BB Interface	X	X			X	X					

F. The resulting beam structures shall be evaluated per the DET beam properties requirements in Para 4.4-D.

G. Objective is to demonstrate the flight BB is acceptable for shuttle operations.

4.9 FLIGHT OPERATIONS

A. The test article BB shall be flown in the space shuttle to low earth orbit (LEO) where it will be used to perform space fabrication experiments.

B. While in LEO a series of beam segments of TBD length shall be manufactured and assembled into a predefined structure.

C. Representative sections of beam shall be returned in the shuttle for evaluation.

D. Objectives

1. To demonstrate the feasibility of BB operations in the space shuttle environments.
2. To produce a usable spacecraft.
3. Provide specimens from orbital fabrication for evaluation, test, and comparison with ground fabricated equivalent specimens.

4.10 POST FLIGHT OPERATION

A. The test article BB shall be returned to the lab at a site to be determined by NASA.

B. A post-flight specimen of beam will be manufactured and evaluated and compared to the preflight and inflight specimens.

C. Post Flight test disassembly and inspection of all critical subsystem elements shall be performed to determine the effects of flight test operation on mechanical and electro-mechanical components.

D. Objective

1. Compare structures made in space to normal ground structures in order to establish future quality control for the next generation of BB.
2. Verify the repeated flight capability of a BB by evaluating re-entry environmental effects and post flight operation.

3. To verify the ability of the BB to function in combined zero-g vacuum environment.
4. To support Space Construction Automated Fabrication Experiments (SCAFE).

5.0 STANDARD TEST OPERATING POLICY

5.1 DET

TEST PLAN → TEST → REPORT

A. The DET test plan will consist of a brief summary to delineate test objectives, test requirements, test methodology to be used during test, a test schedule, and a cost estimate.

B. The testing will be informal with testing tailored to new requirements established due to previous test results.

C. The report shall describe the actual testing performed, the test results and reduced data.

5.2 DPT

TEST PLAN → TEST PROCEDURE → TEST → FORMAL REPORT

A. The DPT test plan will be a brief description of the planned test activity. It shall establish the test objectives, test requirements, and pass/fail criteria.

B. The DPT test procedure shall be a formal controlled document establishing the methods the test agency will use to accomplish the testing required in the test plan.

C. The testing will be formal and shall be as established by the test procedure.

Quality Control Inspection shall verify the testing was conducted per procedure.

D. The test report will be a formal presentation of the test results and test data used to verify the test article is an acceptable flight article.

5.3 FLIGHT

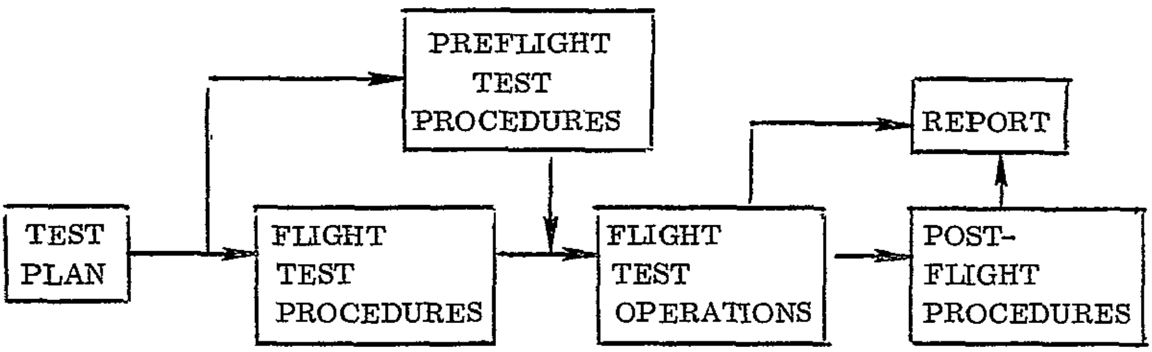

A. The test plan will dictate the GDC support required to provide NASA with a flight article.

B. Preflight, post-flight and flight procedures will dictate the procedural information necessary for operation of the BB.

C. The report will publish the results of the post flight inspection and studies resulting from beams built before, during, and after the flight.

GENERAL DYNAMICS

Convair Division